UNIVERSIDAD COMPLUTENSE DE MADRID

FACULTAD DE GEOGRAFÍA E HISTORIA

TESIS DOCTORAL

Reconstrucción de la paleovegetación y uso de útiles líticos en el yacimiento de homínidos de la garganta de Olduvai (Tanzania) mediante el uso de microfósiles vegetales

Paleovegetation and stone tool use at a selection of hominin sites and their associated landscapes from Olduvai Gorge (Tanzania): a study of plant microfossils

MEMORIA PARA OPTAR AL GRADO DE DOCTOR

PRESENTADA POR

Héctor Arráiz Rodríguez

Directores

Manuel Domínguez-Rodrigo
Doris Barboni

Madrid, 2017

UNIVERSIDAD
COMPLUTENSE
MADRID

Tesis Doctoral

Reconstrucción de la paleovegetación y uso de útiles líticos en el yacimiento de homínidos de la garganta de Olduvai (Tanzania) mediante el uso de microfósiles vegetales

Paleovegetation and stone tool use at a selection of hominin sites and their associated landscapes from Olduvai Gorge (Tanzania). A study of plant microfossils

Autor: **HÉCTOR ARRÁIZ RODRÍGUEZ**

Directores: **MANUEL DOMÍNGUEZ-RODRIGO**

DORIS BARBONI

FACULTAD DE GEOGRAFÍA E HISTORIA

UNIVERSIDAD
COMPLUTENSE
MADRID

Tesis Doctoral

Reconstrucción de la paleovegetación y uso de útiles líticos en el yacimiento de homínidos de la garganta de Olduvai (Tanzania) mediante el uso de microfósiles vegetales

Paleovegetation and stone tool use at a selection of hominin sites and their associated landscapes from Olduvai Gorge (Tanzania). A study of plant microfossils.

Autor: **HÉCTOR ARRÁIZ RODRÍGUEZ**

Directores: **MANUEL DOMÍNGUEZ-RODRIGO**
DORIS BARBONI

FACULTAD DE GEOGRAFÍA E HISTORIA

Agradecimientos

Conviene empezar por los formalismos, pero es justo agradecer al Ministerio de Economía y Competitividad (otrora Ministerio de Ciencia e Innovación) el haberme concedido una beca FPI y posibilitar el desarrollo de este trabajo. Gracias también a la Universidad Complutense de Madrid por haber sido la sede académica de esta tesis y del que esto escribe.

Mil gracias, infinitas gracias, a Doris Barboni y a Manuel Domínguez-Rodrigo, codirectores de esta tesis, sin los que este trabajo hubiera sido imposible. Gracias por acoger a quien desconocía casi todo de la materia a la que se enfrentaba y ahora sólo desconoce gran parte. Doris, merci pour ton soutien, ton patience et ton amitié. Sans toi, l'atterrissage à Aix aurait été impossible.

Gracias a Enrique Baquedano por abrirme las puertas del Museo Arqueológico Regional de la Comunidad de Madrid para poder desarrollar mi tesis doctoral. Qué decir de Belén, César y Mari, quienes han sido mi pequeña familia en esa casa, gracias por vuestros consejos. Gracias a Blanca Ruiz y a María José Gil por prestarme su laboratorio en la Universidad de Alcalá de Henares, a Tomás Martín por su ayuda en ese laboratorio y a los tres por los cafés en el patio. Agradezco a Santos Ballesteros (técnico de la UAH) la ayuda prestada a un extraño a esa institución.

Gracias a todos los que, de alguna u otra manera, habéis colaborado en el trabajo de esta tesis doctoral (junto a los ya mencionados): Fernando Díez-Martín, David Uribelarrea, José Yravedra, Marine Pasturel, Nicolas Barbarin, Luc-Beaufort, Alice Novello, Jean Charles-Mazur… Agradezco, también, la labor de los evaluadores y miembros del tribunal que juzgan esta tesis.

Aixoises, ¡qué momentos! Lo mejor que me llevo de esta tesis es un puñado de amigos y amigas, ¡la familia que hizo de Aix mi segunda casa!: Anita, Meritxell, Fatiha, Olivier Dahan, Vladi, Ghislain, Gaby, Fabrice, Greg, Barbara, Yolaina, Olivier, Paco, Elena… (el orden es aleatorio, no os pongáis celosos). Cito aparte a Adelia y Dave,

porque aparte de brindarme su amistad, he de agradecer su inestimable ayuda con la corrección del inglés de esta tesis. Nos volveremos a juntar muy pronto en el Hublot (gracias también a la "fauna" que allí habitamos y a Fethi por tolerarnos). Je vous aime! Je ne sais pas pourquoi, mais je vous aime!

A los de aquí (o que aquí viven)… Diego, gracias por todo, piso, amistad y gin-tonics intempestivos. Gracias Pablo y Ana Belén por los cafés en la complu y la charleta sobre las penas del doctorando, a Edgar y Rubén por las cervezas por tierra de gatos buscando tascas. Leoneses, cántabros, burgaleses, pucelanos, etc… los de siempre, ya sabéis quienes sois y sois tanto… colegio, instituto, los de la universidad (gracias Félix y Carmen por guiarme en los primeros pasos que di en la ciencia y a Estrella y Alicia por compartirlos). Son muchos años que forjaron mi carácter, por los bares compartidos, por los campings, por las lluvias, el teatro, los jueves santos, por el fútbol (¡aúpa Sporting de Pinilla!), por las tardes perdidas en vuestras casas (o no, según se mire)…

A Ruth por todo.

Y a mi familia, claro, por su cariño y ayuda. Sin vosotros esto hubiera sido imposible.

Resumen

Esta tesis doctoral presenta los resultados de una serie de análisis multidisciplinares que tienen como objeto los microfósiles de plantas. Los objetivos de la tesis fueron mejorar las identificaciones gránulos de almidón mediante el uso de un sistema automatizado, evaluar las muestras modernas como método de inferencia a través del estudio de fitolitos de suelos y plantas relacionadas con áreas húmedas en África, y la reconstrucción del paleoambiente/paleopaisaje de dos yacimientos de la garganta de Olduvai para analizar su influencia en el comportamiento de los homínidos.

Para mejorar la identificación de gránulos de almidón se utilizó un sistema de análisis de imagen que midió 123 caracteres ópticos y morfológicos de aproximadamente 5000 gránulos de 20 especies de plantas comestibles del este de África. Los datos obtenidos se analizaron mediante un sistema estadístico de aprendizaje automático (Random Forest). Los resultados muestran que, a pesar de que el sistema desarrollado no es perfecto, es más eficaz que las identificaciones *de visu,* cuyo acierto medio fue del 25% frente al 53% del sistema automatizado. Se observó que el sistema es sensible al número de especies analizadas y, en un menor grado, al número de caracteres utilizados, por lo que consideramos que reducir las potenciales especies a identificar es crucial para obtener identificaciones precisas y para ello es necesario combinar diversos análisis. De no ser así la identificación automática de gránulos de almidón no será lo suficientemente precisa para ser utilizada en arqueología.

Para mejorar el conocimiento de los conjuntos de fitolitos que permitan obtener inferencias precisas de las muestras fósiles se analizaron los fitolitos de 22 suelos modernos provenientes del entorno de Olduvai y de 14 especies relacionadas con ambientes húmedos. Los resultados del análisis de suelos muestran que los fitolitos reflejan, parcialmente, la estructura vegetación, pero no el tipo de vegetación que los produjo y que las diferencias entre diferentes tipos de formaciones son sutiles. Sin embargo, se observó que dichas diferencias son apreciables cuando se aplican herramientas estadísticas. Los resultados muestran que los fitolitos reflejan mejor que el polen la estructura de la vegetación, pero, como era esperable, el polen traza mejor la

diversidad de especies. El estudio preliminar de 14 especies relacionadas con los ambientes húmedos mostró que los helechos (Pteridophyta) producen fitolitos capaces de marcar su presencia de manera inequívoca en el ambiente. Por otro lado, las otras especies no mostraron fitolitos característicos que permitiesen mejorar la identificación de alguna de las especies analizadas.

El análisis de fitolitos de 27 trincheras del paleopaisaje que incluye los yacimientos del "complejo Zinj" (FLK Zinj, AMK, PTK y DS) reveló una gran área cubierta por vegetación boscosa en los tiempos de deposición de la toba IC (1,832 millones de años). La presencia de palmeras en el área viene a refutar hipótesis previas que sugerían la presencia del cauce de un río de a 50-200 metros al sureste de FLK Zinj. La aparición de fitolitos de helechos indica presencia de hábitats sombríos y húmedos, lo que sugiere presencia de agua dulce (ríos o surgencias) que pudo atraer a homínidos y otros animales. La disponibilidad de agua dulce y los restos animales y útiles líticos encontrados en los yacimientos llevan a pensar que los homínidos no sólo usaron estos lugares como refugio, si no como áreas de procesado de restos animales y otras actividades vinculadas con un modelo de forrajeo central.

El análisis de los fitolitos de 24 muestras del yacimiento BK, muestreados en sentido vertical al de la estratigrafía, permitieron reconstruir la evolución de la paleovegetación que acompañó a la evolución de un sistema fluvial. Los resultados muestran una vegetación que encaja bien con la dinámica fluvial que formó BK. En las zonas donde aparece la vegetación esta estaba dominada por plantas leñosas y se mantuvo estable durante todo el marco de tiempo analizado. Por otro lado, la presencia de muestras estériles coincide con los lugares y momentos donde los suelos se renovaban continuamente debido al arrastre fluvial.

El análisis de fitolitos de 42 útiles líticos del yacimiento FLK West, junto con los paleosuelos que sirvieron de control, mostró que algunas de las piezas recuperadas pudieron ser utilizadas para procesar palmeras y tejidos duros de dicotiledóneas. Los análisis de gránulos almidón efectuados en esas mismas piezas no produjeron resultados concluyentes. Un análisis de arqueología experimental demostró que la distribución de

los fitolitos no se ve afectada por el azar durante la deposición de las piezas líticas o por el manejo de las mismas en el laboratorio.

En conclusión, los resultados de esta tesis muestran que el análisis de microfósiles de plantas ofrece datos útiles en la investigación arqueológica-antropológica capaces de ayudar a desentrañar cuestiones que no pueden ser resueltas mediante otros enfoques. Por otro lado, su uso debe ir acompañado de un desarrollo de estas herramientas para ofrecer resultados que lleven a interpretaciones más precisas.

Abstract

This thesis presents a series of multidisciplinary analysis using plant microfossils. The objectives of this thesis are to improve the identification of starch granules through the use of an automated system, to evaluate modern analogues as an inference method through the study of modern phytolith assemblages and the study of phytoliths from humid areas in Africa, to reconstruct the paleoenvironment/paleolandscape of two Olduvai sites and to analyze the influence of paleovegetation on hominid behavior.

In order to improve the identification of starch granules, an image analysis program was used- a program capable of measuring up to 123 different optical and morphological characters in ~5000 starch granules of 20 different East African edible plant species. The data obtained were analyzed using a machine learning approach (Random Forest). The results show that this automated system is not perfect, but that it is still more powerful than the human eye, for which the average success rate is just 25% for species level identifications, as opposed to 53% for the automated system. In evaluating the performance of the system, I found that accuracy rates in the identification of starch granules are highly sensitive to the number of species being identified and, to a lesser extent, to the number of characters used by the identification system. It is therefore crucial to narrow down as much as possible the number of target species by analyzing additional proxies. If this is not done, the automated identification of starch granules will not be accurate enough to provide acceptable interpretations in archaeological contexts.

In order to increase our knowledge of phytolith assemblages and to obtain accurate inferences from fossil samples, the phytolith assemblages of 22 modern soils and 14 species related to groundwater discharge areas from the Olduvai surroundings were analyzed. The results show that phytolith assemblages can partially reflect the general structure of the environment but do not accurately reflect the vegetation that produced them. There is a subtle variation between the different types of vegetation. However, these subtle differences can be handled and observed when statistical tools are applied. Compared to other microremains, phytoliths are better tracers of the main structure of vegetation than pollen grains, but, as expected, pollen grains trace species diversity better than phytoliths. The preliminary study of 14 species related to groundwater discharge areas showed that only fern species produce phytolith morphologies that unequivocally signal the presence of ferns in the environment. The other species analyzed for phytolith content did not improve on previous knowledge of the phytolith produced by these species.

The phytolith content of 27 trenches of the "Zinj complex" paleolandscape (FLK Zinj, AMK, PTK and DS sites), revealed a large area whose paleovegetation was dominated by forest at Tuff IC deposition times (1.832 Ma). The presence of palm phytoliths in the area refutes previous hypotheses which supposed the presence of a river channel 50 to 200 m southeast of the FLK Zinj site. The presence of ferns in the assemblages suggests shaded and humid habitats, which in turn would suggest the presence of freshwater (rivers or springs) that might have attracted hominids and other animals. The availability of freshwater and the faunal and lithic remains recovered in the sites might suggest a behavioral model for these sites in which hominins used the site not only as a refuge, but also to process animal carcasses and to carry out other activities related to central place foraging.

The analysis of phytolith content of 24 paleosol samples from the BK site, collected along the vertical sequence, made it possible to study the changes in paleovegetation that accompanied the evolution of a riverine system. The vegetation found corresponds well to the fluvial dynamic that formed BK. In the areas in which it appears, the vegetation was clearly dominated by woody plants and it did not change

significantly in the period of time under scrutiny. What is more, the presence of sterile samples was detected in areas where the fluvial traction changed the soils frequently.

The analysis of phytolith remains of 42 FLK West stone tools and paleosols (as control samples) showed that some of the lithic tools recovered could have been used to process palms and dicotyledonous hard tissues. The analysis of starch granule remains found in the same tools, did not provide conclusive results. It is worth noting that an experimental archaeological test demonstrated that deposition processes and laboratory procedures do not create artificial differences between soils and tools with regard to their phytolith assemblages.

In conclusion, the results of this thesis establish that the analysis of plant microfossils provides valuable data for archaeological-anthropological research purposes. Such data can help to clarify issues that cannot be satisfactorily resolved using other approaches. However, the use of plant microfossils must be accompanied by the further refinement of these tools in order to provide results that give more accurate interpretations of the data obtained from fossil samples.

Index

Figure list

Table list

Appendix list

1. Introduction

1.1 General context

The East African Rift Valley can be considered as one of the most important areas to understand hominin evolution. A large number of hominin fossils have been discovered throughout South to North East Africa. In Tanzania, three main sites document hominin evolution over the past 4 million years (Ma): Olduvai Gorge, Laetoli and Peninj. The sites are located in the Ngorongoro Crater Highland Area (**Figure 1.1**). Laetoli is located on the Eyasi plateau and is well-known for the preserved footprints attributed to *Australopithecus afarensis* (Leakey and Hay, 1982) and dated 3.8-3.6 Ma (Deino, 2011). Peninj is situated on the northwestern side of Lake Natron. It has provided one remain of *Paranthropus boisei* dated 1.5 Ma and stone tool artifacts (Domínguez- Rodrigo, 2001; Domínguez- Rodrigo et al., 2009; Isaacs, 1965; Isaacs and Curtis, 1974; Leakey and Leakey, 1964). Olduvai Gorge, which includes many archaeological and paleontological sites dated 2-0.1 Ma, is situated in the eastern foothills of the Ngorongoro volcano. At fossil deposition times around 2 Ma, the area was a basin with a shallow saline/alkaline lake and the Ngorongoro volcano crater was approximately at 4000 m above the sea level in height (Hay, 1976) (**Figure 1.2**). Olduvai Gorge is a major paleoanthropological site considered a cradle of mankind, because it has preserved several species of early humans and abundant artifacts (**Figure 1.3**). At Olduvai Gorge three early hominin species were discovered: *P. boisei* (Leakey, 1959) that occupied the area from 1.9 to 1.3 Ma approx. (Domínguez-Rodrigo et al., 2013); *Homo habilis* (Leakey et al., 1964) that occupied the area from 1.9 to 1.6 Ma approx.; and *H. ergaster/erectus* (Leakey, 1961) whose occurrence at Olduvai is dated ca. 1.2 Ma. Recently, however, new discoveries by the TOPPP team (The Olduvai Paleonthropology and Paleoecology Project) suggest that the earliest occurrence of *H. ergaster/erectus* at Olduvai is likely to be as early as 2 Ma (Domínguez-Rodrigo et al., 2015, and Domínguez-Rodrigo, *pers. comm.*). The Ndutu sedimentary beds on the top of the sedimentary beds at Olduvai have even provided remains of *H. sapiens*. Hence, the sedimentary beds of Olduvai Gorge reveals almost two million years of human evolution.

Olduvai also provides artifacts (stone tools) to trace cultural changes since 2 Ma. These artifacts show the evolution of tool technology from the most basic Oldowan to the elaborate Acheulean (Diez-Martín et al., 2015; Domínguez- Rodrigo, 2001; M. Domínguez-Rodrigo et al., 2014c; Leakey, 1971).

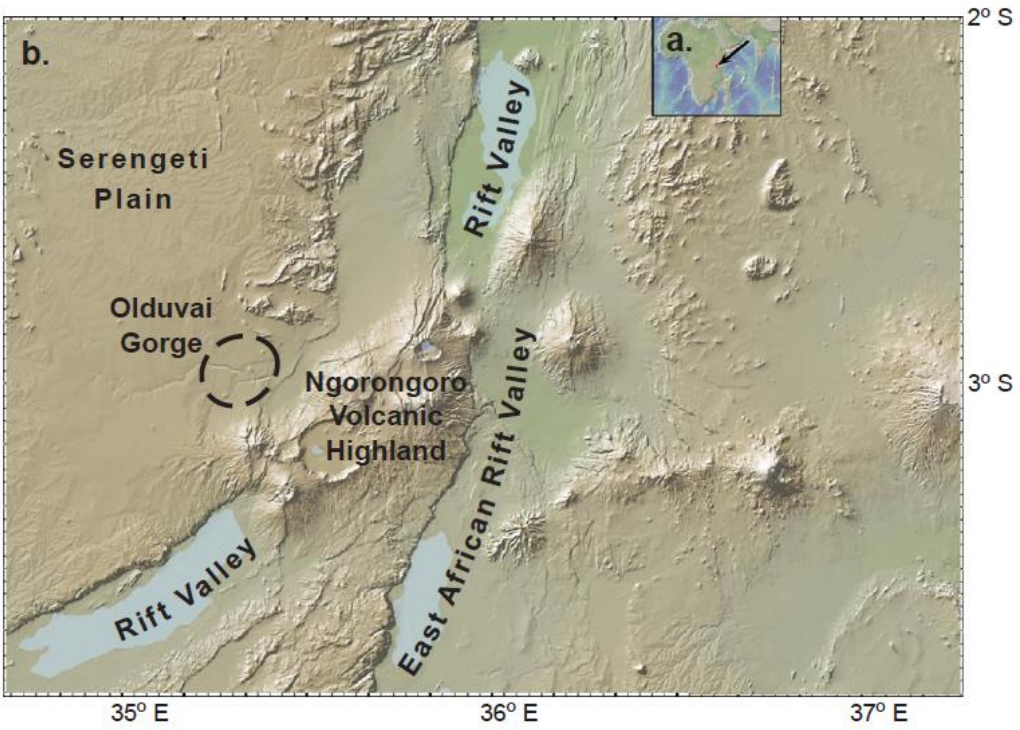

Figure 1.1. Map showing the location of the Olduvai Gorge. **a.** position in Africa. **b.** position in the Ngorongoro area. (Ashley et al., 2014)

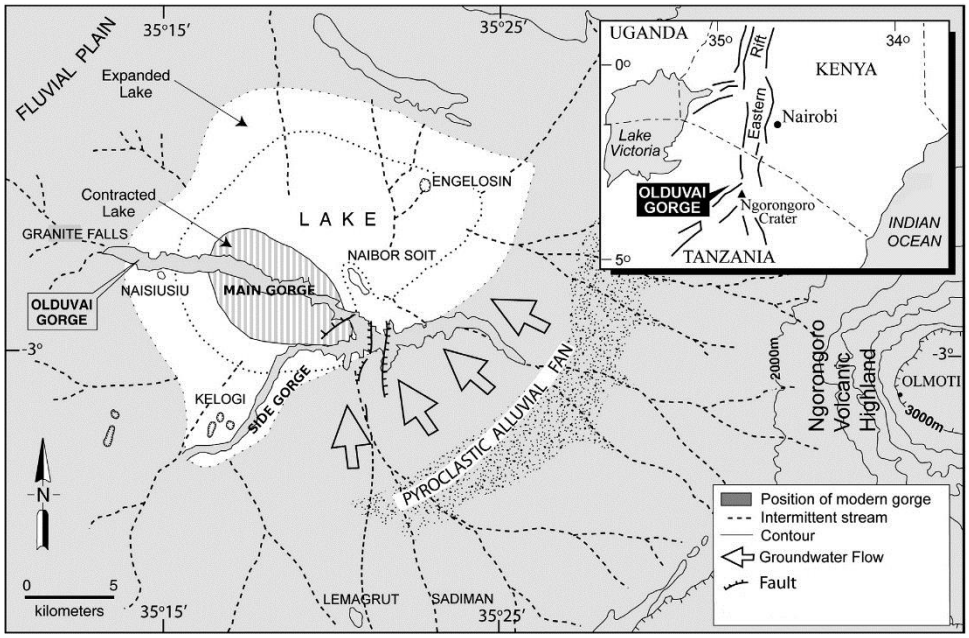

Figure 1.2. Paleogeographic reconstruction of Olduvai Gorge at Bed I time shows location of the Ngorongoro Volcanic Highland, the pyroclastic alluvial fan and the surface of the contracted an expanded paleolake. Modified from Ashley et al. (2010).

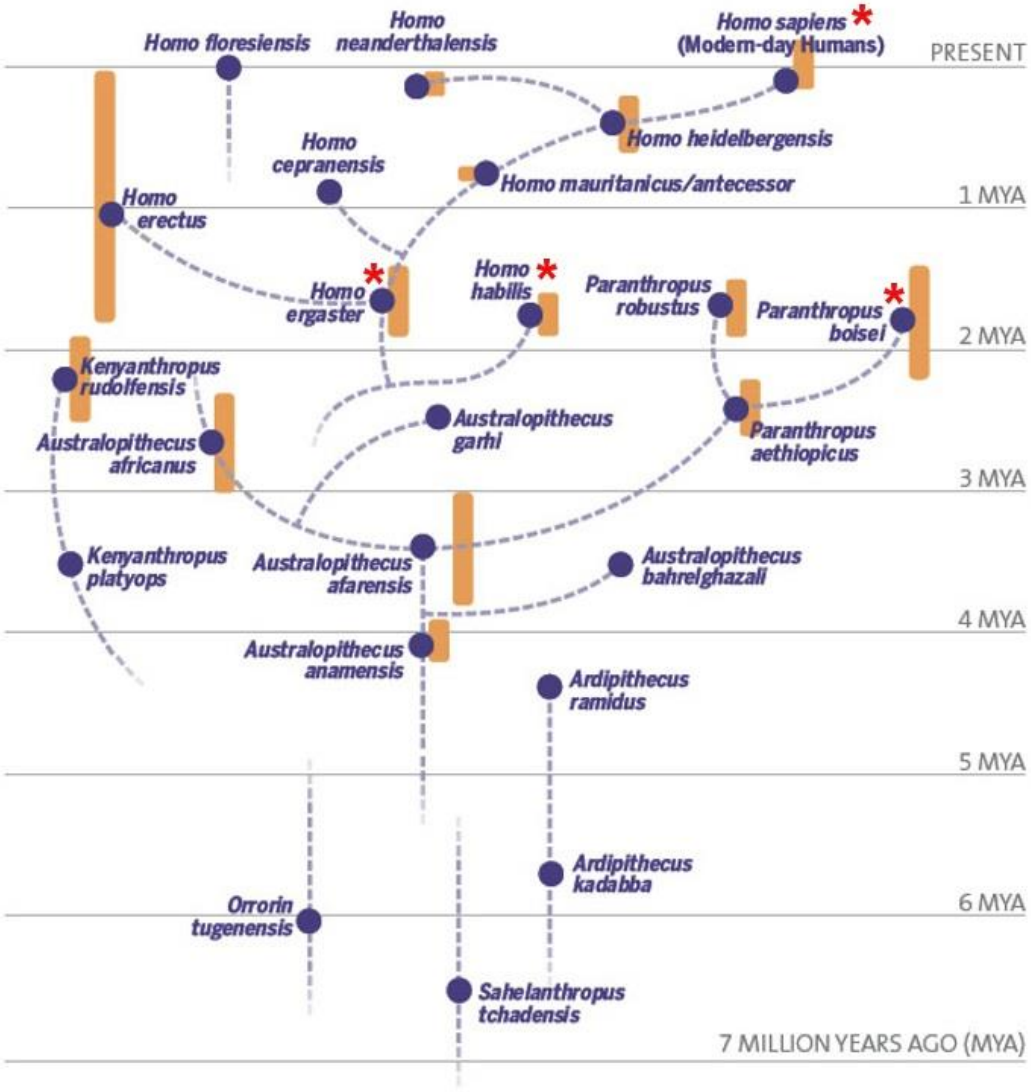

Figure 1.3. Evolutionary tree of hominins. Asterisks denote the species recovered from Olduvai Gorge (American Museum of Natural History, 2015).

If human remains are the basis for evolutionary studies, it is however, mandatory to frame the evolution in context, that is, to identify the various elements that were part of the ecosystem, and that may have contributed to influence hominin evolution since 4 Ma. Hominin evolution was likely triggered by interrelated factors, e.g., environmental-climate changes (Barboni, 2014; Maslin and Christensen, 2007; Potts, 2013; Reed, 1997; Shultz and Maslin, 2013; Thomas and Burrough, 2012; Trauth et al., 2007) and the interaction of hominins with other fauna (Domínguez-Rodrigo et al., 2014b; Plummer and Bishop, 1994). Two aspects of the environment, namely climate and vegetation, may

have played a significant role in early hominin evolution. Indeed, the thermal tolerance of every organism is determined by climate. Hence, climatic changes could have triggered migrations and adaptations (e.g., Maslin et al., 2014; Maslin and Christensen, 2007; Shultz and Maslin, 2013; Trauth et al., 2007). Climate also determines vegetation (e.g., Bonnefille, 2010; Maley, 1996), and therefore, the availability of resources (Magill et al., 2016). Vegetation may also provide refuge. Hence, it is crucial to consider vegetation and climate as determinant factors to explain early hominin evolution. Yet, to date, paleoclimatic and paleovegetation reconstructions at hominin sites are still rare (e.g., Cerling, 2010; Cerling et al., 2011; WoldeGabriel et al., 2009).

Other environmental factors such as the presence and distribution of prey and predators, may have triggered particular hominin behaviors (e.g., migration, hunting, search for refuge, etc.). Very large amounts of faunal remains, such as those found at Olduvai sites indicate interactions of hominins and fauna (Andrews, 1983; Domínguez-Rodrigo et al., 2014a, 2014b). Some bones were clearly cut-marked revealing hominin butchering and carcass-processing activities. The taphonomical studies of these faunal remains have triggered serious controversy. Sites interpretations and inferred human behavior (e.g., their role in carcass processing and sharing) fueled what Domínguez-Rodrigo et al. (2007) called the "home base" debate (e.g., Blumenschine, 1991; Bunn and Kroll, 1986; Domínguez-Rodrigo, 1999; Domínguez-Rodrigo et al., 2007; Leakey, 1971; Oliver, 1994; Rose and Marshall, 1996). The most lively debate was about the potential of early hominins to be scavengers or hunters (e.g., Blumenschine, 1995; Bunn, 1981; Domínguez- Rodrigo, 2002; Domínguez-Rodrigo et al., 2007; Domínguez-Rodrigo and Pickering, 2003; Egeland and Domínguez-Rodrigo, 2008). For the purposes of these studies on early hominid behavior, paleoenvironmental data can provide helpful, and crucial information, notably on the vegetation physiognomy which affects the distribution of animals and interactions among the fauna (including hominids).

Another factor that most likely affected early hominin behavior is how hominins used the technology to interact with the environment, and particularly for feeding purposes. In the early stages of human evolution, the technology (i.e., stone tools) provides insights into meat and plant consumption. Some questions have emerged from the artifacts and their presence/abundance at sites. At some sites, for example, the

accumulation of stone tools could not be related to meat acquisition because cut-marked bones were extremely rare (Bunn et al., 2010), but in others it is the contrary: stone tools are closely associated with modified faunal remains including many cut-marked bones (Diez-Martín et al., 2015). In the analysis of feeding patterns, the consumption of meat is attested by the increasing occurrence of cut-marked bones at early Pleistocene paleontological sites such as FLK Zinj at Olduvai, Tanzania (Bunn and Kroll, 1986; Domínguez-Rodrigo, 1997), Koobi Fora, Kenya (Bunn, 1981; Pobiner et al., 2008) and Kanjera South, Kenya (Ferraro et al., 2013) and there is increasing evidence that meat was probably an important part of hominin diet as early as 2.5 million years ago (Domínguez-Rodrigo et al., 2005, 2012). The study of stone tools can play a prominent role in understanding how these dietary and metabolic changes may have occurred. Evidence for plant consumption by early hominins, however, is rare. Despite the fact that hominoid paleodiet was essentially based on plants (DeMiguel et al., 2014), few studies have traced down the use of plants by early hominins (Wynn et al., 2013). Battering activities seem predominant at several Olduvai Bed I sites (e.g., Diez-Martin et al., 2010), and they are either marginally related or non-functionally related to carcass processing (Domínguez-Rodrigo et al., 2007). For instance, at the FLK North (FLK N) site, Olduvai Gorge (Tanzania), the accumulation of stone tools could not be related to meat acquisition because cut-marked bones were extremely rare (Bunn et al., 2010). Instead, it is suggested that hominins were attracted to the area by fresh water springs (Ashley et al., 2010a) and associated vegetation (Barboni et al., 2010). The dominance of battering activities inferred from the stone tool set (Diez-Martin et al., 2010) suggest that plants, rather than meat were search for at FLK N. To date, few studies have proved useful in directly relating stone tool use by early hominins to the consumption and/or processing of plants, except at sites where phytoliths (silica particles) or starch granules were found preserved. Phytoliths were discovered in the 1.5-1.3 Ma Acheulean assemblage of PEES2 (Peninj, Tanzania), and they indicate wood-working activities (Domínguez- Rodrigo, 2001). No attempt has been made at finding microfossils on early Oldowan tools which could reinforce inferences drawn from the use-wear patterns reported. Micro-residue analyses could potentially contribute to unraveling the functionality of such battering stone tool assemblages. In this regard, the study of paleovegetation can provide some ideas about what type of plants were available and if they were food resources, which, in

turn, can help to explain the associations between stone tools and bones. However, botanical remains that can help document plant resources require further study at Olduvai.

The analysis of the paleoenvironment will help researchers to understand the interactions of hominins with fauna and with their environment, hence, making it possible to frame their evolutionary process. In Olduvai Gorge paleoenvironment studies were first carried out, from a geoarchaeological point of view, by Hay, (1976) who described the saline and shallow paleolake of Olduvai and established the basic stratigraphy of Olduvai Gorge based on the volcanic tuffs produced by the Ngorongoro volcano eruptions. Hay (1976), based on previous work of Reck (1951), subdivided the Olduvai stratigraphy into seven units called beds, that are, from oldest to youngest: Bed I, Bed II, Bed III, Bed IV, Masek Beds, Ndutu Beds and Naisiusiu Beds (**Figure 1.4**). Hay (1976) also identified marker tuffs, some of which could be dated (e.g., Deino, 2012). Ashley (2007) has focused on the carbonate levels, the lake level cycles (that affected spatial variations of vegetation), and paleosols. More recently, Uribelarrea et al. (2014) have made advances in documenting with precision the paleoenvironment at specific sites. From the biological point of view, Bonnefille (1984), Bonnefille et al. (1982) and Bonnefille and Riollet (1980) were the first to document paleovegetation through the study of the pollen record. This record suggests a paleoenvironment dominated by herbaceous species (Poaceae and Cyperaceae) throughout Bed I and Bed II, from 1.85 to 1.5 Ma approx. During Bed I time, herbaceous components were likely and relatively more abundant than today and the paleoenvironment was described as a paleolake surrounded by grasslands, less rich in sedges than today. Afromontane forests (two or three times closer to the Gorge than today) were present in the highlands. During Bed II time (1.8-1.5 Ma) Poaceae are also abundant and the vegetation is similar to Bed I except one site rich in pollen from the halophyte *Suaeda*. At 1.8 Ma, a rich diversity of pollen was described. *Acacia* pollen is abundant suggesting a wooded savannah (Bonnefille and Riollet, 1980) environment or a spring forest (Barboni et al., 2010). There is also presence of *Typha* pollen (Bonnefille and Riollet, 1980) which attests of the presence of freshwater marshes (Barboni et al., 2010). Recent analyses of ^{13}C on leaf wax from lacustrine sediments of paleolake Olduvai provided paleoprecipitations varying between 250 and 700 m during Bed I time, similar to present time (Magill et al., 2013a).

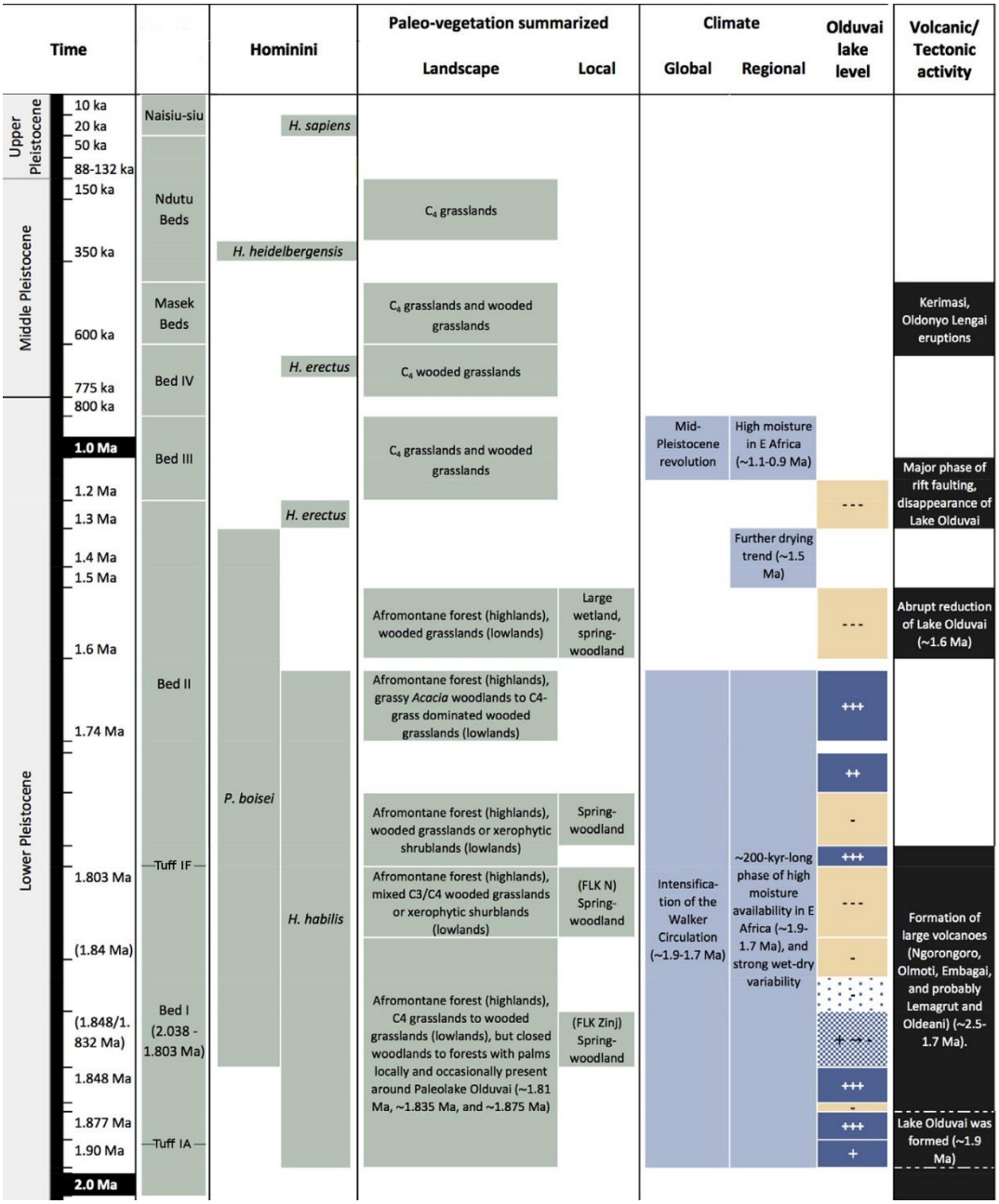

Figure 1.4. Summary of stratigraphy, hominin record, paleovegetation, climate, lake level and volcanic activity in the Olduvai Gorge. As example, tuffs framing Bed I are shown. Modified from Barboni (2014).

Other markers were analyzed to reconstruct paleoenvironment at site scale. Phytoliths have provided botanical evidence for spring associated to woodlands (Gail M. Ashley et al., 2010a, 2010b; Barboni et al., 2010) and open woodlands where trees were not abundant and vegetation was dominated by monocots and herbaceous dicots (Albert et al., 2006; Bamford et al., 2008, 2006) at about 1.8 Ma. Also macroplant remains have been found at some Olduvai sites, especially rhizomes, roots and silicified woody plant stems or branches (Bamford, 2012a; Blumenschine et al., 2012). Carbon and oxygen isotopic studies on paleosoil carbonates have also been used to document paleovegetation and climate changes at Olduvai. Isotopic ratios have been interpreted in a way that reveals major climate changes at 1.67 Ma, 1.3 Ma and 0.6 Ma within an overall drift toward aridity (Cerling and Hay, 1986) but the sampling of this study could be biased because of the mixing of ages and localities in sampling. The fluctuations between wet and dry conditions between 2 Ma and 1.8 Ma were also proved by (Sikes and Ashley, 2007). Also, a more recent study based on the hydrogen isotopic composition of lipid biomarkers has been applied to lake sediments from the center of the paleolake between 2 to 1.8 Ma (Magill et al., 2013a, 2013b) suggesting a variability in precipitations ranging between 200 mm, during arid intervals, and 700 mm, during wetter ones.

The origin of some local paleovegetation variations (e.g., the spring forests) is based on several factors, among them, the most important are the variations in Olduvai paleolake spatial extension. These variations affected depositional environments and paleosol formations (Ashley et al., 2014). Combining sedimentary record studies (Ashley et al., 2009; Liutkus and Ashley, 2003) with palynological records (Bonnefille, 1984, 1979; Bonnefille and Riollet, 1980), isotopic analysis (e.g., Cerling and Hay, 1986; Magill et al., 2013a, 2013b), phytolith analysis (e.g., Albert et al., 2009, 2006; Ashley et al., 2010a; 2010b; Barboni et al., 2010) and macroremains (e.g., Albert and Bamford, 2012; Bamford, 2005; Bamford et al., 2008, 2006), Barboni (2014) summarized the paleovegetation changes in relation to lake level changes (**Figure 1.4**). The periods when the paleolake level was low, vegetation was characterized by xerophytes and halophytes associated to lake margins (e.g., *Suaeda*, Chenopodiaceae, Amaranthaceae, Portulacaceae), and arboreal species characteristic of the Zambezian and Somali-Masai regional centers of endemism (e.g. *Dombeya*, *Syzygium*, *Acacia*). During periods of high lake level, Poaceae and Afromontane taxa are found in higher proportions (±70% and

±15%, respectively) than during low paleolake levels (±40% and <2%, respectively), suggesting that paleoprecipitation increased in the Highlands mainly, without reaching the necessary threshold to trigger large changes in the regional vegetation.

In this regard, according to the variations in vegetation that affected the landscape where hominin developed, reconstructing, in detail, the paleoenvironment at Olduvai may give crucial information about the site structure and, therefore, about hunting, scavenging, living, or gathering particular plant resource by early humans.

1.2 Current research and thesis objectives

Currently, the TOPPP team studies about ten sites in Olduvai Gorge. For this thesis, I analyzed remains from three sites for which the study of paleoenvironment (FLK Zinj/PTK/AMK/DS and BK) and stone tools (FLK-West) is particularly important to understand the relationship of hominins to their environment and to establish behavioral hypotheses. Two types of microbotanical remains have been used for these purposes: phytoliths and starch granules. Phytoliths have been chosen because they are better preserved in sediments than other microbotanical remains such as pollen grains, and because of their low potential for dispersal in the environment, i.e., they allow more spatial resolution in paleovegetation reconstructions. Starch granules have been chosen because they are produced in plant organs that act like energy stores: tubers, roots, fruit, seeds, etc. In this sense, the relation between energy storage and food purposes can be used to trace the connection between plants and tools and their influence on hominin behavior.

1.2.1. Phytoliths

Phytoliths are silica particles produced by vascular plants with a wide variety of functions: e.g., defense against herbivorism or resistance to drought stress (Cooke and Leishman, 2011)**.** Phytoliths are the result of the precipitation of silicic acid as opal in intra- and extracellular spaces. Due to the great variety of places where phytoliths are formed, shape variability of these silica bodies is also large. Phytolith shapes can reflect the shape of the cells within which they were formed (e.g., phytoliths from bulliform cells), or the shape of extracellular spaces (e.g., dendritic elongate phytoliths from grass epidermis) as well as more complex structures (e.g., stomata or tracheary elements) or just amorphous shapes that don't reflect any histological or cellular structure.

Phytoliths have been applied since the mid-20th century (Piperno 1988) on paleoenvironmental reconstruction in a wide variety of studies focusing on several geological periods: Late Devonian, Permian, Triassic (e.g., Carter, 1999), Cenozoic (e.g.,

Baker 1960, Jones, 1964, Jones 1996), Late Eocene (e.g., Meehan 1994; Stromberg 2000), Neogene (e.g., WoldeGabriel et al., 2009) Pleistocene (e.g., Barboni et al., 2010; Blumenschine et al., 2012), Holocene (e.g., Pearsall et al., 2004b), etc. The phytolith contribution to paleoenvironmental reconstruction consists, primarily, in inferring the presence or abundance of some botanical groups or plant taxa using the abundance of phytolith morphotypes in the sediment. Fossil phytolith assemblages are interpreted based on comparison with surface soil phytolith assemblages that sample the modern vegetation. Some studies just describe the phytolith assemblages associated with modern vegetation (e.g., Albert et al., 2015), while others have carried out calibration and developed indices to quantify paleoenvironmental changes using phytoliths as a vegetation or climate proxy (Alexandre et al., 1997; Bremond et al., 2008, 2005a, 2005b; Novello, 2012; Novello et al., 2012). The use of extensive, detailed analogs will enhance the reconstructions of the past. The use of adequate reference collections is necessary to allow accurate identifications. It must be noted that although Pteridophyta species are large phytoliths producers (Piperno, 2006) and are present in a wide variety of environments from the fossil record of Olduvai, ferns have just been reported once in wetlands from FLK at 1.84 Ma (Blumenschine et al., 2012). Pteridophytes are common in tropical Africa, usually in rocky, humid and forest environments (Fournier and Sasson, 1983; Kamau, 2012). Their presence is relevant in all types of Afromontane forests (Hemp, 2002; Wakjira, 2006) but specially in upper montane rainforest (>1830 m) where fern diversity is high (Roux, 2011; Schmitt et al., 2010). In this sense, this work presents the results of the study of several samples from modern soils from the Olduvai region, and areas adjacent to saline Lakes Eyasi and Manyara, and analyze the phytoliths from representative species of humid areas from these modern spring forest and woodlands. In archaeology, phytoliths can have a role revealing dietary behaviors of humans (Henry and Piperno, 2008) or early hominins such as *Australopithecus sediba* (Henry et al., 2012), but they could also be used to reveal stone tool use (e.g., Domínguez- Rodrigo, 2001; Lombard, 2004; Wadley et al., 2011; Mindzie et al., 2001). This work present the results of the analyses of phytoliths recovered from one Olduvai site (FLK West).

Experimental archaeology on stone tools is a useful approach to understand the processes affecting the tools due to their use. In this sense, most of research has been focused on use-wear analysis: e.g., the effects of woodworking on tools (Hardy and

Garufi, 1998; Kononenko et al., 2015) pre and postdepositional alterations (Bamford, 2012b) or blind tests to measure the quality of interpretations (Lemorini et al., 2014). Other approaches are based on physical properties and the carving of stone tools: e.g., the study of debitage and flakes of quartz tools (Driscoll, 2011; Vergès and Ollé, 2011). Even fire as a tool has been studied (Backhouse and Johnson, 2007; Stahlschmidt et al., 2015). Not many studies linking experimental archaeology and phytoliths have been carried out, e.g., polish formation in grinding patches in Australia (Fullagar and Wallis, 2012) or morphological changes in phytoliths due to grinding activities (Portillo and Albert, 2014). Several researches have addressed the mobility of phytoliths in soils. Phytolith transportation is relatively fast (4 cm/year) (Fishkis et al., 2010) and is determined by the size of phytoliths, the soil structure (Hart and Humphreys, 2004) or their dissolution level (Hart and Humphreys, 2003). Taphonomy of phytoliths has been more widely studied, with particular regard to their dissolution (Cabanes et al., 2011; Fraysse et al., 2006), their representativeness in the case of modern and fossil soils (Albert et al., 2006) or fire effects (Elbaum et al., 2003). This work present the result of an experimental archaeological test that will measure the strength of phytolith assemblages recovered from tools.

1.2.2 Starch granules

Starch is the most common energy storage system in plants. Starch is a large chain of glucose molecules joined by covalent bonds. These chains have two spacial conformations: amylose when glucose units are linked in a linear way with α(1→4) glycosidic bonds, and amylopectine when these chains are ramified combining α(1→4) and α(1→6) glycosidic bonds. Starch is accumulated by plants as starch granules that are produced in the amyloplasts by accumulation of layers of amylose and amylopectine that give granules their resistance and optical (birefringence) properties (Whistler and Daniel, 1984).

In Africa, to date, the oldest analysis of starch granules has been carried out in Middle Stone Age archaeological sites in the Niassa Rift in Mozambique (105,000-42,000 years ago). It suggests that the diet of modern humans in East Africa included seeds, fruits, underground storage organs of more than a dozen botanical families among

which Fabaceae, Arecaceae, and Poaceae were the most frequently consumed (Mercader, 2009; Mercader et al., 2008). In this thesis I will present the first results of the analyses of starch granules recovered from one Olduvai site (FLK West).

Previous studies have shown that starch granules could allow plant taxonomic identifications up to the species level (e.g., Torrence et al., 2004; Yang et al., 2009), so their analysis is useful for archaeological purposes. Starch granules, in addition, accumulate in different plant parts (e.g., fruits, seeds, roots). A direct inference of which plant and plant parts were consumed would offer supplementary information regarding hominin behavior. Starch granules exhibit some morphological variations, which may allow taxonomic discrimination among plant species (e.g., Reichert, 1913). These variations are related to the presence or absence of fissures and lamellae, the position of the hilum, surface features, shape, size, etc. In archaeology, starch granules are identified by comparison with reference collections (Horrocks and Nunn, 2007; Mercader et al., 2008; Pearsall et al., 2004a; Yang et al., 2009). However, few studies on the taxonomic potential of starch granules have been backed up by statistical analyses, despite the fact that starch granules exhibit morphological variations within a given species and that a given morphology may be redundant among taxa. Torrence et al. (2004) carried out the first statistical study of starch granules. Other authors applied automated systems to identify starch granules but these methods are limited by their complexity, and feature extraction, or biased by a selection of granules or a limited number of samples to discriminate (Choy et al., 2009; Coster and Field, 2015; Fernández Pierna et al. 2005; Wilson et al., 2010). Also starch granule research is conditioned by modern contaminations in laboratories (Crowther et al., 2014), so one should be able to accurately identify large sources of starch granules to discard those coming from contaminations.

1.2.3 Thesis objectives

To summarize, and considering the foregoing, this thesis has the following objectives:

A. Evaluate modern analogues as an inference method through the study of modern phytolith assemblages and the study of phytoliths of humid areas. I analyzed the phytolith assemblages from modern soils samples from different wooded environments, particularly spring-associated forest and woodlands, occurring today in the Ngorongoro-Manyara-Eyasi region and Olduvai Gorge surroundings to measure the strength of phytolith signals to reveal ecological features. I also analyzed the phytoliths from representative species of humid areas from these modern spring forest and woodlands to increase our knowledge of the phytolith's morphological diversity.

B. To reconstruct the vegetation of two Olduvai sites and to analyze the influence of paleovegetation on human behavior. I analyzed two sites: BK, dated 1.353 Ma, a well-studied locality in a riparian context where no previous paleobotanical studies have been carried out, and the FLK Zinj complex dated 1.832 Ma, with a view to completing spatial analysis of these sites (Gail M. Ashley et al., 2010a, 2010b; Barboni et al., 2010; Blumenschine et al., 2012).

C. To enhance the identification of starch granules for edible East African species by the use of an automated system. I would like to present here a new system that automatically acquires morphometric data from starch granules in all shapes and orientations, and then identifies taxa using a Random Forest statistical classification.

D. To reveal patterns of stone tool usage, to analyze the influence of plant resources on human behavior. I analyzed the phytolith and starch signal from stone tools from FLK West site, dated 1.7 Ma, to discover if these lithics were used to process plant resources by studying. In addition, I carried out experimental archaeology to elucidate if the distribution of phytoliths may be affected by random phenomena during deposition of tools in soil or by extraction protocols. The results of this experiment are useful to evaluate if there is a bias in the deposition of phytoliths.

2. Study area

2.1 Geological context

The East African Rift System (EARS) is an active continental rift system that comprises two main branches that extend from the Afar triple junction (where joins with the Gulf of Aden and the Red Sea) to the Zambezi River (Baker and Wohlenberg, 1971). The Western Branch (2100 km) runs from Lake Albert (Uganda and Democratic Republic of the Congo) in the north, to Lake Nyasa (Tanzania and Mozambique) in the south. Easter Branch (2200 km) starts at the Afar triangle in the north, and comprises the main Ethiopian rift, the Omo-Turkana lows, the Kenyan rifts and ends in the North Tanzanian divergence in the south (Chorowicz, 2005) (**Figure 2.1**).

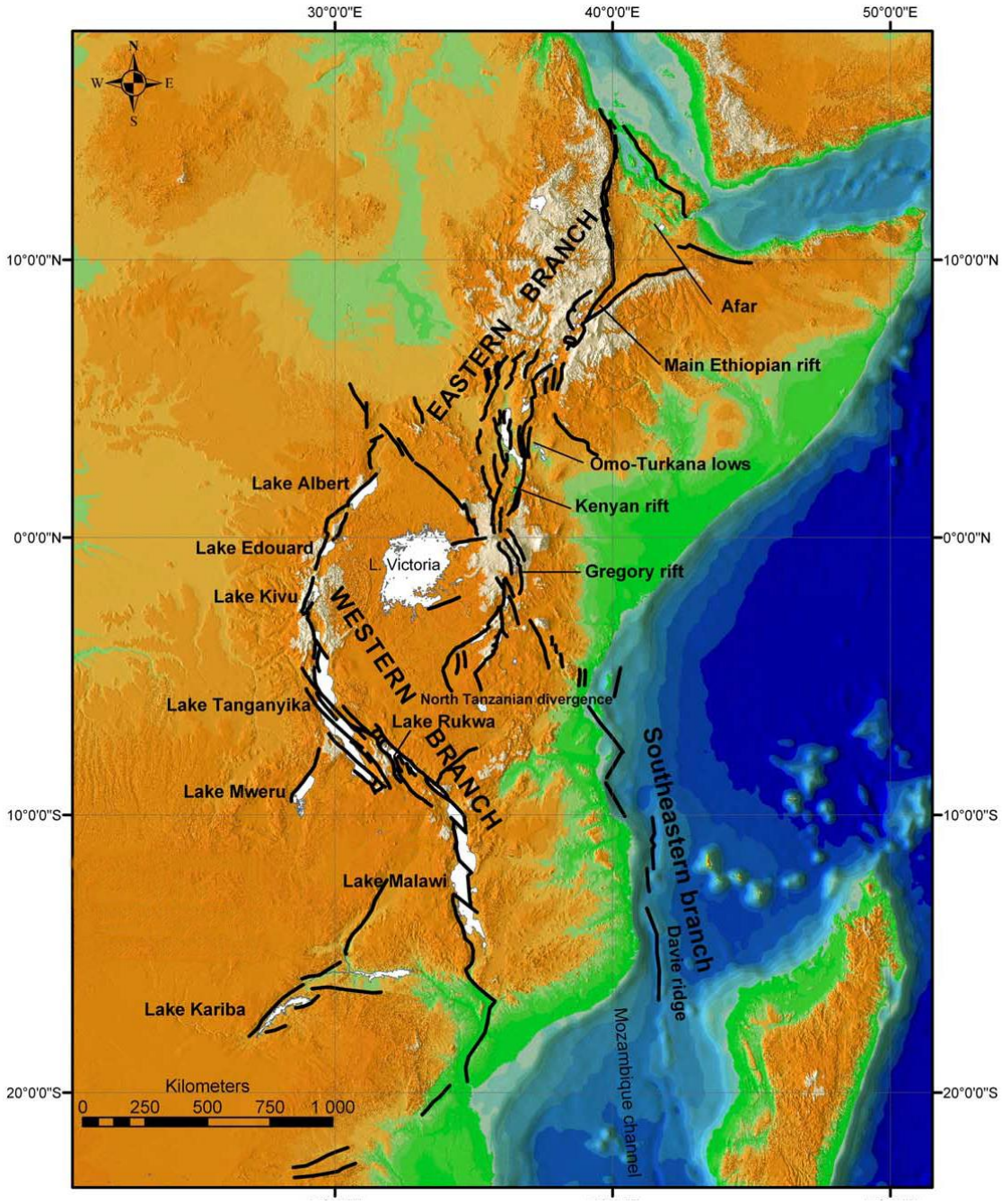

Figure 2.1. EARS map. Black lines: main faults; white surfaces: lakes; dark to light colours (low to high elevations). Modified from Chorowicz (2005).

Olduvai Gorge is located in the eastern part of EARS, in North Tanzania. Located at the south-eastern end of the Serengeti Plains, it is divided into two parts called Main and Side Gorge. The Main Gorge starts at lakes Masek and Ndutu and runs 46 km eastward to the Olbalbal depression which is located at the foot of the Ngorongoro volcano and Crater highlands. The Main Gorge deepens in rapids and falls (Granite Falls) at the western margin of Olduvai Basin. Prior to the Pleistocene, Olduvai Bassin was filled by a low but large lake, paleolake Olduvai, wich was saline/alkaline (Hay, 1976). During the Pleistocene, and due to tectonic activity of the EARS, Olduvai Basin started to tilt to the east, producing several deformations and faultings (Hay, 1976). The current gorge was created by the water erosion that drained from Ndutu Lake to the Olbalbal depression.

The eruptions of the Ngorongoro volcano produced ash flows and air fall tuffs (Mollel and Swisher, 2012) that formed several volcanic tuff layers that are used as chronological markers in the gorge today (Deino, 2012). These volcanic tuffs are the basis of the stratigraphy of the Olduvai deposits (**Figure 2.2**). Olduvai Gorge exposes a sedimentary sequence of one hundred meter thick deposited between 2 Ma to 0.2 Ma. Hay (1976) described the stratigraphy of Olduvai Gorge in seven units called "beds". The samples featured in the present work are from Beds I and II. Bed I is more than 60m thick in the eastern part of the Main Gorge. Sediments of Bed I are bracketed by Tuff IA dated 2.038 Ma and Tuff IF dated 1.803 Ma (Deino, 2012)**.** There are five main lithofacies in Bed I: lava flows, lake deposits, lake margin terrain, alluvial fan and alluvial plain. Bed I is split into two major subdivisions by the Bed I basaltic lavas: Upper and Lower Bed I (Hay, 1963). Ash tuffs from the Ngorongoro volcano eruptions are datable and are the basis on which to establish the chronology of the sediments. Six marker tuffs have been described in Bed I: IA in Lowermost Bed I and IB to IF in Uppermost Bed I (Hay, 1971). Bed II is 20-30 m thick. It overlies Bed I and is slightly larger. There are seven lithofacies in Bed II that represent six depositional environments: alluvial plain, lake, lake margin, aeolian and lake-stream complex. A broad disconformity divides Bed II into two major units: Lowermost and Uppermost Bed II (Peters and Blumenschine, 1995; Blumenschine and Peters, 1998). Lowermost Bed II includes sediments above tuff IF (dated 1.8 Ma) and below tuff IIA (dated 1.15 Ma). Uppermost Bed II includes sediments over tuff IIA to top of Bed II (tuffs IIB, IIC and IID are within Lowermost Bed II). This sequence combines

several types of sediments: fluviatile, lacustrine, wetland, pyroclastic and aeolian sediments (Foster et al., 1997; Hay, 1976). Olduvai hominin sites were placed along the lake margins deposits of a saline lake that fluctuated in level (3m) and extension (7 to 15 km) (Hay, 1976) (**Figure 1.2**). During the deposition of Bed I, Olduvai paleolake became shallow very likely due to increasing aridity and tectonic activity. During Bed II the lake was larger and dry periods increased its salinity (Hay and Kyser, 2001).

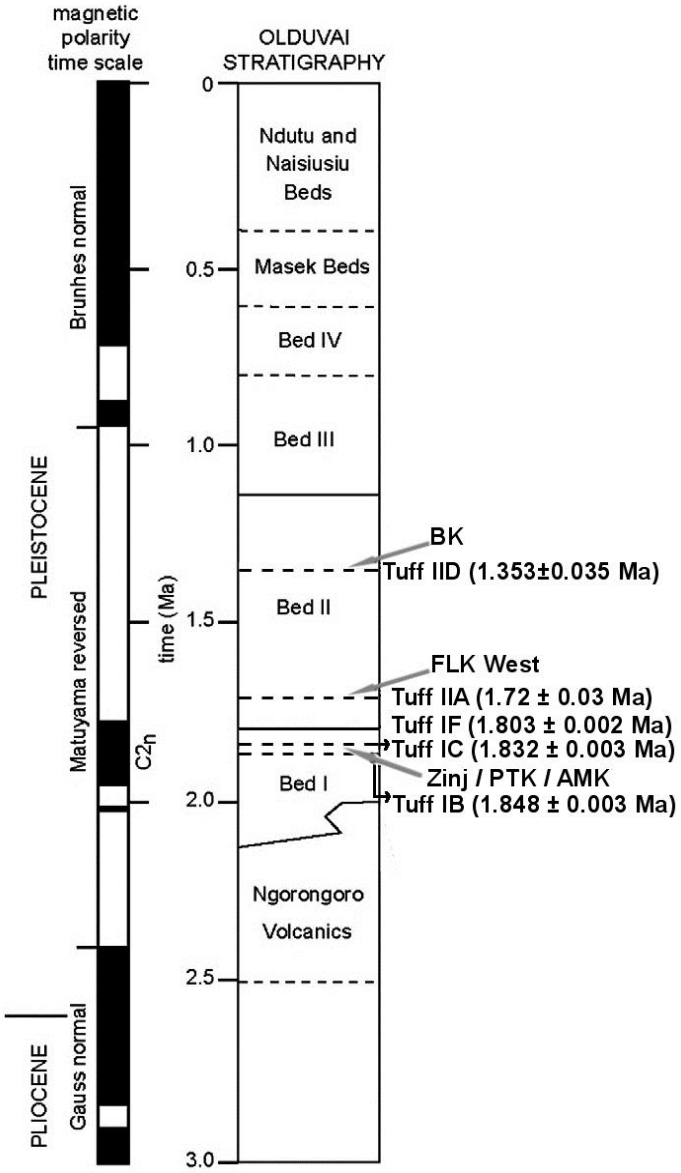

Figure 2.2. Simplified stratigraphy of Olduvai Gorge showing the Beds described by Hay (1976) and the tuffs related to the sites studied in the present work. Modified from Ashley et al. (2010)

2.2 Present-day climate and vegetation in the study area

The climate of East Africa is strongly influenced by the Indian Ocean and the Inter-Tropical Convergence Zone (ITCZ). The variations in the position of the ITCZ affects equatorial zones of the planet producing a bimodal rainfall regime (dry and wet season). In the study area, wet seasons occur between March-May and November-December. The steep relief of the area causes zonal variations in temperature and rainfall distribution. Because of this, precipitations range from 750-1250 mm/year in Crater Highlands, Serengeti Plains or Lakes Manyara and Eyasi to 250-500 mm/year around Lake Natron (Barboni, 2014). This rainfall distribution varies from year to year due to El Niño–southern oscillation (ENSO), which is the main cause of interannual climate variability in East Africa (Nicholson and Kim, 1997). On the other hand, despite the fairly high precipitation values in the area, the high levels of evaporation (Dagg et al., 1970; Nyenzi et al., 1981) limit the amount of water available, which explains the arid sub-desert region. These seasonal variations in the rainfall, but especially in evapotranspiration (which depends on temperature, humidity and wind), causes variations in the saline lake surfaces (e.g., lakes Manyara and Eyasi). From 2000 to 2011, Lake Manyara, for example, showed important surface variation, and almost dried up in 2005 and 2011 (Deus and Gloaguen, 2013).

The study area is located in the administrative Ngorongoro Conservation Area, which falls into the Somali-Masai regional center of endemism (White, 1983). The present-day vegetation represents the influence of climate, soil, topography (Anderson, 2008) and human managements of the environment (Holdo et al., 2009). The vegetation of the Ngorongoro can be classed as four vegetation areas influenced by climate and geomorphology (Herlocker and Dirschl, 1972): the Serengeti plains (Western plains), dominated by short and medium grasslands with a significant presence of both *Sporobolus* and *Digitaria* species; the escarpments, dominated by low woodlands (*Commiphora* sp. and *Acacia* sp.) and bushlands of *Lippia-Lantana-Solanum incanum* formation; the crater highlands where the Afromontane forests grow above 2500 m on the slopes, dominated by montane taxa (e.g., *Olea*, *Podocarpus*, *Hagenia*); and the

lowlands, with sparse grassland and bushland vegetation. The Olduvai Gorge area is located in the western plains, and the vegetation may be divided into three physiogeographic units (Herlocker and Dirschl, 1972). 1) In the western section of the gorge, the vegetation is characterized by low woodland of *Commiphora madagascarensis, Acacia mellifera* and *A.tortilis* as the arboreal dominant species. The shrub layer consists of the suculent *Sansevieria ehrenbergiana, Cissus quadrangularis* and *C. cactiformis*. The grass layer throughout the area is not continuous, and is dominated by *Sporobolus* spp. And other annual grasses. 2) In the eastern section of the gorge, the broken canyon walls cause a more heterogeneous vegetation, and low woodlands are usually more open than in the western section. The composition of the arboreal and bush layers is dominated by *Commiphora* and *Acacia* sp. but in the bush layer *Salvadora persica* appears as one of the characteristic species. Also some *Euphorbia* spp., *Cordia* spp., and *Justicia* spp. are present. 3) In the South fork tributary area, the vegetation is characterized by shrublands rich in *Sansevieria ehrenbergiana, Salvadora persica,* and *Cissus* spp. The presence of strips of low woodland is noticeable.

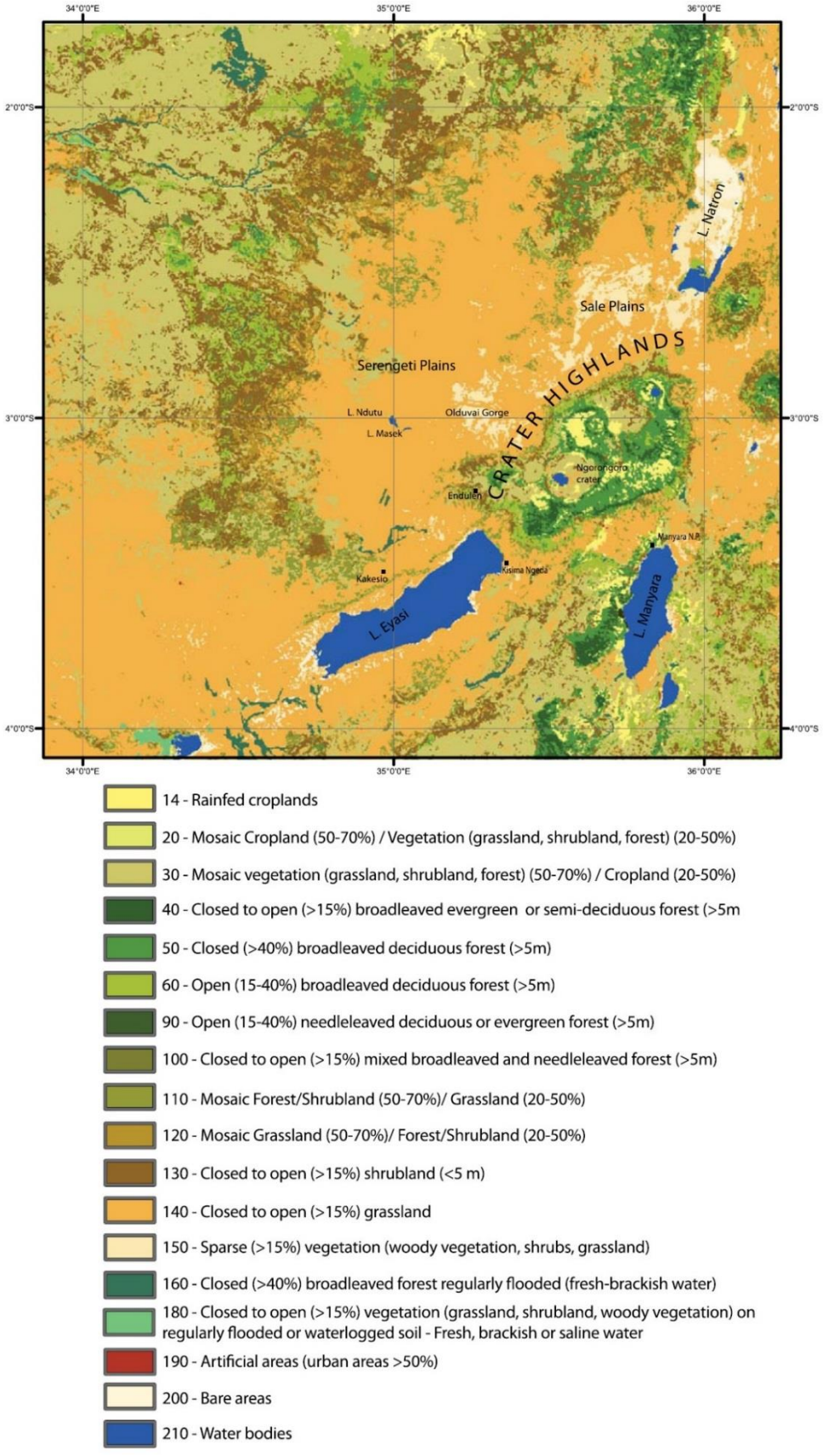

Figure 2.3. Detailed vegetation map for the Serengeti and Crater Highlands region. ESA/ESA Globcover Project, led by MEDIAS-France/POSTEL.

In addition to the vegetation patterns produced by climate and topography, the fluctuation of lake levels has an influence on the area, producing local variations associated with the lake margin and with the freshwater springs. In the past, the Olduvai environment was influenced by a shallow and saline lake whose fluctuations caused local variations in vegetation. Nowadays two shallow and saline lakes occur south of the Ngorongoro area and their fluctuations alternately expose mudflats. Grasslands are typical of these areas around and along the edge of the maximal extension of the lake and consist of halophyte *Sporobolus consimilis* with clumps of Cyperaceae (Herlocker and Dirschl, 1972). At Lake Mayara two communities have been described for these alkaline grasslands: *S. spicatus – Cynodon dactylon* and *S. spicatus – Cyperus laevigatus* (Loth and Prins, 1986). In the north end of the lake, *Typha angustifolia* is the dominant plant in the swamp herbage (Greenway and Vesey-Fitzgerald, 1969). In very localize areas, freshwater seeps out of geologic faults and allows for the development of a vegetation that is not the usually associated with such an arid zone as that of the study: wetlands dominated by *Typha* and sedges or spring forests. These groundwater forests are dense and composed of several species of evergreen tall trees, such as *Trichilia emetica, Ficus sycomorus*, *Tabernaemontana ventricosa*, *Rauvolfia caffra* and the palm *Phoenix reclinata.* When the influence of water diminishes these dense forests are replaced by woodlands or bushlands of *Acacia xanthophloea* and the palm *Hyphaene petersiana* where accompanying species are drought resistant (Greenway and Vesey-Fitzgerald, 1969; Loth and Prins, 1986).

2.3 The paleoanthropological and archaeological sites studied at Olduvai

More than 70 localities with faunal, hominin and archaeological remains have been described at Olduvai Gorge. Many sites occur in the main Gorge (Leakey, 1971). In this thesis I analyzed samples essentially from three sites: "Zinj complex" (FLK Zinj/PTK/AMK), FLK West, and BK (**Figures 2.2 and 2.4**).

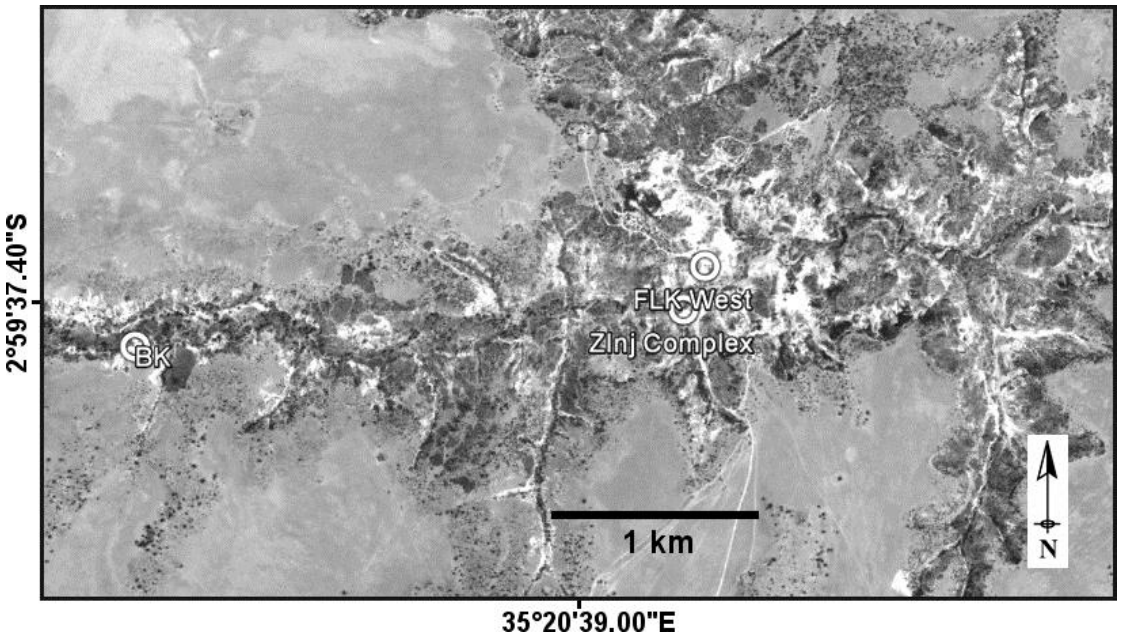

Figure 2.4. Approximate position of the sites studied in this thesis. "Zinj complex" includes FLK Zinj, PTK, AMK and DS sites.

2.3.1 FLK Zinj/PTK/AMK/DS sites ("Zinj complex")

FLK level 22 is more commonly known as FLK Zinj due to the the discovery of the holotype of *Paranthropus* (=*Zinjanthropus*) *boisei* (Leakey, 1959). FLK level 22 is located to the North of the area that comprises FLK sites (**Figure 2.5**). The main sequence of FLK Zinj is located in Bed I between Tuffs IB and IC (**Figure 2.6**), which are easily recognizable and can be traced from the FLK Zinj site, down south to PTK, AMK and even to the west near the KK fault (Uribelarrea et al., 2014) (**Figure 2.5**). Tuff IB is an ash-fall tuff dated 1.848 ± 0.003 Ma (Deino, 2012). Between IB and Tuff IC there is a clayey tuff/tuffaceous clay formed primarily of clay and a variable proportion of ashes, silt, and fine sand. Above this clayey tuff/tuffaceous clay, there is a laminated and reworked tuff called Chapati Tuff (CHT). Above CHT, up to Tuff IC is the Zinj clay that corresponds to the archaeological level 22 at FLK Zinj or level 1 at FLKNN (Uribelarrea et al., 2014).

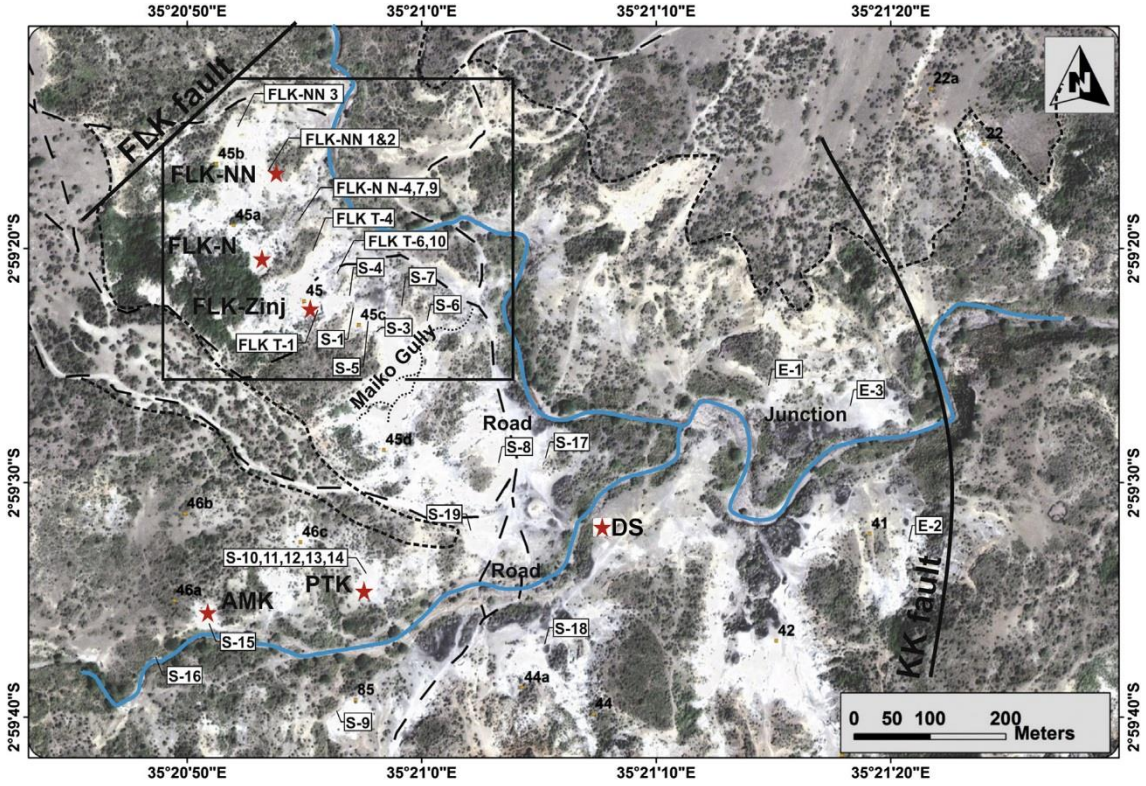

Figure 2.5. Map showing main localities of FLK Zinj complex and faults. Modified from Uribelarrea et al. (2014).

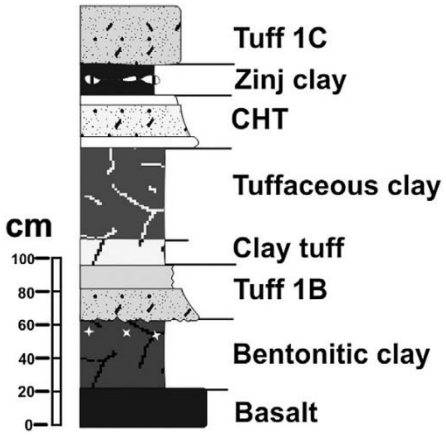

Figure 2.6. Schematic type section corresponding with the main units described in the lower-middle Bed I in the area sampled, from the basalt to Tuff IC. Uribelarrea et al. (2014).

FLK Zinj and now the FLK Zinj Complex is an important site for the knowledge and understanding of early hominin behavior, the interpretation of which is still a matter of debate since Leakey (1971) suggested that the site acted as a "living floor". The abundance of skull and limb bones has been interpreted, so far, in three different ways (Domínguez-Rodrigo et al., 2007): hominins carried selected parts from carcasses to the site, and hence were most likely hunters (Bunn and Kroll, 1986; Domínguez- Rodrigo, 2002; Domínguez-Rodrigo, 1997; Domínguez-Rodrigo and Pickering, 2003; Oliver, 1994; Rose and Marshall, 1996); secondly, hominins transported complete skeletons from partially defleshed carcasses (Capaldo, 1997) and thirdly, hominids scavenged the brain and marrow-bearing long limb bones from carcasses, model called "carnivore-hominid-carnivore" (Blumenschine, 1995, 1991).

In order to throw light on the interpretation of human evolution, it is crucial to frame behavioral hypotheses into a landscape and characterize the local habitat. Phytolith analyses of samples from FLK Zinj and surrounding areas (~2 ha) suggest a densely wooded environment near freshwater springs (Ashley et al., 2010a). Macroremains indicate the presence of grasses and sedges in the wetlands close to a river channel, 50 to 200 m southeast of FLK Zinj site including FLK-S (Blumenschine et al., 2012). Close to this southern area, the Olduvai Paleoanthropology and Paleoecology Project (TOPPP) Team discovered, in 2012, new archaeological sites in the same stratigraphic interval as

FLK Zinj level 22 that were named PTK (in memory of Phillip Tobias), AMK (in memory of Amin Turi) and DS. These sites, are close to the junction of the main and side gorges (Domínguez-Rodrigo et al., 2015, Uribelarrea et al., 2014) (**Figure 2.5**). These sites are located 500m south of FLK Zinj site and comprise three archaeological levels, two of which are below tuff IC at the same level as Clay level 22 from FLK Zinj. PTK's third archaeological level underlies the Zinj clay, within the tuffaceous layer known as the 'Chapati Tuff'. In PTK a modern hand phalanx belonging to an indeterminate species has been discovered (Domínguez-Rodrigo et al., 2015).

2.3.3 FLK West site

The new FLK West site was discovered in 2012 by TOPPP. It is the oldest Acheulean site to date (1.7 Ma, Diez-Martín et al., 2015). FLKW is situated in the lowermost Bed II, 1.5 m above Tuff IF, which is dated 1.809 ± 0.003 Ma (Deino, 2012). Above Tuff IF, close to FLKW and between Maiko Gully and the FLK fault (**Figure 2.5**), 3m of waxy clay (similar to that which is below Tuff IF in Bed I) was deposited. Within this clay, and overlying 1m Tuff IF, a yellowish eolian tuff, partially transformed into waxy clay, has been documented. This tuff has been called Tuff FLKWa and has a chronology of 1.7 Ma (Diez-Martín et al., 2015). In FLKW, the waxy clays are partially eroded by the fluvial channel, and just above the channel, another tuff (30 cm thick, laminated aspect) was deposited. This tuff named FLKWb has a greater lateral continuity than Tuff FLKWa and has been dated 1.664 ± 1.9 Ma (Diez-Martín et al., 2015) (**Figure 2.7**). These recent dates place FLKW, in the lowermost bed II, right above Tuff IIA, as having a weighted mean age of 1.74 ± 0.03 Ma (Manega, 1993) although other authors (Stanistreet, 2012) apply the date of 1.72 ± 0.03 Ma which represents a weighted mean biotite age (Manega, 1993).

As described in Diez-Martín et al. (2015), the stratigraphy and sediments indicate that it is a 40 m wide fluvial channel with a maximum depth of 1.2m, embedded in the clays that form the base of bed II. The central and deepest part of this channel has a width of 20 m. It is composed of six geological levels that represent different fluvial events. Each geological layer has an archaeological level associated with it, but the lowest levels

(5 and 6) are the most important in terms of density of lithics and/or archaeological materials. Granulometry and flow structures decrease towards the top. There are no marks of prolonged subaerial exposure, with incipient formation of soil horizons, crusts or bioturbation. The lowest level (level 6), 15 cm thick, is a bed load composed of gravel and blocks (mostly basalt blocks) up to 20 cm in diameter. A high proportion of these are hammerstones (Diez-Martín et al., 2015). The matrix is formed by coarse sand. It is at archaeological level 6 that stone tool samples were collected and analyzed for phytolith content.

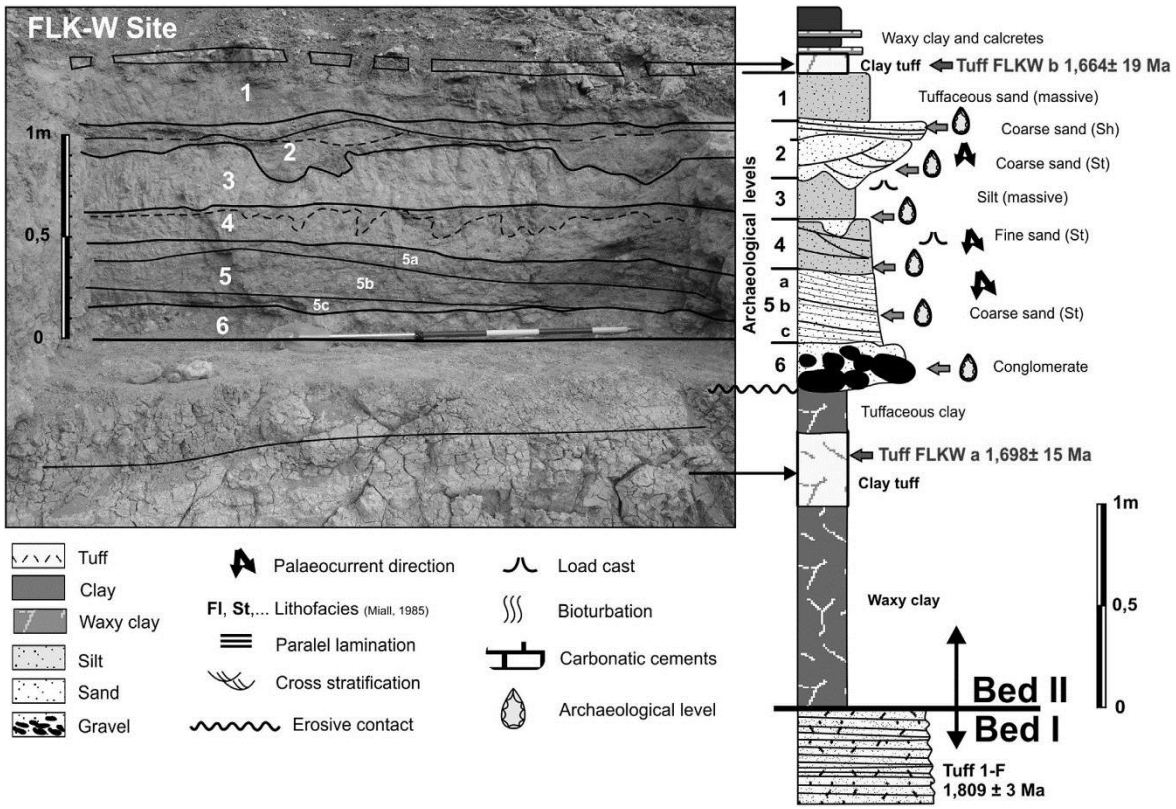

Figure 2.7. Left, detail of geometry and contacts of geological levels 1 to 6 in FLKW site. Right, stratigraphic section from Tuff 1-F to Tuff FLKW b. Drawing and photo by D. Uribelarrea. (Diez-Martín et al., 2015)

2.3.3 BK sites

The BK (Bell's Korongo) site was discovered in 1935 (Leakey, 1971; Hay, 1976). It is located on the South wall of the southern branch of the Side Gorge. Placed at the top of Bed II in lateral connection with Tuff IID it is dated 1.353±0.035 Ma (Domínguez-Rodrigo et al., 2013). It represents a riverine system where conglomeratic sandstone filled channels eroded into siliceous earthy claystone. (Domínguez-Rodrigo et al., 2014; Hay, 1976; Leakey, 1971). The trench analyzed by TOPPP was divided into 13 geological levels in which most sediments are fine-grained showing that, most likely, a distal alluvial sedimentary environment created this sequence (Domínguez-Rodrigo et al., 2009) (**Figure 2.8**). From the archaeological and taphonomical point of view, it is a well-studied site where numerous artifacts and animal remains were recovered. Several excavations were carried out in the 1950's and 1960's, revealing a very rich assemblage of stone tools (over 6800 items), classified as belonging to the Developed Oldowan B complex, as well as bones (Leakey, 1971). BK bone assemblage shows a low frequency of bones with marks made by hominins (Egeland et al., 2007; Monahan, 1996). More recent studies have recovered over 1500 lithic pieces (Diez-Martín et al., 2009) and among them, cutting tools supporting the consumption of small carcasses by hominins in BK site. Recent analyses support the idea of BK as a site where hominins were modifying and consuming small and middle-sized carcasses (Domínguez-Rodrigo et al., 2009), which is concordant with previous interpretations (Egeland and Domínguez-Rodrigo, 2008; Monahan, 1996). In this regard, the reconstruction of the paleoenvironment will provide a vegetation framework that will help to interpret this site.

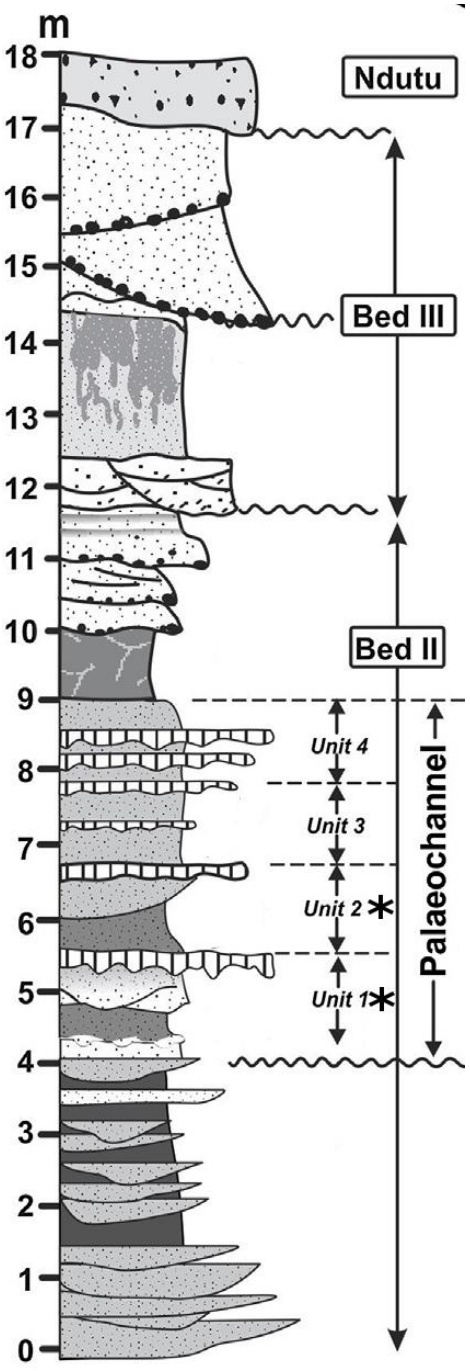

Figure 2.8. Stratigraphy of BK and position of the paleochannel. Asterisks denote archeological levels.

3. Materials

3.1 Surface soil and plant samples

Modern soil samples

Twenty-two modern soil samples from the Crater Highland Area were analyzed for their phytolith content, to test how they reflect vegetation features and for their usefulness as ecological indicators for paleoenvironmental inferences. These samples were collected from various environments to document the phytolith signal of present day vegetation types **Table 3.1.1**, including wooded grasslands, groundwater woodlands and riparian woodlands (**Figure 3.1.1**). At each sampling site, vegetation was described and photographs of the canopy were taken to quantify the tree cover. Before sampling the soil, litter was removed. Each sample is composed of 10-20 sub-samples collected, at random, over an area of about $100m^2$. Modern soils and photographs of the canopy were collected/taken by Doris Barboni in the 2011 field season.

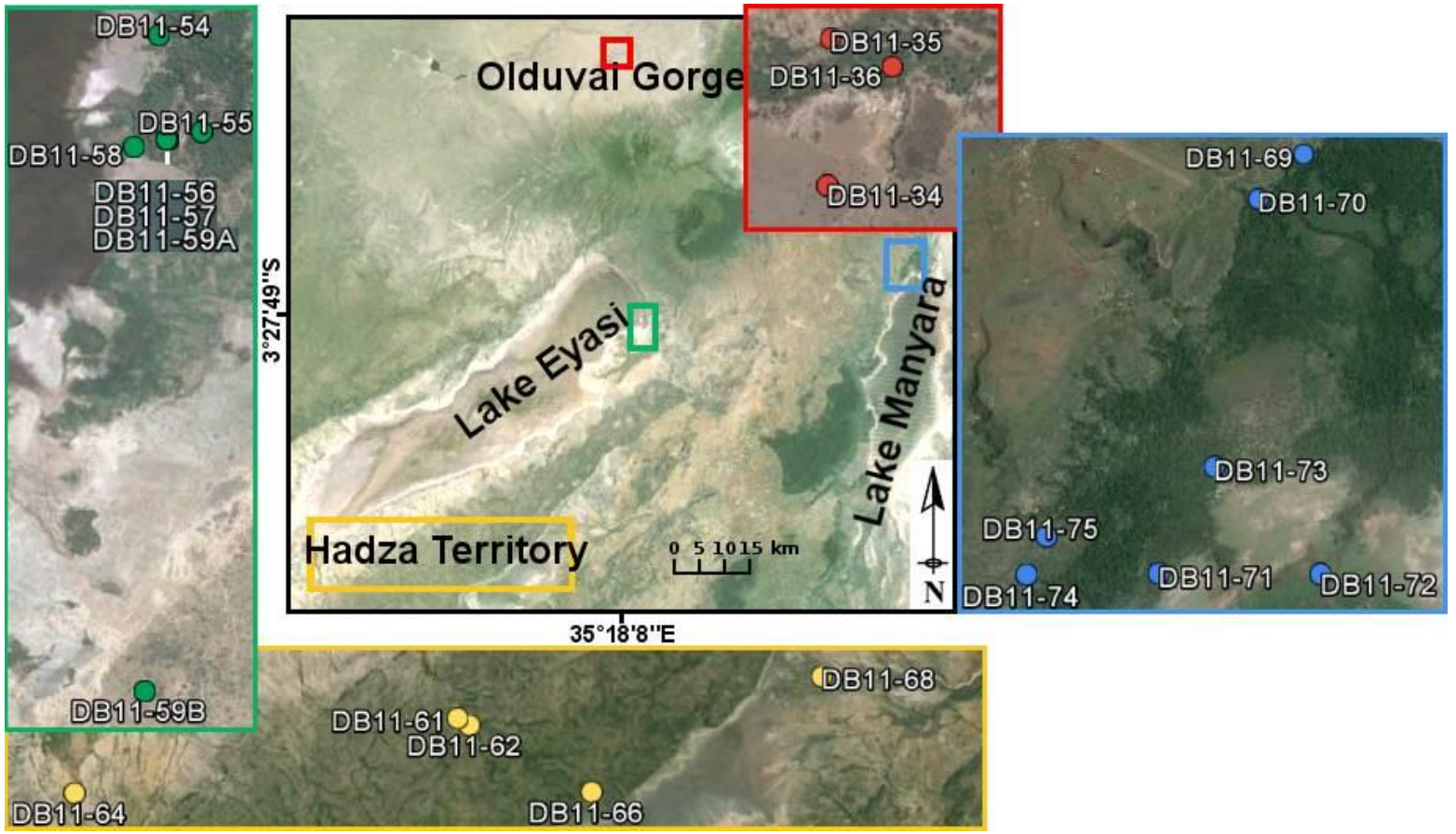

Figure 3.1.1. Map showing the position of modern soils samples from Olduvai Gorge area (red), lake Eyasi (green), Hazdabe Territory (yellow) and lake Manyara (blue).

Table 3.1.1. List of modern soil samples. Full sample ID are DB11-34 (e.g.), but abbreviated labels are given here for clarity.

Sample ID	Locality	Vegetation at sampling site	Elevation (m)	Latitude (S)	Longitude (E)
O34	Olduvai	Wooded grassland with *Commiphora* and *Acacia*	1472	-2.99811	35.32428
O35	Olduvai	Riparian wooded bushland with *Sanseveria*, *Euphorbia tirucali*, *Leonotis leonurus, Acacia*, other dicots and grasses	1457	-2.99542	35.32547
O36	Olduvai	Riparian woodland with *Acacia*, lianas, other tall trees with microphylous, rigidly-coriaceous leaves	1440	-2.99531	35.32572
E54	Lake Eyasi, Kisima Ngeda	Woodland with trees of *Hyphaene* palm, *Acacia xanthophloea*, and tall grasses	1029	-3.47103	35.35042
E55	Lake Eyasi, Kisima Ngeda	Woodland with trees of *Hyphaene* palm and *Acacia xanthophloea*, *Balanites*, and tall grasses	1041	-3.47572	35.35247
E56	Lake Eyasi, Kisima Ngeda	Woodland with *Hyphaene* dominant and *Acacia xanthophloea*. No grasses	1037	-3.47608	35.35075
E57	Lake Eyasi, Kisima Ngeda	Woodland with *Acacia xanthophloea* dominant and *Hyphaene* palm. Abundant grasses	1037	-3.47608	35.35075
E58	Lake Eyasi, Kisima Ngeda	Ecotone between the *Typha* swamp and the groundwater woodland with *Acacia/Hyphaene*. Abundant trees of *Sesbania sesban* and Cyperaceae.	1026	-3.47642	35.34914
E59A	Lake Eyasi, Kisima Ngeda	*Typha* swamp at coring site III	1037	-3.47608	35.35075
E59B	Lake Eyasi, Gorofani	Groundwater forest, very disturbed, with tall evergreen trees of *Ficus*, *Tamarindus indica*, *Cordia* and *Commiphora*	1050	-3.50278	35.34978
H61	Hadzabe territory, Ukumako river	Riparian woodland with *Adansonia, Tamarindus, Sclerocarya, Commiphora, Sesbania, Hyphaene, Euphorbia tirucali, Typha, Cyperus papyrus* and other Cypercaeae	1212	-3.86117	34.97939
H62	Hadzabe territory, Ukumako river	Riparian woodland with *Adansonia, Acacia, Sesbania, Hyphaene, Typha, Cyperus papyrus* and Cyperaceae	1234	-3.86539	34.98647
H64	Hadzabe territory	Wooded grassland with *Adansonia*, *Cordia* and medium-size grasses	1291	-3.85458	34.34300
H66	Hadzabe territory	Woodland with *Adansonia*	1353	-3.90503	35.05847

Sample ID	Locality	Vegetation at sampling site	Elevation (m)	Latitude (S)	Longitude (E)
H68	Hadzabe territory, Yaida swamp	Bushland or wooded bushland with shrubs and small trees with rigidly coriaceous and succulent leaves. *Acacia*	1306	-3.83572	35.19589
M69	Lake Manyara	Groundwater forest with tall evergreen trees of *Ficus, Rauvolfia caffra, Tamarindus indica, Kigelia africana*, *Phoenix reclinata* in understory, Cyperaceae (*Cyperus alternifolius* and others)	989	-3.37444	35.83517
M70	Lake Manyara	Groundwater forest with tall evergreen trees of *Ficus, Rauvolfia caffra, Tamarindus indica, Kigelia africana,* Palm *Phoenix reclinata* in understory, Cyperaceae (*Cyperus alternifolius* and others)	998	-3.37944	35.83053
M71	Lake Manyara	Small swamp herbage enclosed within the groundwater forest, surrounded by *Phoenix, Ficus, Cyperus alternifolius*, and grasses. No *Typha*	1010	-3.41761	35.82100
M72	Lake Manyara	Swamp herbage with Cyperaceae dominant and some grasses	958	-3.41761	35.83633
M73	Lake Manyara	Groundwater woodland with *Acacia xanthophloea, Rauvolfia caffra*, and thick understory of non-gramineous plants	967	-3.40722	35.82622
M74	Lake Manyara	Forest fringing a perennial spring-fed stream	982.9	-3.41781	35.80858
M75	Lake Manyara	Bushed woodland with *Acacia tortilis*, non-gramineous plants in understory. *Adansonia* within 100 m distance	996	-3.41414	35.81033

Modern edible plant samples (starch granules analysis)

Twenty plant species were collected to develop an automated identification method that allows for an accurate identification of starch granules **Table 3.1.2**. The 20 species were chosen randomly to avoid a subjective preselection of shapes and sizes of the granules, from a list of 187 edible plants from East Africa that are part of the diet of modern humans, chimpanzees and baboons listed in Copeland (2007) and Peters (1993). Several of these plants are consumed by the Hadza, one of the last ethnic groups of hunter-gatherers in Africa that are found near lake Eyasi (Mabulla, 1996; Marlowe and Berbesque, 2009). The selected taxa do not represent specific nutritional values and were only used to test the automated system. I analyzed 22 samples from the 20 species, which represent nine botanical families. One family (Poaceae) was over-represented to study intra-familial variations. Two species, *Faidherbia albida* and *Cyperus rotundus* were duplicated. Sampling was made in the following herbaria: ALF (CIRAD, Montpellier, France), MA (*Royal Botanical Garden of Madrid, Spain*) and MPU (University of Montpellier 2, France). Starch granules occur in many plant parts (including leaves, and stems), but are most abundant in storage organs. Starch granules were therefore extracted from fruits (mesocarp, n=8), seeds (n=7) and underground storage organs (n=7) (**Figure 3.1.2**).

Table 3.1.2. Plant species considered for starch granules study. Herbarium codes as per Index Herbariorum. USO: underground storage organ.

Family	Species	Sample origin	Part sampled
Araceae	*Zantedeschia aetiopica* (L.) Spreng.	MPU	USO
Capparaceae	*Cadaba farinosa* Forssk.	MA 653027	Mesocarp
Capparaceae	*Capparis fascicularis* DC.	ALF 28342	Mesocarp
Cyperaceae	*Cyperus rotundus* L.	MA 385928	Seed
Cyperaceae	*Cyperus rotundus* L.	MA 760568	USO
Fabaceae	*Faidherbia albida* (Delile) A. Chev.	MA 205330	Mesocarp
Fabaceae	*Faidherbia albida* (Delile) A. Chev.	MPU	Mesocarp
Fabaceae	*Eminia antennulifera* (Baker) Taub.	H.Bunn's collection	USO
Fabaceae	*Vigna frutescens* A. Rich.	H.Bunn's collection	USO
Fabaceae	*Vigna vexillata* (L.) A. Rich.	MPU	USO
Malvaceae	*Adansonia digitata* L.	H.Bunn's collection	Mesocarp
Malvaceae	*Hibiscus micranthus* L. f.	MPU	Mesocarp
Moraceae	*Ficus salicifolia* Vahl	MPU	Mesocarp
Poaceae	*Brachiara deflexa* (Schumach.) C.E. Hubb. ex Robyns	MA 377254	Seed
Poaceae	*Cynodon dactylon* (L.) Pers.	MA 516133	USO
Poaceae	*Echinochloa colona* (L.) Link	MA 770794	Seed
Poaceae	*Olyra latifolia* L.	MA 535568	Seed
Poaceae	*Panicum subalbidum* Kunth	MA 586518	Seed
Poaceae	*Setaria pumila* (Poir.) Roem. & Schult.	MA 627337	Seed
Polygonaceae	*Persicaria senegalensis* (Meisn.) Soják	MPU	Mesocarp
Portulacaceae	*Portulaca oleracea* L.	MPU	USO
Typhaceae	*Typha latifolia* L.	MPU	USO

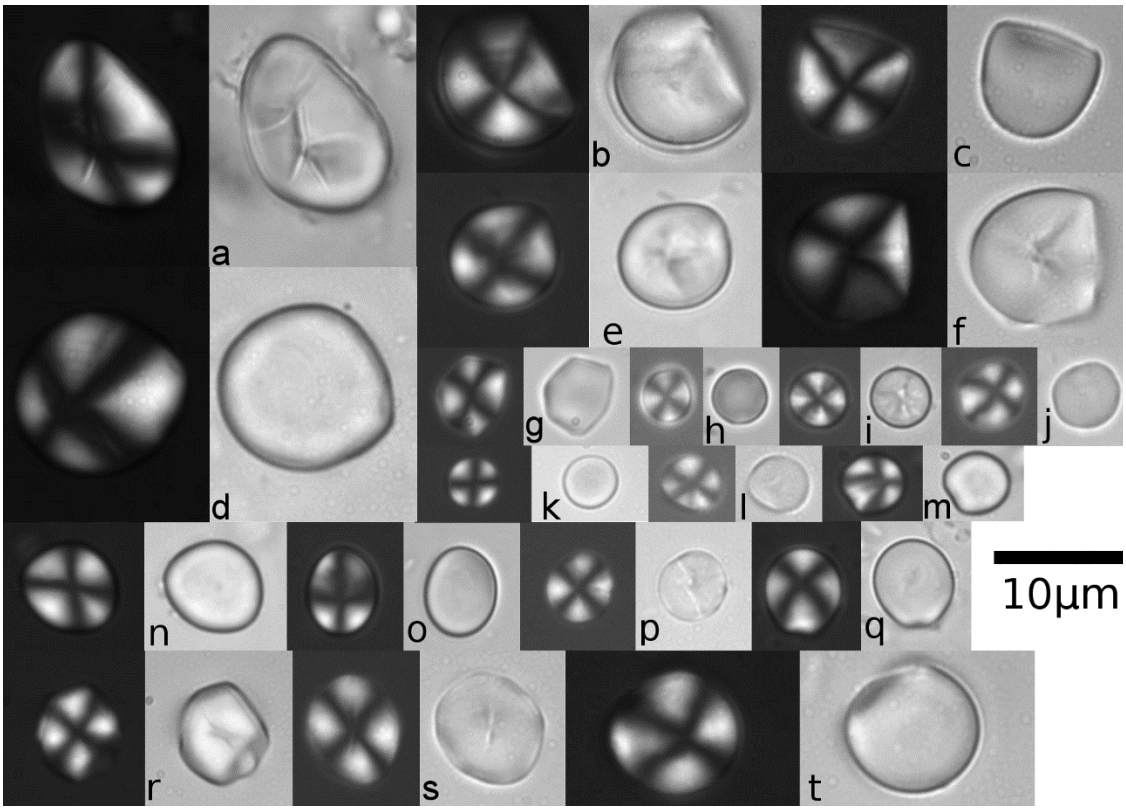

Figure 3.1.2. Selection of starch granules of all the species used in our study, viewed under polarized light (left) and natural light (right) (1000X). **a**: *Faidherbia albida* (mesocarp), **b**: *Vigna vexillata* (USO), **c**: *Emina antennulifera* (USO), **d**: *Portulaca oleracea* (USO), **e**: *Ficus salicifolia* (mesocarp), **f**: *V. frutescens* (USO), **g**: *Echinochloa colona* (seed), **h**: *Persicaria senegalensis* (mesocarp), **i**: *Setaria pumila* (seed), **j**: *Cadaba farinosa* (mesocarp), **k**: *Olyra latifolia* (seed), **l**: *Adansonia digitata* (mesocarp), **m**: *Hibiscus micranthus* (mesocarp), **n**: *Typha latifolia* (USO), **o**: *Cyperus rotundus* (USO), **p**: *Brachiaria deflexa* (seed), **q**: *Capparis fascicularis* (mesocarp), **r**: *Cynodon dactylon* (USO), **s**: *Panicum subalbidum* (seed), **t**: *Zantedeschia aethiopica* (USO).

Modern plant phytolith reference collection

Fourteen modern plant species from spring-associated vegetation types were analyzed for their phytolith content to improve phytolith identifications of fossil samples. Among the set of species, six are pteridophytes (ferns). Fern phytoliths content have been poorly studied and described. In our study area, ferns are commonly found near watercourses and water springs (Kamau, 2012). Other non-fern species, such as the Amarathaceae *Achyrantes aspera*, very common as an understory forb, or typical trees such as Adansonia digitata (baobab) have also been studied. Complete list is given in table (**Table 3.1.3**). Samples were collected principally from leaves, but some branches and petioles were also collected (**Table 3.1.3**). Plants were collected by Doris Barboni in the 2014 field season.

Table 3.1.3. Plant species considered for phytolith reference collection. *: fern species.

Family	Species	Analyzed plant part
Amaranthaceae	*Achyranthes aspera* L.	Leave and inflorescence
Apocynaceae*	*Rauvolfia caffra* Sond.	Pinna
Aspleniaceae*	*Asplenium pumilum* Sw.	Rachis and pinna
Cyperaceae	*Cyperus papyrus* L.	Leave and stem
Euphorbiaceae	*Croton macrostachyus* Hochst. ex Delile	Leave and petiole
Fabaceae	*Tamarindus indica* L.	Leave and petiole
Hymenophyllaceae*	*Trichomanes* sp. L	Rachis and pinna
Malvaceae	*Adansonia digitata* L.	Leave, petiole and stem
Malvaceae	*Thespesia garckeana* F. Hoffm.	Leave and petiole
Pteridaceae*	*Pteris vittata* L.	Rachis and pinna
Pteridaceae*	*Adiantum poiretti* Wikstr.	Rachis and pinna
Pteridaceae*	*Aleuritopteris farinosa (Forssk.) Fée*	Rachis and pinna
Pteridaceae*	*Pteris muricella* Hook.	Rachis and pinna
Zygophyllaceae	*Balanites aegyptiaca* (L.) Delile	Leave and stem

3.2 Paleosol samples

"Zinj complex" paleosol samples

To further characterize the local habitat within the FLK Zinj area, which is likely heterogeneous because of the presence of fresh-water springs (Ashley et al., 2010a), 27 new samples from the same paleosurface as FLK Zinj but at FLK Zinj, PTK, AMK and DS sites were analyzed here (**Figure 3.2.1**) (**Table 3.2.1**). Most samples were collected immediately below Tuff IC (**Figure 2.6**) to ensure contemporaneity of phytolith assemblages. This sampling, therefore allows the analysis of the vegetation pattern during Tuff IC deposition times at about 1.84 Ma, (Deino, 2012). The surface covered by the sampling is approximately 900m from West to East and 600m from North to South. Three samples (DB12-67, DB12-68 and DB 12-69) were collected vertically in stratigraphy at 10, 20 and 40 cm below Tuff IC respectively, to study the changes in vegetation over time. Each sample is composed of 3-5 sub-samples collected less than 50 cm apart Under Tuff IC.

Table 3.2.1. List of Zinj Complex paleosol samples.

Sample ID	Locality	Latitude S	Longitude E
DB14-27	AMK	-2.993333	35.347583
DB14-29	AMK	-2.993361	35.347500
MDR14-1	DS	-2.992222	35.352222
MDR14-2	DS	-2.992222	35.352222
DB14-32	External simple (E4)	-2.990639	35.355139
DB12-67	FLK Zinj	-2.989617	35.348900
DB12-68	FLK Zinj	-2.989617	35.348900
DB12-69	FLK Zinj	-2.989617	35.348900
DB12-85	FLK Zinj	-2.990233	35.350217
DB12-112	FLK Zinj	-2.989633	35.349600
DB12-116	FLK Zinj	-2.989867	35.349517
DB12-135	FLK Zinj	-2.990050	35.350017
DB12-79	FLK Zinj	-2.988933	35.348283
DB12-130	Zinj-PTK Junction (FLK S)	-2.991150	35.350883
DB12-10	PTK	-2.992486	35.350969
DB12-121	PTK	-2.992933	35.349483
DB12-124	PTK	-2.994317	35.349083
DB12-144	PTK	-2.994317	35.349083
DB12-159	PTK	-2.992933	35.349483
DB12-160	PTK	-2.992933	35.349483
DB12-161	PTK	-2.992933	35.349483
DB14-09	PTK	-2.993056	35.349528
DB14-11	PTK	-2.993056	35.349528
DB14-40	PTK	-2.992917	35.349667
DB14-46	PTK	-2.992750	35.350139
DB14-47	PTK	-2.992917	35.350139
DB14-48	PTK	-2.992917	35.350139

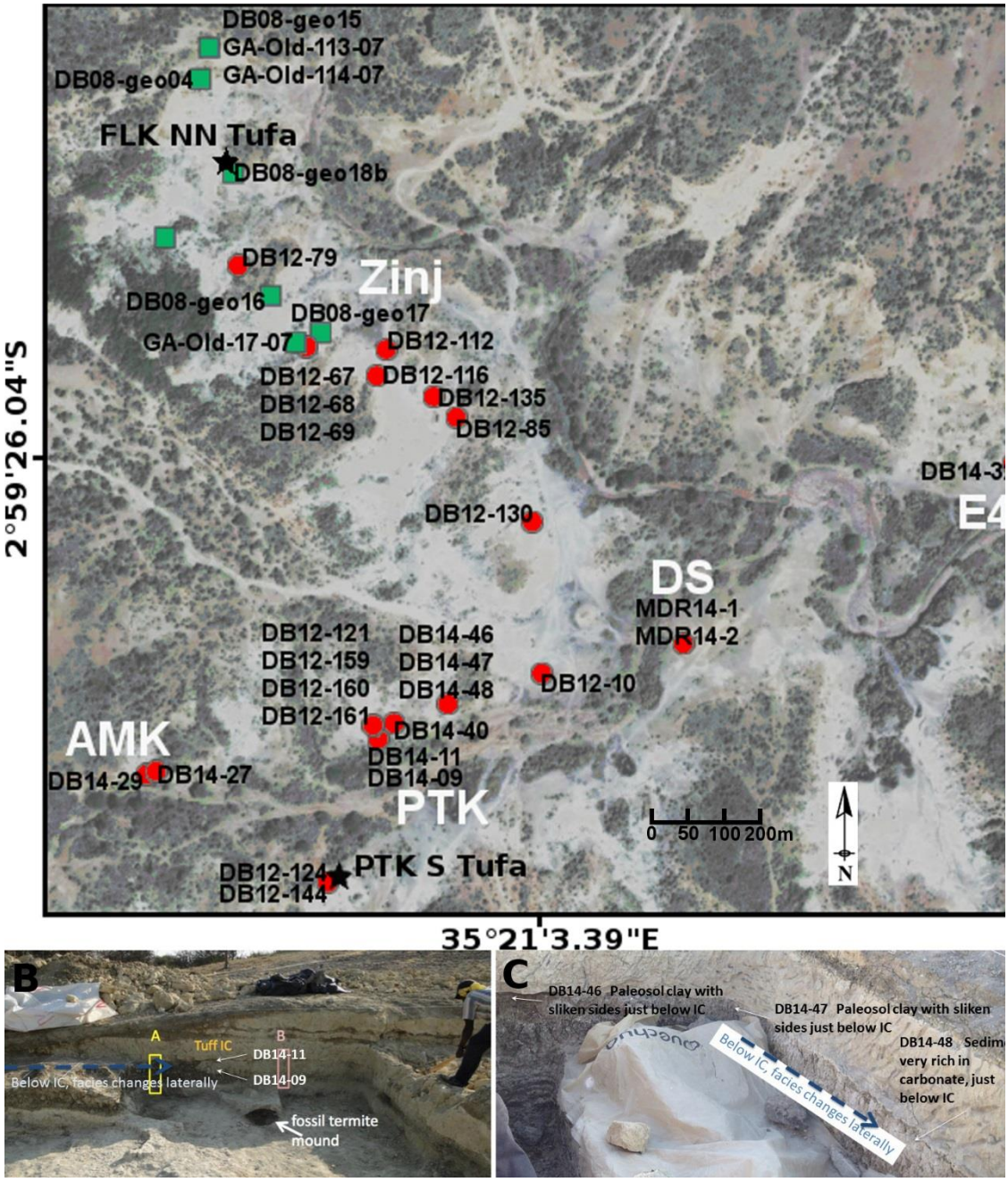

Figure 3.2.1. A) Map showing the position of paleosol samples from Zinj complex. Red circles: Samples analyzed in this thesis, green squares: samples analyzed by Ashley et al. (2010a), stars: tufa position. **B)** Example of vertical facies changes at PTK. **C)** Example of lateral facies changes at PTK.

BK paleosol samples

The BK site is, from the archaeological and taphonomical point of view, a well-studied site where numerous artifacts and animal remains were recovered (Diez-Martín et al., 2009; Domínguez-Rodrigo et al., 2014a, 2009). To study the evolution of vegetation, 24 paleosol samples from BK were analyzed (**Table 3.2.2**). Samples were collected in three different trenches (1, 2 and 14) along the vertical sequence to study the changes in paleovegetation over time (**Figure 3.2.2**). Samples from trench 1 comprise archaeological levels 1 to 3 and trench 2 includes the level 4. These trenches are placed where the highest concentration of cut-marked bones have been recovered. Trenches 1 and 2 were placed in the paleo-river flood plain. Trench 14 was placed to the east of trenches 1 and 2 and is placed in the paleo-river channel. Two additional samples (DB12-18 and DB12-19) were collected a hundred meters east of the site from a yellow siliceous clay layer below a carbonated tuff but these samples are not contemporaneous to BK archaeological site. Each sample is composed of 3-5 sub-samples collected from a square surface whose sides were less than 50cm. After collection, samples were immediately deposited in clean polyethylene ziplock bags. Paleosoils from BK and the "Zinj complex" were collected by Doris Barboni and Manuel Domínguez-Rodrigo during the 2011, 2012 and 2014 field seasons.

Table 3.2.2. List of Zinj Complex paleosol samples.

Sample ID	Locality	Trench/Unit/Archaeological level	Latitude S	Longitude E
DB11-8	BK	Trench 1. Unit 1. Archaeological level IIIa	2.996000	35.324361
DB11-9	BK	Trench 1. Unit 1. Archaeological level IIIa	2.996000	35.324361
DB11-10	BK	Trench 1. Unit 1. Archaeological level IIIb	2.996000	35.324361
DB11-1	BK	Trench 1. Unit 2. Archaeological level I	2.996000	35.324361
DB11-2	BK	Trench 1. Unit 2. Archaeological level II	2.996000	35.324361
DB11-3	BK	Trench 1. Unit 2. Archaeological level II	2.996000	35.324361
DB11-4	BK	Trench 1. Unit 2. Archaeological level II	2.996000	35.324361
DB11-5	BK	Trench 1. Unit 2. Archaeological level II	2.996000	35.324361
DB11-6	BK	Trench 1. Unit 2. Archaeological level II	2.996000	35.324361
DB11-7	BK	Trench 1. Unit 2. Archaeological level II	2.996000	35.324361
DB11-19	BK	Trench 2. Unit 1. Archaeological level IVa	2.996000	35.324361
DB11-20	BK	Trench 2. Unit 1. Archaeological level IVb	2.996000	35.324361
DB11-21	BK	Trench 2. Unit 1. Archaeological level V	2.996000	35.324361
DB12-71	BK	Trench 14. Unit 1. Archaeological level V	2.983333	35.316667
DB12-72	BK	Trench 14. Unit 1. Archaeological level V	2.983333	35.316667
DB12-73	BK	Trench 14. Unit 1. Archaeological level V	2.983333	35.316667
DB11-13	BK	Trench 14. Unit 2. Archaeological level II	-2.996083	35.324250
DB11-14	BK	Trench 14. Unit 2. Archaeological level II	-2.996083	35.324250
DB11-15	BK	Trench 14. Unit 2. Archaeological level II	-2.996083	35.324250
DB11-16	BK	Trench 14. Unit 3	-2.996083	35.324250
DB11-17	BK	Trench 14. Unit 3	-2.996083	35.324250
DB11-18	BK	Trench 14. Unit 3	-2.996083	35.324250
DB12-18	BK	Under Tuff IID	-2.983333	35.316667
DB12-19	BK	Under Tuff IID	-2.983333	35.316667

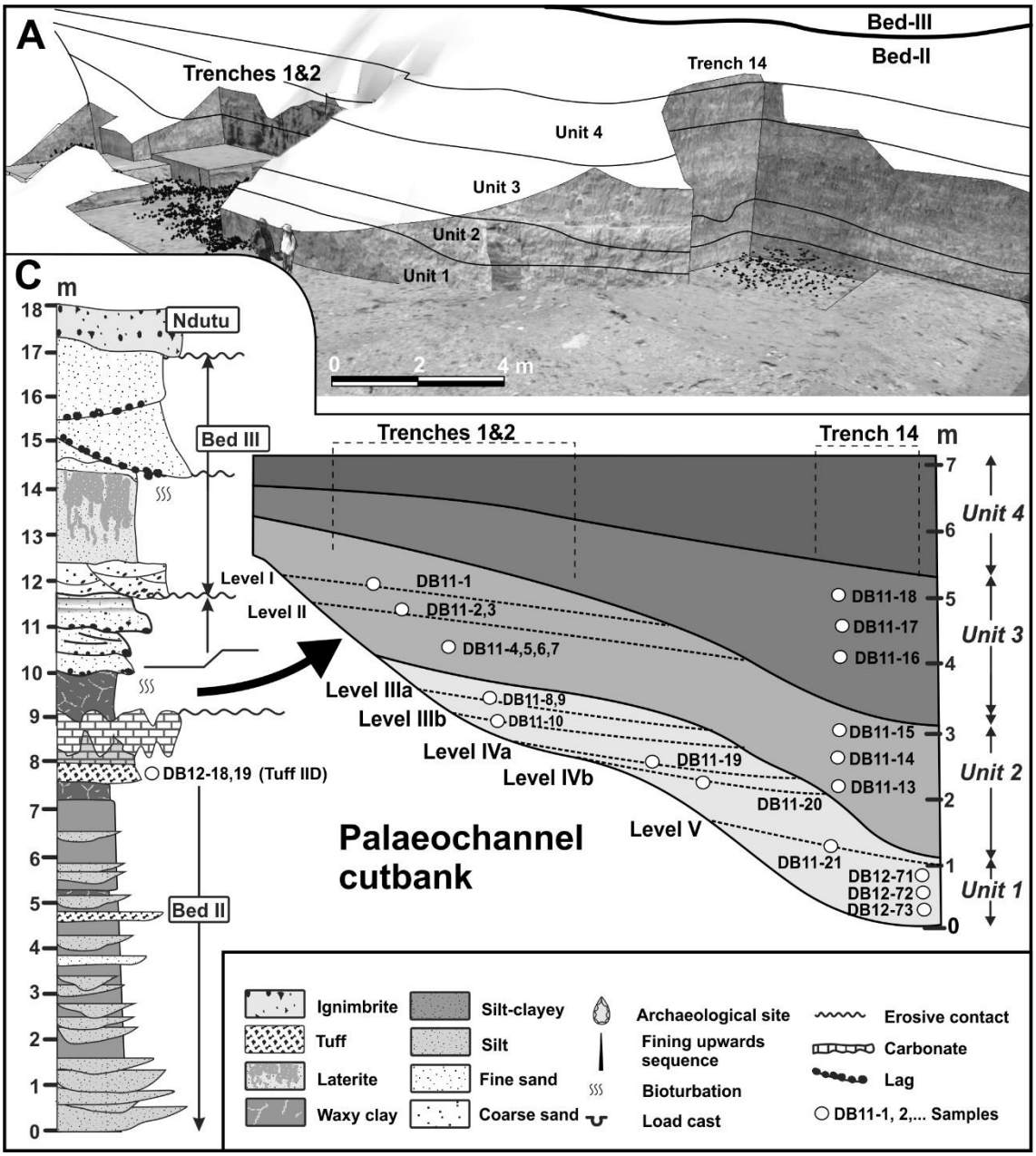

Figure 3.2.2. Figure showing the position of paleosol samples from **BK site. A)** 3D scheme showing position of trenches**. C)** Stratigraphic section across the Bed II-Bed III and Ndutu units in (left). Detailed stratigraphic and sample position (right). Modified from Domínguez-Rodrigo et al. (2014).

3.3 Stone tool samples for micro-botanical remains analysis

FLK West is a site recently discovered by TOPPP with the earliest (1.7 Ma) Acheulian stone tools discovered to date (1.7 Ma). The site is located approximately at 2º59´20.44´´S - 35º20´55.66´´E. It has been suggested that the analysis of plant micro remains opens up new ways to understand how these lithic remains were used (Diez-Martin et al., 2015). The analysis of phytoliths and stone tools was carried out on stone tools from archaeological level 6, which was one of the densest and most important levels in terms of artifact remains. Stone tools were collected with an attached soil layer (also analyzed), unwashed, and minimally handled to avoid modern contamination. During excavation, stone tools were placed in self-sealing plastic bags awaiting analysis. Forty-two samples from the complete collection of tools were chosen randomly in order to analyze the pattern between used and unused tools (those showing no flaking or percussion stigma). Selected stone tool types included flakes, hammerstones, anvils, cores, pebbles, spheroids and fragments. **(Table 3.3.1, Figure 3.3.1).** Sampling was carried out by Fernando Diez-Martin's team during 2013 field season.

Table 3.3.1. List of FLK West stone tool samples.

Tool ID	Material	Lenght (mm)	Width (mm)	Thickness (mm)	Mass (g)	Tool type
15	Quartz	95	94	45	565	Bifacial unipolar core/chopper
17	Quartz	144	93	46	773	LCT
24	Quartz	89	63	25	140	Retouched Flake: distal point
28	Basalt	76	62	54	422	Multifacial/Multipolar core,
29	Quartz	57	25	14	27	Flake
33	Quartz	144	65	57	673	LCT, cleaver
41	Basalt	70	41	23	91	Pebble, no percussion stigma
42	Basalt	65	54	39	218	Unifacial unipolar core
45	Quartz	71	53	50	403	Bifacial unipolar core
47	Quartz	76	64	59	394	Spheroid
54	Gneiss	146	84	64	869	Anvil
56	Phonolite	81	68	56	369	Unipolar circular core
62	Quartz	40	67	26	95	Flake
68	Basalt	91	68	67	471	Test core
77	Quartz	79	79	52	617	Bipolar core
82	Basalt	113	86	50	584	Pebble, no percussion stigma
87	Quartz	64	83	46	342	Bipolar core
90	Basalt	91	81	79	844	Hammerstone
99	Chert	52	49	43	159	Multifacial/Multipolar core,
100	Phonolite	69	50	36	175	Pebble, no percussion stigma
174	Quartz	40	36	12	22	Flake
178	Phonolite	79	64	57	487	Multifacial/Multipolar core,
184	Quartz	94	97	42	337	Flake
185	Quartz	62	50	22	75	Flake
186	Quartz	53	53	21	59	Flake
188	Phonolite				110	Fragment
189	Basalt	126	70	65	697	Pebble, no percussion stigma
190	Basalt	77	58	50	272	Pebble, no percussion stigma
191	Basalt	78	63	59	350	Pebble, no percussion stigma
197	Basalt	59	67	64	282	Pebble, no percussion stigma
198	Quartz				77	Fragment
201	Basalt				75	Fragment
203	Quartz				195	Fragment
208	Quartz	85	60	46	315	Uniporlar circular core with percussion
218	Quartz	77	70	46	363	Test core
219	Quartz	29	27	10	11	Flake
225	Quartz	71	49	29	119	Flake
226	Phonolite	60	42	27	95	Flake
227	Quartz	74	49	45	257	Unifacial core
228	Quartz	55	47	21	77	Flake
231	Quartz	117	111	104	1848	Multifacial/Multipolar core,
237	Quartz	47	51	41	135	Bifacial multipolar orthogonal core

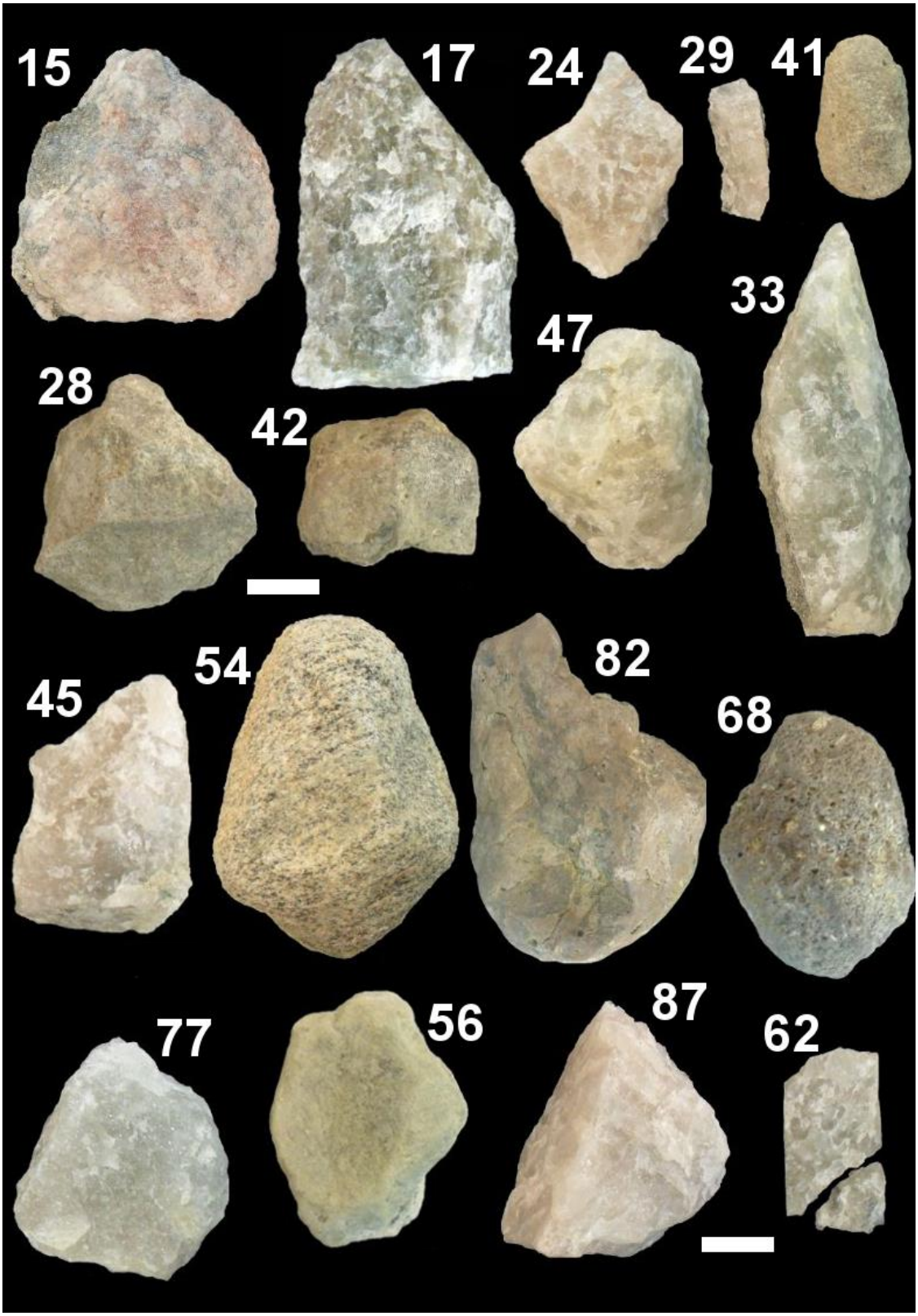

Figure 3.3.1. Stone tools analyzed from FLK West site. Scale bar = 3 cm.

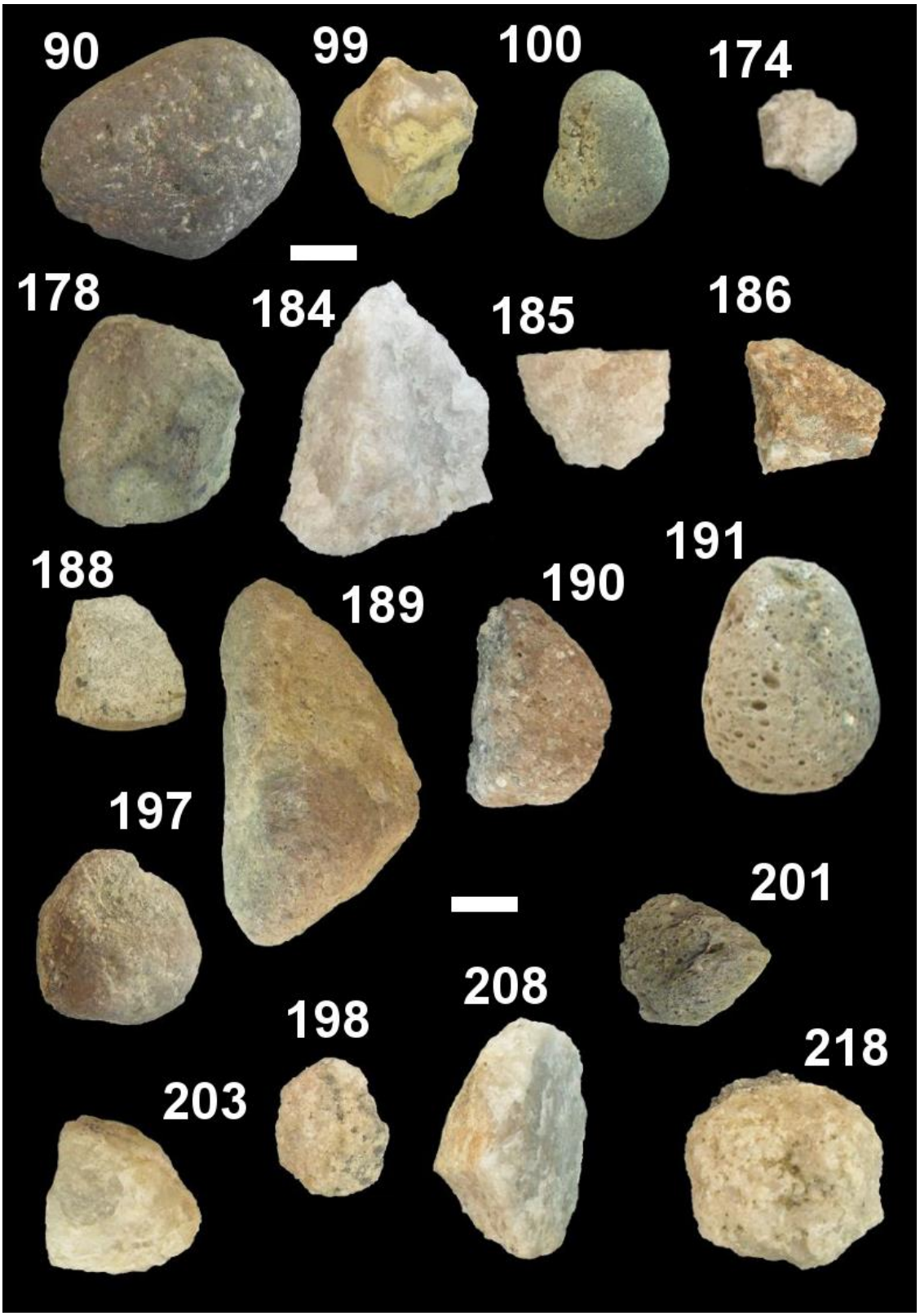

Figure 3.3.1. Cont.

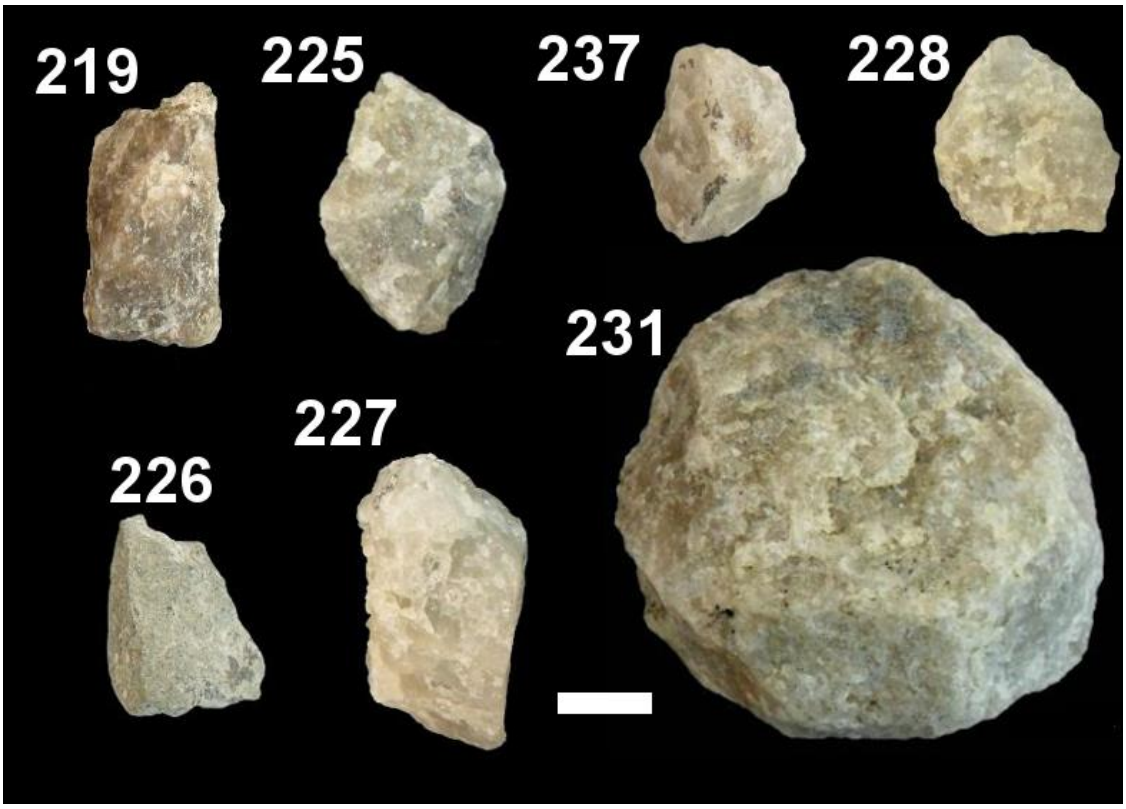

Figure 3.3.1. Cont.

To analyze if the phytolith assemblages on tools are biased by depositional processes or by laboratory procedures, an experimental archaeological test was carried out involving a total of 28 experimental stone tools. Twenty-three of these stone tools were made of quartz, three of nephelinite and two of basalt (**Table 3.3.2**). Tools made of quartz from Madrid were provided by José Yravedra in Madrid (Spain). Modern stone tools from Tanzania were provided by Fernando Diez-Martin. For the experimental archaeology we used two types of soils (one rich in grasses and the other rich in leguminous plants, 12 kg of each type of soil). The experimental soils were enriched by the addition of coconut (*Cocos nucifera*) fruits extract (phytolith extraction from 100 g of fresh coconut fruit). Raw soils were collected in Alcalá de Henares (Spain). In **table 3.3.2** "sample weight" refers to the internal matrix obtained for each tool or the weight of soil samples. "Residue sample" refers to the fraction of soil that remains after phytolith extraction.

Table 3.3.2. List of experimental stone tool and soil samples.

Sample	ID	Sample weight (g)	Sample residue (g)	Tool weight (g)	Length	Width	Thickness
Tool	2	0.12	0.007	45.2	68	58	20
Tool	3	0.42	0.094	107.2	75	66	23
Tool	4	0.215	0.059	126.5	92	87	21
Tool	5	0.64	0.004	80.3	74	42	28
Tool	6	0.34	0.005	81.9	80	39	32
Tool	7	0.241	0.038	65.5	54	56	26
Tool	8	1.619	0.203	24.6	50	40	15
Tool	9	0.775	0.083	47.2	50	35	17
Tool	10	0.485	0.073	44.3	59	37	17
Tool	11	0.569	0.071	28	54	35	13
Tool	12	0.154	0.008	119.8	99	55	23
Tool	13	0.172	0.003	53.4	71	44	16
Tool	14	0.161	0.047	44.5	64	40	13
Tool	15	1.18	0.103	70.9	90	51	20
Tool	16	0.382	0.146	123	86	67	28
Tool	17	0.097	0.014	103.6	71	54	28
Tool	18	0.62	0.003	33.9	56	50	13
Tool	19	0.66	0.099	45.6	57	52	17
Tool	20	0.07	0.039	25.3	62	50	12
Tool	21	0.143	0.143	55.2	69	66	13
Tool	22	0.187	0.05	139.8	81	61	28
Tool	23	0.016	0.019	47.4	69	52	13
Tool	24	0.12	0.054	272.2	77	70	44
Tool	25	0.41	0.001	63.5	68	50	20
Tool	26	0.13	0.045	216.3	100	60	31
Tool	27	0.74	0.02	95	73	62	28
Tool	28	0.14	0.044	78.5	82	46	21
Tool	29	0.153	0.035	198	62	57	40
Soil	A	2	0.025				
Soil	B	2	0.025				
Soil	C	2	0.078				
Soil	D	2	0.043				
Soil	E	2	0.042				
Soil	F	2	0.064				
Soil	G	2	0.053				
Soil	H	2	0.049				
Soil	I	2	0.0134				
Soil	J	2	0.16				
Soil	K	2	0.031				
Soil	L	2	0.062				
Soil	M	2	0.039				
Soil	N	2	0.024				
Soil	O	2	0.066				

4. Methods

4.1 Phytolith analysis

4.1.1 Phytolith extraction procedures

External adhering sediment from tools was removed by brushing delicately and thoroughly. Then, tools were placed in beakers (in an ultrasonic bath) and immersed in ultrapure water. Tools were sonicated for 5-10 minutes to extract the embedded sediment in pores and fissures because there is little risk that it will be affected by contamination (Hart, 2011). Due to strict anti-contamination protocol for starches, spot sampling for phytoliths was not used to obtain stone tool matrices. Stone tool sediment from cracks and micro-cavities in the stone surface was extracted by using a single step extraction protocol (Perry, 2010).

Paleosols, modern soils, and external brushing remains and matrices from stone tool samples were prepared for phytolith analyses by treatment of dry sediments (6-8 g from soils, 2 g from external brushing from tools, and all the matrices recovered from tools) with pure HCL (33%) for 1-2h to remove carbonates, and then with H_2O_2 (110 volumes) at 80ºC to remove organic matter. Clays were deflocculated using a solution of sodium hexametaphosphate $(NaPO_3)_6$ at pH 7, and removed by decantation. Separation of phytoliths was made using a $ZnBr_2$-HCl heavy liquid in the case of modern soils and paleosols from Olduvai, or Sodium Polytungstate heavy liquids in the case of stone tools from Olduvai, and modern soils and stone tools from the experimental archaeology test. Density of the heavy liquid was set at 2.3 g/cm^3. The residue was mounted in benzyl benzoate.

Plant samples were prepared for phytolith analyses by treatment of dry samples with pure HNO_3 and $HClO_4$ at 50ºC for 1-2 days, and then with H_2O_2 (110 volumes) at 50ºC to remove organic matter.

The residue was mounted in benzyl benzoate. Slides were sealed using paraffin. Observations and counting were done under optical microscope at 400× magnification. Observations and photographs of the samples were made by using a Carl Zeiss© optical microscope equipped with a Canon EOS 550D© camera and an Olympus BX51© optical microscope with an Olympus DP71© camera that uses CellA v.2.7© software to take photographs and measurements.

4.1.2 Phytolith description and identification databases

Phytolith descriptions follow the international code for phytolith nomenclature (Madella et al., 2005). Phytolith identifications were based on compare phytoliths with photographs and descriptions from previous works (Albert et al., 2016, 2009; Barboni et al., 2010; Collura and Neumann, 2016; Eichhorn et al., 2010; Garnier et al., 2012; Mercader et al., 2010, 2009; Novello, 2012; Stromberg, 2004, 2003, 2002). Phytoliths were classified according to their morphology and size and subsequently grouped according to their most probable botanical origin. Some of the main categories used in the present work that are clearly related to the plants that produced them are: Grass Silica Short Cells (GSSC) (Twiss et al., 1969) and bulliform cells from grasses (Poeaceae) and sedges (Cyperaceae) (Novello et al., 2012; Rossouw, 2009), sedges (Cyperaceae) "hat shaped" plates (Piperno, 1988; Ollendorf, 1992), globular echinate phytoliths from Palms (Arecaceae) (Fenwick et al., 2011; Piperno, 2006) or globular rugose-granulate from woody plants (Collura and Neumann, 2016; Garnier et al., 2012). Other morphological categories are not specific to a single plant group but their occurrence is more frequent in certain groups than in others. These morphologies are for example some blocky morphologies, sclereids and tracheids from woody plants (e.g., Albert et al., 2014; Collura and Neumann, 2016; Mercader et al., 2009), also angular polyhedral bodies from fern epidermis (Pteridohyta) (Mazumdar, 2011; Mazumdar and Mukhopadhyay, 2011; Sundue, 2009), polygonal prisms with rugose tops from Commelinaceae (Eichhorn et al., 2010), or small cylindrical branching bodies and elongated tabular or slightly cylindrical tuberculate phytoliths from grasses and sedges (Albert et al., 2014). Due to this ubiquitous production from plants a great number of categories were not attributed to any plant

groups, e.g., elongated smooth glass-rod type bodies, acicular hair-cell bodies, papillae, etc., and all the altered morphologies. An additional non botanical category including all dicotyledonous remains (forest indicators) was used in paleoenvironmental studies as previous authors had done (e.g., Ashley et al., 2010a, 2010b; Barboni et al., 2010). Most phytoliths considered here are illustrated (**Figure 4.1.1)** and their taxonomical attribution is given in **Table 4.1.1**.

In our analysis we considered two main groups of globular phytoliths, in which we include those globular phytoliths considered by Collura and Neumann (2016) as diagnostic of wood/bark tissues, which are also used to calculate D/P indices. We also considered as FI phytoliths (named "other FI" in our results) those morphologies produced by other tissues, including leaves, which are produced, especially but not only, by woody plants (Albert et al., 2016; Mercader et al., 2009). If we had only considered as FI phytoliths those of wood/bark suggested by Collura and Neumann (2016), we would have left out some phytoliths from leaves, which in tropical forest trees, are one of the major producers of phytoliths (Collura and Neumann, 2016). This method may overestimate the presence of woody plants, but trees and high and low shrubs cover most of the landscape in wooded areas of Lake Manyara National Park (Loth and Prins 1986), so this overestimation would be weak. Furthermore, this approach allows us to compare our results with other studies that used as FI most of the phytoliths produced by dicotyledonous plants (e.g.; Albert et al., 2015 and Esteban et al., 2016).

Diatom remains were counted but not classified nor analyzed. Relative phytolith abundance is expressed as the percentage on the total phytolith sum. Percentages of diatoms are calculated on the basis of the sum of diatoms plus phytoliths.

Tabla 4.1.1. List of phytolith morphologies and attributions used in this thesis. L: longitude, h: height, d: diameter. NA: Photo not available. *: photo from fossil sample.

ID	Description	Taxonomical attribution	Environmental signal	Dicot plant part signal (if distinctive)	Bibliography
GRASS SILICA SHORT CELLS (GSSC)					
Rondels					
GSSC1	Rondel conical, top pointed (d6-12)	Poaceae	Grass		Albert et al., 2016 (Fig. 692)
GSSC2	Rondel base slightly constricted, top keeled (d<15)	Poaceae	Grass		Albert et al., 2016 (Fig.1321)
GSSC3*	Rondel conical, top truncated (d<15)	Poaceae	Grass		Garnier et al., 2013 (Fig C.q)
GSSC4*	Rondel cylindrical short, base round/oblong (d6-12)	Poaceae	Grass		Garnier et al., 2013 (Fig C.o)
GSSC5*	Rondel cylindrical short, base round/oblong (d15-18)	Poaceae	Grass		Garnier et al., 2013 (Fig C.o)
GSSC6	Rondel cylindrical tall, base round/oblong (d10, h20)	Poaceae	Grass		Albert et al., 2016 (Fig. 301)
GSSC7	Rondel base slightly constricted, conical, top truncated (d8)	Poaceae	Grass		Albert et al., 2016 (Fig. 872)
GSSC8	Rondel base slightly constricted, conical, top truncated (d15-20)	Poaceae	Grass		Albert et al., 2016 (Fig. 872)
GSSC9 NA	Rondel sinuous/oblong base, conical, top pointed (d8-10)	Poaceae	Grass		
GSSC10 NA	Rondel tabular hexagonal (d8-12)	Poaceae	Grass		
Trapeziforms					
GSSC11	Trapeziform shortcell (b10-16)	Poaceae	Grass		

ID	Description	Taxonomical attribution	Environmental signal	Dicot plant part signal (if distinctive)	Bibliography
Bilobates					
GSSC12*	Bilobate, trapeziform, with concave lobes (L<15)	Poaceae	Grass		Albert et al., 2016 (Fig. 524)
GSSC13*	Bilobate, trapeziform, with concave lobes (L>15)	Poaceae	Grass		Albert et al., 2016 (Fig. 524)
GSSC14	Bilobate, trapeziform, with round lobes (L10-20)	Poaceae	Grass		Garnier et al., 2013 (Fig C.c)
GSSC15	Bilobate straight lobes (L10-12)	Poaceae	Grass		Garnier et al., 2013 (Fig C.a)
Crosses					
GSSC16*	Cross 4-lobed tabular (d>15)	Poaceae	Grass		Mercader el al., 2010 (Fig 2.25)
GSSC17	Cross 4-lobed tall (pyramidal) (b10)	Poaceae	Grass		Garnier et al., 2013 (Fig C.h)
Polylobates					
GSSC18	Polylobate tabular, lobes round/straight (L<20)	Poaceae	Grass		Albert et al., 2016 (Fig. 5484)
GSSC19	Polylobate tabular, lobes round/straight (L>20)	Poaceae	Grass		Albert et al., 2016 (Fig. 5484)
GSSC20	Polylobate tabular, concave end lobes (L15-20)	Poaceae	Grass		Mercader el al., 2010 (Fig 3.14)
Saddles					
GSSC21*	Saddle regular (L6-12)	Poaceae	Grass		Mercader el al., 2010 (Fig 2.31)
GSSC22	Saddle short convex edges (8-15)	Poaceae	Grass		Mercader el al., 2010 (Fig 2.7)
GSSC23	Saddle long convex edges (L6-15)	Poaceae	Grass		Mercader el al., 2010 (Fig 2.6)

ID	Description	Taxonomical attribution	Environmental signal	Dicot plant part signal (if distinctive)	Bibliography
Unidentified GSSC					
GSSC24 [NA]	Dubious GSSC (broken, damaged, indistinguishable shape)	Poaceae	Grass		
NON GSSC Globular bodies					
Glo1	Globular echinate body with distinc spines (d5-10)	Arecaceae	Palms	Leaves/Fruit	Albert et al., 2016 (Fig. 1503); Piperno 1998
Glo2	Globular echinate body with distinc spines (d11-15)	Arecaceae	Palms	Leaves/Fruit	Albert et al., 2016 (Fig. 1503); Piperno 1998
Glo3	Globular echinate body with distinc spines (d>16)	Arecaceae	Palms	Leaves/Fruit	Albert et al., 2016 (Fig. 1503); Piperno 1998
Glo4	Globular echinate body with distinc spines (d>20)	Arecaceae	Palms	Leaves/Fruit	Albert et al., 2016 (Fig. 1503); Piperno 1998
Glo5*	Globular micro-echinate or micro-granuate body (L10-40)	Dicotyledons	Globular FI	Wood/Bark	Albert et al. 2016 (Fig. 502)
Glo6	Globular faceted (d10-20)				Garnier et al., 2013 (Fig B.a)
Glo8*	Discoid tabular, sub-globular, tuberculate or microechinate, half-spherical in side view (d10-30)	Dicotyledons	Globular FI		Garnier et al., 2013 (Fig B.d)
Glo9	Globular smooth/psilate (d10-20)		Globular FI		Garnier et al., 2013 (Fig. B.e.)
Glo10	Globular granulate body spherical (d8-15)	Dicotyledons	Globular FI	Wood/Bark	Garnier et al., 2013 (Fig. B.b.)
Glo11	Globular granulate body spherical (d15-20)	Dicotyledons	Globular FI	Wood/Bark	Garnier et al., 2013 (Fig. B.b.)

ID	Description	Taxonomical attribution	Environmental signal	Dicot plant part signal (if distinctive)	Bibliography
Glo12	Globular granulate body spherical (d20-25)	Dicotyledons	Globular FI	Wood/Bark	Garnier et al., 2013 (Fig. B.b.)
Glo13*	Globular granulate irregular body (multiple globules) (d>20)	Dicotyledons	Globular FI	Wood/Bark	Garnier et al., 2013 (Fig. B.c.)
Plates					
Pla1	Irregular edge "algae like" (20-50x28-60)	Podostemataceae			Garnier et al., 2013 (Fig. D.b)
Pla2	Plate, thick, irregular contour, irregular granulate surface (L-W20-60)	Dicotyledons	Other FI		Mercader el al., 2009 (Fig 3-q)
Pla3*	Plate, angular shard-like, psilate-rugose (L-W20-50)	Dicotyledons	Other FI	Leaves	Albert et al., 2014 (Fig 1175)
Pla4*	Plate, thin, irregular contour, wavy surface, finely rugose (L-W-20-50)	-			
Pla5	Hexagonal-roudend platelet with rounded apex “hat-shaped” (L10-20)	Cyperaceae	Sedge (Other G/S)		Ollendorf, 1992 (Fig 5.5e)
Pla6	Thin plate, edge or surface lacunate (L30)	-			
Pla7	Thin plate, smooth (L30-50)	-			
Pla8 [NA]	Subspherical plate with bulliform-type texture (L40-100)	Poaceae/ Cyperaceae	Grass/Sedge (Other G/S)		
Pla9*	Tabular thick smooth, usually contorted (L20-40)	Dicotyledons	Other FI		Mercader et al., 2009 (fig 6.a.b)
Elongate bodies					
El1	Elongate tabular, irregular edges, rough surface (L25-60)	Dicotyledons	Other FI		Albert et al., 2016 (Fig 324), Mercader el al., 2009 (Fig 4-q)

ID	Description	Taxonomical attribution	Environmental signal	Dicot plant part signal (if distinctive)	Bibliography
El2*	Elongate cylindrical, sinuous edges (L20-40)	Poaceae/ Cyperaceae	Grass/Sedge (Other G/S)		Albert et al., 2016 (Fig 5464)
El3	Elongate cylindrical body, surface psilate to slightly lacunate (L20-30)	Dicotyledons	Other FI		Mercader el al., 2009 (Fig 2-q)
El4	Elongate cylindrical body sinuous, smooth surface (L15-45)	Cyperaceae	Sedge (Other G/S)		Albert et al., 2016 (Fig. 839)
El5	Elongate tabular or slightly cylindrical, surface perforated-granulate (L30)	Poaceae/ Cyperaceae	Grass/Sedge (Other G/S)		Albert et al., 2016 (Fig. 767)
El6*	Elongate quadrangular section, body curved, surface spilate to slightly rugose(L22-70)	-			
El7	Elongate tabular with sinuous edges (L10-30)	Poaceae/ Cyperaceae	Grass/Sedge (Other G/S)		Mercader et al., 2010 Fig 5.6
El8*	Elongate segmented cylindroid psilate (L60-100)	Cyperaceae	Sedge (Other G/S)		Albert et al., 2016 (Fig 923)
El9	Elongate smooth glass-rod type straight body (L15-30)	-			
El10	Elongate cylindrical/subcylindrical body granulate (L20-120)	Dicotyledons	Other FI		Albert et al., 2016 (Fig 284)
El11	Elongate triangular transverse section smooth edges (L20)	-			
El12 NA	Dubious elongates, altered.	-			
El13	Vertebral column body (L24)	Poaceae	Grass (Other G/S)		Mercader el al., 2010 (Fig 2.28)

ID	Description	Taxonomical attribution	Environmental signal	Dicot plant part signal (if distinctive)	Bibliography
El14	Blocky body parallelepipedal, pinch-pointed, smooth edges, surface psilate (L30-70)	-	-	-	
El15	Helical tracheary element (L15-30)	Dicotyledons	Other FI	Leaves	Stromberg 2003 (Figure 4.8f)
Blocky/irregular bodies					
Blo1 [NA]	Orange slice body (L20-40)	-			
Blo2	Parallepiped body, bulliform-type texture (L20-40)	Poaceae/ Cyperaceae	Grass/Sedge (Other G/S)		Albert et al., 2016 (Fig. 789)
Blo3*	Tabular thick lacunate body (20-70)	Dicotyledons	Other FI	Leaves	Mercader el al., 2009 (Fig 6-k,l,m)
Blo4	Parallepiped/cubic body, sinous edges, psilate surface (L10-40)	Dicotyledons	Other FI		Mercader et al., 2009 (Fig 5.i)
Blo5	Parallelepiped/cubic/ ovate body, granulate surface (L15-20)	Dicotyledons	Other FI		Albert et al., 2016 (Fig 406)
Blo6	Parallelepiped/cubic/ ovate body, granulate surface (L20-70)	Dicotyledons	Other FI		Albert et al., 2016 (Fig 556)
Blo7	Parallelepiped lacunate body (L15-60)	Dicotyledons	Other FI		Mercader et al., 2009 (Fig 5.h)
Blo8	Blocky body, parallelepipedal irregular, smooth irregular edges, sharp, surface psilate (L15-40)	Dicotyledons	Other FI	Wood	Collura and Neumann (2016) (Fig 7.f.)
Blo9*	Blocky body cuneiform, likely sicilified bulliform cell (L20-30)	Poaceae	Grass (Other G/S)		
Blo10 [NA]	Discoidal/spheroidal psilate body, vaguely fan-shaped (d20-30)	-			

ID	Description	Taxonomical attribution	Environmental signal	Dicot plant part signal (if distinctive)	Bibliography
Blo11	Fan shaped bulliform cells (L-W15-50)	Poaceae/ Cyperaceae	Grass/Sedge (Other G/S)		Albert et al., 2016 (Fig. 2189)
Blo12*	Narrow fan shaped bulliform cells (L40-100,W10-30)	Poaceae/ Cyperaceae	Grass/Sedge (Other G/S)		Albert et al., 2016 (Fig. 2217)
Blo13*	Paralleleipedal. Faceted, sharp edges (L20-80)	Pteridophyta	Fern		Ferns reference collection
Blo14	Blocky irregular, smooth edges, longitudinal facets, surface psilate (L20-60)	Dicotyledons	Other FI		Garnier et al., 2013 (Fig A.b)
Blo16	Blocky body with sinuous edges, psilate surface (L25-50)	Pteridophyta	Fern		Ferns reference collection
Blo17	Blocky body trapeziform, psilate (L30)	-			
Acicular bodies					
Ac1	Acicular body (L16-20)	-			
Ac2	Acicular body, lacunate (L15-20)	-			
Ac3*	Small trichome, half sphere (L<10)	-			
Other structures					
Mes*	Mesophyl dicot cell	Dicotyledons	FI	Leaves	Stromberg 1997(fig 4.4)
Com1	Basal part polygonal prismatic to subcylindric.Scrobiculate margin on top (L15-40)	Commelinaceae	FI		Eichhorn et al., 2010 (Fig.4)
Com2[NA]	Polygonal platelet of Commelinaceae	Commelinaceae	FI		Eichhorn et al., 2010 (Fig.3)
Pap1 [NA]	Papillae	-			
Sto	Stoma (L10)	-			

ID	Description	Taxonomical attribution	Environmental signal	Dicot plant part signal (if distinctive)	Bibliography
Epi1*	Epidermis structure (L30-60)	Dicotyledons	FI	Leaves	Mercader el al., 2009 (Fig 2-l,m,n)
Epi2	Irregular and complex flat bodies with wavy edges and many protuberances. “Puzzle” (L-W>50)	Pteridophyta	Ferns		Ferns reference collection
Undefined					
Und1	Dubious globular	-			
Und2	Dubious body made of imbricate cubes	-			
Und3 [NA]	Dubious silicified haircell	-			
Und4 [NA]	Dubious lacunate or altered body	-			

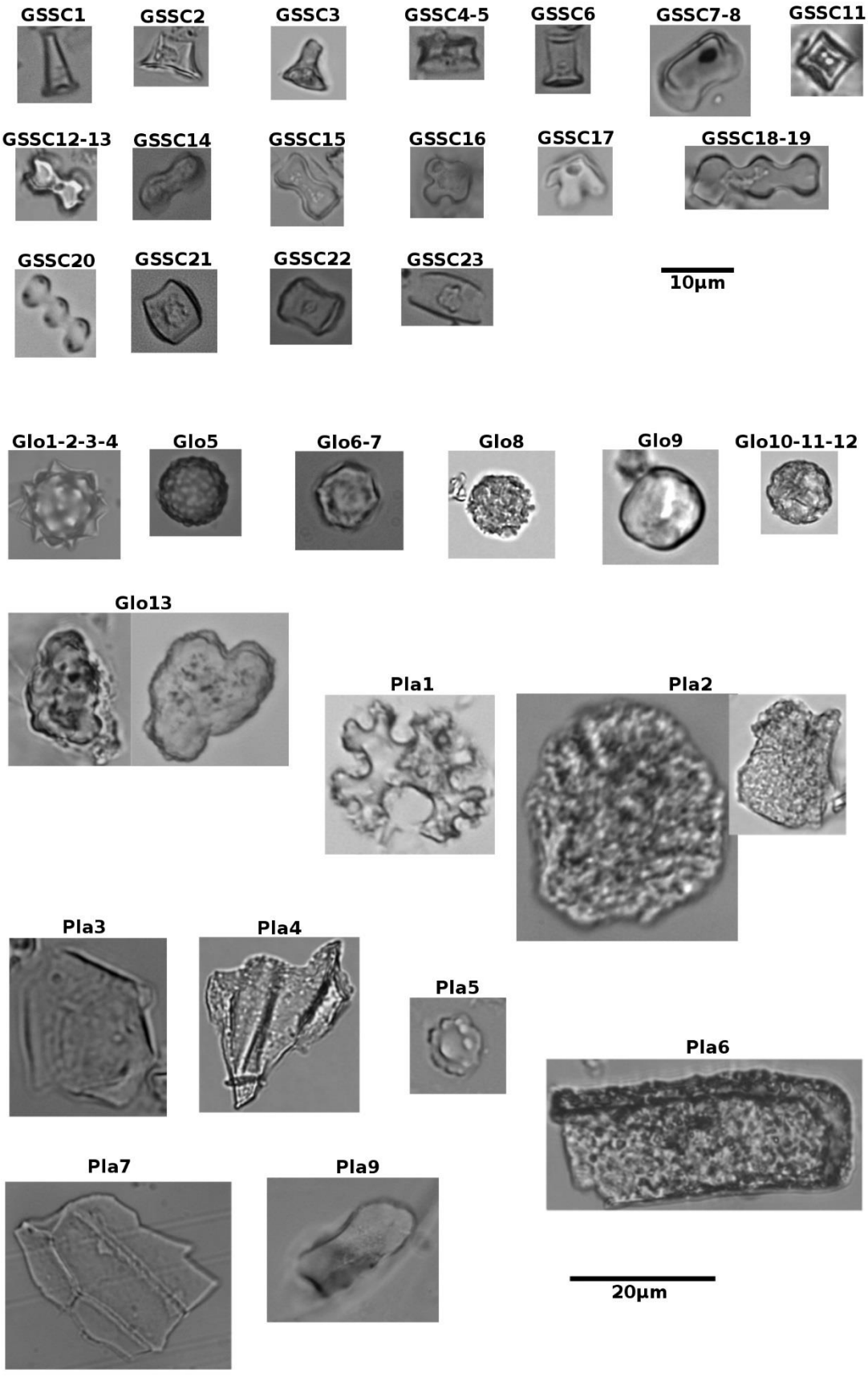

Figure 4.1.1. Selection of photographs of the phytolith morphotypes described in this thesis.

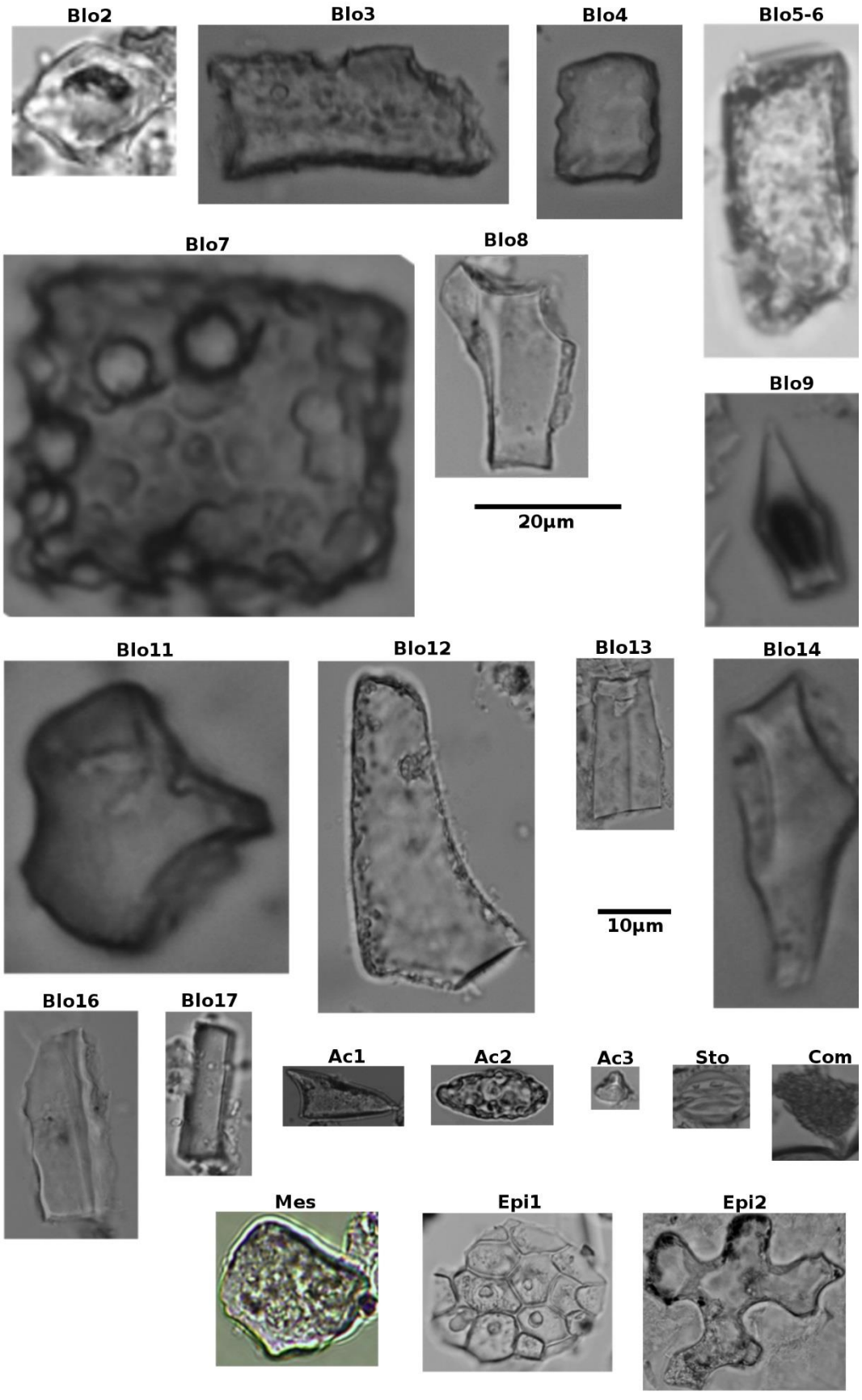

Figure 4.1.1. Cont.

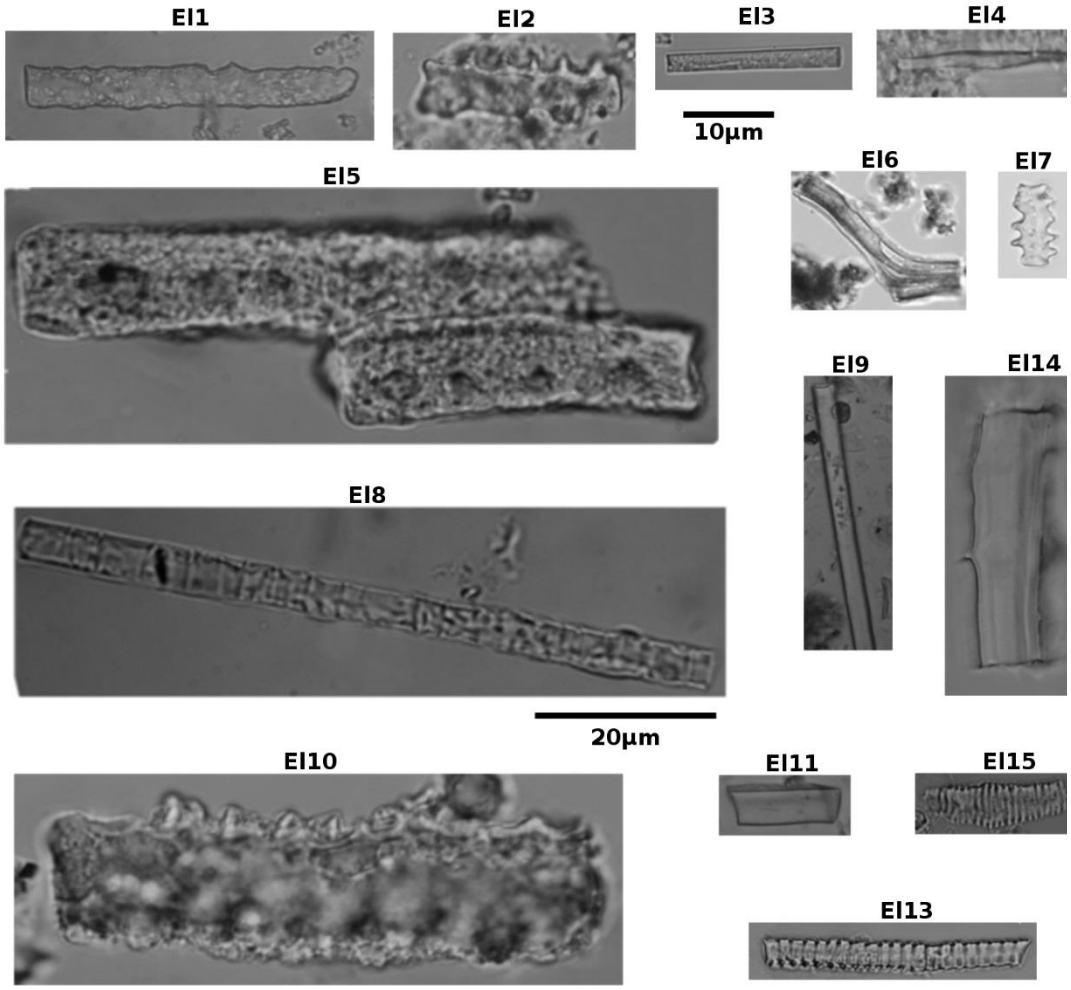

Figure 4.1.1. Cont.

4.1.3 Experimental archaeology based on phytoliths

The experimental archaeological test (to evaluate the random distribution of phytoliths during deposition and the possible bias introduced by laboratory procedures) was carried out under laboratory conditions to avoid the effect of environmental conditions. The experimental soil was prepared with natural soil enriched with the extract of coconut fruit (*Cocos nucifera*). The extract of coconut was produced by treating 50 g of exosperm and outer leaves of coconut fruits with HNO_3 at 80ºC for three hours and thereafter with H_2O_2 at 80ºC for 12 hours. The residue was rinsed with distilled water and then added to two litres of distilled water. This water (with phytoliths) was then poured on the soils, which were then thoroughly mixed for homogenization. The use of a soil rich in grasses ensures the presence of grass silica short cells (GSSC) and the coconut extract provides globular echinate phytoliths.

Stone tools were thoroughly washed with distilled water and sonicated for 15 minutes and then placed in the bucket containing the experimental soil for two months. Tools were placed on top of the soil.

4.1.4 Statistical and analytical approaches on phytolith analysis. Ecological indices

To ensure the statistical relevance of phytolith assemblages, different countings were carried out. In modern samples, countings were carried until reaching 200 GSSC phytoliths per sample to obtain representative groups and indices not biased by the small size of groups (Stromberg, 2009). In paleosols from BK, “Zinj complex”, and in soils and stone tool matrices from FLKW and in experimental stone tools, countings were carried out up to 200-300 phytoliths per sample (when possible).

To evaluate the impact of taxonomy on the representativeness of phytolith assemblages I used a method proposed by Madella and Lancelotti (2012). This method suggests that long cells have a weaker typology than short cells so assemblages with a higher number of long cells than short cells could mean a higher degree of preservation. To compare long cells presence, I used as control data the results obtained from the analyses of the 27 modern soils (**Table 3.1.1**).

To evaluate differences between groups, several statistical analyses were carried out. Tests were performed using the R software (R Core Team, 2013) and the following libraries: ade4 (Dray and Dufour, 2007) and FactoMineR (Husson et al., 2016). Phytolith assemblages were analyzed by grouping phytoliths according to their original morphological descriptions, to large morphological groups (i.e., GSSC, rondels, blocky bodies, elongates, etc) or to possible producers (i.e., forest indicators, palms, grasses, etc.). Multivariate analysis of variance (MANOVA) test (Mathew, 1989) was used to compare all variables (phytolith categories) between two groups. Resampling tests (via permutation) to ensure the statistical significance between groups for which the MANOVA test found a difference (between soils and tools) were carried out. The procedure consisted of two-sample randomization tests based on the Monte Carlo simulation of the two samples being compared. A Monte-Carlo p-value was computed by permutating data 4999 times. This method includes a correction suggested by Davison and Hinkley (1997). Significant p-values (from two-sided tests) show differences between samples obtained across the permutation distribution (all permutation resamples). The correlation between phytolith percentages, indices and ecological features was studied by calculating coefficients of correlation and determination, and by simple and multiple regression analyses (e.g., Shaw, 2003). Unless otherwise specified, the confidence level used is set at 95% as it is commonly used in paleoenvironmental reconstructions (e.g., Lytle and Wahl, 2005). To analyze how variables explain differences between groups (i.e., the different vegetation types in modern soil assemblages), or to observe the similarities between groups (i.e., to compare paleosol samples with modern soil samples), multivariate principal component analysis (PCA) and discriminant analysis (DA) were used. PCA and DA statistical tools are complementary but use different approaches. PCA finds the

variables that explain the maximum variance and DA finds the variables that maximize class separation (Martinez and Kak, 2001).

Phytolith assemblages are often interpreted using ratios (e.g., Barboni and Bremond 2009; Bremond et al., 2005). The relationship between phytolith ratios or indices with ecological characteristics of the environment (e.g., woody cover) provides a way to interpret the fossil assemblages. For the analysis of modern samples and paleosols from BK and "Zinj complex". I used three phytolith indices:

D/P (Bremond et al., 2005a) index is the ratio of the sum of globular rugose, globular microechinate and globular echinate phytoliths, over the sum of GSSC phytoliths to evaluate woody cover. This index is calculated as follows:

$$D/P = \frac{\text{Glob. echinate (Glo1-4)} + \text{Glob. microechinate (Glo5)} + \text{Glob. granulate (Glo10-13)}}{\Sigma\ \text{GSSC}}$$

Ic index is used to compare several groups of Grass Silica Short Cells to describe grassland composition with regard to the ratio between Pooideae and all the grasses. (Barboni and Bremond, 2009). This index is calculated as follows:

$$Ic = \frac{\text{Rondel >15 µm (GSSC5, GSSC8)} + \text{Polylobate tabular (GSSC18-20)}}{\Sigma\ \text{GSSC}}$$

Iph index (humidity-aridity index) is a good proxy to estimate moisture in the environment by comparing Chloridoideae short cell phytolith types relatively to the sum of Panicoideae and Chloridoideae short cell phytoliths (Barboni and Bremond, 2009; Bremond et al., 2008, 2005b). This index is calculated as follows:

$$Iph = \frac{\text{Saddle (GSSC21-23)}}{\text{Saddle (GSSC21-23)} + \text{Cross (GSSC16-17)} + \text{Bilobate (GSSC12-15)}}$$

In order to evaluate the relationship between phytolith groups and D/P index to the tree cover, photographs of the canopy from modern soil sampling points were taken. Photographs were taken by Doris Barboni in Olduvai at 2011 by using a camera equipped with a fisheye lens in forested environments, fisheye lens was positioned at a height of 130 cm from the ground. Height was set at 70 cm in woodlands and grasslands by adjusting the tripod length. Color images were converted into grey images, in which each pixel contains the information of light intensity. Grey images were converted into black and with images by calculating the optimal threshold in which the variance between black and white, and grey pixels is minimal. To convert the black and white images in % of canopy cover we used Otsu's method (Otsu, 1979). Canopy was calculated by measuring the proportion of black pixels in the image (**Figure 4.1.2**). The tree cover measurements were performed using MATBLAB®, and they were conducted by Philippe Dussouillez at CEREGE (France).

4.2 Starch analysis

4.2.1 Starch extraction procedures and anti-contamination measures

For starch granule extraction I used the protocol suggested by Perry (2010), compiling and modifying previous works by Loy (1994), Perry (2001) and Piperno (2009). This methodology was used in paleosols from FLK-West. The sediment which adhered to stone tools was sampled by brushing. Three samples were lost during laboratory procedures, so just 39 sedimentary adherences were analyzed. Internal matrices from cracks and micro-cavities of stone tool surfaces (previously brushed) were recovered by sonication of the tools. Clays were deflocculated using a solution of sodium hexametaphosphate $(NaPO_3)_6$ at pH 7, and removed by decantation. Starch remains were separated from matrices and sedimentary adherences by heavy liquid flotation (with sodium polytungstate) at 1.8 g/cm^3. Then, supernatants were concentrated by the addition of ultrapure H_2O and centrifugation. Slides were prepared using glycerol-water (50/50) as mounting medium and sealed with nail polish.

For starch granule extraction from plants, plant samples were macerated (12h in ultrapure water), then crushed and sonicated for 10-15 minutes. The mixture was sieved at 150 μm and then centrifuged. The residue was mounted in a water and glycerol mixture (50/50). Slides were sealed using nail polish.

Contamination with modern starch granules is common (Crowther et al., 2014) and test are therefore necessary to ensure that recovered starch granules from lithics are fossil material anti-contamination measured were implemented. I followed standard protocols and sterilized of the laboratory. Precautions were taken also during excavations and sampling in the field (Loy, 1994; Piperno, 2006). In the lab I tested surfaces (workbenchs and soils), equipment (hoods, centrifuges, shakers, pHmeter, microwave, refrigerator, scale, shaker sonicator and autoclave), autoclave or boiled tools/reactives (beakers, tips, slides, coverslips, Eppendorf tubes, sodium

polytungstate and ultrapure water), and no autoclave or boiled tools (vinyl and polystyrene gloves, Falcon tubes and nail polish). Also control test extractions (blank test, using all reactives and performed with all steps but without sample) were carried out. Modern starch granules were found on laboratory surfaces and equipment (78 granules) but just two granules were found in the sterilized material that was directly in contact with samples. No granules were found in blank tests (**Appendix 4.2.A**).

4.2.2 Microscopical and statistical analysis of starch samples

All the residue from FLK-W paleosols, stone tools' adhering matrices, stone tools' internal matrices and anti-contamination test starch extraction was mounted on slides and observed at 400x magnification with the same optical equipment used for phytolith analysis (see 4.1.4 "*Microscopical observations*"). All the starch granules found in the fossil material observed were photographed except when the sediment made it impossible to take a clear view. Starch identifications were made by comparing them with published photographs and descriptions (e.g., Mercader et al., 2009; Reichert, 1913) and with our own plant reference material. Starch descriptions follow the International Code for Starch Nomenclature (ICSN, 2011).

To measure if the frequency of appearance of the starch granule remains on the stone tools matrices, and if paleosols, surrounding soils and anti-contamination samples were significantly different, an analysis of variance (ANOVA) test was carried out.

4.2.3 Starch automated identification system

This project has been carried out in collaboration with Luc Beaufort and Nicolas Barbarin (CEREGE, France) who have developed this system of automated morphometry for coccolithophores.

Image acquisition

The reference image collection is composed of starch granules randomly selected from the slides photographed in natural light and in crossed-Nichols using an automated light microscope (Leica DM 6000B© with a Spot Flex Mono 15.0© camera) and following the methodology described in Beaufort et al. (2014). Four images were taken for each granule: one under natural light and three under different polarization angles (0°, 35°, and 45°). The three polarized images were then combined to suppress the extinction pattern of the starch (**Figure 4.2.1**), so that for each starch granule, two images were used for feature extraction. For each species, 180 to 240 granules photographed. In total, the reference image collection includes 5028 different starch granules. i.e., 20112 pictures (under polarized and natural light).

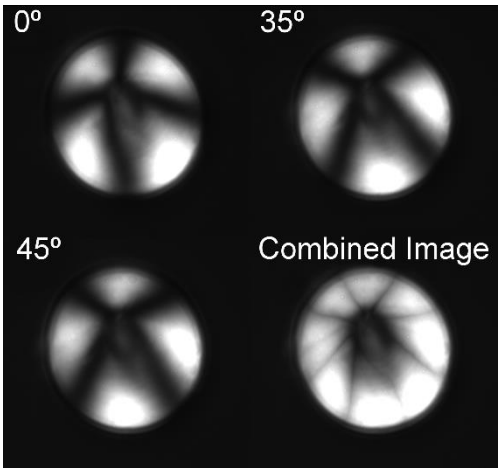

Figure 4.2.1. Combination of three polarized photographs (0°, 35°, 45°) of a *Portulaca oleracea* starch granule to suppress the extinction cross.

Feature extraction and measurements

Starch granules were individually segmented from the images using a threshold detection method under polarized light by computing the average of the clustering and metric algorithm and using an edge detection method under natural light (**Figures 4.2.2 and 4.2.3.**). Measurements were then applied to the images of the same individual in polarized and natural light. This second step extracts 123 descriptive parameters (characters), such as the area, the major and the minor axes of the fitted ellipse, their ratio (i.e., ellipticity), the circularity, the presence or absence of a central depression (with area, axes length etc.), the relative mass using the methodology from Beaufort et al. (2014), the extracted profile from the major axis which gives the number of major intensities, a degree-9 polynomial curve that is fitted to this profile, some measurements on the outline (length, regularity, spectral analysis, flattening etc.), measurements of the texture of the object with Haralick features (Haralick, 1979; Haralick, et al., 1987) and some classic signal analysis on the pixel intensities of the object (spectral analysis, regularity, flattening etc.) (Barbarin, 2014) (**Appendix 4.2.B**). In using this classification system, I have not considered some of the characters used in the classical taxonomic identification (e.g., fissures, lamellae surface) for several reasons: firstly, because these characters may be subjective (i.e., some analysts

will see a crack others will not, and fissures can be confused with simple cracks), and secondly, because these characters need extensive coding to be measured objectively. Other characters, such as features related to the polarization cross, were not used because cross shape and size vary depending on the point of focus. Similarly I have not measured the hilum because its position is also related to the extinction cross, and the presence of the hilum can be masked by the point of focus.

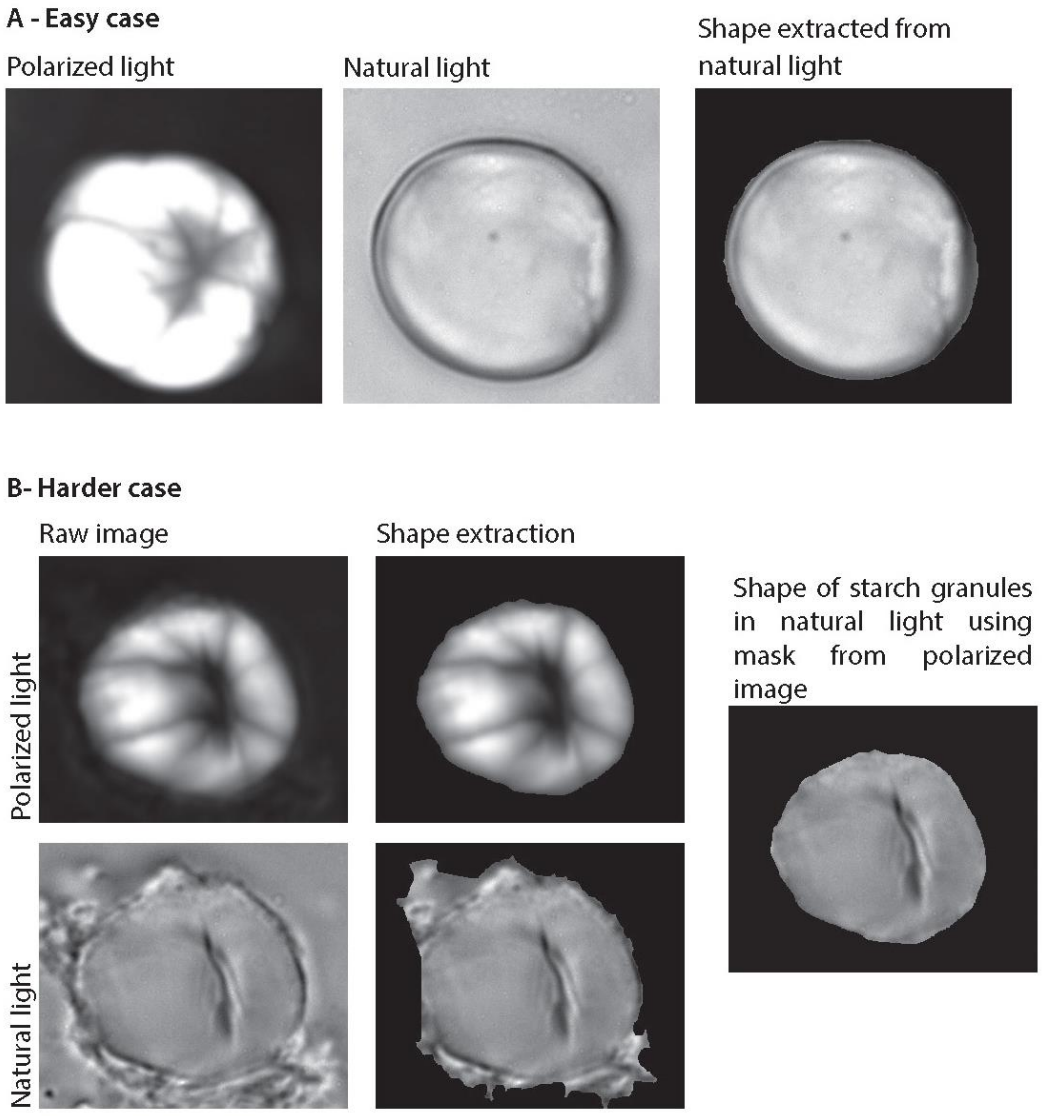

Figure 4.2.2. Differences between an easy and a hard outline extraction case. Advantages of the use of images under polarized light.

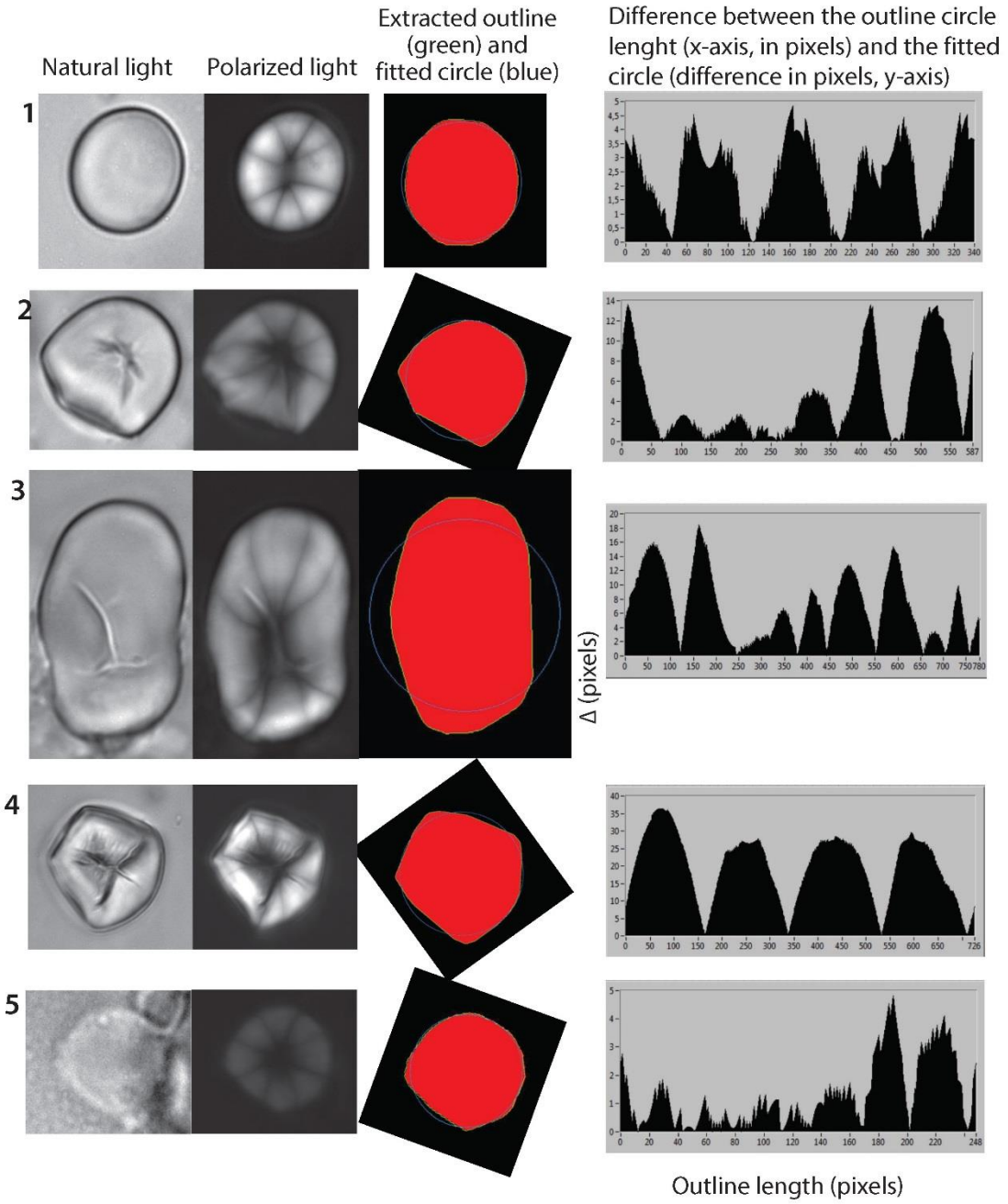

Figure 4.2.3. Photo of different sized and shaped starch granules in natural and polarized light, the extracted binary image and the extracted outline. 1: *Cyperus rotundus*, 2-3: *Vigna vexillata*, 4: *Faidherbia albida*, 5: *Persicaria senegalensis*. The example 5 shows the advantage of using the polarized light to extract the shape. The (absolute) difference between the outline of the granule and its fitted/normalized circle permits to measure the shape of the granule. If it is perfectly round, the difference will be very small (less than 5 pixels) and, confused with the noise of few pixels (Example 1 is round and regular and 5 is also round but irregular). If the granule has a more complex shape, the variations (of number of pixels) will reflect it with larger variations and asymmetry (examples 2, 3 and 4). The larger variations express the global shape but the smaller variations express if a face is flattened or rounded. Some parameters are measured to quantify those variations (length, kurtosis, skewness, mean, standard deviation, fundamental frequency, amplitude, SINAD, frequency, phase...).

Tests and statistical classifications

Statistical analyses were performed using the R software (R Core Team, 2013) with the following libraries: ade4 (Dray and Dufour, 2007) and rattle (Williams, 2011). Random Forest (RF) tests were used to identify the most discriminant characters and RF confusion matrices were used to evaluate the classification system (Breiman, 2001). RF has been repeatedly shown to be the best algorithm classifier available to date. Even when compared with neural networks, trees, multiple regression, multiple discriminant analyses or other classifying methods, RF systematically scores higher classification rates. The only algorithm that performs better than RF is C5, but this last algorithm is only effective when dealing with large numbers of variables. In contrast, RF performs equally well when variable number is limited. RF is also not affected by processes such as non-lineal distribution of variables or, most importantly, collinearity, which is the number one handicap of multiple regression. For full discussion see Kuhn and Johnson (2013). We used discriminant analysis to explain the correspondence between characters and the different groups (defined according to taxonomy -species, families- or to part sampled -seed, mesocarp, underground storage organs-) (**Table.3.1.2**) (Shaw, 2003). An additional RF test was performed only with herbaceous species, namely Poaceae, Typhaceae and Cyperaceae. Herbaceous species were chosen for their phylogenetic proximity and their identification reliability using phytoliths.

Given the size of the dataset in terms of the number of granules, the number of characters, and the numbers of groups to identify, I carried out several tests. Based on previous work, which showed that grains measured in centric view provided unreliable identifications (Torrence et al., 2004), I checked whether excluding small (<5µm), irregular granules looking like transient granules (Buléon et al., 1998), as well as round and centric oriented granules would improve the classification system. I retained for the analyses all the granules for *Adansonia digitata*, *Brachiaria deflexa*, *C. rotundus*, *Persicaria senegalensis* and *Setaria pumila* because these species produce almost exclusively round granules.

In order to test whether a selection of characters could improve the discrimination of groups, I calculated the average rate of correct allocations, firstly by using the 24 most important characters (i.e., those with the highest RF test values), (**Appendix 4.2.C**) and, then, by using a random selection of a number of characters (from 10 to 123). In order to test the correlations between the numbers of characters, the numbers of groups and the average ARI for the starch granules of the reference collection, I created 32 datasets of two to 19 species randomly selected.

Finally, to evaluate the strength of this automated method against the most widely used human eye identification, I performed a blind test based on the recognition of 189 randomly selected granules from the set of photographs used in the statistical analysis, and within these, those photographs showing the classical characters that could allow for proper identification. On average, 10 photos per species were tested (range 2-11 species).

5. The phytolith signal of present-day soils and plants

5.1 Modern soils analysis

Description of phytolith assemblages

In the 22 modern soil samples collected in the Olduvai-Eyasi-Manyara-Hadzabe region, 67 phytoliths morphotypes were described **(**summarized in **Figure 5.1.1**). Most types could be attributed to a possible botanical producer group/signal (**Figure 5.1.2**). Detailed phytolith counts are given in **Appendix 5.A.**, along with measured canopy.

Phytoliths attributed to forest indicators (hereafter "FI") are dominant in most samples (μ=39%±10%, range: 13-58%). Phytoliths from grasses and sedges are the second largest group represented (μ=33%±11.7%, range: 15-64%). Palm phytoliths occur in 17 samples with a mean value of 5%±6.8% (range 0-27%). Fern phytoliths are present in 14 out of 21 samples in small proportions (μ=1%±1.5%, range: 0-6%). Non-diagnostic phytoliths reach a high percentage in most samples (μ=23%±10.9%, range: 5-42%). The most common FI phytolith types are sclereids, described as irregular blocky bodies with facets (including globular granulate bodies) (Glo-13), that are present in all samples. Among the GSSC the most common categories are rondels and bilobates. Diatom remains are present, in most samples, with values under 5% (relative to the total of silica remains), except for three samples from swamp environments (E58, M71 and M72), in which diatom percentages are above 20%.

Figure 5.1.1. Relative abundance in percentage of phytoliths grouped by morphological groups. Percentages of diatoms are calculated on the basis of the sum of diatoms plus phytoliths.

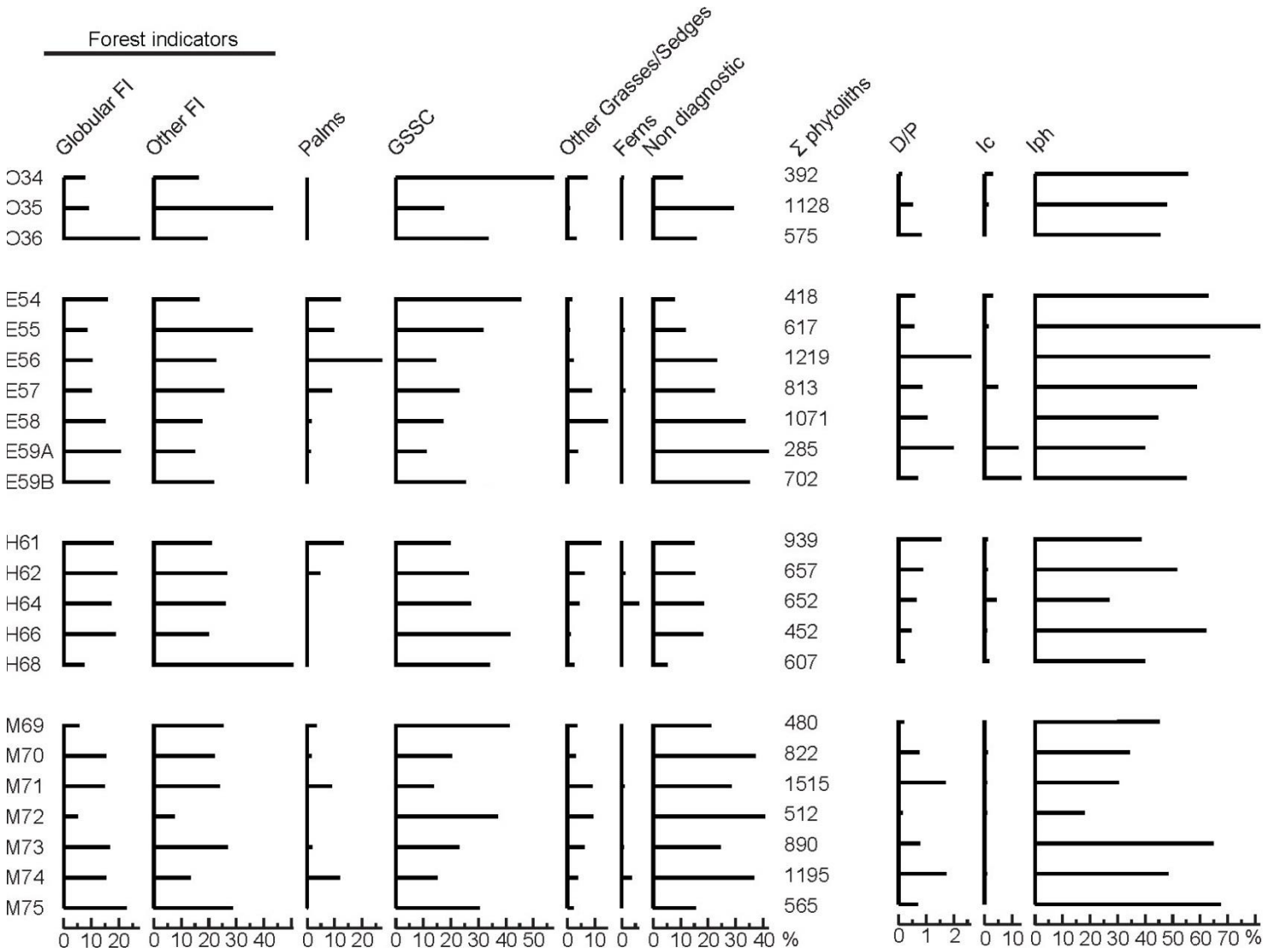

Figure 5.1.2. Relative abundance in percentage of phytoliths grouped by botanical attribution and ecological index values.

Samples from Olduvai Gorge (n=3, O34 to O36), placed along a transect from the steppe (O34) to the escarpment area (O35) and to the seasonal river bed (O36), exhibit values up to 50% (O35) for FI phytoliths, in agreement with the presence of bushes and *Acacia* trees. Riparian wooded bushland O35 is rich in "parallepiped/cubic body, sinous edges, psilate surface" (Blo4) and riparian woodland O36 is rich in globular decorate phytoliths (Glo5-13). O34, a grassland with rare small *Commiphora* trees, shows a value of 64% for grasses phytoliths (57% of GSSC). Palm phytoliths are absent in these assemblages, in agreement with the absence of palms in the present-day vegetation sampled in the area of BK site at Olduvai Gorge. Despite the significant presence of unidentified sedge species in the grassland at O34 sampling site, we did not observe hat-shaped -Pla5- (Cyperaceae) phytoliths.

Samples on the northeastern end of Lake Eyasi (n=6, E54 to E59B) represent spring associated woodlands (E54-57-59B) and *Typha* swamps (E59A). FI phytoliths represent ~40% in most samples. The highest variations in assemblages are shown in grass-sedge phytoliths (17% to 47%), with a notable presence of rondel phytoliths (GSSC1-10). Palm phytoliths (Glo1-5) are present in samples where *Hyphaene* plants occur, and are absent where the latter were not described (E59B). Gorofani sample (E59B) represents a highly disturbed spring forest, and E54-E57 represent Eyasi woodlands rich in *Acacia* and Palms. Small differences between these two types of vegetation are observed (acicular bodies (Ac-Ac3) are present in Gorofani in higher percentages than in Eyasi samples, and diatoms are almost absent in Gorofani sample but considering the large variability observed in samples E-54-E57 and the fact that E59B is the only sample from Gorofani, it is not possible to observe major differences. In the sample E59A (*Typha* swamp) FI phytoliths duplicate percentage of grass-sedge phytoliths (36% and 15% respectively), but non-diagnostic phytoliths represent 42% of total assemblage, so these values are not significant.

Samples from Hadzabe territory (n=5, H61 to H68) cover a variety of woodlands in the Mbulu Highlands between lake Eyasi and Lake Manyara. H61 and H62 were collected in a riparian woodland with a large variety of dicotyledonous trees. The percentages of FI and grasses are almost equal for both samples (39% and 46% respectively), but H61 shows higher percentage of palm phytoliths (13%) than H62

(5%), and H64 is a wooded grassland in which FI phytoliths represent 40% and grass-sedge phytoliths 32%. This difference is not significant. In this sample, the percentage of fern phytoliths is up to 6%. H66 sample was collected in a woodland dominated by grasses and *Adansonia* (baobab) trees. Grass phytoliths represent 43% of the assemblage and FI 39%. H68 was collected in a woodland located on the occasionally flooded Yaeda swamp. FI phytoliths clearly dominate the assemblage (58%, being the most of them non-globular FI) and grass phytoliths represent 37% of the assemblage.

Samples from Lake Manyara (n=7, M69 to M75) are related to wet environments and were sampled on the northern end of the lake. M71 and M72 are swamp herbages, but M71 is a small patch enclosed in the groundwater forest. M71 is dominated by FI phytoliths (39%), and M72 phytolith assemblage is dominated by grasses, which represent 46% (37% GSSC), whereas FI phytoliths represent 13%. Both samples (M71 and M72) are rich in diatom remains. M70 and M73 are groundwater forests whose phytolith assemblages are dominated by FI phytoliths (FI ~40%, grasses-sedges ~25%). M70 and M73 assemblages are similar to M71 phytolith assemblage (except for palm phytoliths: 9% in M71, <2% in M70 and M73). Sample M69 was also collected in a groundwater forest, but the assemblage reflects a great amount of grass phytoliths (45%). M74 is a sample from a forest fringing a perennial spring-fed stream in which FI phytoliths represent 29%, grass-sedge 19%, and palm phytoliths 12%. M75 represents an exception in Manyara samples because it was collected in a woodland non-related to water in which FI are clearly dominant, reaching up 52%.

Phytolith indices and multivariate analysis. Relationship with ecological features

In the studied samples, D/P index (the ratio between the sum of globular rugose, globular microechinate and globular echinate phytoliths, and GSSC phytoliths, see **chapter 4.1.4**) ranges from 0.1 to 2.5 ($\mu=0.9\pm0.6$). Sixteen out of 21 samples have D/P values lower than 1, which theoretically represent grass-dominated habitats. The D/P values obtained in the modern samples represent more likely open spaces. Low D/P

values <1 are typical for African grasslands (Alexandre et al., 1997; Bremond et al. 2005a, Novello, 2012) and in riparian forests where trees and shrubs are scarce (Barboni et al, 1999). The low values obtained in our results can be explained by the likely over-representation of grasses in phytolith assemblages. For the studied region, the correlation between D/P index and canopy cover was calculated using tree cover values measured at the sites. The coefficient of correlation (r=0.72) shows that there is a correlation between this two variables, but the coefficient of determination (R^2=0.504) does not allow to use this correlation to make accurate inferences based on regression analysis. Even if these inferences are significant (p-value=0.0005), the confidence interval is too large (**Figure 5.1.3**). The coefficient of determination between GSSC percentage and tree cover (R^2=0.528) is slightly (but not significantly) higher than in the previous correlation. Percentage of GSSC and D/P index cannot be used together in a multiple regression to infer tree cover because these two parameters are collinear. Hence, inferring canopy cover based on D/P index only is not sufficient. Regression can be used cautiously and assuming that the error of estimation will be large for an acceptable level of confidence. In previous studies, D/P index seem to be best correlated with other ecological features that measure tree cover as Leaf Area Index (LAI, m^2 of leaves per m^2 of ground) (Aleman et al., 2012, Bremond et al., 2005a), so our low values of correlation could be caused by the method chosen to measure canopy cover, rather than to the lack of correlation between D/P index and tree cover.

Iph index varies from 18% to 80% (μ=50%±15.3%). Most samples exhibit Iph values >40% in agreement with the abundance of xerophytic grasses in the Olduvai-Nogorongoro-Manyara-Eyasi region. Five samples have values below 40%, which is considered the limit between grasslands dominated by Panicoideae with warm and humid climate and moist soil conditions (<40%), and grasslands dominated by Chloridoideae with warm and dry climatic conditions (Bremond et al., 2005b; Novello et al., 2015). Three of the five with Iph index values below 40% were sampled near Lake Manyara (M70, M71 and M72). These values are in agreement with the presence of Panicoideae species such as *Cenchrus, Digitaria, Panicum, Brachiaria, Cymbosetaria*, etc., which are common in the *Acacia* groundwater woodlands at Lake

Manyara National Park (Greenway, 1969; Loth and Prins, 1986). In our samples, the values of Iph index seem to reflect the climatic conditions of the area rather than the water resources.

Ic index varies from 1% to 13% (μ=2%±2.9%) in agreement with the fact that present-day communities are dominated by, low-elevation, non-Pooideae (high elevation) grasses at the sampling sites. In the Olduvai-Nogorongoro-Manyara-Eyasi area Chloridoideae are well represented, e.g., *Cynodon* and *Sporobolus* are the most abundant grasses in the *Acacia* groundwater forest of Lake Manyara communities (Greenway, 1969; Loth and Prins, 1986), and *Sporobolus* predominates in the low woodlands of the western section of the gorge (Herlocker and Dirschl, 1972).

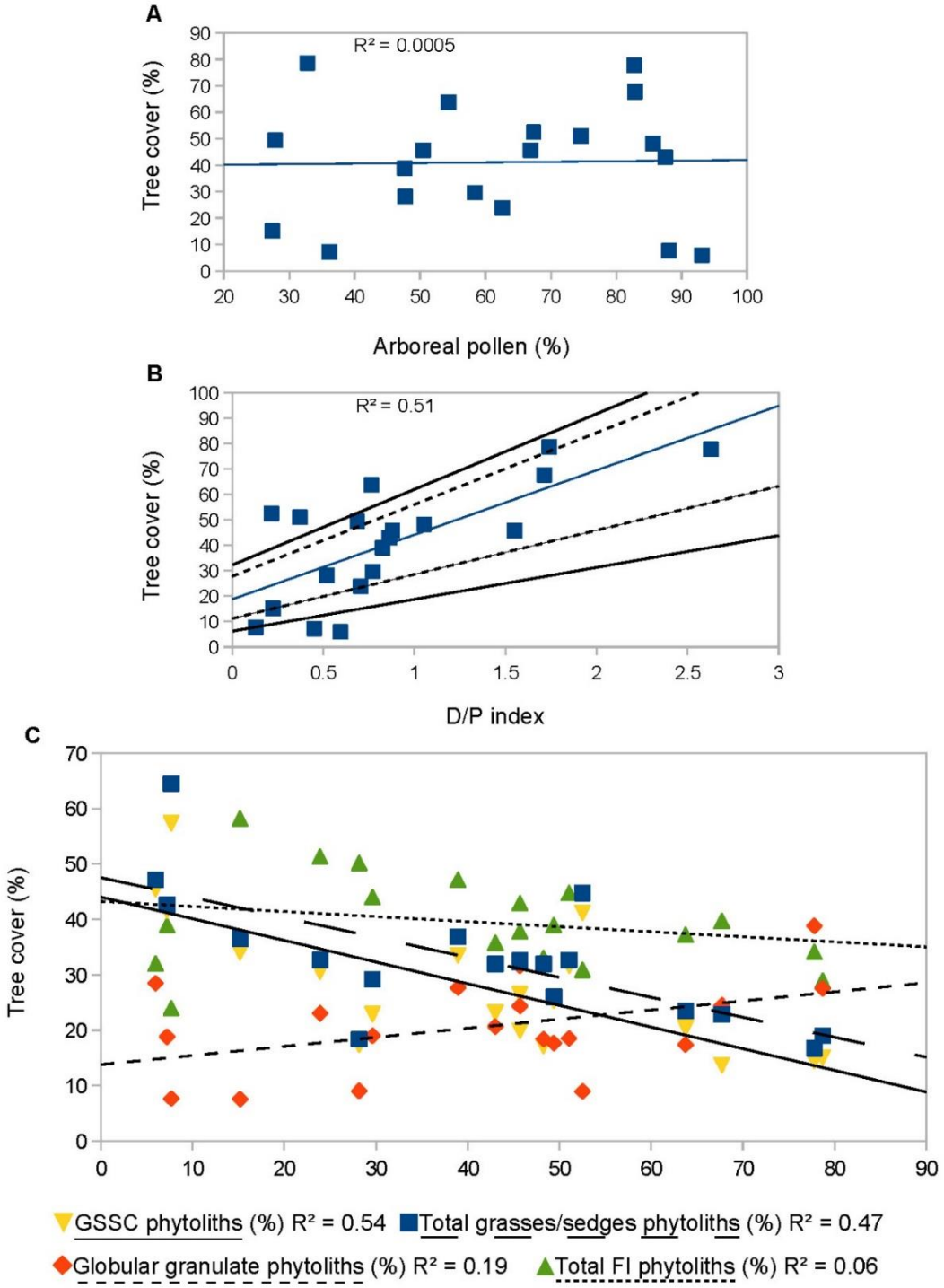

Figure 5.1.3. (A) Correlation between the percentage of arboreal pollen and tree cover. (B) Correlation between D/P index values and canopy cover. Solid lines indicate 95% confidence interval. Dotted lines indicate 80% confidence interval. (C) Correlation between the percentage of GSSC, total grass/sedge, globular, and FI phytoliths and tree cover.

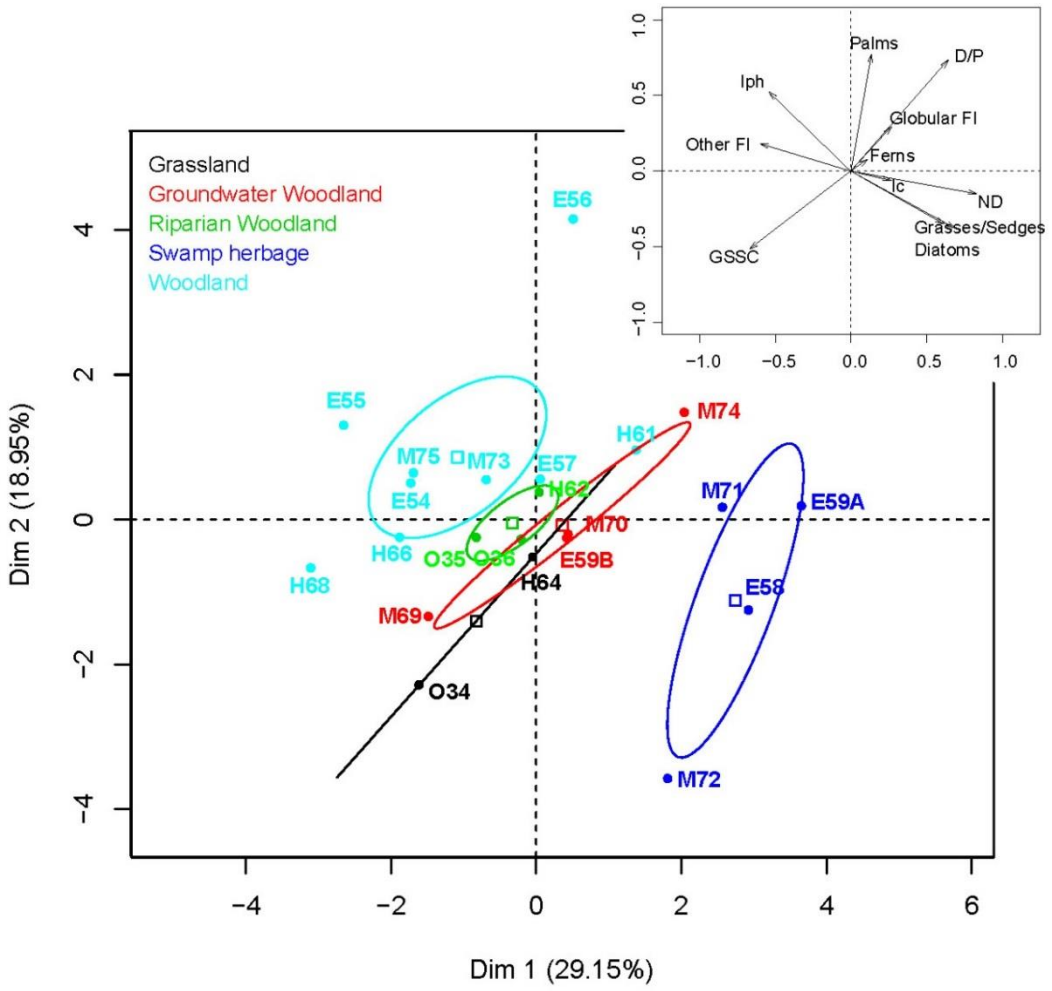

Figure 5.1.4. PCA showing differences between our modern samples grouped by vegetation type. Arrows figure shows the relative significance/importance of the different variables.

PCA analysis using percentages of all phytolith categories indicates that the first two axes explain 24% of the variance. A second PCA using FI phytoliths indicates that the first two axes explain 23% of the variance, and no separation between wooded environments was found. Another PCA using plant groups (globular FI, non-globular FI, palms, GSSC, other grasses/sedges, ferns and non-diagnostic phytoliths), percentage of diatoms, and the indices (D/P, Ic and Iph) explains more of the variance (48% with axes 1 and 2). In the third analysis, different vegetation types tend to be distinguished (**Figure 5.1.4**). Vegetation types are better discriminated when large morphological groups and indices are used, instead of detailed morphological groups.

To confirm the results obtained in PCA analysis, a discriminant analysis (DA) was performed (**Figure 5.1.5**). PCA and DA plots show that swamp herbages are clearly discriminated by the phytolith category "other grasses/sedges" (which includes bulliform cells and non-GSSC morphologies attributed to grasses/sedges) and "diatoms" components. Woodlands are separated from riparian and groundwater woodlands by "Palms" and "D/P" components (some "woodland" outliers are woodlands in which palms are present, e.g., E56, E57 or H61). Riparian and Groundwater woodlands are not separated in PCA. Grasslands are separated by GSSC. H64 grassland is placed within groundwater woodlands, but this is explained considering that it is a grassland with more wooded vegetation than O34 grassland. As expected, a correlation between "D/P", "palms", and "globular FI" is observed in PCA analysis. On the contrary "other FI" are slightly correlated to these components (positive values of Y axis), but also to "GSSC" (negative values of X axis). The "other FI" component is particularly related to E54, E55, M73 and M75 woodlands. This unexpected result does not appear in the results of DA, and, analyzing in detail the phytolith assemblages, we do not find any particular morphology that explains the PCA result.

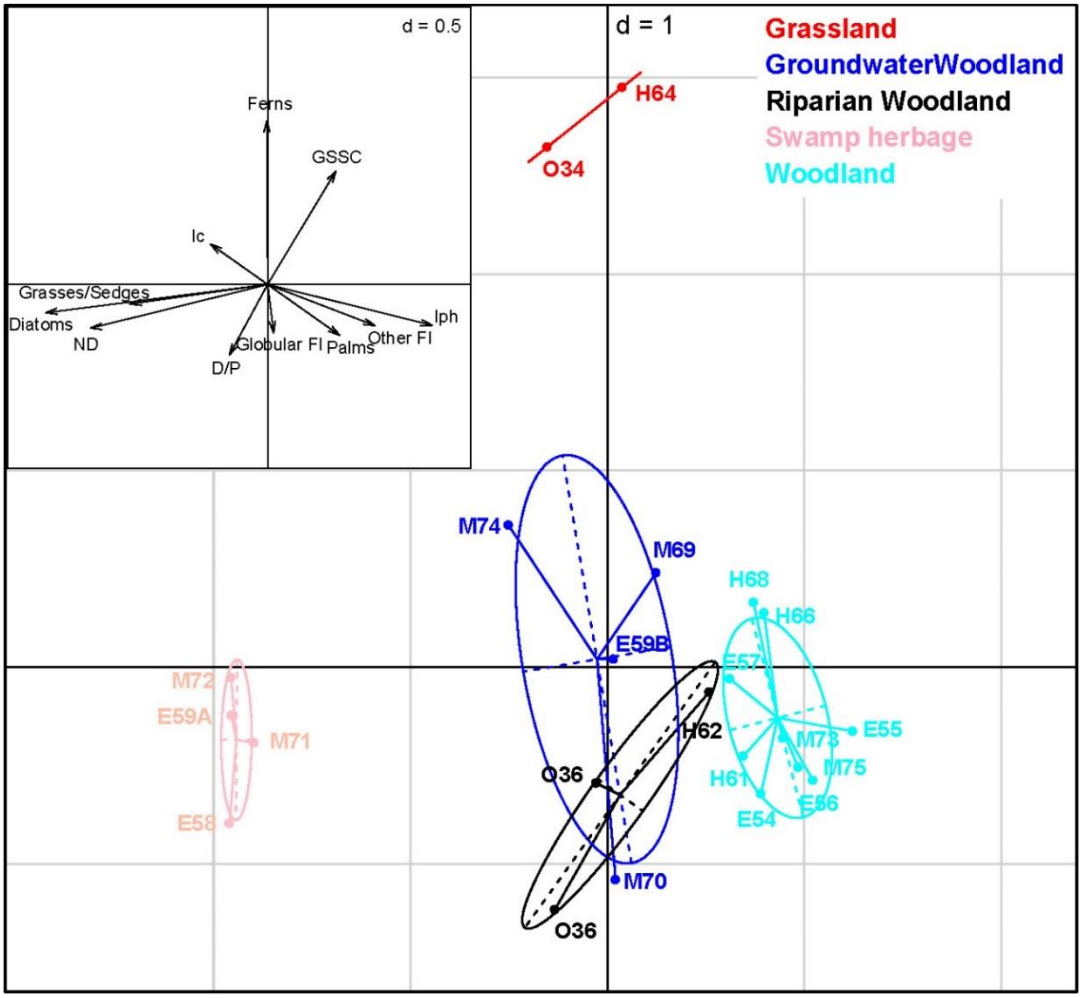

Figure 5.1.5. Discriminant analysis showing differences between samples grouped by vegetation type. Ellipses show 95% confidence interval. Arrows figure shows the relative significance/importance of the different variables.

Our samples were analyzed together with 134 modern soil samples of different environments from Cameroon (Bremond et al., 2005a), Chad (Novello, 2012), Democratic Republic of Congo (Runge, 1999), Ethiopia (Barboni et al., 1999), Kenya (Bremond, 2003), Mauritania (Bremond et al., 2005b), Senegal (Alexandre et al., 1997; Bremond et al., 2005b) and Tanzania (Bremond, 2003). To standardize samples, we only compared the morphological categories which were undoubtedly considered in the same way. These phytolith categories are: globular smooth, globular echinate, globular granulate, rondel shortcells, bilobate shortcells, cross shortcells, saddle shortcells, polylobate shortcells, trapeziform shortcells, and bulliform cells. D/P, Iph

and Ic indices were also used as variables. D/P index was recalculated in all samples to standardize values with the formula used in this thesis (which uses globular echinate phytoliths, but not globular smooth phytoliths). The environmental diversity of 156 samples was grouped in seven categories: Dune vegetation (n=2), fern ecotone (n=3), grasslands (n=22), wooded grasslands (n=64), swamps (n=11), woodlands (n=39), and moist woodlands (n=15). In the PCA performed using 156 samples (**Figure 5.1.6, Appendix 5.B**), the two first axes explain 45% of the variance. The 95% confidence ellipses are clearly separated, but most of the samples are outside these ellipses. "Wooded grasslands" are separated by "saddle", "cross", and "bilobate" shortcells, and "bulliform cells", "grassland" are separated by "Iph", but also slightly by "saddle" and "cross" shortcells. Woody environments (i.e., "moist woodlands" and "woodlands" are separated by globular phytoliths ("echinate", "smooth", and "granulate") and "D/P index". Finally, "swamps" are slightly separated by "globular smooth" phytoliths. The "diatoms" component that separated swamps in the 22 samples PCA is not considered now, so it can explain the weak separation of "swamp" samples. The 22 samples from Olduvai/Manyara/Eyasi/Hadza ("Olduvai surroundings") fall near the woody samples, which indicates the influence of woody plants even in environments rich in grasses. Also, the woodlands from Olduvai surroundings are plotted closer to the "humid woodlands", rather than "woodlands", which can be explained by the climatic conditions of the area, which affect all the samples from the same region. A PCA performed grouping the 156 modern soil samples by country (**Figure 5.1.7, Appendix 5.B**) shows that the variability reflects geographical areas instead of vegetation types. These results suggest that the use of multivariate statistics should include samples of the same climatic region as those samples that could be analyzed to infer vegetation structure, and should also include a large number of modern samples from different environments to infer climatic conditions.

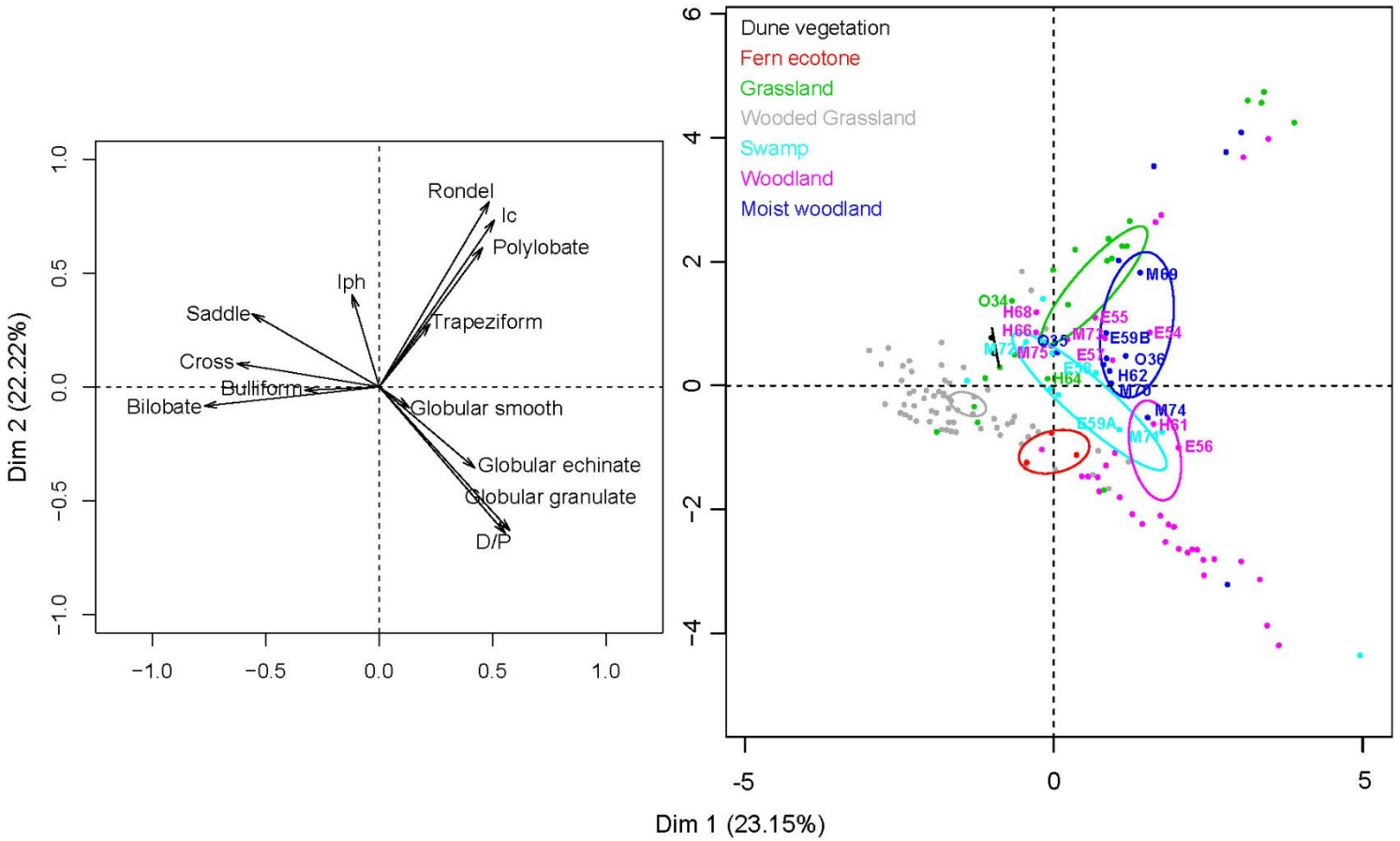

Figure 5.1.6. PCA showing differences between 156 African modern vegetation samples grouped by vegetation type. Arrows figure shows the relative significance/importance of the different variables.

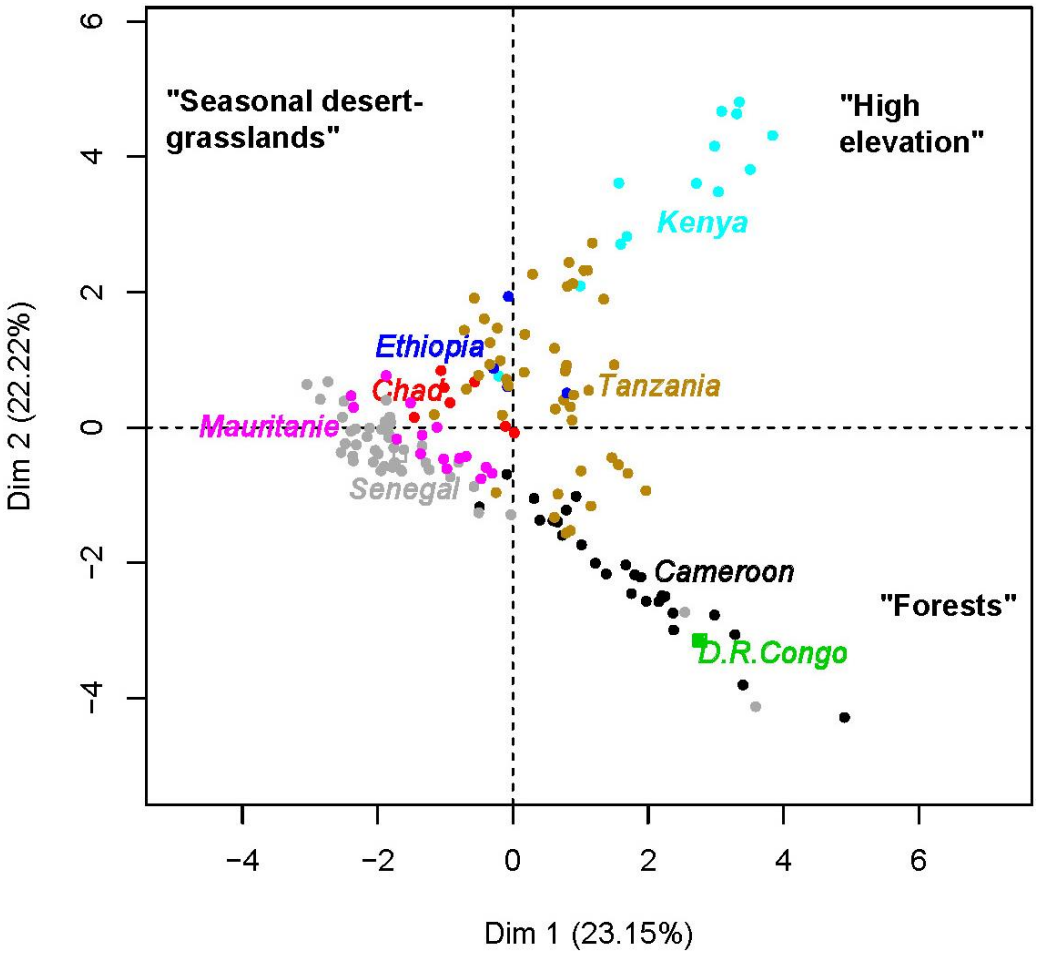

Figure 5.1.7. PCA showing differences between 156 African modern vegetation samples grouped by country. Quotation marks indicate main vegetation characteristics.

Are phytolith assemblages and indices good enough to infer vegetation patterns?

In broad terms, phytolith assemblages do not reflect accurately the vegetation that produces them. It must be noted that the assemblages reflect, less than expected, the composition of the vegetation, and the variation of several factors between different types of vegetation is subtle. It also has to be taken into account that vegetation inferences are more accurate when phytolith assemblages show one specific signal as clearly dominant over the others (e.g., 90% signal A and 10% signal B), as suggested by Stromberg (2009). Considering that the statistical approach is able to find

patterns that cannot be appreciated with "classical" analyses, it is mandatory to use statistics (e.g., multivariate PCA or DA tests) to handle this subtle differences and the large number of distinctive variables, to discriminate different environments and to infer past vegetation from paleosol samples.

In the studied samples, woody plants have a not-so clear representation in assemblages. Although phytoliths indicators of forest environments are very abundant (especially globular phytoliths [Glo 10-13], which occur in all assemblages, and represent almost half of FI), it is not possible to properly infer the amount of woody vegetation present at the sampling sites. Woodland-wooded bushlands (samples E54, E55, E56 E57, H68, M69 and M75) are not well defined according to the main phytolith groups. In woodland-wooded bushlands samples (E54, E55, E56 E57, H68, M69 and M75) FI percentage ranges from 31% to 58%. This is also well shown by D/P index. These inconsistent results have been shown by previous studies (Neumann et al., 2009; Novello, 2012), which reported that the abundance of trees/shrubs at several local sites is not well estimated by D/P index. D/P index only considers as woody indicators the globular "decorated" phytoliths, but these phytoliths are not the only ones produced by woody plants, and they are not produced by all woody plants (Collura and Neumann, 2016; Mercader et al., 2009). This index formulation could explain the discordances between D/P and tree cover. When environments with assemblages clearly dominated by globular FI phytoliths are analyzed, D/P index results reflect well the abundance of woody vegetation (Bremond et al., 2005a). With the use of globular psilate phytoliths as FI, despite being largely produced by woody plants (but also produced by certain non-woody monocots e.g., *Sporobolus consimilus* [Albert et al., 2016], or *Melinis nerviglumis* [Mercader et al., 2010]), the risk of over-representation of tree cover caused by the use of these phytoliths as FI is negligible, due to the low amount of globular psilate phytoliths recovered from modern soils.

Grasses seem to be over-represented in the phytolith assemblages, suggesting a vegetation more open than it actually is. In wooded grasslands (O34 and H64), grass-sedge phytoliths represent 64% and 32% of the assemblage, respectively (GSSC 57% and 27% respectively). In swampy environments (E58, M71 and M72), grass-sedge phytoliths represent from 23% to 46% of the assemblage (GSSC 14%-37%). In

woodlands whose understories are rich in grasses, grass-sedge phytoliths represent from 32% to 47% of the assemblage. In woody environments where grasses or sedges are not characteristics (or absent), grass and sedges phytoliths vary from 17% to 47% (over-represented), so no big differences are revealed by phytolith assemblages. Grasses are the largest phytolith producers within Spermatophyta (Hodson, 2005), which can explain the over-representation of grass phytoliths in soil assemblages, also reported by other authors (Albert et al., 2015; Neumann et al., 2009; Novello et al., 2012).

Cyperaceae hat-shaped phytoliths are absent in phytolith assemblages despite their presence in the areas where samples were collected (O34, E58, H62 and M72). Exclusive phytolith morphologies of sedges (e.g., hexagonal-rounded platelet with rounded apex "hat-shaped" or cylindroid bulbous bodies, Pla5) are not present, and other morphologies (e.g., small, cylindrical branching bodies) are not exclusive to Cyperaceae, being attributable to both grasses and sedges. The absence of typical sedges phytolith morphologies has been frequently observed (e.g., Albert et al. 2015, Garnier et al., 2013) and may be explained by taphonomical processes that cause that hat shaped and cylindroid bulbous morphologies tend to disappear from the soil record (Albert et al., 2006; Cabanes et al., 2011).

Palm globular echinate phytoliths (Glo1-4) represent properly the presence/absence of palm plants in samples or adjacent samples. On the contrary, globular echinate phytoliths percentage seems to over-represent the amount of palm trees in the samples, taking into account their presence in modern environments, where their presence is not as dominant as in phytolith assemblages. This is consistent with results obtained previously in taphonomical studies that suggested that Arecaceae are large phytolith producers (Bamford et al., 2006).

Fern phytoliths (Epi2) have been observed in our modern samples from Olduvai, Lake Manyara, Lake Eyasi and Hadza Territory. To our knowledge, this is the first time that fern phytoliths are described in the area. Despite many studies of surface soil samples in Africa, fern phytoliths have never been mentioned, even for samples collected in similar environments (Albert et al., 2015).

Pre- and post-depositional phenomena can explain many of the inconsistencies found in phytolith assemblages. In the case of samples from Lake Manyara (M69 to M75) possible pre-depositional phenomena have to be considered, such as the fact that *Hyphaene petersiana* and *Phoenix reclinata* are the most frequent palms reported in the area and their fruits are eaten by humans and baboons (present in the study area), thus zoochory may be a taphonomical process that affects phytolith assemblages. Furthermore, undergrowth disturbances (as produced by elephants, for example) can affect modern phytolith assemblages. This can explain the presence of palm phytoliths in samples where palms were not described (but they are present in nearby samples). Other taphonomical processes affect the assemblages, notably the representation of phytolith from sedges that are absent in the samples, despite the presence of Cyperaceae plants in the environment.

The results obtained are consistent with those of Albert et al. (2015): subtle differences between different plant formations, over-representation of grass phytoliths and under-representation of sedge phytoliths. However, Albert et al. (2015) only describe 30 phytolith morphotypes, which cannot cover the variability of morphotypes extant in these soils, and which made more imprecise the attribution of phytolith. In addition, this study attributes almost all morphologies to a determinate group of plants (except weathered phytoliths). Given that previous studies have attributed some morphologies to diverse plant groups (e.g., some tabular crenate *sensu lato* can be indistinguishable from dicotyledonous or Poaceae; all the "cylindroid" phytoliths cannot be attributed to Poaceae; "hairs" are not unique to dicotyledonous; and not all the "parallelepiped thin" are from grasses; Mercader et al., 2010, 2009; Stromberg, 2003), or simply unidentifiable (Piperno, 2006; Shillito, 2013), it can be considered that the approach of Albert et al. (2015) is inaccurate and that their attributions may largely bias the results of the analysis. Therefore, a more cautious approach should be adopted, openly showing the percentage of phytoliths that cannot be attributed to a specific group, rather than attributing them to a specific plant category.

Are phytoliths more powerful than others microbotanical remains?

Phytolith remains are usually considered better markers of vegetation at site scale than other e.g., pollen, which are easily transported. Pollen content of our analyzed samples (Barboni, *unpublished data*; **Figure 5.1.8**) show that the main disparity between phytolith and pollen remains concerns sedge remains, which occur in pollen samples but are absent (or cannot be distinguished from grasses) in phytolith remains. In this regard, pollen is a better indicator/tracer of environments where Cyperaceae plants are abundant (see E58, H62 and M72 samples). On the contrary, in some samples where grasses are abundant, the Cyperaceae presence seems to be over-represented by pollen remains (see O34), and grasses are largely under-represented. Considering grasses-sedges a single group, both pollen grains and phytoliths over-represent the presence of these plants in the environment. *Typha* presence is traced by pollen, but not by phytoliths (due to the absence of unique morphotypes). *Typha* pollen grains are well-represented in swamps (E58, E59A, M71 and M72) and riparian forests (H61 and H62) where *Typha* is present, as well as in woodlands where *Typha* presence is secondary (E55, E56, E57 and E59B). In phytolith assemblages, the presence of *Typha* seems to be marked or related to some elongate morphologies (El7 and El9, except in E59A sample) attributed to grasses-sedges. Yet, in the PCA the environments rich in *Typha* are best discriminated by the percentage of "diatoms", "grasses-sedges" and "non-diagnostic" components.

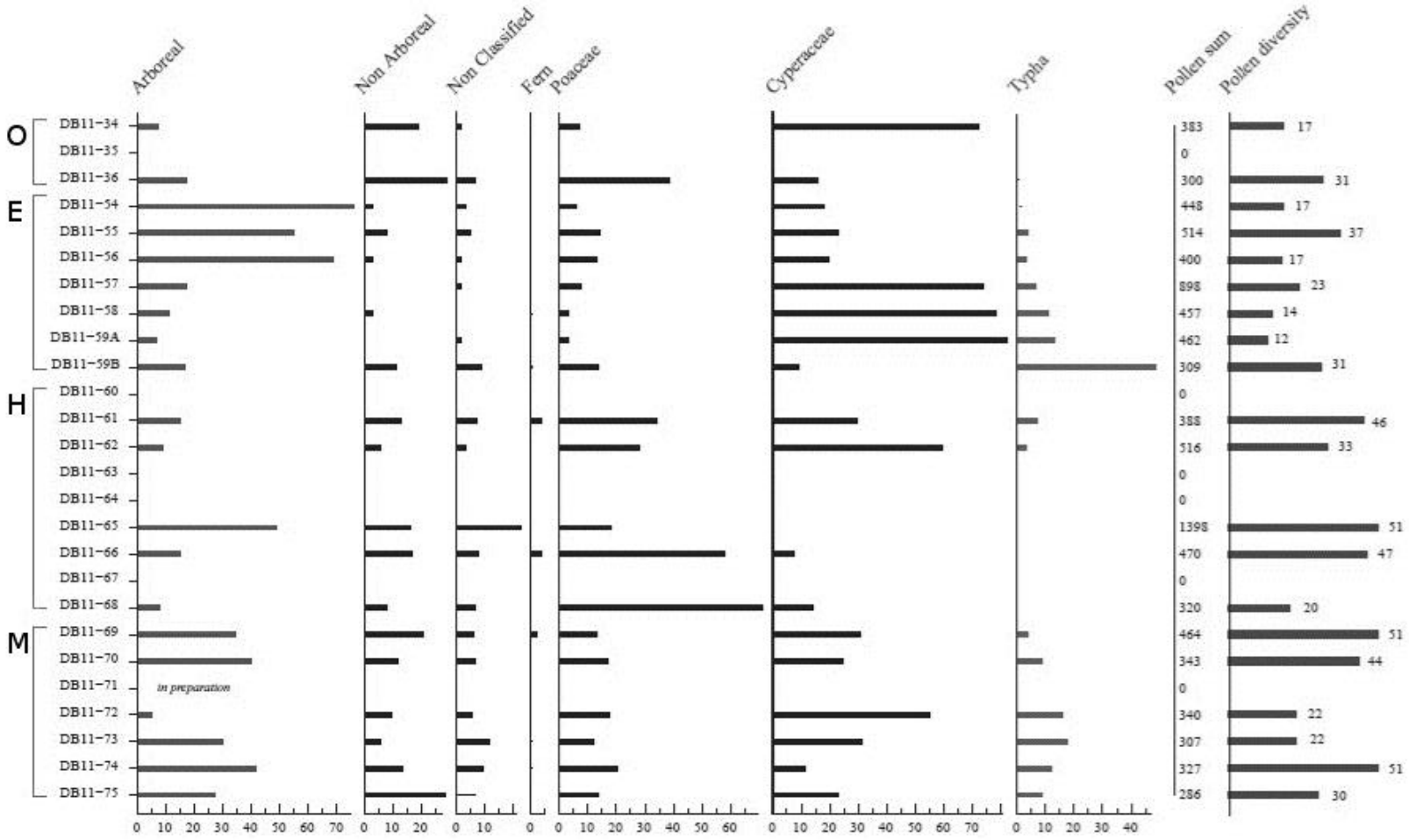

Figure 5.1.8. Relative abundance of pollen grains grouped by taxa. (Barboni, *unpublished data*). O: Olduvai samples, E: Eyasi samples, H: Hadza Territory samples, M: Manyara samples

Arboreal pollen and FI phytoliths seem to be under-represented in phytolith and pollen analysis respectively, but considering canopy (tree) cover as a good descriptor of vegetation structure phytoliths are a better approach /method/proxy to infer the main vegetation structure than pollen remains. This can be appreciated in the comparison of correlation values between D/P index of phytoliths and arboreal pollen grains percentage with tree cover values. Correlation between arboreal pollen percentage and tree cover value shows a coefficient of determination (R^2) of 0.08, that is significantly lower than the value (R^2=0.504) obtained in the correlation between D/P index and tree cover values (**Figure 5.1.3**). This lack of correlation between pollen and tree cover can be explained by pollen grains biology. Pollen grains are reproductive structures produced in very different amounts by plants. Trees as *Adansonia* or *Acacia* are pollinated by animals (Baum, 1995; Tybirk, 1993), so their pollen production is lower than in other wind-pollinated (anemophilous) plants such as grasses and palms (Shukla et al., 1998). Our results are in agreement with those obtained by Bremond et al. (2005a) and Barboni et al. (2007), which show that D/P indices are better correlated with values that measure tree cover (Leaf Area Index or satellite estimations) than with the arboreal pollen percentage. Bremond et al. (2005a) explain this discrepancy by the presence of young trees, which produce phytoliths but not pollen grains.

Pollen is a better tracer of species diversity than phytoliths, due to the taxonomical resolution allowed by these microremains. However, pollen grains do not trace properly the components of vegetation. In this regard, *Hyphaene* pollen seems to overestimate the presence of this species in the environment with values higher than 50% of the total pollen grains (Barboni, *unpublished results*), and, on the contrary *Acacia* and *Adansonia* pollen abundance underestimates the presence of these two major components of actual vegetation (with values below 5% or close to 0% Barboni, *unpublished results*). In samples where palms are present, pollen seems to better trace arboreal vegetation than in samples where palms are absent. This is consistent with the results obtained in phytolith analysis, in which globular echinate palm phytoliths largely influence D/P index, which is an estimate of tree cover (as shown in PCA and DA results).

5.2 Modern plants reference collection

A small number of representative species found near groundwater discharge areas of the Olduvai-Nogorongoro-Manyara-Eyasi region were analyzed for their phytolith content. The aim of this experiment/analysis was to improve the characterization of ferns, of spring marker species (*Rauvolfia caffra, Tamarindus indica and Croton macrostachys*), shade-loving species (*Achyranthes aspera*), typical species of woodlands (*Adansonia digitata, Balanites aegyptiaca and Thespesia garckeana),* and of a sedge species (*Cyperus papyrus*).

The species that exhibit the most characteristic phytoliths are pteridophytes. Three major morphotypes have been found in the six species analyzed: tabular, irregular "puzzle" bodies (**Figure 5.2.1**).

Blocky parallelepiped phytoliths. These phytoliths were found in modern soils and paleosols analysis and were coded as Blo13/Blo16. This phytolith category is subdivided in two types. Type "Blo13" shows blocky parallelepiped quadrangular section and striped surface with 1-2 stripes parallel to the longitudinal axis. Its size is 30-110 μm. Type "Blo16" is blocky parallelepiped with crenate edges and trapeziform section. Its surface is psilate or finely rugose and its size is 30-80 μm. Attention should be paid to Blo16 morphology because it can be confused with GSSC polylobate phytoliths. However, the lobes of fern phytoliths are more irregular and they are thinner (thickness/width ratio) than those of grasses.

Elongate, polygonal section, rugose or slightly psilate surface (80-160 μm). These very big phytoliths were not found in modern soils or paleosols analysis. Code El16.

Irregular and complex flat bodies with wavy edges and many protuberances. These bodies that look like "puzzle pieces", were found in few quantities in modern soils and paleosols analysis and coded Epi2. Attention should be paid to this morphology because it can be confused with Fabaceae leaves

polylobate phytoliths, but latter are more regular and thinner than fern phytoliths (Mercader et al., 2009).

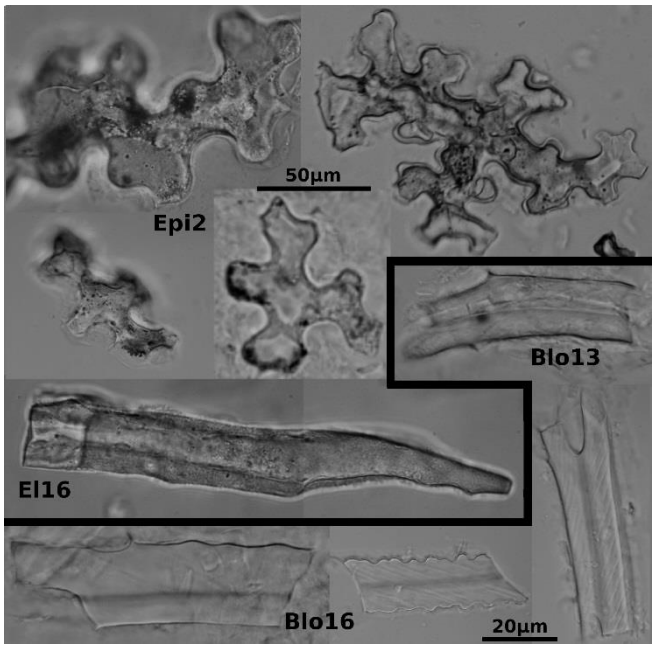

Figure 5.2.1. Selection of phytoliths found in modern fern samples. El16: elongate, polygonal section, rugose or slightly psilate surface. Blo13: blocky parallelepiped quadrangular section. Striped surface. 1-2 Parallel stripes to the longitudinal axis.Blo16: blocky parallelepiped with crenate edges. Trapeziform section. Psilate or finely rugose surface. Epi2: Irregular "puzzle" bodies

These phytoliths are associated to analyzed species as follows:

	Blo13	Blo16	El16	Epi2
Adianthum poiretti	+	+	+	+
Asplenium pumilum		+	+	+
Aleuritopteris farinosa	+		+	
Pteris muricella		+	+	+
Pteris vittata	+	+	+	+
Trichomanes sp.				+

Mazumdar and Mukhopadhyay (2011) and Chauhan et al. (2009) described large epidermal plates (Epi2) and *heavy* deposited plates in *Pteris vittata*. These heavy deposited plates have not been observed in our samples. Mazumdar (2011) and Sundue (2009) did not found phytoliths in *P. vittata*. I found in *P. vittata* Blo13, Blo16 and El16, not cited in the aforementioned studies, but considering that these studies analyzed Asian samples and the ubiquity of *P. vittata*, large intra-specific variations are expected. Blo16 and Epi2 were found in other *Asplenium* species (Chaerle and Viane (2004). Blo13 were described in Cheilantoideae species (Lellinger, 1968). Our results did not show differences in morphologies between species and are concordant with Sundue (2009), who did not found diagnostic phytoliths in *Cheilanthes* sp. Sundue (2009) notes the importance of blocky parallelepiped morphologies and uses them to establish a systematic classification and reveals a large inter-specific variability. Epi2 phytoliths appears in five ferns and no differences between species have been found. This is consistent with previous studies that described this morphology as non-diagnostic (between ferns) (Piperno, 2006; Sundue, 2009).

In the seven dicotyledonous species I analyzed, the phytoliths found match with the common patterns found in previous studies (Albert et al., 2016; Garnier et al., 2012; Mercader et al., 2009). Negligible amounts of phytoliths were found in stem extraction from *Balanites aegyptiaca* and *Adansonia digitata*, and petioles from *Croton macrostachys*, *A. digitata*, *Tamarindus indica* and *Thespesia garckeana*. Not many species have morphologies that can be considered specific for leaves. Most of the phytoliths found do not allow distinguishing between soft and hard plant tissues, except for tracheid phytoliths (El15). Tabular plates are the most common group in the species sampled that occur in our samples. Angular shard-like plates with psilate-rugose surface (Pla3) have been found in *Achyranthes aspera* (forb), *A. digitata* (tree), *C. macrostachys* (tree) and *T. indica* (tree). Tracheids (El15) were noted in *Achyranthes aspera*, *B. aegyptiaca* (tree), *C. macrostachys and Rauvolfia caffra* (tree). Small parallelepiped/cubic/ovate bodies with granulate/tuberculate surface (Blo5), that cannot be undoubtedly attributed to dicotyledonous plants but are more often associated with them, appear in *A. aspera* and *T. garckeana* (tree). Globular faceted bodies (Glo6 and Glo7) were found in *A. digitata* and *R. caffra*. Acicular bodies seem to be wider in dicotyledonous species than in monocotyledonous species, according to

reference collections, but this is unclear. In this sense, triangular bodies with smooth surface and as long as wide were found in *T. indica*.

Cyperus papyrus (sedge) was analyzed for phytolith content. Hexagonal-rounded platelets with rounded apex (Pla5, "hat-shaped" phytoliths) represent ~70% of total phytolith content. In stems the amount of phytoliths is negligible, but the presence of elongate cylindrical body with sinuous and smooth surface (El4) is noted. Despite the apparent high production of sedge "hat-shaped" phytoliths, these have been found in negligible amounts in modern soils and paleosols. No new morphologies have been observed in our *C. papyrus* analysis.

6. Starch granules automated identification system

6.1 Results

With a selection the 24 characters with the highest RF test values (**Appendix 4.2.C**), group classifications did not significantly improve. Classifications were not significantly improved by filtering granules either (**Appendix 6**). Yet, the best accuracy rates of identification (ARI) were obtained by using the selection of granules and the whole set of characters. Only these results obtained with 3416 selected granules out of 5028 are presented here (**Tables 6.1-6.2, Figures 6.1 to 6.4**).

The Random forest (RF) test for the 20 species shows that with 52.2±16.4% of correct allocations on average, species identification based on starch granules is low (**Table 6.1a**). Success rates range from 23% for *Cadaba farinosa* to 75% and 76% for *C. rotundus* and *Echinochloa colona*, respectively. The confusion matrix shows that incorrect allocations are evenly distributed for most species (**Table 6.2**). Species with uneven distributions (they are uneven towards a particular group or species) include for example *Cadaba farinosa* (Capparaceae), for which 43% of the granules are misclassified into Poaceae, particularly into *B. deflexa* (14%) and *E. colona* (17%). For several species, *Cyperus rotundus* acts as an attractor for several granules incorrectly identified (e.g. 25% of *Olyra latifolia* granules). This could be explained by the fact that *Cyperus rotundus* presents high values of importance (RF test value) for a large number of characters. Surprisingly, misclassification between the two species of genus *Vigna* is low. Starch granules of the *Vigna* species are separated by two different sets of characters, with few important characters in common (**Appendix 4.2.C**). In the confusion matrix it is true that for many taxa the majority of the granules are missclassified, but it is still highly significant that each taxon had a higher percentage correctly classified for it than any of the other taxa. For example, *C. farinosa* has only 23% of the granules classified correctly, but no other taxon has a higher percentage (the next closest is *E. colona* with 17% of the *C. farinosa* granules classified to it. At the family level, highest values of classification are obtained for the Fabaceae (79%) and Poaceae (83%) (**Table 6.1b**). Such high values could be considered as statistical artifacts because these two families include large numbers of species. Within the Poales order species, highest identification values are of ~80% for *Cyperus rotundus*, *Brachiara deflexa*, *Echinochloa colona* and *Panicum subalbidum*

(**Table 6.1c**). Among the plant parts, highest accuracy values are of 80% for underground storage organs (**Table 6.1c**).

Table 6.1. Summary table of success rates (in percent) obtained from confusion matrices using granules grouped by a) species, b) families, c) order Poales, d) histological origin (plant parts). And e) results of the human eye identification blind test. Species names are coded using the three first characters of genus and specific epithet.

	Automated test	**Blind test[e]**		**Automated test**
Species[a]	**Accuracy %**	**Success/Total**	**Poales[c]**	**Accuracy %**
Ada_dig	53	5/10	Bra_def	78
Bra_def	71	8/13	Cyn_dac	64
Cad_far	23	1/9	Cyp_rot	84
Cap_fas	50	0/9	Ech_col	82
Cyn_dac	63	5/11	Oly_lat	55
Cyp_rot	75	1/16	Pan_sub	81
Ech_col	76	2/8	Set_pum	44
Emi_ann	33	1/11	Typ_lat	66
Fai_alb	64	11/17	**Mean Poales**	**69±14.29**
Fic_sal	47	0/3		
Hib_mic	56	4/9	**Families[b]**	
Oly_lat	42	0/11	Cappareceae	31
Pan_sub	63	2/8	Fabaceae	79
Per_sen	61	0/2	Malvaceae	53
Por_ole	71	1/3	Poaceae	83
Set_pum	38	0/10	**Mean families**	**62±24**
Typ_lat	31	0/10		
Vig_fru	53	7/20*	**Plant part[d]**	
Vig_vex	63	7/20*	Mesocarp	67
Zan_aet	25	0/9	Seed	69
			USO	80
Mean species	**53±16.4**	**Total 48/189**	**Mean plant parts**	**72±7.3**

Table 6.2. Random Forest test confusion matrix with rates of allocations in percentage using the dataset of selected granules and all characters. Species names are coded using the three first characters of genus and specific epithet.

	Ada_dig	**Bra_def**	**Cad_far**	**Cap_fas**	**Cyn_dac**	**Cyp_rot**	**Ech_col**	**Emi_ann**	**Fai_alb**	**Fic_sal**	**Hib_mic**	**Oly_lat**	**Pan_sub**	**Per_sen**	**Por_ole**	**Set_pum**	**Typ_lat**	**Vig_fru**	**Vig_vex**	**Zan_aet**
Ada_dig	**53**	5	3	2	4	11	3	4	1	2	0	2	0	6	1	1	0	3	0	1
Bra_def	6	**71**	1	0	2	5	5	0	0	0	0	2	0	6	0	2	0	0	0	1
Cad_far	7	14	**23**	3	1	4	17	1	0	1	6	4	4	7	0	3	0	0	0	1
Cap_fas	4	0	0	**50**	0	12	3	4	2	4	5	0	2	7	0	0	0	0	0	7
Cyn_dac	1	0	1	0	**63**	2	0	2	5	5	1	1	9	1	0	1	1	3	1	1
Cyp_rot	3	1	0	4	1	**75**	1	2	2	0	1	2	0	1	0	3	1	0	2	0
Ech_col	1	3	6	1	0	2	**76**	1	2	2	2	2	0	2	0	0	0	1	0	1
Emi_ann	1	0	0	0	0	1	12	**33**	7	6	2	0	13	0	2	2	3	15	2	2
Fai_alb	0	0	0	4	0	2	1	3	**64**	4	1	0	5	0	1	0	1	6	6	3
Fic_sal	2	1	0	2	2	4	4	2	5	**47**	2	1	2	2	1	0	5	5	5	8
Hib_mic	4	1	1	7	2	15	0	0	0	3	**56**	2	0	7	0	1	0	0	1	1
Oly_lat	5	5	0	0	6	25	0	0	0	2	2	**42**	0	11	0	5	0	0	0	0
Pan_sub	2	2	2	0	0	0	6	11	6	3	0	1	**63**	0	0	0	3	0	0	2
Per_sen	10	2	1	2	0	11	3	1	0	0	2	5	0	**61**	0	2	0	1	0	1
Por_ole	0	0	0	0	0	7	0	1	3	0	0	0	1	0	**71**	0	3	2	10	3
Set_pum	1	5	1	4	4	23	3	0	0	3	1	4	0	8	0	**38**	4	0	0	0
Typ_lat	1	0	0	3	1	14	3	2	8	10	6	0	1	4	1	2	**31**	1	6	7
Vig_fru	3	0	0	0	4	0	2	5	8	5	1	1	4	0	3	0	0	**53**	8	4
Vig_vex	0	0	0	1	0	0	1	0	6	9	3	0	1	2	3	0	2	7	**63**	2
Zan_aet	4	0	1	4	3	5	3	7	5	17	5	1	3	1	1	0	7	7	4	**25**

Discriminant analysis (DA) shows that several characters are implied in the discrimination of groups. However, although the RF test confirms that there is significant difference between these groups, the first two axes of DA just explain 27% of the variance. Plotting granules grouped by species, the groups tend to separate but the ellipses that include 95% of confidence intervals largely overlap (except *Portulaca oleracea*). The plotting of class scores shows that taxa tend to separate into three or four groups (**Figure 6.1**). The plot of variable scores shows that single species or groups of species are separated by different sets of characters (**Figure 6.2**). *P. oleracea*

is clearly separated by characters related to size (e.g. Longest axis, Shortest axis length, Area) measured under polarized and natural light. Fabaceae species (*Eminia antennulifera*, *F. albida*, *Vigna frutescens* and *Vigna vexillata*) are separated by characters related to the shape (e.g. Longest/Shortest axis, Dissymmetry) measured under natural light. About four to six Poaceae species (particularly *B. deflexa*, *Echinochloa colona*, *O. latifolia* and *S. pumila*) are separated by characters of textures (e.g. Peaks, Contrast, Central area) measured under polarized and natural light.

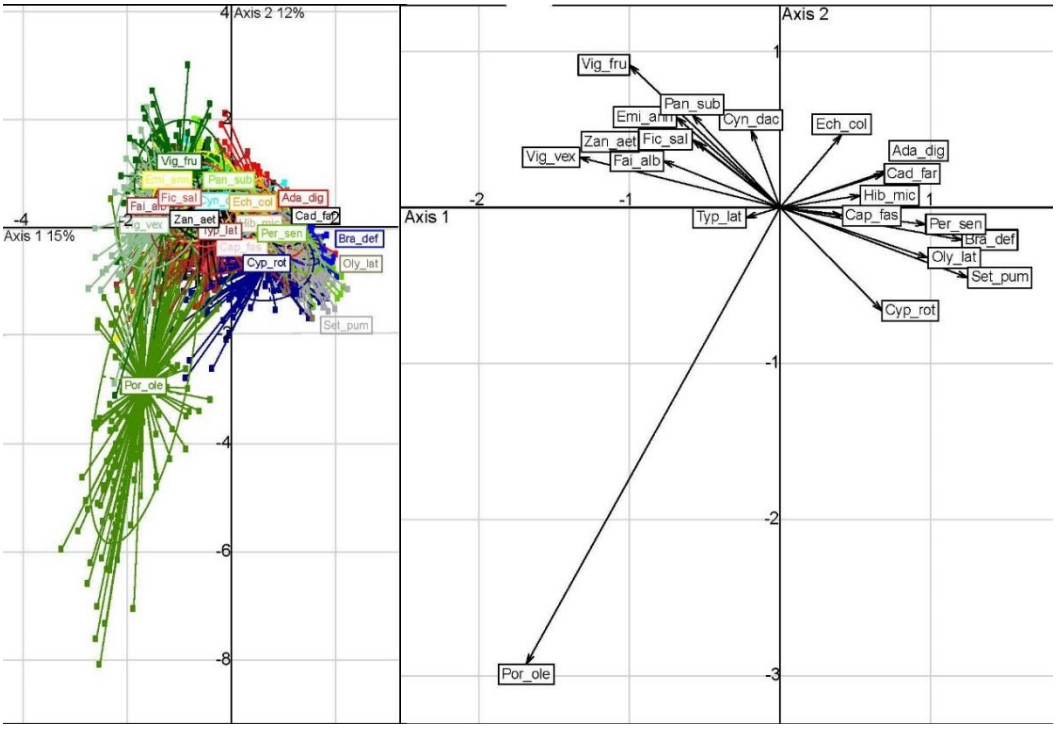

Figure 6.1. Discriminant analysis. Plot with all granules showing differences between groups (left graph) and vectorial graph showing class scores for granules grouped by species (right). In the left plot, ellipses show 95% confidence intervals for each taxonomic group (note the intense overlap). In the right plot, arrow length shows the amount of variance explained by each taxa group. Species names are coded using the three first characters of genus and specific epithet. See **Figure 6.2** for variables scores.

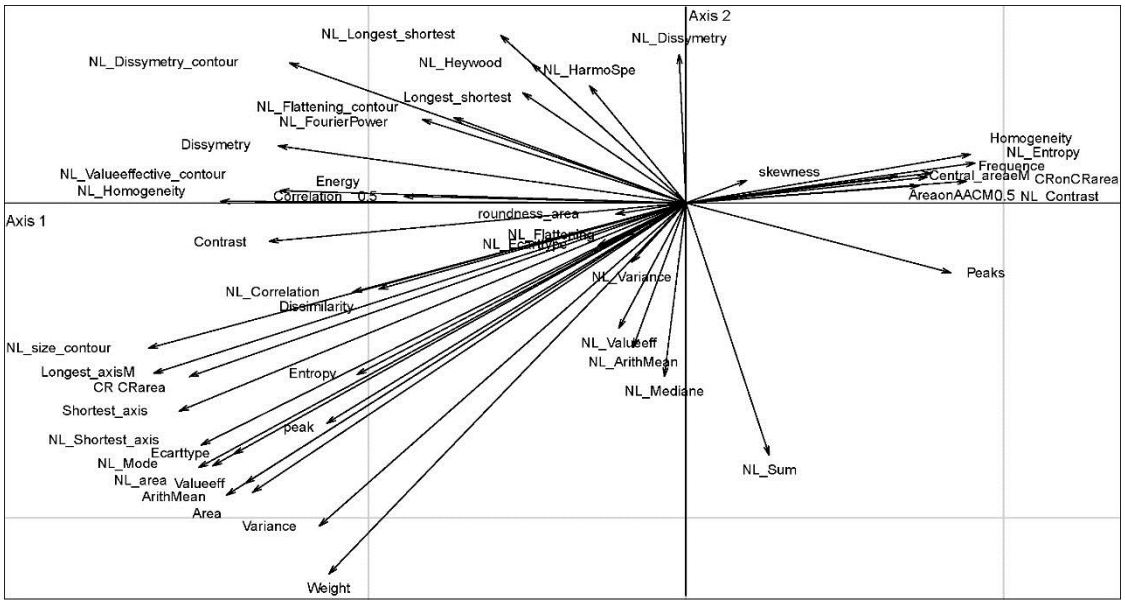

Figure 6.2. Vectorial graph showing variables scores for the test with granules grouped by species. The 50 variables (characters) with highest Random Forest mean decrease accuracy and mean decrease gini values are plotted in the graph. Arrow length shows the importance and contribution of each variable to the final multidimensional solution. Variables are described in **Appendix 4.2.B**.

DA using granules grouped by histological origin provides a clearer separation than with species or families, with 99% of the variance being explained by the first two axes (Figure 5.3). It is not clear, however, which are the characters implied for separating each group. The nature of characters is diverse for each group, with USO being separated by the larger group of characters (**Figure 6.4**).

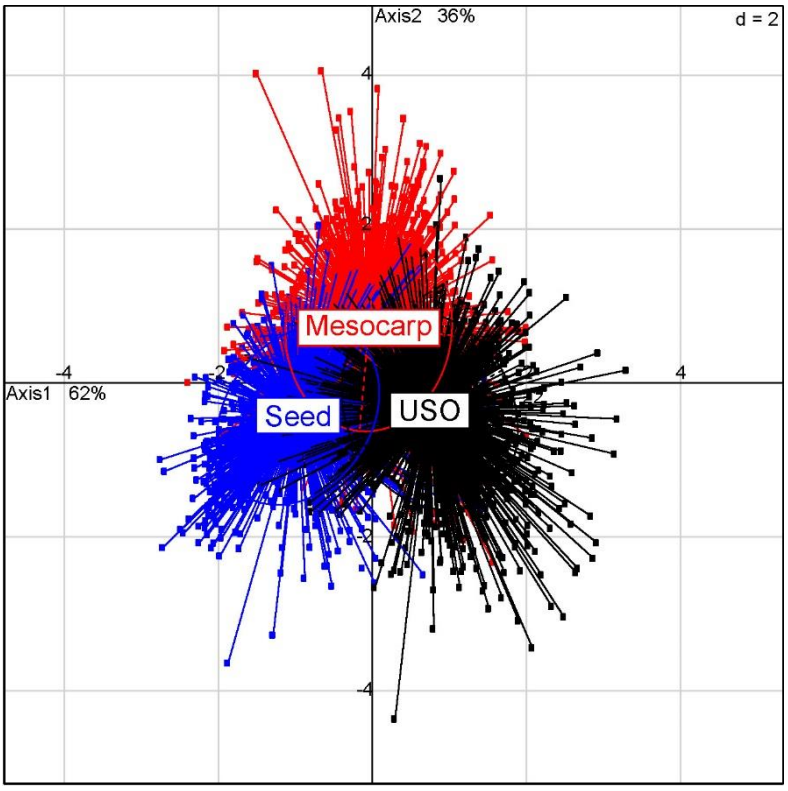

Figure 6.3. Discriminant analysis showing differences between granules grouped by plant part origin (seed, mesocarp, and underground storage organs). Ellipses show 95% confidence interval. See **Figure 6.4** for variable scores.

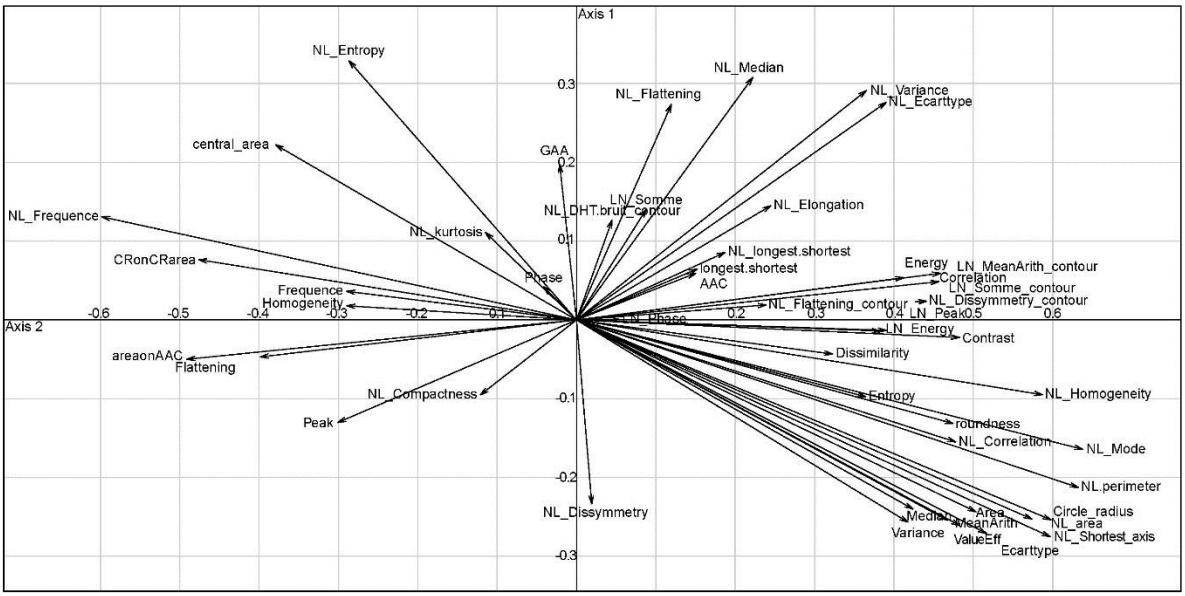

Figure 6.4. Vectorial graph showing variables scores for the test with granules grouped by plant part origin. The 50 variables (characters) with highest Random Forest mean decrease accuracy and mean decrease gini values are plotted in the graph. Arrow length shows the importance and contribution of each variable to the final multidimensional solution. Variables are described in **Appendix 4.2.B**.

We also tested how the number of characters or the number of groups to discriminate would influence ARI. We found that both the number of characters taken into account in the discrimination of groups and the number of groups to discriminate influence the ARI in starch granule identification (**Figure 6.5**). Our test with randomly selected characters shows that average accuracy rates increase with increasing number of characters following a log correlation (**Figure 6.5a**). The correlation is strong (R^2= 0.83). Best average accuracy rates for our dataset of 20 species reach a maximum value of about 53% with a maximum of 123 characters. With 123 characters a maximum accuracy rate of 75% is obtained for *Cyperus rotundus*. The addition of new characters does not considerably improve starch granule identifications: by increasing the number of characters by an order of magnitude (from 10 to 100 for example), the mean ARI registers an increase of about 10% in absolute value (i.e. about 20% improvement).

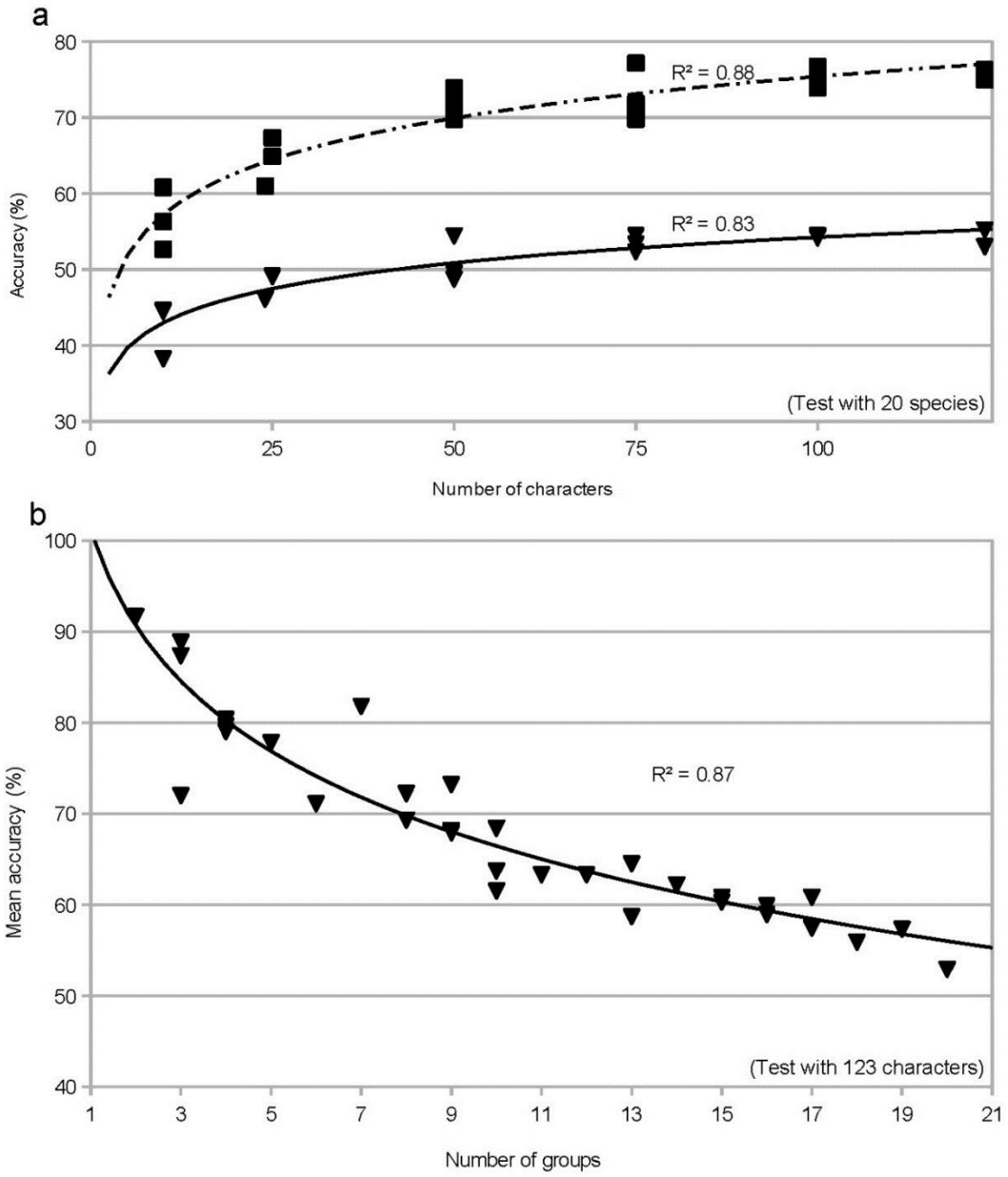

Figure 6.5. Correlations between the numbers of characters (a), the numbers of groups (b) and the average accuracy rates of identification for the starch granules of our reference collection. Squares: *Cyperus rotundus*; Triangles: average rate.

The number of groups to discriminate also influences the ARI in starch granule identification (**Figure 6.5b**). Average ARI are of 53±16% at the species level (n=20). They are higher at the family level (61±24%, n=4) and when granules were grouped according to their histological origin (72±7.3%, n=3,) (**Table 6.1d**). At the species level, but with a dataset reduced to the Poales (Poaceae, Cyperaceae and Typhaceae) we obtained similarly good results (69±14%, n=8). Differences of mean values between species and Poales or histological origins are significant. The correlation obtained is strong (R2 = 0.87) and shows that the greater the number of groups to identify the lower the average ARI of starch granules (**Figure 6.5b**).

We evaluated our automated method against the subjective, but trained, human eye identification. The accuracy of the researcher was of 25.4% (48 correct identifications over 189 tested), which is incontestably worse than the automated and statistically aided classification method that we have developed here (**Table 6.1**). A rate of 0% of accuracy was obtained for seven species. However, for two species the results were close: 62% of accuracy with human eye and 64% with our automatic system for *F. albida*, and 62% and 71% for *B. deflexa*. Also there is a group formed by *V. frutescens*, *V.vexillata*, *Eminia antenulifera* (Fabaceae), *Zantedeschia aethiopica* and *T. latifolia*, which are all underground storage organs samples, and which were identified with an accuracy of 71% (percentage of granules from USO samples that were classified as others USO samples). We were surprised to see that there seem to be no relationship between granules gross morphology and ARI. Species with rounded morphologies, such as *Cyperus rotundus* or *Persicaria senegalensis* have rates of accuracy (of 75% and 61%, respectively) that are as high as for species with what our subjective human eye would qualify as "distinctive" (e.g. *P. oleracea*) (**Table 6.1**). And similarly, some species with "distinctive" morphology (to our subjective human eye) (e.g. *Z. aethiopica*) show low rates of accuracy (of 25-50%), the same as species with rounded morphology (e.g. *S. pumila*).

6.2 Discussion

Is this system powerful enough to establish accurate identifications?

Our system provides an estimation of how well a given taxon can be identified by using a fixed set of 123 characters. Despite the high number of morphological and optical characters taken into account here, we never obtained 100% correct taxa identification. At best, we obtained 84% correct identifications for the species *Cyperus rotundus* when the initial dataset of 20 species was reduced to those of the Poales order (8 species only, **Table 6.1c**). The species we considered here may be too similar in morphology or regarding their optical properties to allow a proper discrimination. Using a different set of species could have improved our results. It should be noted, however, that accuracy rates of identifications (ARI) are not absolute, but relative to the species dataset. They also depend on the character dataset, the image quality and analysis (notably the edge detection) and the classification method. It is therefore impossible to assess which species are better identifiable than others.

It may also be argued that our system is not powerful enough to provide reliable starch granule identifications, but yet it uses optimized features extraction procedures notably regarding the outline detection (Barbarin, 2014). In this regard, a comparison of methods with other studies is hardly possible because species and character datasets are different than the one we have considered (Coster and Field, 2015; Fernández Pierna et al., 2005; Liu et al., 2014; Torrence et al., 2004; Wilson et al., 2010). Comparing our methodology with a previous approach we note that Wilson et al. (2010) used low quality images (border very pixelized) and worked on complex samples with aggregates. We avoided this situation using only images of "individuals" (to test properly the possibility of classification). The smoothing of the shape induced by the thresholding of the polarized images is negligible because we use higher resolution images. The only smoothing problem is the convex hull processing we kept in the program to reduce potential noises induced by the thresholding. Unfortunately, this parameter is not adjustable under LabVIEW, but we think that the resulting approximation is negligible (**Figures 4.2.2 and 4.2.3**). Coster and Field's (2015) work gives good results, but, there are some points that have to be taken into account: these

authors try to identify all the specific variability, but their study focuses on (only) 8 species. Our results show that the lower group number, the greater the rate of recognition (**Figure 6.5b**). Furthermore, Coster and Field's (2015) work does not have a separate test set and the "re-substitution" method re-uses the training set on which the learning of their model was based.

Yet, our automated approach to identify starch granules appears to be more reliable than human eye identifications for which, on average, a mere 25% of correct identifications were produced. Our automated system improved substantially the taxonomic value of all taxa. For example, *Cyperus rotundus* is almost unidentifiable with human eye (1/16 correct identifications) but is correctly identified at 75% by our automated system (**Table 6.1**). For this test of identification using human eye, however, the best conditions would have been to observe granules in a liquid mounting medium. Instead, the identification was carried out on the photographs taken for the automated experiment. In these conditions, starch granules could not be observed in the three dimensions, which may have improved the ARI by human eye. The ARI of starch granule with human eye may have been higher, also, if performed by an analyst with more experience. The replicability of identification needs to be tested thoroughly as done in some phytolith studies (e.g. dealing with maize identifications (Pearsall et al., 2003). This is particularly needed when plant species inference (e.g. maize (*Zea mays*) against non-maize *Zea* and non-*Zea* grasses) is based on a single proxy (e.g. phytoliths [Pearsall et al., 2003]), which can easily be questioned by other researchers (e.g. Pearsall et al., 2004; Rovner, 2004). An automated system like the one we have used here also enables carrying out statistical analysis and measuring and analyzing a large number of starch granules, (i.e. to handle the large intraspecific variability that one can observe in starch granules).

Support our results the taxonomic value of starch granules?

Our results do not question the taxonomic value of starch granules, because if just two species are considered e.g. *B. deflexa* and *F. albida*, the discrimination can be made with both human eye and our automated system (**Table 6.1**). The difficulty arises when the pool of target species is large. When dealing with the identification of plants processed by early hominin stone tools for example, the pool includes several hundreds of target species, as diets of both modern human and other African primates should be considered (Copeland, 2007; Peters, 1993). The use of a large reference collection, however, implies the use of a large set of characters (e.g Dollfus and Beaufort, 1999). Our results show that ARI decrease when the size of the reference collection increases (**Figure 6.5b**), but ARI increase when the number of morphological and optical characters considered for the discrimination increases (**Figure 6.5a**). In this regards, our study makes an important contribution to the field of starch granule identification by enlarging the number of characters to 123. Previous studies used less than 20 characters although up to 29 species were included in the reference collections (e.g. Torrence et al., 2004, Wilson et al., 2010).

Despite using a set of 123 characters, we obtained a relatively low averaged ARI of about 53% (**Table 6.1**). It is possible that better results could be obtained by implementing our automated system with morphological qualitative characters (e.g. the three-dimensional shape, the presence/absence of hilum, vacuoles, etc.) as in Torrence et al., (2004), or optical features (e.g. chord length distribution) as in Choy et al. (2010). We observed, however, that although the addition of new characters does increase the rates of identification, these tend to stabilize at a plateau (**Figure 6.5a**). Two different approaches may therefore be implemented to improve starch granules identification: modifying the set of characters, and/or reducing the pool of target species (or groups).

Our results show that by reducing the number of target species, ARI improves (**Figure 6.5b**). If the number of target species cannot be reduced, the chances for getting wrong identifications are very high. As an example, we can consider two species that are poorly discriminated by our system such as *Zantedeschia aethiopica*

and *Cadaba farinosa*. If just those two are considered in the "reference collection", our system easily separates them (ARI are of 90% and 86% respectively). If our full "reference collection" of 20 species is considered, then ARI for *Z. aethiopica* and *C. farinosa* drop to 25% and 23%, respectively. We note that we obtained averaged ARI as high as 72% in the test for discriminating among three plant parts mesocarp, seed and underground storage organs (**Table 6.1d**). Yet, it is likely that such high ARI relates to the fact that just three groups were considered rather than to real differences between granules from different histological origins. It is therefore crucial to constrain as much as possible the pool of target species. To reduce the pool of target species, it may be useful to combine the analysis of starch granules with the analysis of other proxies e.g. resins, fibers (Gibson et al., 2004; Lombard, 2004), phytoliths (Dickau et al., 2012; Ezell et al., 2006; Piperno, 2009), or the analysis of use-wear (Barton et al., 1998; Kealhofer et al., 1999).

7. Phytolith paleosols analysis. Paleoenvironmental reconstruction

7.1 Zinj complex (FLK Zinj, PTK, AMK and DS)

Description of phytolith assemblages

In the 25 paleosol samples collected in the "Zinj complex" (hereafter ZC), which include samples from FLK Zinj, AMK, PTK and DS localities, 51 phytoliths morphotypes were described **(**summarized in **Figure 7.1.1**). Most types can be attributed to a possible botanical producer group/signal (**Figure 7.1.2**). Detailed countings are shown in **Appendix 7.A**. Non-diagnostic phytoliths that, to date, cannot be attributed to any specific taxon represent 6% to 53% (μ=24%±11.8%). Samples exhibit a great heterogeneity in the abundance of forest indicator (hereafter FI) phytoliths (excluding palms) (12% to 77%, μ=53%±16.3%). In FI phytoliths, globular rugose/granulate/psilate phytoliths (Glo4-13) represent 4% to 48% (μ=21%±13.4%) and the other FI phytoliths represent 5% to 60% (μ=32%±14.3%). The other component of forest formations are palm phytoliths, which represent up to 56% of the assemblages (μ=6%±11.4%). The phytoliths attributable to grasses and sedges represent up to 68% of the assemblages (μ=16%±10.5%; GSSC phytoliths μ=9%±7.2%, range 0-28%). The majority of GSSC found in the assemblages were trapeziform shortcells (GSSC11). Fern phytoliths are present in the ZC assemblages in low frequencies (<9%, μ=1%±2.6).

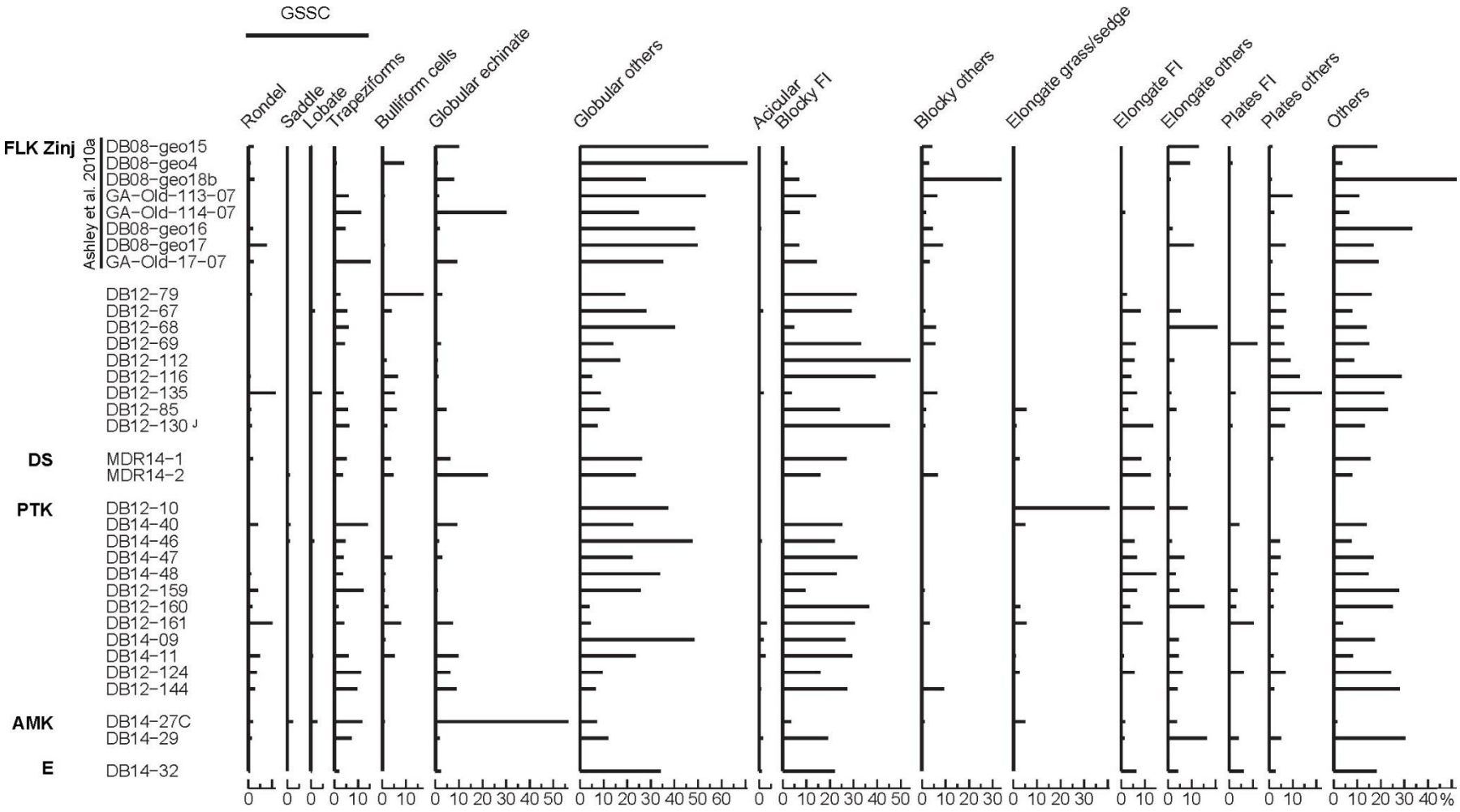

Figure 7.1.1. Relative abundance in percentage of phytoliths grouped by morphological group. [J]: Junction FLK Zinj-PTK. Samples are ordered North to South within the same site. [J]: Junction FLK Zinj-PTK. Samples are ordered North to South within the same site.

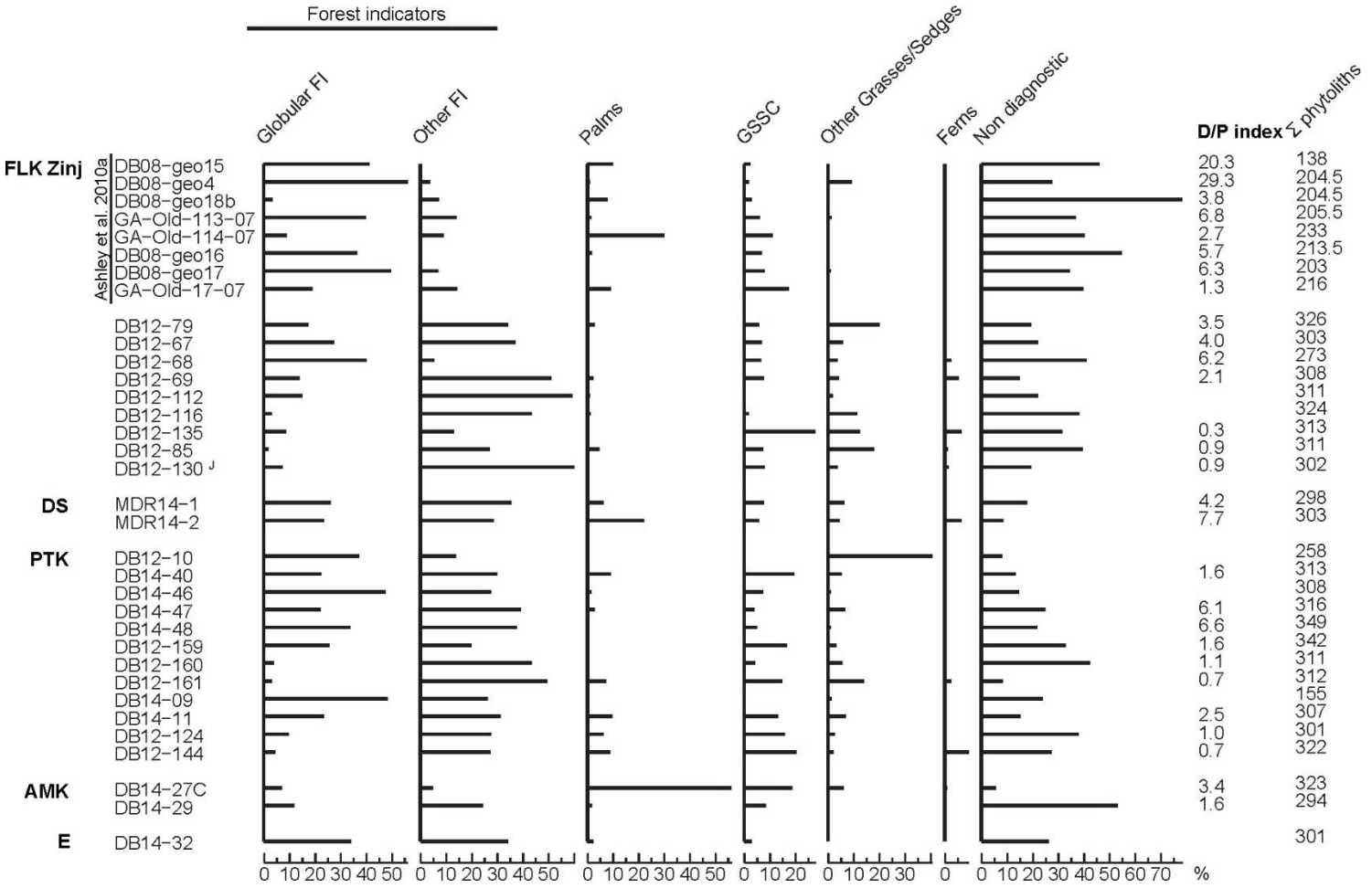

Figure 7.1.2. Relative abundance in percentage of phytoliths grouped by botanical attribution and ecological index values. [J]: Junction FLK Zinj-PTK. Samples are ordered North to South within the same site.

Only two samples from AMK and two from DS sites were analyzed. The AMK site shows strong/significant differences between samples: in DB14-27C, palm phytoliths represent 56%, and just a mere 2% DB14-29. On the contrary, DS samples have a homogeneous signal dominated by FI phytoliths. In seven of the eight samples from FLK Zinj percentages of FI phytoliths (that vary from 22% to 65%, excluding palm phytoliths) are higher than percentages of grass-sedge phytoliths (2%-40%). The Only one sample (DB12-135) shows a different pattern, with FI phytoliths representing 22% and grass-sedge phytoliths 40%. Most samples exhibit palm phytolith percentages of about 5% except at FLK Zinj and AMK. Fern phytoliths are present in four samples and reach up to 6%. Samples from the PTK site show a pattern similar to those from FLK Zinj. FI phytoliths represent the strongest signal in 12 out of 14 samples (FI: 32%-75%, grasses-sedges: 1-41%), and grasses-sedges in one. Sample DB12-121 is sterile. The PTK samples are richer in GSSC than FLK Zinj samples. Palm phytoliths are present in nine samples with values below 10%. Fern phytoliths are present in four samples, reaching up to 9% in one of them (DB12-144).

Phytolith indices and multivariate analysis

GSSC are relatively rare in the samples (counts <100 in all samples), which leads to very high D/P index values. D/P index was calculated for 21 samples (samples with low values of GSSC were discarded), with values ranging from 0.3 to 12.2, and values >1 (associated to forests, Alexandre et al., 1997; Bremond et al. 2005) occur in 19 samples (**Figure 7.1.2**). The phytoliths indices based on GSSC (Iph and Ic) were not calculated because the count of GSSC was lower than 100.

The PCA does not provide powerful results, but fossil samples are closer to wooded environments than to grass-dominated environments. As discussed in the previous chapter concerning modern soil assemblages (chapter 5.1), statistical approaches are very useful to infer paleovegetation from fossil assemblages. A first PCA was performed combining Zinj samples and the complete collection of modern soil samples from Africa (n=156), classifying samples by country and using the same variables (excluding Iph and Ic) (**Figure 7.1.3, Appendix 5.B**). A second PCA was performed using the same samples and the same variables used in the analysis performed with

our modern soils samples (i.e., large groups based on attributions [FI, palms, GSSC, other grasses/sedges, ferns and non-diagnostic phytoliths], percentage of diatoms, and the indices [excluding Iph and Ic]) including data from the Zinj samples (**Figure 7.1.4**). The first PCA plot Zinj samples near woodlands and samples from Tanzania and Kenya. Threesamples are plotted close to Cameroon (DB12-112, DB12-10 and DB14-09) due to the higher values of D/P caused by the scarcity of GSSC. The information provided by these results is in agreement/consistent with the interpretations made through the study of phytolith assemblages. In the second PCA there is absolutely no overlap with our modern samples. This can be explained by taphonomy, which affects GSSC more than others morphologies (Albert et al., 2006), by the dominance of globular FI in ZC samples, or by the presence of a completely different type of vegetation which we have not been able to describe.

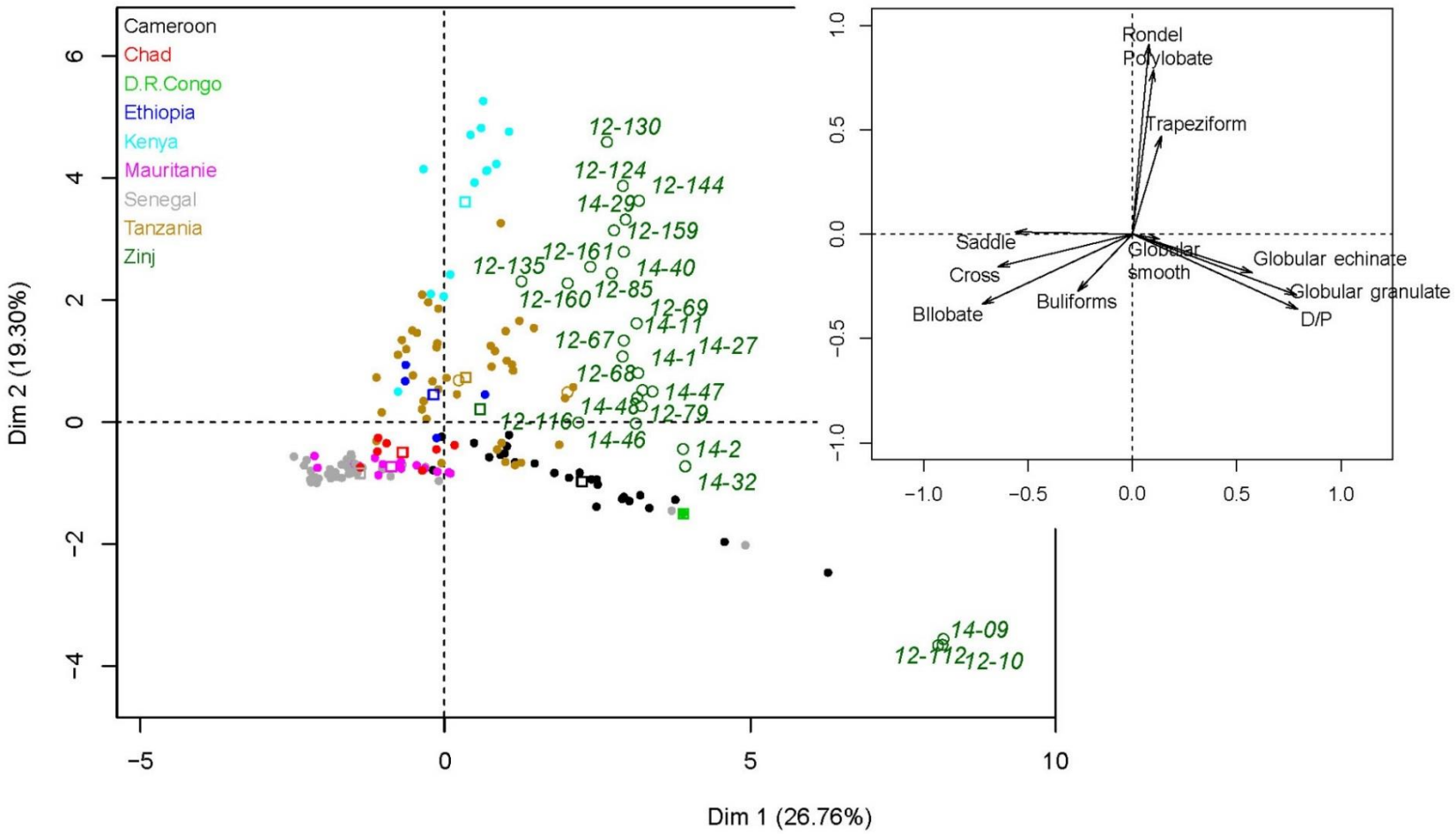

Figure 7.1.3. PCA showing differences between Zinj samples and 156 African modern soil samples (chapter 6), grouped by country of sampling (except Zinj samples, labeled).

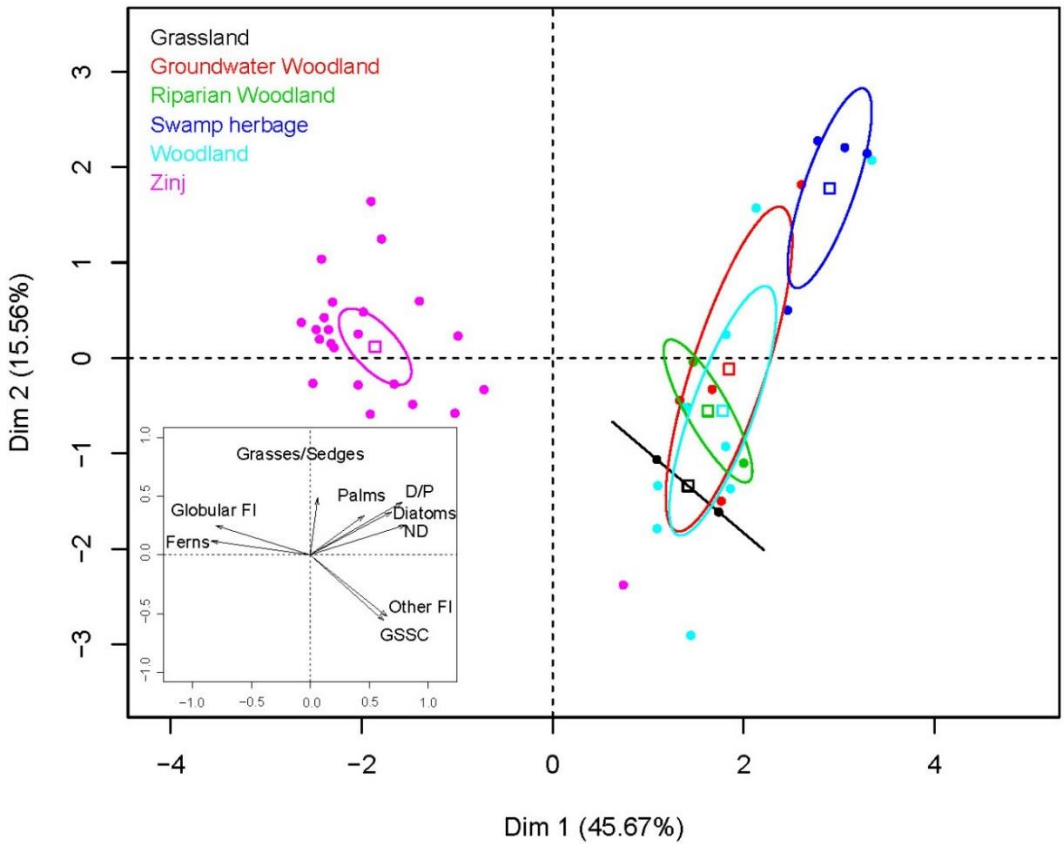

Figure 7.1.4. PCA showing differences between Zinj samples and 22 modern samples analyzed in chapter 6, grouped by vegetation type.

Paleoecological and paleovegetation reconstruction

The studied samples show a mixed paleovegetation dominated by forest. D/P index values clearly indicate a woody vegetation in more than 80% of samples. The common presence of palms in most assemblages indicates that they were regular component of the forests. Previous studies found high percentages of globular echinate phytoliths in palm swamp of *Raphia* sp. (~60%, Bremond et al. 2005a) but the results obtained in the modern soils analysis from lakes Manyara and Eyasi (**Figure 6.1.2, Appendix 7.A**) and by Albert et al. (2015) suggest that environments where palms are dominants can be characterized by percentages around ~10% of globular echinate phytoliths. Despite the low presence of fern phytoliths in the assemblages, their remains were found in all sites and their presence is important to analyze the relation

between environment and hominins because the occurrence of ferns suggests a shady and wet habitat (Kamau, 2012). A recent study using biomarkers to reconstruct paleovegetation, has also suggested the presence of ferns in samples from FLK Zinj (Magill et al., 2016).

The ZC results are similar to those obtained by Ashley et al. (2010b), who provided evidence for a freshwater spring and closed wooded vegetation in FLK NN (sampled north of the study area analyzed in the thesis) using $\delta^{13}C$ and $\delta^{18}O$ isotopes and phytolith remains. In Ashley et al. (2010a) the number of "other FI" is lower than in our samples. This implies that in our study area the presence of bushes, saplings or non woody dicotyledonous plants could be larger than in the paleovegetation reconstruction of FLK NN (Ashley et al., 2010). The whole FLK Zinj area was likely covered by closed wooded vegetation before the deposition of Tuff IC, which is a suitable habitat for ferns. The abundance of fern phytoliths at PTK and FLK Zinj may reflect the presence of watercourses (Uribelarrea et al., 2014) or springs (Ashley et al., 2010a). Diatoms were found in large quantities in modern samples related to watercourses and they could be used to interpret freshwater presence in paleoenvironmental reconstructions (Albert et al., 2015; Hay, 1976), but some diatom species develop in alkaline water (Hecky and Kilham, 1973), so their presence is not diagnostic of freshwater presence. Diatoms are absent in ZC paleosols. Diatom and fern remains were not observed in the FLK Zinj samples previously analyzed (Ashley et al., 2010a), this may be due to a lack of information about fern phytoliths. In our samples, GSSC are found systematically with very low abundance and we note that the majority of them are trapeziform shortcells (GSSC11). This contrasts with the results obtained in modern soil samples (**Figure 6.1.2, Appendix 7.A**), where these phytoliths rarely occur in the assemblages, as is also the case of many surface soil samples from Africa (e.g., Alexandre et al., 1997; Barboni et al., 1999; Bremond, 2003; Bremond et al., 2005a; Novello, 2012; Runge, 1999). Trapeziform shortcells occurs in the 32% of fynbos (Mediterranean shrubland from South Africa) grass species, and in the 24-55% of montane grasslands grass species (Rossouw, 2009). Considering that the climatic reconstructions suggest a dry period during those times in the ZC landscape (Magill et al., 2013a, 2013b), and Trapeziform shortcells are attributed to Pooideae, Ehrhartoideae and Danthonioideae (which are associated to

wetter and colder conditions than those of the area), three hypotheses can explain these relatively high levels of trapeziform shortcells: 1) there were some cooler, humid and shady spots, caused by spring water and associated vegetation, 2) trapeziform shortcells are more resistant to dissolution than other GSSC, and 3) at the moment of deposition of these phytolith assemblages the Ngorongoro volcano crater had an approximate altitude of 4000 m (Hay, 1976), so the high slopes of the volcano may have been a source of vegetation that produced trapeziform shortcell phytoliths. As discussed before, trapeziform shortcells are typical in formations that currrently occur in colder areas than our study area. What if climate was cooler than we think? Previous studies suggest that 2.0-1.8 Ma, the region was under an arid-semiarid environment (Bonnefille, 1984; Magill et al., 2013a), with mean annual precipitation between 250 and 700 mm/yr. (Magill et al., 2013a). Restionaceae are monocotyledonous graminoid plants that are abundant nowadays in the Mediterranean-like scrub, also called fynbos formations, in the Cape Region of South Africa (Allsopp et al., 2014), which occurs in infertile soil areas where mean annual temperatures vary between 3ºC (median minimum temperature) and 25°C (median maximum temperature), and mean annual precipitations range enormously between 200 and 3000 mm/yr. (Bradshaw and Cowling, 2014). They also occur in East Africa, but are not frequent (Beentje, 2005). In Tanzania today, Restionaceae occur in swamps in Morogoro Region (Beentje, 2005). Restionaceae phytoliths show a potential for reconstructing the extent of winter rainfall during the colder stages of the Pleistocene (Cordova, 2013). Restionaceae produce a variety of discoidal phytoliths (diameter: 5-25 µm, Cordova, 2013; Esteban et al., 2016) that is hardly distinguishable from those produced by woody plants (Esteban et al., 2016). We attributed these globular phytoliths to FI considering that no other diagnostic phytoliths of Restionaceae (Cordova, 2013) were found. Also, in our assemblages, most of the globular phytoliths attributed to FI are in the category Glo13, undoubtedly attributed to wood/bark tissues (Collura and Neumann, 2016). Phytoliths categorized as Glo10-11-12 can be confused with some globular regulate phytoliths found in Restionaceae, but none exhibit the spiraling decoration or the double ring on the edges, common in Restionaceae. In addition, our approach was conservative about attributions (as seen in the large percentages of non-diagnostic phytoliths). We consider that the main source of globular phytoliths in our assemblages

was woody dicots. We suggest that this approach must be further explored to discern this issue in future works.

Our paleovegetation reconstruction indicates a dense vegetation in PTK and AMK sites, which does not match previous results. Using phytoliths and macroremains, Blumenschine et al. (2012) suggested the existence of grasses and sedges in the wetlands close to a river channel 50 to 200 m southeast of FLK Zinj site (between PTK and FLK Zinj). Furthermore, palm phytoliths are incompatible with the river channel proposed by Blumenschine et al. (2012), where no mature soils should have been present. Our paleovegetation inference supports the geo-archaeological and geometrically corrected reconstruction of the FLK Zinj paleolandscape proposed by Uribelarrea et al. (2014), and not that proposed by Blumenschine et al. (2012). Uribelarrea et al. (2014) proposed that the studied area may have been divided in three zones according to the flooding pattern. Therefore, different distributions of vegetation are expected in each of the zones. The AMK site was situated in the supralittoral belt (i.e., the border of the lake), an area that was rarely flooded by the lake. The FLK-Zinj and PTK sites were situated in an area interpreted as a lacustrine terrace, which was occasionally flooded, and the DS site was likely placed in an elevated area surrounded by a depression that was more frequently flooded (Uribelarrea et al., 2014). The FLK-Zinj and PTK lacustrine terrace match with the Typha imprints found at the base of Tuff IC in PTK and FLK Zinj (Barboni and Domínguez-Rodrigo, *pers. comm.)*, which suggest the presence of a sort of *Typha* swamps in those areas (maybe in the areas occasionally flooded). The DS samples were sampled in an area that may have been a former land elevation, during phytolith deposition, an anomaly that may explain the presence of palms (Uribelarrea, *pers. comm.*). As shown in **Figure 7.1.5,** the distribution of samples rich in grasses-sedges or palms does not indicate differences between sites, suggesting a similar paleovegetation in the entire area. Even the most remote and isolated sample (DB14-32) exhibits a similar pattern to the ZC samples. In addition, the spatial flooding model (Uribelarrea et al., 2014) suggests the presence of freshwater inputs from the south (associated with an alluvial fan), which could promote wet habitats compatible with the presence of ferns.

There is a debate about the possible presence of a freshwater source in PTK site. Driese and Ashley (2015) have suggested that supplementary soil moisture by spring discharge during low lake levels in PTK surroundings (that could explain the presence of fern phytoliths). No geological evidence has been found of spring waters in PTK (Uribelarrea *pers. comm.*). Uribelarrea (*pers. comm.*) suggests that the carbonates, used by Driese and Ashley (2015) to indicate the presence of a water spring, are, actually, of diagenetic origin (formed underground after deposition of the sediment). Also, the proposed water spring is associated to a fault formed after Tuffs IC, ID and IE, so, it is subsequent to level 22 of PTK. However, a river or spring bringing subterraneous water can explain high FI percentage, so, with the phytolith analysis results, we are not able to support or reject any hypothesis.

Our results do not support the paleoenvironmental reconstruction based on δ13C analysis of Magill et al. (2016). These biomarkers provide evidence of open vegetation close to our PTK samples. The results of Magill et al. (2016) are biased by incorrect sampling. Three samples were collected in the floodplain, not in the PTK archaeological site, which could explain the low signal of wooded vegetation. Another sample was collected in mud filling a cavity produced by erosion of the original sediment (Domínguez-Rodrigo, *pers. comm.*), so results do not reflect the vegetation at the time of deposition. The northern area analyzed by Magill et al. (2016) and our results both suggest the same wooded paleolandscape.

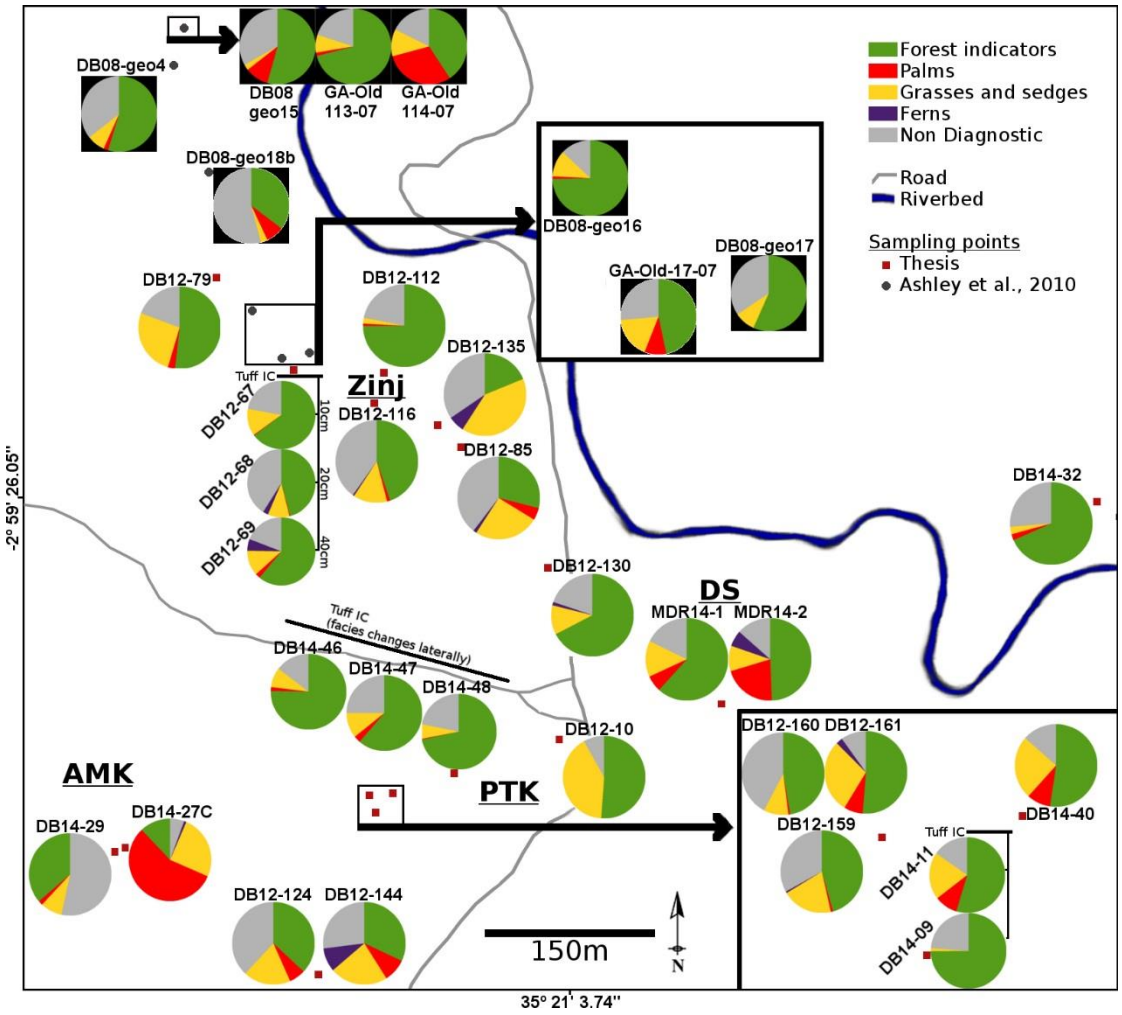

Figure 7.1.5. Location map of the ZC soil samples and phytolith signal of botanical groups. FI, forest indicators, do not include palm phytoliths. Graphs represent phytolith signal at sampling points (red square: samples analyzed in this thesis, black dots: samples analyzed in Ashley et al., 2010). Tuff schemes indicate the stratigraphic position of samples.

The analysis of samples collected vertically through the stratigraphic succession shows no vegetation changes over time. In the three samples from FLK Zinj northwest "corner" (DB12-67, 68 and 69, collected at 10, 20, and 40 cm under the Tuff 1C respectively), FI phytoliths represent 65%, 46% and 65%, respectively, palm phytoliths just represent 2% in DB12-69 (absent in the others), grass-sedge phytoliths represent 13%, 10% and 12%, respectively, and fern phytoliths represent 3% and 6% in samples DB12-68 and 69, respectively (absent in DB12-67). This indicates that no significant change is observed in the main vegetation groups during

the sedimentation period of the three samples analyzed. This sampling covers a time-span of about 15000 years, if a deposition rate of 0.5 mm/yr is considered (Ashley, 2007; Hay and Kyser, 2001). Another sample set from PTK (DB14-09, 11) was also used to evaluate the changes in vegetation over time. Palm signal shows a major change, since it represents 30% of the assemblage in DB14-11 but is absent in DB14-09. DB14-09 remains are largely damaged, which may explain this wide variation. The abundance of FI phytoliths (particularly at FLK Zinj over a long period 15000 of years) is consistent with the results of previous studies on phytolith remains from FLK NN below Tuff IC (Ashley et al., 2010a), with δ13C and δ18O isotopes analysis (Ashley et al., 2010b) and with phytolith remains from FLK N under Tuff IF (Barboni et al., 2010), which suggest that vegetation of the area was densely wooded during deposition of middle and uppermost Bed I. In addition, faunal remains such as bovids (Kappelman, 1984; Potts, 1988), rodents (Fernandez-Jalvo et al., 1998; Jaeger, 1976) or freshwater invertebrates (Hay, 1973) also support the presence of densely wooded environments.

The samples DB14-46, 47, and 48, sampled under Tuff IC but in three different sediments do not show changes in vegetation over short spatial distance, despite clear sediment changes. These PTK samples are dominated by FI phytoliths (61% to 75%). Grasses/sedges phytoliths represent 6 to 11%, and palm phytoliths are present in DB14-46 (2%) and DB14-47 (3%). In samples DB14-09 (oldest) and DB14-11 (youngest) FI phytoliths represent 75% and 55% of the total assemblages, respectively, and grasses-sedges 1% and 20%.

During deposition times (through Beds I and II, from 1.85 to 1.5 Ma, approx.), the study area was located in a large scale paleolandscape characterized by open spaces dominated by grasses and sedges with scarce presence of arboreal plants (*Bonnefille 1984, Bonnefille et al., 1982; Bonnefille and Riollet, 1980)*. Our results support the importance of zonal variations in water supplies in the Olduvai area vegetation. It seems that in the southern area of the Zinj Peninsula the presence of spring-associated woodlands was recurrent (Ashley et al., 2010b; Ashley et al., 2010c; Barboni et al., 2010). This patched vegetation of groundwater woodlands mixed with wooded

grasslands is currently common around lakes Manyara and Eyasi, which are modern analogues of paleolake Olduvai (Barboni, 2014).

Implications for human behavior

The results presented here show an extension of the area covered by wooded vegetation to the south of FLK Zinj, including the southern part of FLK Zinj, AMK, PTK and DS. In the southern part of FLK Zinj, the lack of archaeological remains does not suggest a hominin occupation, but PTK and DS exhibit a dense accumulation of cut-marked faunal remains associated with large stone tool assemblages (Arriaza and Domínguez-Rodrigo, 2016) in the same clay stratum and paleosurface deposit underlying Tuff IC, which contains FLK Zinj. In PTK, the earliest modern human-like hand bone was found (Domínguez-Rodrigo et al., 2015). The presence of these remains, along with the evidence of a paleovegetation similar to that previously described in FLK Zinj (Ashley et al., 2010a), lead to explain the relation between hominins, fauna and environment as in the case of FLK Zinj. FLK Zinj is well known for the dense concentration of archaeological remains found associated to Tuff IC (Domínguez-Rodrigo et al., 2010a, 20010b; Leakey, 1971)**.** FLK Zinj is interpreted as a site with an anthropogenic origin, where lithic remains and bones processed by hominins are functionally-related (Domínguez-Rodrigo et al., 2007). A behavioral model has been proposed, in which hominins used the site to process animal carcasses in a central-place foraging behavior, and not only as refuge (e.g., Ashley et al., 2010; Domínguez-Rodrigo et al., 2007). These areas were intensively occupied and hominins developed a wide range of activities (Bunn and Kroll, 1986). This model refuted the idea that hominins were attracted by vegetation, for shade and refuge, to act only as passive scavengers that transport carcasses acquired in more open areas over long distances to processed them (e.g., Blumenschine, 1995; Blumenschine et al., 2012). The presence of freshwater springs and watercourses served as source of potable water and were attractive both to hominins and animals during dry periods. The profiles of bovid mortality found in FLK Zinj show that hominins could have acted as ambush predators (Bunn and Pickering, 2010), and that they may have had early access to intact carcasses (Pickering and Domínguez-Rodrigo, 2006). If predators or hominins killed animals on the spot, it seems likely that hominins played an active role in obtaining

animal resources from nearby sites and transported carcasses short distances to butchering sites. This hypothesis is plausible in the case of the PTK site, which appears to be placed in the middle of a densely wooded area in which long transportation of carcasses may have been difficult. Despite the well traced relation between tools and cut-marked bones, the interpreted environment may have been also a source of plants for feeding purposes (Rose and Marshall, 1996), according to previous studies that suggested plant processing in wooded habitats (Diez-Martin et al., 2010), the multiple purposes suggested for cutting and hacking tools (e.g., butchering, wood working, plant processing, tuber digging) (Diez-Martín et al., 2015), and according to the palm and woody plants processing observed in FLK West site (Chapter 8).

7.2 BK

Description of phytolith assemblages

In the 24 paleosol samples collected in the BK site, six samples are sterile (DB11-3, 4, 6, 7, and 9 collected in Trench 1 and DB11-19 collected in Trench 2). 52 phytoliths morphotypes were described (summarized in **Figure 7.2.1**). Most types could be attributed to a possible botanical producer group/signal (**Figure 7.2.2**). Detailed counts are shown in **Appendix 7.B**. Forest indicator (hereafter FI) phytoliths (excluding palms) clearly dominate the assemblage and are the largest group in all samples. FI phytoliths represent 46% to 92% of the assemblages (μ=67%±13.9%). In FI phytoliths, globular rugose/granulate phytoliths (Glo5, 8, 10-13) represent 6% to 49% of total assemblages (μ=24%±12.3%), whereas the other FI phytoliths represent 11% to 77% (μ=43%±17.4%) of total assemblages. Palm phytoliths are the other component of forest formations, and represent up to 10% of the assemblages (μ=2%±3.1%). The phytoliths attributable to grasses and sedges represent up to 15% of assemblages (μ=6%±5.4; GSSC phytoliths μ=4%±4.4%, range 0-15%), and fern phytoliths represent up to 15% (μ=2%±4.4). Non-diagnostic phytoliths that to date cannot be attributed to any specific taxon represent 6% to 48% (μ=23%±11.3%) of total assemblages.

There are no significant differences between units, trenches or between samples collected above and under Tuff IID, therefore no detailed descriptions of different trenches or units will be provided. The only exceptions to this point are the lower presence of grass/sedge phytoliths in samples from Unit 3, compared to samples collected in Units 1 and 2 and to those collected under Tuff IID; and the presence of palm phytoliths, which only occur in samples from Units 1 and 2 (**Figure 7.2.2**, **Appendix 7.B**). Analyzing the percentages of phytoliths grouped by morphology, we do not observe great variations over time for most groups. Trapeziform shortcells (GSSC11) seem to be more frequent in samples from upper units 1 and 2, elongate morphologies from dicotyledonous plants (El1, 3, 10 and 15) only appear significantly in the three oldest samples (DB12-73 above Tuff IID and DB12-18 and 19 under Tuff IID) and in the most modern sample (DB11-18). (**Figure 7.2.1**, **Appendix 7.B**).

Although the percentage of FI phytoliths does not variate largely among samples, the distribution of these FI between “globular FI” and “other FI” does. “Other FI” phytoliths are slightly more frequent in samples collected under Tuff IID, in the older samples of Unit 1, and in Unit 3, but these differences are not significant and do not change the overall paleovegetation descriptions.

D/P, Iph, and Ic indices were not calculated due to the scarcity of GSSC recovered from BK samples. Multivariate tests to compare BK samples with modern samples were not performed considering the results obtained in “Zinj complex” (chapter 7.1) multivariate tests and the scarcity of phytolith assemblages.

Diatoms were sparsely observed in BK paleosols. Only 30 diatoms were counted in the analyzed samples (6 under Tuff IID). Only sample DB11-18 (unit 3, trench 14) provided a slightly relevant number of diatoms (n=18) **(Appendix 7.B).**

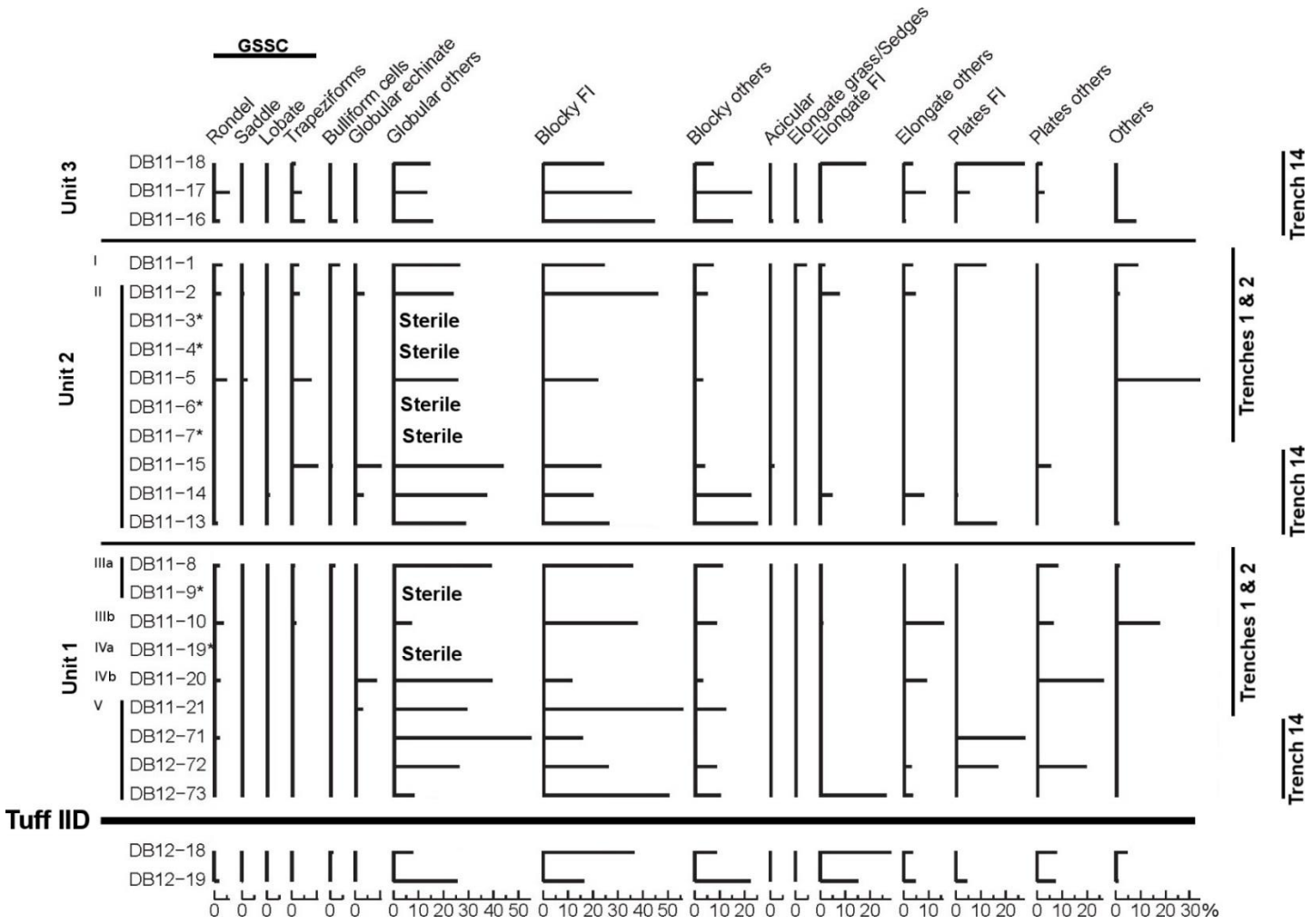

Figure 7.2.1. Relative abundance in percentage of phytolith main categories. *: sterile samples.

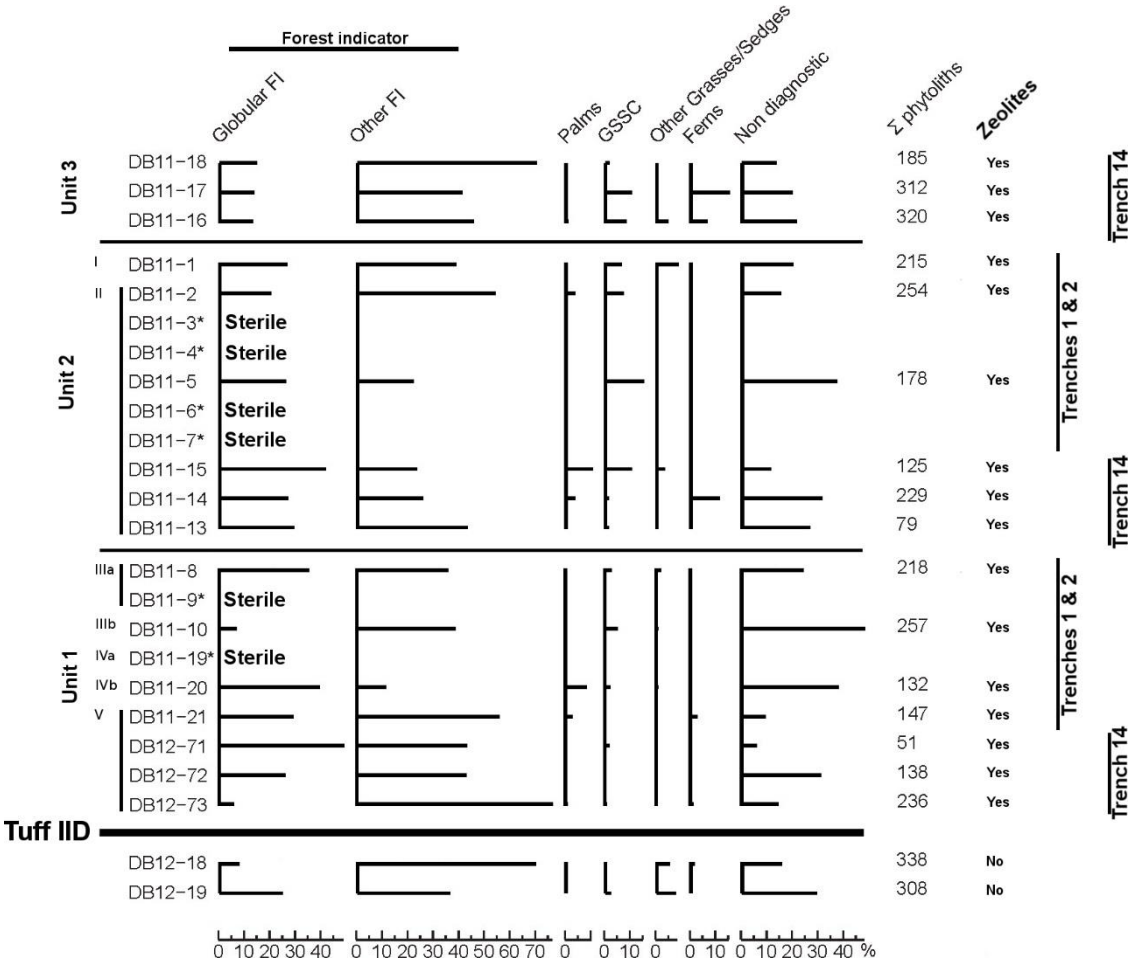

Figure 7.2.2. Relative abundance in percentage of phytoliths grouped by botanical attribution, and ecological index values. *: sterile sample. Roman numerals indicate archaeological level.

In the BK paleosol samples, large percentages of phillipsite zeolites and analcime zeolites have been recovered (**Figure 7.2.3**). Two hypotheses can explain the abundance of these minerals: (1) the volcanic origin of sediments. Phillipsite zeolites and analcime zeolites are volcanic minerals (Myrbo et al., 2011) and their presence in paleosols may be explained by the transport of sediment from the nearby slopes. The sediment of BK was formed by the erosion of the slopes of Lemagrut volcano, which was located southeast of BK (Domínguez-Rodrigo et al., 2014a)**.** (2) Zeolites came from the paleolake. Zeolites of the central basin of Olduvai were formed principally by reaction of pore fluid with detrital clay and particles of volcanic glass (Hay, 1970).

Zeolites are very common in sediments formed under highly evaporative conditions (Hay, 1976; Hay and Kyser, 2001). Ashley (*pers. comm.)* suggests that the BK archaeological site was formed during a dry period when the lake contracted and the river eroded older sediments generating and incised valley.

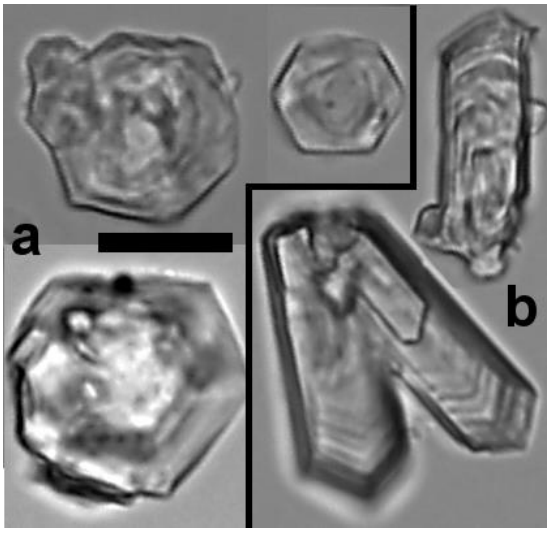

Figure 7.2.3. Volcanic mineral remains found in BK samples. **a)** Analcime zeolites**. b)** Phillipsite zeolites. Scale bar 10 μm.

Paleoenvironmental reconstruction. Concordance with the geological reconstruction of BK

According to the assemblages, the vegetation of BK was clearly dominated by forest components, but in BK, non-globular FI phytoliths are more abundant than globular phytoliths, in contrast with other paleosols (e.g., Ashley et al., 2010a; Barboni et al., 2010; see also "Zinj Complex" results in this thesis, chapter 7.1). This could indicate that the presence of bushes, saplings or non-woody dicotyledonous plants in this environment could be larger than in previous paleovegetation reconstruction that

describe wooded vegetation (e.g., the ZC reconstruction proposed in this thesis or Ashley et al., 2010a), which fits with the rich understories such as those found in gallery forest in riverine environments. These reconstructed vegetation fits well with the avifauna remains found at BK which suggest a low energy river with presence of trees and bushes near the river bank (Pernas-Hernández, *pers. comm.*)

The results reflect a vegetation that fits well with the geological reconstruction of BK (Uribelarrea et al., 2014). The sedimentary environment in which BK was formed was a low energy alluvial system with alternating distributary channels (chute-channels) and low energy interchannel areas (Domínguez-Rodrigo et al., 2014a). The whole system evolved into a final phase in which the fluvial channel was filled with sediments (silting phase). Sediments from trenches 1 and 2 were sampled in the point-bar, where chute-channels eroded and mobilized fine sediments due to water traction. This water erosion changed soils frequently, so vegetation could not develop or developed difficulty, which may explain the possible abundance of non woody dicotyledonous plants. The chute-channels alternated with small interfluves where fine sediment was retained, allowing the development of soil and vegetation. This alternation may explain the occurrence of sterile samples (DB11-3, 4, 6, 7, 9, and DB11-19) near productive samples. This geological reconstruction, and the dominance of phytoliths that cannot be attributed undoubtedly to woody dicots ("Other FI", Figure 7.2.2) suggest that dicot plants in these areas were (as at present) bushes, saplings and non-woody dicots (**Figure 7.2.4**). On the contrary, trench 14 was located in the river channel but in a more evolved state in which floodplain sediments (silts and decantation clays) accumulated. This low energy system retained humidity and allowed the development of deep and mature soils.

Figure 7.2.4. Modern river in the study area. The picture shows the alternation of areas covered by bushes and herbaceous plants and areas uncovered by vegetation as proposed for trenches 1 and 2 of BK (Photo provided by David Uribelarrea).

The presence of six sterile samples (DB11-3, 4, 6, 7, 9, and DB11-19), and sub-sterile samples with less than 100 phytoliths counted (DB11-13 and DB17-71), as well as the sparse presence of GSSC phytoliths, may be the result of taphonomical processes. Taphonomy has to be taken into account because it can affect the representativeness of phytolith assemblages. Taphonomy affects phytolith conservation in assemblages and is one of the causes that produce unidentifiable phytoliths. Basic (high pH) environments concentration affect phytoliths by increasing their solubility, but it seems to affect more the surface decoration/details than the three dimensional shape of phytoliths (Fraysse et al., 2006). It is also important to take into account the differential stability of phytolith morphologies: if phytoliths from grasses lose their surface decoration they could be identified as other simpler morphotypes. Furthermore, long and decorated morphologies are largely affected by basic pH (Cabanes et al., 2011). Other taxonomical bias is the under-representation of the amount of phytoliths in paleosols in comparison to modern samples. This could imply the over-representation of several groups, such as dicotyledonous from wood/bark or

globular, the under-representation of grass/sedge groups and the reasonably accurate representation of palm phytoliths (Albert et al., 2006). In the BK samples the large predominance of FI phytoliths leads to consider that taphonomical processes have affected the assemblages facilitating the dissolution of other plant remains. A measure to evaluate the impact of taphonomy on the representativeness of phytolith assemblages, based on the ratio of long and short morphologies (Madella and Lancelotti, 2012), was carried out. The percentage of long cells in modern samples (chapter 6) is 26%±9% (range: 9%-47.6%), whereas in the BK samples it is 19%±12.5% (range: 0-43%). However, differences within the same sample set (modern and paleosols) are too high and differences between sites are too weak to establish if low long cell rates are due to taphonomy or to natural variability. The absolute predominance of FI phytoliths, the good conservation of some "fragile" phytoliths, and the consistency between the phytolith assemblage results with the geological description, allow us to consider that paleovegetation patterns, rather than partial dissolution of phytoliths due to taphonomical processes, are responsible for the phytolith assemblages obtained here. Nevertheless, we advise cautiousness when proposing hypotheses derived from these results and we suggest that further analyses should be carried out in order to confirm these preliminary results of phytolith analysis, because they have to be considered all the issues previously discussed about phytolith attributions (chapters 4, 5 and 7.1), and because the presence of zeolites suggests alkaline environments that could induce high rates of phytolith dissolution (Cabanes et al., 2011; Cabanes and Shahack-Gross, 2015),

Implications for human behavior

BK site was formed when the Olduvai paleolake was almost disappeared during a dry period (Hay, 1976; Kovarovic et al., 2013). According to previous descriptions, during other moments when the paleolake was low, the paleovegetation was dominated by wooded grasslands (Bonnefille, 1984; Bonnefille and Riollet, 1980), which fits with the open-habitat suggested by the analysis of the faunal remains found at BK (Domínguez-Rodrigo et al., 2014).

In a general dry context, the presence of both vegetation, which provides resources and refuge, and a river, which provides freshwater, suggest that BK acted as an oasis that attracted hominins and other animals. In BK, as well as in the "Zinj complex" sites, a large number of bones exhibit percussion marks and cut marks. These bone remains are associated with large assemblages of stone tools. All these data suggest primary access to fleshed carcasses by hominins. BK has been described as an anthropogenic site created by butchering activities over time (Diez-Martín et al., 2009; Domínguez-Rodrigo et al., 2009; Egeland and Domínguez-Rodrigo, 2008). Level IVb in BK has been interpreted as a site in which hominins not only carried out butchering activities. The outstanding amount of lithic raw material, seems to exceed the amount necessary to produce the tools for butchering. Thus, in level IVb, other hominin activities besides butchery were carried out (Domínguez-Rodrigo et al., 2014a). To summarize, the dense paleovegetation, together with the watercourse, attracted animals and hominins, as in Zinj/PTK/AMK/DS site. It is mandatory to complete the spatial analysis of BK by studying surrounding areas to evaluate whether the described paleovegetation was part of an extensive wooded area or it was truly a gallery forest whose surroundings were a dry area with sparse/open vegetation, as suggested by the study of faunal remains that proved the existence of open-habitat faunas (Domínguez-Rodrigo et al., 2014a).

8. FLK West stone tools analysis and experimental archaeology

8.1 Experimental archaeology

Can phytolith assemblages be biased by depositional processes and laboratory procedures?

An experimental archaeology test to evaluate whether phytolith assemblages are biased by random deposition causing false positives was carried out. The goal of this experiment was detecting if significant differences between phytolith count on stone tool surfaces and those from the encasing sediment could be interpreted as random or functionally related (see the Methods section, Chapter 4). Twenty-one phytolith morphological categories were described from experimental soils and tools. Detailed countings are given in **Appendix 8.A**. When the 21 morphological groups were compared between soil and tools, MANOVA test gave a *p*-value of 0.4113. A *p*-value greater than 0.05 means that the null hypothesis (covariances are unequal) must be rejected. Therefore, the obtained value indicates that there is no difference between soils and tools. Partial results in MANOVA test gave *p*-values below 0.05 for three phytolith categories. These three categories that are significantly different between soils and tools are "GSSC Rondel" (*p*-value = 0.02), "blocky irregular psilate" (*p*-value = 0.0298) and "globular echinate" (*p*-value = 0.0007). To confirm or discard these three differences, Monte-Carlo permutation test were carried out. The results of these tests showed that soils and tools are different in "GSSC Rondel" (*p*-value = 0.015) and "globular echinate" (*p*-value = 0.003), but differences in "blocky irregular psilate" category (*p*-value = 0.978) are not significant. We repeated the MANOVA test by grouping phytoliths in different ways. Firstly, MANOVA test only using grasses/sedges phytoliths (GSSC and bulliform cell) was carried out. The *p*-value obtained was 0.643 (no difference between groups), and no partial difference between soils and tools was observed. Secondly, by grouping phytoliths according to their morphology in seven categories (GSSC, elongate, blocky, platelets, globular, acicular and bulliform phytoliths) the obtained *p*-value was 0.008 (difference between groups), but concerning partial results, just two groups showed differences: "blocky" category (*p*-value = 0.0002) and "globular" category (*p*-value = 0.0003). Monte-Carlo permutation test showed that difference between soils and tools for "blocky" category is not significant (*p*-value = 1), but it is for "globular" category (*p*-value = 0.002).

Finally, in the last test, phytoliths were grouped according to their taxonomical attribution in five categories (grasses/sedges, dicots -except those from hard tissues-, hard tissue, palms -i.e., same values than "globular echinate"-, and non-diagnostic phytoliths). MANOVA test produced a *p*-value of 0.018 (difference between groups). Partial differences were significant only in "palms" category (*p*-value = 0.0007125).

According to these results, statistical tests did not find differences between tools and soils for most groups, however, for several groups these differences are statistically significant. Comparing tools and soils using the original 21 categories, differences between tools and soils are not significant, but "globular echinate" and "GSSC rondel" category values are significantly different. Were there some tools pointed as "false positives"? Regarding the range of values for "globular echinate" and "GSSC rondels" categories, five tools (in each of these two categories) exhibit phytolith percentages out of the range of values obtained in soil samples. Anyway, these values are under the lower limit of soil values and the difference between them (in percentage) is weak. Hence, these tools would not have ever been considered as "used tools" in a hypothetical stone tools analysis.

It is also important to note that the number of countings (200 phytoliths in total) can be considered insufficient according to previous analyses that suggested counting a minimum of 200 diagnostic phytoliths to reduce the bias caused by smaller countings (Strömberg, 2009). The amount of countings was set as the same as in the FLK West stone tool analysis (200 phytoliths counted at least for each sample) in order to standardize the results. Even with this apparently insufficient total number of phytoliths, the variability due to random/stochastic processes is irrelevant. To summarize, the results of the experiment show that depositional processes and laboratory procedures do not create artificial differences in phytolith assemblages between soils and tools.

8.2 FLK West stone tool analysis

Microbotanical remains from FLK West stone tools

Fifty-three phytolith morphotypes were described and then attributed to a possible botanical group based on their morphological features (shape, size, texture, etc.) (**Figure 8.1**). Detailed phytolith counts are given in **Appendix 8.B**. From the total of 41 analyzed stone tools, two were sterile, and 12 exhibited phytolith patterns distinguishable from those of paleosol samples (**Figure 8.1**). Two distinguishable phytolith signals between paleosols and some tools were found. The strongest signal is for palm phytoliths (globular echinate, Glo10-11). Palm phytoliths occur at low abundance in paleosols (0-3%, μ=1.5%±1.2%, of the total phytolith assemblage). In four stone tools (41, 87, 90 and 208) palm phytoliths represent more than 10% of the phytolith assemblage. The result of the permutation test for palm phytoliths shows that the mean difference between paleosols and the selected stone tool samples is significant (*p*-value 0.002, mean difference 9.6%). Therefore, the high proportion of palm phytoliths on the selected stone tools contrasts with the low percentage of palm phytoliths in paleosols.

The second distinguishable signal is for dicotyledonous hard tissue phytoliths (wood and/or bark). Hard tissue phytoliths in paleosols represent 10% (±3.7%, range: 5-17%). Five stone tools exhibit values over 29% (42, 68, 174, 208 and 219). The permutation test for hard tissue phytoliths showed that the difference between paleosol and the five tool samples is significant (*p*-value 0.001, mean difference 36%). Therefore, the percentages of hard tissue phytoliths in the selected stone tools contrast with those percentages of paleosols. The origin of this marked signal is observed especially in one phytolith category, (Blo8). In paleosols, these phytoliths represent 7% (±3.4%, range: 1-11%), whereas in the selected tools they represent 100% of the dicots hard tissue phytoliths found. Actually, only regarding the percentages of Blo8 phytolith percentages, a second group of four tools (45, 56, 185 and 186), exhibits percentages of 23-24% for these phytoliths, which duplicate the highest value found in soil samples. Adding these tools to the tools previously selected for their percentages of dicots hard tissue phytoliths, and using permutation to compare Blo8 phytolith

percentages, the difference is also significant (*p-value* 0.001, mean difference 34%). Therefore, we consider that these tools exhibit a pattern of phytoliths clearly different from that of paleosols.

A PCA carried out using the five main categories of phytoliths ("Grasses/sedges", "palms", "hard tissues", "other dicots" and "non-diagnostic" phytoliths) (**Figure 8.2**) shows that stone tools with distinguishable signal for palm phytoliths (41, 87, 90 and 208), and the first group of tools with distinguishable signal for dicots hard tissue phytoliths (42, 68, 174, 208 and 219) are separated from paleosol samples. On the contrary, the second group of tools with distinguishable signal for dicots hard tissue phytoliths (45, 56, 185 and 186) is not clearly separated from other tool samples. It is important to note that a group of samples, plotted in the third quadrant (negative values in Axes X and Y), tends to separate from soil samples by the "non-diagnostic" phytoliths component. These samples are rich in "Unid 4" phytoliths (dubious lacunate or altered bodies), which makes it impossible to attribute them to any plant taxon.

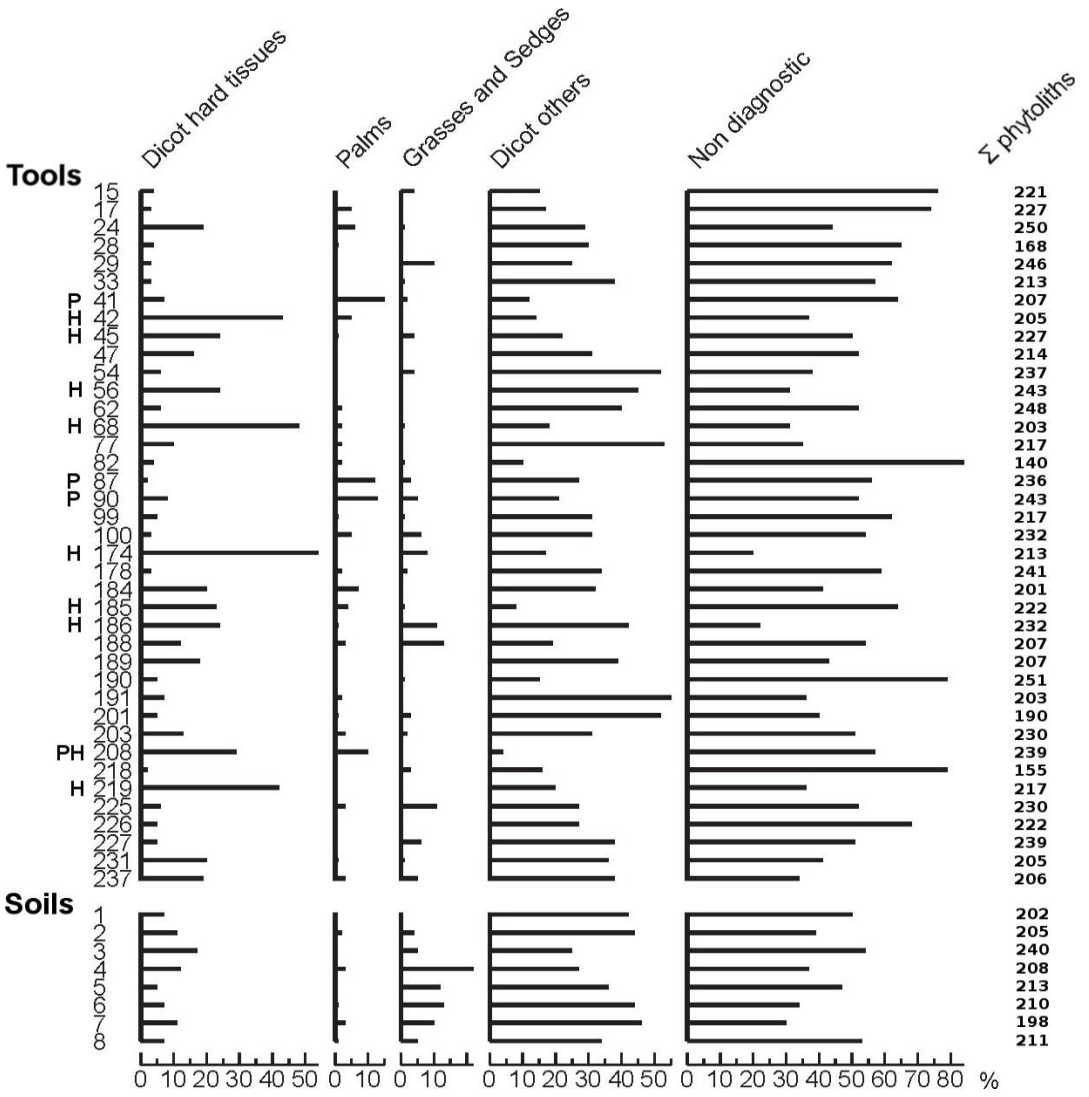

Figure 8.1. Relative abundance in percentage of phytoliths grouped by botanical attributions. In bold, values marked as distinguishable signal. H: distinguishable signal for dicotyledonous hard tissue phytoliths, P: distinguishable signal for palm phytoliths.

To summarize, 12 stone tools exhibit phytolith assemblages that differ from those of paleosols. Four stone tools present a distinguishable pattern for palm phytoliths, eight for dicots hard tissue phytoliths, and one for both signals. Distinctive assemblages of dicot hard tissue (wood and/or bark) phytoliths were found in five cores and four flakes (five in quartz, two in basalt, and one in phonolite). The hard tissues signal may tentatively be related to scrapping, cutting or battering activities. Distinctive assemblages of palm phytoliths occur in two cores, one pebble, one

hammerstone and one flake (two in quartz, and two in basalt). The palm signal may tentatively be related to battering activities. The analyzed tools were selected randomly from the complete collection recovered in FLK West, so some samples cannot be undoubtedly categorized as tools or do not show use-wear. From the total 41 tools studied, three fragments were analyzed and they did not exhibit distinguishable phytolith patterns different to those of soils. Seven pebbles without percussion stigma were analyzed, and in 6 of these pebbles we did not find significant differences between soil and tool samples. One of these pebbles showed a distinctive signal for palm phytoliths. No correlations were observed between size, weight, or raw material of stone tools and phytolith patterns.

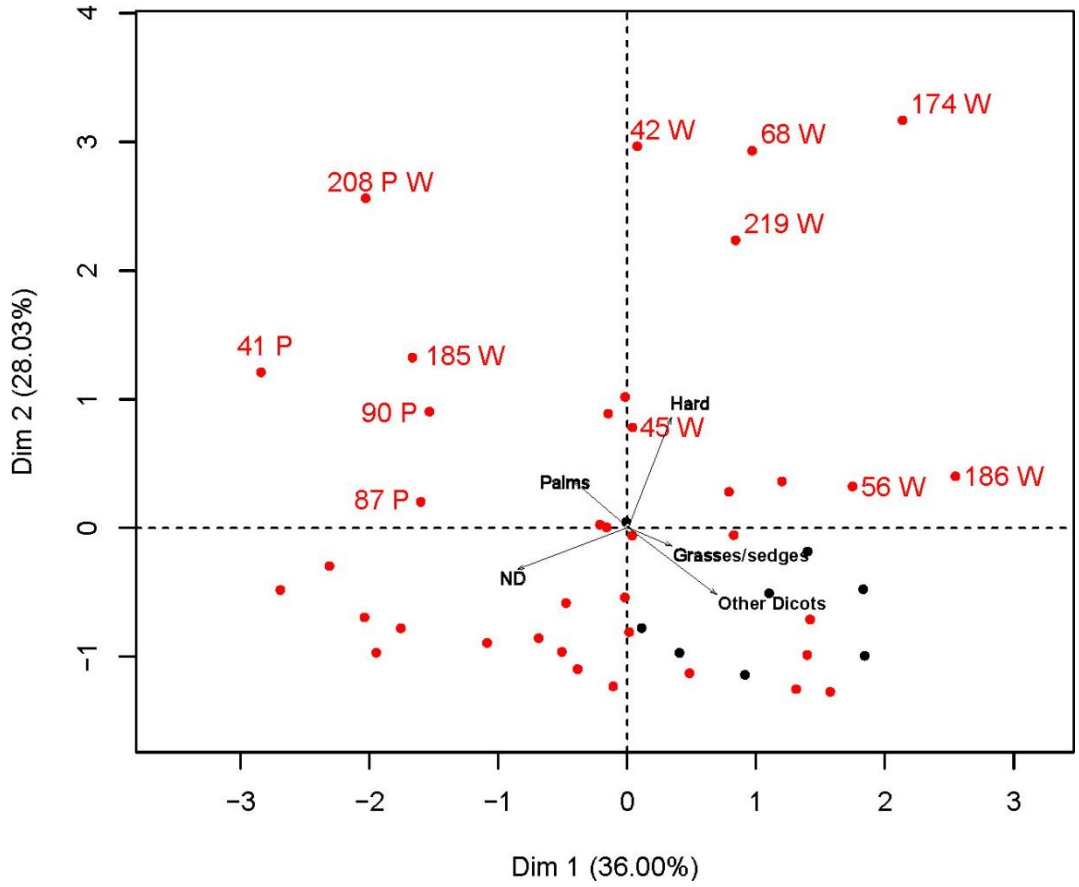

Figure 8.2. PCA showing differences between FLK West paleosol samples and stone tool samples grouped by phytolith attributions. P: distinguishable pattern for palms phytoliths. W: distinguishable pattern for dicots hard tissue phytoliths. Red: stone tool sample, Black: paleosol sample.

Starches analyses at FLK West yielded a total of 210 granules on stone tools. Seven stone tools present countings significantly higher (10 to 21 granules, **Table 8.1**) than those from surrounding sediments, paleosols, and anti-contamination tests. Starch granules were found in significant amounts in two LCT (large-cutting tools), two cores, one anvil, one pebble and one flake. Two types of starch granules were described on stone tools: a majority of polyhedral and fissured granules attributed to type A, and less common ellipsoidal and fissured granules attributed to type B **(Figure 8.3)**. The ellipsoidal granules cannot be identified and their botanical origin remains uncertain. On the other group, the granules (polyhedral, fissured) look like those described in Poaceae samples in our reference collection and Poaceae granules observed elsewhere

(Mercader, 2009), including modern contamination analyses (Crowther et al., 2014). In our anti-contamination tests, we found that type A starch granules are similar in shape but not in size to those found associated with stone tools. In surrounding sediment analysis, 10 granules were found in five samples. In anti-contamination tests, just two granules were found on materials that are directly in contact with samples from a total of 80 granules, **Appendix 4.2.A**).

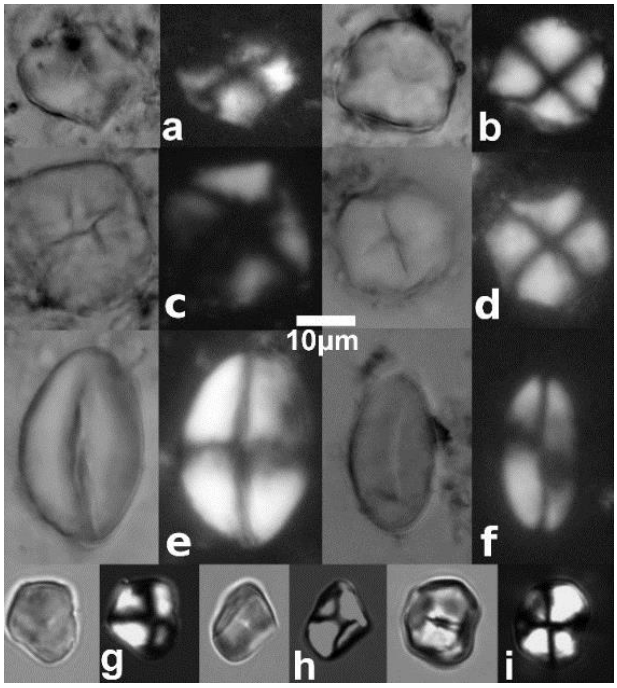

Figure 8.3. Selection of optical micrographs of starch granules found in stone tools and anti-contamination tests (400x). a-d: polyhedral granules from stone tools attributed to grasses (Type A); e-f: unidentified ellipsoidal granules from stone tools (Type B); g-i: polyhedral granules from anti-contamination tests.

Table 8.1. Starch granules analysis results. *: tools mentioned in text. Only surrounding sediments in which starch granules were recovered are mentioned in the table.

Sample ID	Type A	Type B	Sample ID	Type A	Type B
15	4		**191**		
17*	17		**197**		
24	9		**198**		
28*	8	3	**201**		
29	2		**203**	4	
33*	5	5	**208**	2	
41			**218**		
42	6		**219**	6	
45			**225**	2	
47	3		**226**	7	
54*	6	5	**227**	2	
56	6		**228**	6	1
62	8		**231***	18	
68			**237**	7	
77	3		**SOIL 1**		2
82*	18	3	**SOIL 2**		
87	8		**SOIL 3**		
90			**SOIL 4**		
99	5		**SOIL 5**		
100			**SOIL 6**		
174	1		**SOIL 7**		
178			**SOIL 8**		
184	2		**Sediment 189**	4	
185			**Sediment 190**	3	
186*	15	2	**Sediment 191**	1	
188	5		**Sediment 198**	1	
189	5		**Sediment 203**	1	
190	4	1			

Does starch remains indicate signals of plant use at FLK West site?

Out of 216 starch granules found in FLK West stone tools, 90% were classified into type A (polyhedral and fissured granules). The type A granules (polyhedral, fissured) are similar in morphology to Poaceae starch granules (Mercader, 2009; Reichert, 1913).

Our results show that there is a significant difference between the amount of starch granules found in stone tools and the control test performed on paleosols, surrounding sediment, and laboratory, but in our anti-contamination tests we recovered starch granules similar in shape, but not in size, to those described as type A on stone tools. Moreover, in the 41 samples of soils surrounding the tools we only found ten granules (in five samples) similar to those found in anti-contamination tests. If these granules come from grass samples, our results could potentially agree with previous works that suggest consumption of C4 grasses by early hominins (Stewart, 2014; Wynn et al., 2013). Further support that the starch granules come from stone tools is provided by the fact that in anti-contamination tests only two granules were found on materials that are directly in contact with samples (**Appendix 4.2.A**).

Three facts argue against the hypothesis that starch granules on stone tools are the result of plant processing: the similarity between granules found in the other anti-contamination test and type A from stone tools; the fact that most starch granules used in modern industry (which may contaminate archaeological samples) are grass starch granules (Crowther et al., 2014); and the fact that starch granules were recovered in almost all stone tools. The main source of recovered starch granules should be the remains of stone tools, but the sparse remains found, the possibility of contamination, their dubious attribution and the potential unknown phenomena of concentration of granules from modern contamination sources make us discard the deliberate transference of granules from plants to stone tools, that is, to discard plant processing.

Does phytolith analysis reveal signals of plant use at FLK West site?

The results show a different distribution of palm and dicot hard tissue phytoliths between paleosols and some tools. The results at FLK West indicate that phytoliths found in paleosols and those of some stone tools had different sources. Hence, transference of phytoliths from plants to some stone tools is different from the transference from plants to paleosols. The most likely explanation for this, is that this transference is caused by the deliberated use of stone tools and not by the result of random phenomena. Previous analyses suggest woodworking activities by the analysis of Acheulian tools from PEES2 (Peninj, Tanzania; Dominguez- Rodrigo, 2001). In addition, our results agree with previous analyses carried out on stone tools from Olduvai Gorge, on which a distinctive signal of palm phytoliths has been found (Barboni, *unpublished data*), and with modern consumption of palms by humans and baboons in the study area (Copeland, 2007). The distinguishable signal of palm phytoliths in stone tools argues for an active selection of plant resources.

Are these hypotheses consistent with the climatic conditions at FLK West deposition times? FLK West is located in a fluvial paleochannel incised in the clay unit that forms the base of Bed II (Diez-Martin et al., 2015). The presence of a river in the area implies that the Olduvai paleolake was retracted, and therefore that climate was becoming more arid. It has been suggested that around the time of deposition of level 6 of FLK West (1.698 ± 0.015 Ma) the Olduvai paleolake reduced its surface to a minimal extension coinciding with an arid period before Tuff IIB (Hay, 1976). During periods when the paleolake was low, vegetation was characterized by wooded grasslands (based on pollen samples between Tuff IF and Tuff IIA; Bonnefille, 1984; Bonnefille and Riollet, 1980), which is consistent with the faunal assemblages of FLK West, dominated by open-habitat taxa (Diez-Martín et al., 2015). This paleolandscape suggest that FLK West may have been a freshwater oasis that attracted hominids and fauna. This water supply could allow the development of water-related vegetation that provided plant resources to early hominins, as well as access to trees (dicot hard tissue signal) and palms, which can be currently found in low proportion in the riverine vegetation of Lake Manyara National Park (*Phoenix* sp. and *Hyphaene* sp), in the

ecotone between saline lake and the foothills where groundwater seeps out. (Copeland, 2007; Loth and Prins, 1986; Barboni *pers. comm.*).

In the FLK West site there is a strong association between stone tools and faunal remains, suggesting that carcass processing must have been the primary function for stone tools, particularly considering the large number of tools prepared for cutting activities (Diez-Martín et al., 2015). However, considering the presence of tools prepared for battering activities and the fact that cutting or hacking tools could be used for a wide diversity of purposes (e.g., butchery, wood working, plant processing, tuber digging), Diez-Martín et al. (2015) suggested that plant processing may have been an activity that was carried out by hominins at FLK West site.

Despite the significant difference in phytolith assemblages between paleosol samples and some stone tools, the consistency with archaeological data, and the fact that depositional processes and laboratory procedures do not create artificial differences in phytolith assemblages, there are several issues that impel us to be cautious about the relationship between phytolith assemblages and plant processing. Phytolith identifications are commonly based on reference collections and some morphologies are attributed to a botanical group without ambiguity [e.g., Palm globular echinate (Piperno, 2006) or silica short cells from grasses (Twiss et al., 1969)]. However, some attributions are based on the probability that phytoliths are produced by a particular group, in which case, some attributions are probably correct but not unequivocal. To evaluate plant uses, we only considered as dicot hard tissue phytoliths those attributed to wood and/or bark by Collura and Neumann (2016), who question some of the phytolith morphologies attributed to woody plants (e.g., Albert et al., 2016, 2006), and those that are also produced in other plant parts. Moreover, a considerable number of analyzed phytoliths remains unidentifiable, so percentages have to be considered cautiously. In addition, the differences in phytolith assemblages between paleosols and stone tools were constrained by the extraction method used to reduce modern contaminations in starch granule analysis. This sampling method, which extracts all the sediment from a stone tool, could not completely provide phytolith groups distinguishable between tools and soils (because the assemblages recovered from unused tool parts should be similar to those from soils), but it could

provide different phytolith group frequencies that can be tested statistically to prove whether this difference is significant. Previous studies used single-spot sampling (e.g., Dominguez- Rodrigo, 2001; Pearsall et al., 2003), which allows to obtain greater differences in phytolith assemblages between soils and lithics than by using complete matrices extraction, but these methods increase the risk of modern contamination, which is crucial to avoid if other microremains (as starch granules) are analyzed.

The presence of one pebble without percussion marks showing a significant palm signal can be interpreted as an evidence of random transference of phytoliths from plants to tools, but the experimental archaeology results and the low presence of palm phytoliths in the FLK West paleosols lead to discard this hypothesis. This can also be discarded because even slight and short uses of stone tools may transfer large amounts of palm phytoliths to them, considering that: (1) globular echinate phytoliths are common in palm leaves (Cabanes and Shahack-Gross, 2015); (2) leaf tissues cover the trunks and fruits in palms; (3) palms are large phytolith producers (Bamford et al., 2006), and (4) impact marks are less common during nut cracking (Dubreuil et al., 2015),

To summarize, having considered all the processes that may affect phytolith assemblages we interpret that the distinct phytolith assemblages found in several stone tools in FLK West are the result of deliberate use. The adoption of large-format tools must be a reflection of new activities previously undocumented during the Oldowan. These new activities probably opened new ecological niche opportunities for Acheulian hominins. However, early Acheulian stone tool assemblages are morphologically diverse and probably represent a diversity of stone tool functions. We suggest the need to improve the analysis by combining phytolith remains analysis with use-wear analysis to accurately correlate plants and tool use (Kealhofer et al., 1999; Lucarini et al., 2016). Also, it is advisable to increase the number of stone tool samples to elaborate strong hypotheses about lithic and plant processing at a given site, as well as to increase the number of anthropological sites analyzed to elaborate early hominin behavioral hypotheses.

9. Conclusions and perspectives

The research presented in this thesis was focused on two types of botanical microremains (phytoliths and starch granules), applied to the paleo-anthropological sites of Olduvai. Some results have improved the applicability of plant microremains to these sites by developing a starch granule automated identification system, and by the study of modern soil and plant samples to improve phytolith identifications. In addition, phytolith analyses have been applied to archaeological sites to reconstruct the paleoenvironment ("Zinj site" complex), to study paleovegetation changes through time (BK site), and, in combination with starch granule analysis, to study plant processing in stone tools from FLK West site.

The study of **modern soil samples from the Olduvai area, Lake Eyasi and Lake Manyara surroundings, and from Hadzabe territory** (**chapter 5.1**) shows that phytolith assemblages can partially reflect the general structure of the vegetation (particularly when statistical tools are used), but do not reflect accurately the vegetation that produce them. In our studies, the assemblages reflect the composition of the vegetation worse than expected, and they also show that the variation of several factors between different types of vegetation is subtle. Concerning the main components of vegetation, we observe: a) that woody plants have a not-so-clear representation in assemblages; b) that grasses seem to be over-represented in the phytolith assemblages, suggesting a more open vegetation than the actual one; c) that Cyperaceae plant representation is absent in phytolith assemblages, despite their presence in the areas where samples were collected; d) that palm phytoliths represent properly the presence/absence of palm plants (but seem to over-represent the amount of palm trees in samples, taking into account their presence in modern environments); and e) that fern phytoliths are present in samples associated to water courses, being the first time (to our knowledge) that fern phytoliths are described in the area. However, the statistical approach shows that the subtle differences observed between vegetation types can be handled using multivariate statistical tools, so their use is proposed in order to discriminate different environments and to infer past vegetation from paleosol samples. Compared to other microremains, phytoliths are better tracers of the main structure of vegetation and of canopy cover than pollen grains. Pollen grains trace species diversity better than phytoliths, but they do not trace properly the local

components of vegetation, and do not estimate well the proportion of major components of vegetation as palms or trees.

In the **modern species collected near groundwater discharge areas** (**chapter 5.2**) and analyzed for their phytolith content, only fern species produce phytolith morphologies that can be used to indicate their presence in the environment. Three morphotypes have been found in the six species analyzed: 1) blocky parallelepiped with trapeziform section, with crenate edges and/or striped surface; 2) tabular elongate with polygonal section and rugose or slightly psilate surface; and 3) "puzzle" bodies (irregular and complex flat bodies with wavy edges and many protuberances). The results obtained are consistent with previous studies that describe these morphologies as distinctive for ferns. The other species analyzed for phytolith content do not improve the previous knowledge of phytoliths produced by these species. The dicotyledonous species analyzed do not produce morphologies that can be considered specific for leaves, except for tracheid phytoliths, and no new morphologies have been observed in our *C. papyrus* analysis.

In perspective, for the analyzed area, a large number of species, including a variety of plant parts have to be analyzed to allow a proper identification of phytoliths recovered from modern soils and paleosol. In the area analyzed for modern soils, the sampling should have covered a wider variety of environments and a larger number of samples for each vegetation type, which could have led to a better differentiation of environments based on phytolith assemblages. Nevertheless, in our opinion, further analyses of phytolith modern soil assemblages must be combined with other botanical remains and statistical approaches, to improve the inferences that can be made from archaeological soil samples. Moreover, it is advisable to obtain a large collection of phytolith assemblages along with ecological data from modern environments in order to try modern statistics (e.g., machine learning methods) for obtaining stronger relationships between ecological data and phytolith assemblages, and more accurate inferences from fossil samples measurable in terms of their statistical robustness. In sum, further research is required to better understand phytolith variability, and it is necessary to improve the knowledge about the relationship between phytolith morphologies and phytolith producers to allow proper inferences from fossil samples. To date, there is still a significant ambiguity due to the misidentification of phytoliths because different plant groups produce similar morphologies, or caused by the large amount of phytolith morphologies that are still non-

attributable to any taxa.The selection of modern plants for the phytolith reference collection should be enlarged, so it is not restricted only to parts of Olduvai Gorge and the analogues from lakes Eyasi and Manyara. The use of herbarium collections is advisable (e.g., African plant collections from Kew -K- or Arusha -NHT- herbariums).

Although our proposed **starch granules automated classification system** (**chapter 6**) largely improves the identifications of starch granules compared to the human eye, for the 20 species we considered, and taking into account that the human eye identification test was made on 2D-photographs, the identification of starch granules seems hard to achieve without the aid of an objective classification method. Some species and taxa can be very difficult to discriminate, and our set of 20 species may include particularly unidentifiable species. In contrast to the human eye, an automated system allows taking into account a large number of characters, which can seize the subtle morphological and optical differences that exist among starch granules. It also allows handling the vast intra- and inter-specific variability of starch granules, which is particularly helpful when the use of large reference collections is mandatory to avoid preconceived plant inferences. In archaeology, particularly when dealing with early hominin behavior, a plausible reference collection should include all plants that were potentially used or processed. In our opinion, in the present state of knowledge, our automated system of identification of starch granules remains unsatisfactory to provide acceptable plant inference for archaeological purposes.

In perspective, considering additional proxies may help narrowing down the list of potential plants and, therefore, improving plant identifications using starch granules; but additional proxies may not always be available, so further investigations should focus on the study of new characters with higher taxonomic value and the combination of several automated methods that will lead to accurate identifications.

Our phytolith-based **paleoenvironmental reconstruction of the "Zinj complex" (FLK Zinj, AMK, PTK and DS sites, chapter 7.1)** completes the knowledge of paleovegetation of sites to the south of FLK Zinj sites. Our results indicate a mixed paleovegetation dominated by forest in which palms would have been a regular component. This paleovegetation description matches that previously described

for FLK NN and is consistent with the studies that suggest that vegetation of the area was densely wooded during middle and uppermost Bed I times. The presence of ferns in the assemblages suggest shady and wet habitats, which is supported by the geological reconstruction that proved the existence of a river east of PTK site. Our study re-evaluates areas previously studied and, based on the presence of palm phytoliths, we discard the presence of a river channel 50 to 200 m southeast of FLK Zinj site. The presence of hominin remains and stone tools in PTK, AMK and DS sites leads to suggest a behavioral model for these sites in which hominins used the site to process animal carcasses and not only as refuge.

Our results of the **analysis of phytolith assemblages of paleosols from BK site** (collected along the vertical sequence to study the changes in paleovegetation over time) (**chapter 7.2**), reflect a vegetation clearly dominated by forest components. This vegetation fits well with the environment that formed BK, whose deposits represent a low energy alluvial system with alternating distributary channels and low energy interchannel areas. The vegetation of BK did not change significantly over time. The behavioral interpretation of BK fits well with the interpretations made for Zinj, PTK, AMK, and DS sites.

In sum, further analyses should include areas adjacent to the "Zinj complex" sites to get an overview of the environment, and anthropological sites should be analyzed at higher resolution to better understand how hominins interacted with the environment. For BK, it is mandatory to complete the spatial analysis by studying surrounding areas to evaluate whether the described paleovegetation was part of an extensive wooded area or it was truly a gallery forest whose surroundings were a dry area with sparse/open vegetation. We also recommend the use of other proxies to reveal the structure of vegetation, which cannot be obtained by the study of phytolith assemblages.

The results of the **analysis of FLK West stone tools** (**chapter 8**) indicate plant processing by hominins. The transference of phytoliths from plants to some stone tools was different from the transference from plants to paleosols. The most likely explanation for this is that the transference was caused by the deliberate use of stone tools and not as result of random phenomena. The distinguishable signal of palm and wood tissue phytoliths in the stone tools argues for the active selection of plant resources

by early hominins. On the contrary, it seems unlikely that the transference of starch granules from plants to stone tools was caused by the deliberate use of stone tools. We also proved, through an experimental archaeology test, that deposition processes and laboratory procedures do not create artificial differences in phytolith assemblages between soils and tools. Nevertheless, we consider that interpretations should be cautious, considering the sampling method, which did not discern used and un-used surfaces of stone tools (for phytoliths) and did not ponder the possibility of modern contaminations (for starch granules).

In sum, we recommend to increase the number of stone tool samples to elaborate strong hypotheses about lithic and plant processing at a given site, and to increase the number of anthropological sites analyzed to elaborate early hominin behavioral hypotheses. At present, if the analysis of starch granules is not developed, and their taxonomical attributions remain ambiguous, we consider that analyzing the same tools for both microremains is useless and results in loss of information. We consider that phytolith analyses have to be carried out in work surfaces and/or edges, and not in the entire tool, in order to obtain completely different assemblages.

Bibliography

Albert, R.M., Bamford, M.K., 2012. Vegetation during UMBI and deposition of Tuff IF at Olduvai Gorge, Tanzania (ca. 1.8 Ma) based on phytoliths and plant remains. J. Hum. Evol. 63, 342–350. doi:10.1016/j.jhevol.2011.05.010

Albert, R.M., Bamford, M.K., Cabanes, D., 2009. Palaeoecological significance of palms at Olduvai Gorge, Tanzania, based on phytolith remains. Quat. Int. 193, 41–48. doi:10.1016/j.quaint.2007.06.008

Albert, R.M., Bamford, M.K., Cabanes, D., 2006. Taphonomy of phytoliths and macroplants in different soils from Olduvai Gorge (Tanzania) and the application to Plio-Pleistocene palaeoanthropological samples. Quat. Int. 148, 78–94. doi:10.1016/j.quaint.2005.11.026

Albert, R.M., Bamford, M.K., Esteban, I., 2015. Reconstruction of ancient palm vegetation landscapes using a phytolith approach. Quat. Int. 369, 51–66. doi:10.1016/j.quaint.2014.06.067

Albert, R.M., Esteve, X., Portillo, M., Rodríguez-Cintas, A., Cabanes, D., Esteban, I., Hernández, F., 2016. Phytolith CoRe, Phytolith Reference Collection [WWW Document]. URL http://phytcore.org/ (accessed 2.1.16).

Aleman, J., Leys, B., Apema, R., Bentaleb, I., Dubois, M.A., Lamba, B., Lebamba, J., Martin, C., Ngomanda, A., Truc, L., Yangakola, J.-M., Favier, C., Bremond, L., 2012. Reconstructing savanna tree cover from pollen, phytoliths and stable carbon isotopes. J. Veg. Sci. 23, 187–197. doi:10.1111/j.1654-1103.2011.01335.x

Alexandre, A., Meunier, J.-D., Colin, F., Koud, J.-M., 1997a. Plant impact on the biogeochemical cycle of silicon and related weathering processes. Geochim. Cosmochim. Acta 61, 677–682.

Alexandre, A., Meunier, J.-D., Lézine, A.-M., Vicens, A., Schwartz, D., 1997b. Phytoliths: indicators of grassland dynamics during the late Holocene in intertropical Africa. Palaeogeogr. Palaeoclimatol. Palaeoecol. 136, 213–229.

Allsopp, N., Colville, J.F., Verboom, G.A. (Eds.), 2014. Fynbos: Ecology, Evolution, and Conservation of a Megadiverse Region. Oxford University Press, Oxford.

Anderson, M., 2008. Plant compositional change over time increases with rainfall in Serengeti grasslands. Oikos 0, 080227085440234–0. doi:10.1111/j.2008.0030-1299.16516.x

Andrews, P., 1983. Small mammal faunal diversity at Olduvai Gorge, Tanzania. Anim. Archaeol. 1, 77–85.

Arriaza, M.C., Domínguez-Rodrigo, M., 2016. When felids and hominins ruled at Olduvai Gorge: A machine learning analysis of the skeletal profiles of the non-anthropogenic Bed I sites. Quat. Sci. Rev. 139, 43 – 52. doi:http://dx.doi.org/10.1016/j.quascirev.2016.03.005

Ashley, G.M., 2007. Orbital rhythms, monsoons, and playa lake response, Olduvai Basin, equatorial East Africa (ca. 1.85–1.74 Ma). Geology 35, 1091–1094.

Ashley, G.M., Barboni, D., Domínguez-Rodrigo, M., Bunn, H.T., Mabulla, A.Z.P., Diez-Martin, F., Barba, R., Baquedano, E., 2010a. A spring and wooded habitat at FLK Zinj and their relevance to origins of human behavior. Quat. Res. 74, 304–314. doi:10.1016/j.yqres.2010.07.015

Ashley, G.M., Barboni, D., Domínguez-Rodrigo, M., Bunn, H.T., Mabulla, A.Z.P., Diez-Martin, F., Barba, R., Baquedano, E., 2010b. Paleoenvironmental and paleoecological reconstruction of a freshwater oasis in savannah grassland at FLK North, Olduvai Gorge, Tanzania. Quat. Res. 74, 333–343. doi:10.1016/j.yqres.2010.08.006

Ashley, G.M., Beverly, E.J., Sikes, N.E., Driese, S.G., 2014. Paleosol diversity in the Olduvai Basin, Tanzania: Effects of geomorphology, parent material, depositional environment, and groundwater on soil development. Quat. Int. 322-323, 66–77. doi:10.1016/j.quaint.2013.12.047

Ashley, G.M., Tactikos, J.C., Owen, R.B., 2009. Hominin use of springs and wetlands: Paleoclimate and archaeological records from Olduvai Gorge (~1.79–1.74 Ma). Palaeogeogr. Palaeoclimatol. Palaeoecol. 272, 1–16. doi:10.1016/j.palaeo.2008.10.016

Backhouse, P.N., Johnson, E., 2007. Where were the hearths: an experimental investigation of the archaeological signature of prehistoric fire technology in the alluvial gravels of the Southern Plains. J. Archaeol. Sci. 34, 1367–1378. doi:10.1016/j.jas.2006.10.027
Baker, B.H., Wohlenberg, J., 1971. Structure and Evolution of the Kenya Rift Valley. Nature 229, 538–542. doi:10.1038/229538a0
Baker, G., 1960. Fossil Opal Phytoliths. Micropaleontology 6, 79–85.
Bamford, M.K., 2012a. Fossil sedges, macroplants, and roots from Olduvai Gorge, Tanzania. J. Hum. Evol. 63, 351–363. doi:10.1016/j.jhevol.2011.07.001
Bamford, M.K., 2012b. Pre- and post-depositional alteration of botanical macro-remains: A case study from Olduvai Gorge, Tanzania. Quat. Int. 275, 97–103. doi:10.1016/j.quaint.2011.10.023
Bamford, M.K., 2005. Early Pleistocene fossil wood from Olduvai Gorge, Tanzania. Quat. Int. 129, 15–22. doi:10.1016/j.quaint.2004.04.003
Bamford, M.K., Albert, R.M., Cabanes, D., 2006. Plio–Pleistocene macroplant fossil remains and phytoliths from Lowermost Bed II in the eastern palaeolake margin of Olduvai Gorge, Tanzania. Quat. Int. 148, 95–112. doi:10.1016/j.quaint.2005.11.027
Bamford, M.K., Stanistreet, I.G., Stollhofen, H., Albert, R.M., 2008. Late Pliocene grassland from Olduvai Gorge, Tanzania. Palaeogeogr. Palaeoclimatol. Palaeoecol. 257, 280–293. doi:10.1016/j.palaeo.2007.09.003
Barbarin, N., 2014. The automatic recognition of calcareous nannofossils of the Cenozoic. Université Aix-Marseille, Aix en Provence, France.
Barboni, D., 2014. Vegetation of Northern Tanzania during the Plio-Pleistocene: A synthesis of the paleobotanical evidences from Laetoli, Olduvai, and Peninj hominin sites. Quat. Int. 322-323, 264–276. doi:10.1016/j.quaint.2014.01.016
Barboni, D., Ashley, G.M., Domínguez-Rodrigo, M., Bunn, H.T., Mabulla, A.Z.P., Baquedano, E., 2010. Phytoliths infer locally dense and heterogeneous paleovegetation at FLK North and surrounding localities during upper Bed I time, Olduvai Gorge, Tanzania. Quat. Res. 74, 344–354. doi:10.1016/j.yqres.2010.09.005
Barboni, D., Bonnefille, R., Alexandre, A., Meunier, J.-D., 1999. Phytoliths as paleoenvironmental indicators, west side Middle Awash Valley, Ethiopia. Palaeogeogr. Palaeoclimatol. Palaeoecol. 152, 87–100.
Barboni, D., Bremond, L., 2009. Phytoliths of East African grasses: An assessment of their environmental and taxonomic significance based on floristic data. Rev. Palaeobot. Palynol. 158, 29–41. doi:10.1016/j.revpalbo.2009.07.002
Barboni, D., Bremond, L., Bonnefille, R., 2007. Comparative study of modern phytolith assemblages from inter-tropical Africa. Palaeogeogr. Palaeoclimatol. Palaeoecol. 246, 454–470. doi:10.1016/j.palaeo.2006.10.012
Barton, H., Torrence, R., Fullagar, R., 1998. Clues to stone tool function re-examined: Comparing starch grain frequencies on used and unused obsidian artefacts. J. Archaeol. Sci. 25, 1231–1238.
Baum, D.A., 1995. The Comparative Pollination and Floral Biology of Baobabs (Adansonia-Bombacaceae). Ann. Mo. Bot. Gard. 82, 322. doi:10.2307/2399883
Beaufort, L., Barbarin, N., Gally, Y., 2014. Optical measurements to determine the thickness of calcite crystals and the mass of thin carbonate particles such as coccoliths. Nat. Protoc. 9, 633–642. doi:10.1038/nprot.2014.028
Beentje, H.J., 2005. Restionaceae, Flora of East Africa. Royal Botanic Gardens Kew, Richmon, UK.
Blumenschine, R.J., 1995. Percussion marks, tooth marks, and experimental determinations of the timing of hominid and carnivore access to long bones at {FLK} Zinjanthropus, Olduvai Gorge, Tanzania. J. Hum. Evol. 29, 21 – 51. doi:http://dx.doi.org/10.1006/jhev.1995.1046
Blumenschine, R.J., 1991. Hominid carnivory and foraging strategies, and the socio-economic function of early archaeological sites. Philos. Trans. R. Soc. Lond. B. Biol. Sci. 334, 211–9; discussion 219–221. doi:10.1098/rstb.1991.0110

Blumenschine, R.J., Peters, C.R., 1998. Archaeological predictions for hominid land use in the paleo-Olduvai Basin, Tanzania, during lowermost Bed II times. J. Hum. Evol. 34, 565–607.

Blumenschine, R.J., Stanistreet, I.G., Njau, J.K., Bamford, M.K., Masao, F.T., Albert, R.M., Stollhofen, H., Andrews, P., Prassack, K.A., McHenry, L.J., Fernández-Jalvo, Y., Camilli, E.L., Ebert, J.I., 2012. Environments and hominin activities across the FLK Peninsula during Zinjanthropus times (1.84 Ma), Olduvai Gorge, Tanzania. J. Hum. Evol. 63, 364–383. doi:10.1016/j.jhevol.2011.10.001

Bonnefille, R., 2010. Cenozoic vegetation, climate changes and hominid evolution in tropical Africa. Glob. Planet. Change 72, 390–411. doi:10.1016/j.gloplacha.2010.01.015

Bonnefille, R., 1984. Palynological research at Olduvai Gorge, in: Lea, J.S., Link Powars, N., Swanson, W. (Eds.), National Geographic Society Research Reports. Washington, DC, pp. 227–243.

Bonnefille, R., 1979. Methode palynologique et reconstitutions paleoclimatiques au Cenozoique dans le Rift est-africain. Bull. Soc. Geol. Fr., 7 XXI, 331–342.

Bonnefille, R., Lobreau, D., Riollet, G., 1982. Fossil Pollen of Ximenia (Olacaceae) in the Lower Pleistocene of Olduvai, Tanzania: Palaeocological Implications / Pollen fossile de Ximenia (Olacaceae) dans le Pleistocene Inferieur d'Olduvai en Tanzanie: implications paleoecologiques. J. Biogeogr. 9, 469–486. doi:10.2307/2844614

Bonnefille, R., Riollet, G., 1980. Palynologie, végétation et climats de Bed 1 et Bed 2 á Olduvai, Tanzanie, in: Leakey, R.E., Ogot (Eds.), Proceedings of the 8th Pan-African Congress of Prehistory and Quaternary Studies. Tillmiap, Nairobi, pp. 123–127.

Bradshaw, P.L., Cowling, R.M., 2014. Landscapes, rock types, and climate of the Greater Cape Floristic Region. Fynbos Ecol. Evol. Conserv. Megadiverse Reg. Oxf. Univ. Press Oxf. 26–46.

Breiman, L., 2001. Random forests. Mach. Learn. 45, 5–32.

Bremond, L., 2003. Calibration des fonctions de transfert entre assemblages phytolithiques, structure des végétations et variables bioclimatiques actuelles, pour l'intégration de la dynamique des biomes herbacés dans les modèles de végétation. Aix-Marseille 3.

Bremond, L., Alexandre, A., Hely, C., Guiot, J., 2005a. A phytolith index as a proxy of tree cover density in tropical areas: calibration with Leaf Area Index along a forest?savanna transect in southeastern Cameroon. Glob. Planet. Change 45, 277–293. doi:10.1016/j.gloplacha.2004.09.002

Bremond, L., Alexandre, A., Peyron, O., Guiot, J., 2005b. Grass water stress estimated from phytoliths in West Africa. J. Biogeogr. 32, 311–327.

Bremond, L., Alexandre, A., Wooller, M.J., Hély, C., Williamson, D., Schäfer, P.A., Majule, A., Guiot, J., 2008. Phytolith indices as proxies of grass subfamilies on East African tropical mountains. Glob. Planet. Change 61, 209–224. doi:10.1016/j.gloplacha.2007.08.016

Buléon A., Colonna P., Planchot V., Ball S., 1998. Starch granules: structure and biosynthesis. Int. J. Biol. Macromol. 23, 85–112.

Bunn, H.T., 1981. Archaeological evidence for meat-eating by Plio-Pleistocene hominids from Koobi Fora and Olduvai Gorge. Nature 291, 574–577. doi:10.1038/291574a0

Bunn, H.T., Kroll, E.M., 1986. Systematic Butchery by Plio/Pleistocene Hominids at Olduvai Gorge, Tanzania. Curr. Anthropol. 27, 431–452.

Bunn, H.T., Mabulla, A.Z.P., Domínguez-Rodrigo, M., Ashley, G.M., Barba, R., Diez-Martín, F., Remer, K., Yravedra, J., Baquedano, E., 2010. Was FLK North levels 1–2 a classic "living floor" of Oldowan hominins or a taphonomically complex palimpsest dominated by large carnivore feeding behavior? Quat. Res. 74, 355–362. doi:10.1016/j.yqres.2010.06.004

Bunn, H.T., Pickering, T.R., 2010. Bovid mortality profiles in paleoecological context falsify hypotheses of endurance running–hunting and passive scavenging by early Pleistocene hominins. Quat. Res. 74, 395–404. doi:10.1016/j.yqres.2010.07.012

Cabanes, D., Shahack-Gross, R., 2015. Understanding Fossil Phytolith Preservation: The Role of Partial Dissolution in Paleoecology and Archaeology. PLOS ONE 10, e0125532. doi:10.1371/journal.pone.0125532
Cabanes, D., Weiner, S., Shahack-Gross, R., 2011. Stability of phytoliths in the archaeological record: a dissolution study of modern and fossil phytoliths. J. Archaeol. Sci. 38, 2480–2490. doi:10.1016/j.jas.2011.05.020
Capaldo, S.D., 1997. Experimental determinations of carcass processing by Plio-Pleistocene hominids and carnivores at FLK 22 (Zinjanthropus), Olduvai Gorge, Tanzania. J. Hum. Evol. 33, 555–597.
Carter, J.A., 1999. Late Devonian, Permian and Triassic phytoliths from Antarctica. Micropaleontology 45, 56–61.
Cerling, T.E., 2010. Ardipithecus ramidus Comment on the Paleoenvironment of. science 1185274, 328.
Cerling, T.E., Hay, T., 1986. An Isotopic Study of Paieosol Carbonates from Olduvai Gorge. Quat. Res. 25, 63–78.
Cerling, T.E., Mbua, E., Kirera, F.M., Manthi, F.K., Grine, F.E., Leakey, M.G., Sponheimer, M., Uno, K.T., 2011. Diet of Paranthropus boisei in the early Pleistocene of East Africa. Proc. Natl. Acad. Sci. 108, 9337–9341.
Chaerle, P., Viane, R.L., 2004. Leaf anatomy and the occurrence of false veins in Asplenium (Aspleniaceae, Pteridophyta). Bot. J. Linn. Soc. 145, 187–194.
Chandler-Ezell, K., Pearsall, D.M., Zeidler, J.A., 2006. Root and tuber phytoliths and starch grains document manioc (Manihot esculenta) arrowroot (Maranta arundinacea) and llerén (Calathea sp.) at the real alto site Ecuador. Econ. Bot. 60, 103–120.
Chauhan, D.K., Tripathi, D.K., Sinha, P., Tiwari, S.P., 2009. Biogenic silica in some Pteridophytes. Bionature 29, 1–9.
Chorowicz, J., 2005. The East African rift system. J. Afr. Earth Sci. 43, 379–410. doi:10.1016/j.jafrearsci.2005.07.019
Choy, S.-K., Tong, C.-S., Zhao, Z.-Z., 2009. A novel and effective multistage classification system for microscopic starch grain images. Microsc. Res. Tech. 73, 77–84. doi:10.1002/jemt.20758
Collura, L.V., Neumann, K., 2016. Wood and bark phytoliths of West African woody plants. Quat. Int. doi:10.1016/j.quaint.2015.12.070
Cooke, J., Leishman, M.R., 2011. Is plant ecology more siliceous than we realise? Trends Plant Sci. 16, 61–68. doi:10.1016/j.tplants.2010.10.003
Copeland, S., 2007. Vegetation and plant food reconstruction of lowermost Bed II, Olduvai Gorge, using modern analogs. J. Hum. Evol. 53, 146–175. doi:10.1016/j.jhevol.2007.03.002
Cordova, C.E., 2013. C3 Poaceae and Restionaceae phytoliths as potential proxies for reconstructing winter rainfall in South Africa. Quat. Int. 287, 121–140. doi:10.1016/j.quaint.2012.04.022
Coster, A.C.F., Field, J.H., 2015. What starch grain is that? – A geometric morphometric approach to determining plant species origin. J. Archaeol. Sci. 58, 9–25. doi:10.1016/j.jas.2015.03.014
Crowther, A., Haslam, M., Oakden, N., Walde, D., Mercader, J., 2014. Documenting contamination in ancient starch laboratories. J. Archaeol. Sci. 49, 90–104. doi:10.1016/j.jas.2014.04.023
Dagg, M., Woodhead, T., Rijks, D.A., 1970. EVAPORATION IN EAST AFRICA. Int. Assoc. Sci. Hydrol. Bull. 15, 61–67. doi:10.1080/02626667009493932
Davison, A.C., Hinkley, D.V., 1997. Bootstrap Methods and their Application. Cambridge University Press.
Deino, A., 2011. 40Ar/39Ar Dating of Laetoli, Tanzania, in: Harrison, T. (Ed.), Paleontology and Geology of Laetoli: Human Evolution in Context, Vertebrate Paleobiology and Paleoanthropology Series. Springer Netherlands, pp. 77–97.

Deino, A.L., 2012. 40Ar/39Ar dating of Bed I, Olduvai Gorge, Tanzania, and the chronology of early Pleistocene climate change. J. Hum. Evol. 63, 251–273. doi:10.1016/j.jhevol.2012.05.004

DeMiguel, D., Alba, D.M., Moyà-Solà, S., 2014. Dietary Specialization during the Evolution of Western Eurasian Hominoids and the Extinction of European Great Apes. PLoS ONE 9, e97442. doi:10.1371/journal.pone.0097442

Deus, D., Gloaguen, R., 2013. Remote Sensing Analysis of Lake Dynamics in Semi-Arid Regions: Implication for Water Resource Management. Lake Manyara, East African Rift, Northern Tanzania. Water 5, 698–727. doi:10.3390/w5020698

Dickau, R., Whitney, B.S., Iriarte, J., Mayle, F.E., Soto, J.D., Metcalfe, P., Street-Perrott, F.A., Loader, N.J., Ficken, K.J., Killeen, T.J., 2013. Differentiation of neotropical ecosystems by modern soil phytolith assemblages and its implications for palaeoenvironmental and archaeological reconstructions. Rev. Palaeobot. Palynol. 193, 15–37. doi:10.1016/j.revpalbo.2013.01.004

Diez-Martín, F., Sánchez, P., Domínguez-Rodrigo, M., Mabulla, A., Barba, R., 2009. Were Olduvai Hominins making butchering tools or battering tools? Analysis of a recently excavated lithic assemblage from BK (Bed II, Olduvai Gorge, Tanzania). J. Anthropol. Archaeol. 28, 274–289. doi:10.1016/j.jaa.2009.03.001

Diez-Martin, F., Sanchez Yustos, P., Domínguez-Rodrigo, M., Mabulla, A.Z.P., Bunn, H.T., Ashley, G.M., Barba, R., Baquedano, E., 2010. New insights into hominin lithic activities at FLK North Bed I, Olduvai Gorge, Tanzania. Quat. Res. 74, 376–387. doi:10.1016/j.yqres.2010.07.019

Diez-Martín, F., Sánchez Yustos, P., Uribelarrea, D., Baquedano, E., Mark, D.F., Mabulla, A., Fraile, C., Duque, J., Díaz, I., Pérez-González, A., Yravedra, J., Egeland, C.P., Organista, E., Domínguez-Rodrigo, M., 2015. The Origin of The Acheulean: The 1.7 Million-Year-Old Site of FLK West, Olduvai Gorge (Tanzania). Sci. Rep. 5, 17839. doi:10.1038/srep17839

Dollfus, D., Beaufort, L., 1999. Fat neural network for recognition of position-normalised objects. Neural Netw. 12, 553–560.

Domínguez- Rodrigo, 2002. Hunting and Scavenging by Early Humans: The State of the Debate. J. World Prehistory 16, 1–54.

Domínguez-Rodrigo, 1999. The study of skeletal part proflles: anambiguoust zaphonomic tool for zooarchaeology. Complutum 10, 15.

Domínguez-Rodrigo, 1997. Meat-eating by early hominids at the FLK 22 Zinjanthropus site, Olduvai Gorge (Tanzania): an experimental approach using cut-mark data. J. Hum. Evol. 33, 669–690.

Domínguez- Rodrigo, M., 2001. Woodworking activities by early humans: a plant residue analysis on Acheulian stone tools from Peninj (Tanzania). J. Hum. Evol. 40, 289–299. doi:10.1006/jhev.2000.0466

Domínguez- Rodrigo, M., Alcalá, L., Luque, L., 2009. Peninj: A Research Project on Human Origins (1995-2005). Oxbow Books, Oxford.

Domínguez-Rodrigo, M., Barba Egido, R., Egeland, C.P., 2007. Deconstructing Olduvai a taphonomic study of the Bed 1 sites. Springer, Dordrecht, Netherlands.

Domínguez-Rodrigo, M., Bunn, H.T., Mabulla, A.Z.P., Ashley, G.M., Diez-Martin, F., Barboni, D., Prendergast, M.E., Yravedra, J., Barba, R., Sánchez, A., Baquedano, E., Pickering, T.R., 2010a. New excavations at the FLK Zinjanthropus site and its surrounding landscape and their behavioral implications. Quat. Res. 74, 315–332. doi:10.1016/j.yqres.2010.07.003

Domínguez-Rodrigo, M., Bunn, H.T., Mabulla, A.Z.P., Baquedano, E., Uribelarrea, D., Pérez-González, A., Gidna, A., Yravedra, J., Diez-Martin, F., Egeland, C.P., Barba, R., Arriaza, M.C., Organista, E., Ansón, M., 2014a. On meat eating and human evolution: A taphonomic analysis of BK4b (Upper Bed II, Olduvai Gorge, Tanzania), and its bearing on hominin megafaunal consumption. Quat. Int. 322-323, 129–152. doi:10.1016/j.quaint.2013.08.015

Domínguez-Rodrigo, M., Bunn, H.T., Yravedra, J., 2014b. A critical re-evaluation of bone surface modification models for inferring fossil hominin and carnivore interactions through a multivariate approach: Application to the FLK Zinj archaeofaunal assemblage (Olduvai Gorge, Tanzania). Quat. Int. 322-323, 32–43. doi:10.1016/j.quaint.2013.09.042

Domínguez-Rodrigo, M., Diez-Martin, F., Mabulla, A., Baquedano, E., Bunn, H.T., Musiba, C., 2014c. The evolution of hominin behavior during the Oldowan–Acheulean transition: Recent evidence from Olduvai Gorge and Peninj (Tanzania). Quat. Int. 322-323, 1–6. doi:10.1016/j.quaint.2014.01.017

Domínguez-Rodrigo, M., Mabulla, A., Bunn, H.T., Barba, R., Diez-Martín, F., Egeland, C.P., Espílez, E., Egeland, A., Yravedra, J., Sánchez, P., 2009. Unraveling hominin behavior at another anthropogenic site from Olduvai Gorge (Tanzania): new archaeological and taphonomic research at BK, Upper Bed II. J. Hum. Evol. 57, 260–283. doi:10.1016/j.jhevol.2009.04.006

Domínguez-Rodrigo, M., Mabulla, A.Z.P., Bunn, H.T., Diez-Martin, F., Baquedano, E., Barboni, D., Barba, R., Domínguez-Solera, S., Sánchez, P., Ashley, G.M., Yravedra, J., 2010b. Disentangling hominin and carnivore activities near a spring at FLK North (Olduvai Gorge, Tanzania). Quat. Res. 74, 363–375. doi:10.1016/j.yqres.2010.07.004

Domínguez-Rodrigo, M., Pickering, T.R., 2003. Early hominid hunting and scavenging: A zooarcheological review. Evol. Anthropol. Issues News Rev. 12, 275–282. doi:10.1002/evan.10119

Domínguez-Rodrigo, M., Pickering, T.R., Almécija, S., Heaton, J.L., Baquedano, E., Mabulla, A., Uribelarrea, D., 2015. Earliest modern human-like hand bone from a new >1.84-million-year-old site at Olduvai in Tanzania. Nat. Commun. 6, 7987. doi:10.1038/ncomms8987

Domínguez-Rodrigo, M., Pickering, T.R., Baquedano, E., Mabulla, A., Mark, D.F., Musiba, C., Bunn, H.T., Uribelarrea, D., Smith, V., Diez-Martin, F., Pérez-González, A., Sánchez, P., Santonja, M., Barboni, D., Gidna, A., Ashley, G., Yravedra, J., Heaton, J.L., Arriaza, M.C., 2013. First Partial Skeleton of a 1.34-Million-Year-Old Paranthropus boisei from Bed II, Olduvai Gorge, Tanzania. PLoS ONE 8, e80347. doi:10.1371/journal.pone.0080347

Domínguez-Rodrigo, M., Pickering, T.R., Diez-Martín, F., Mabulla, A., Musiba, C., Trancho, G., Baquedano, E., Bunn, H.T., Barboni, D., Santonja, M., Uribelarrea, D., Ashley, G.M., Martínez-Ávila, M. del S., Barba, R., Gidna, A., Yravedra, J., Arriaza, C., 2012. Earliest Porotic Hyperostosis on a 1.5-Million-Year-Old Hominin, Olduvai Gorge, Tanzania. PLoS ONE 7, e46414. doi:10.1371/journal.pone.0046414

Domínguez-Rodrigo, M., Pickering, T.R., Semaw, S., Rogers, M., 2005. Cutmarked bones from Pliocene archaeological sites at Gona, Afar, Ethiopia: implications for the function of the world's oldest stone tools. J. Hum. Evol. 48, 109–121. doi:10.1016/j.jhevol.2004.09.004

Dray, S., Dufour, A.-B., 2007. The ade4 package: implementing the duality diagram for ecologists. J. Stat. Softw. 22, 1–20.

Driese, S.G., Ashley, G.M., 2015. Paleoenvironmental reconstruction of a paleosol catena, the Zinj archeological level, Olduvai Gorge, Tanzania. Quat. Res. doi:10.1016/j.yqres.2015.10.007

Driscoll, K., 2011. Vein quartz in lithic traditions: an analysis based on experimental archaeology. J. Archaeol. Sci. 38, 734–745. doi:10.1016/j.jas.2010.10.027

Dubreuil, L., Savage, D., Delgado-Raack, S., Plisson, H., Stephenson, B., de la Torre, I., 2015. Current Analytical Frameworks for Studies of Use–Wear on Ground Stone Tools, in: Marreiros, J.M., Gibaja Bao, J.F., Ferreira Bicho, N. (Eds.), Use-Wear and Residue Analysis in Archaeology. Springer International Publishing, Cham, pp. 105–158.

Egeland, C.P., Domínguez-Rodrigo, M., 2008. Taphonomic perspectives on hominid site use and foraging strategies during Bed II times at Olduvai Gorge, Tanzania. J. Hum. Evol. 55, 1031–1052. doi:10.1016/j.jhevol.2008.05.021

Egeland, C.P., Domínguez-Rodrigo, M., Barba, R., 2007. Geological and paleoecological overview of Olduvai Gorge, in: Deconstructing Olduvai: A Taphonomic Study of the Bed I Sites. Springer, pp. 33–38.

Eichhorn, B., Neumann, K., Garnier, A., 2010. Seed phytoliths in West African Commelinaceae and their potential for palaeoecological studies. Palaeogeogr. Palaeoclimatol. Palaeoecol. 298, 300–310. doi:10.1016/j.palaeo.2010.10.004

Elbaum, R., Weiner, S., Albert, R.M., Elbaum, M., 2003. Detection of Burning of Plant Materials in the Archaeological Record by Changes in the Refractive Indices of Siliceous Phytoliths. J. Archaeol. Sci. 30, 217–226. doi:10.1006/jasc.2002.0828

Esteban, I., De Vynck, J.C., Singels, E., Vlok, J., Marean, C.W., Cowling, R.M., Fisher, E.C., Cabanes, D., Albert, R.M., 2016. Modern soil phytolith assemblages used as proxies for Paleoscape reconstruction on the south coast of South Africa. Quat. Int. doi:10.1016/j.quaint.2016.01.037

Fenwick, R.S.H., Lentfer, C.J., Weisler, M.I., 2011. Palm reading: a pilot study to discriminate phytoliths of four Arecaceae (Palmae) taxa. J. Archaeol. Sci. 38, 2190–2199. doi:10.1016/j.jas.2011.03.016

Fernández-Jalvo, Y., Denys, C., Andrews, P., Williams, T., Dauphin, Y., Humphrey, L., 1998. Taphonomy and palaeoecology of Olduvai Bed-I (Pleistocene, Tanzania). J. Hum. Evol. 34, 137–172.

Fernández Pierna, J.A., Volery, P., Besson, R., Baeten, V., Dardenne, P., 2005. Classification of Modified Starches by Fourier Transform Infrared Spectroscopy Using Support Vector Machines. J. Agric. Food Chem. 53, 6581–6585. doi:10.1021/jf0501544

Ferraro, J.V., Plummer, T.W., Pobiner, B.L., Oliver, J.S., Bishop, L.C., Braun, D.R., Ditchfield, P.W., Seaman, J.W., Binetti, K.M., Seaman, J.W., Hertel, F., Potts, R., 2013. Earliest Archaeological Evidence of Persistent Hominin Carnivory. PLoS ONE 8, e62174. doi:10.1371/journal.pone.0062174

Fishkis, O., Ingwersen, J., Lamers, M., Denysenko, D., Streck, T., 2010. Phytolith transport in soil: A field study using fluorescent labelling. Geoderma 157, 27–36. doi:10.1016/j.geoderma.2010.03.012

Foster, A., Ebinger, C., Mbede, E., Rex, D., 1997. Tectonic development of the northern Tanzanian sector of the East African Rift System. J. Geol. Soc. 154, 689–700.

Fournier, F., A. Sasson. 1983. Écosystèmes Forestiers Tropicaux d'Afrique. Orstom and Unesco. Recherches Sur Les Ressources Naturelles 19.

Fraysse, F., Pokrovsky, O.S., Schott, J., Meunier, J.-D., 2006. Surface properties, solubility and dissolution kinetics of bamboo phytoliths. Geochim. Cosmochim. Acta 70, 1939–1951. doi:10.1016/j.gca.2005.12.025

Fullagar, R., Wallis, L.A., 2012. Usewear and phytoliths on bedrock grinding patches, Pilbara, north-western Australia.

Garnier, A., Neumann, K., Eichhorn, B., Lespez, L., 2012. Phytolith taphonomy in the middle- to late-Holocene fluvial sediments of Ounjougou (Mali, West Africa). The Holocene 0959683612463102.

Gibson, N.E., Wadley, L., Williamson, B.S., 2004. Microscopic residues as evidence of hafting on backed tools from the 60 000 to 68 000 year-old Howiesons Poort layers of Rose Cottage Cave, South Africa. South. Afr. Humanit. 16, 1–11.

Greenway, P.J., Vesey-Fitzgerald, D.F., 1969. The Vegetation of Lake Manyara National Park. J. Ecol. 57, 127–149. doi:10.2307/2258212

Haralick, R.M., 1979. Statistical and structural approaches to texture. Proc IEEE 67, 786–804.

Haralick, R.M., Sternberg, S.R., Zhuang, X., 1987. Image Analysis Using Mathematical Morphology. Pattern Anal. Mach. Intell. IEEE Trans. PAMI 9, 532–550.

Hardy, B.L., Garufi, G.T., 1998. Identification of woodworking on stone tools through residue and use-wear analyses: experimental results. J. Archaeol. Sci. 25, 177–184.

Hart, D.M., Humphreys, G.S., 2004. Distribution and mobility of spherical opaline phytoliths in a podzol (Podosol), in: 3rd Australian New Zealand Soils Conference. pp. 5–9.

Hart, D.M., Humphreys, G.S., 2003. Phytolith depth functions in surface regolith materials, in: Advances in Regolith: Proc. CRC LEME Regional Regolith Symp., Adelaide, Canberra, and Perth. pp. 13–28.

Hart, T.C., 2011. Evaluating the usefulness of phytoliths and starch grains found on survey artifacts. J. Archaeol. Sci. 38, 3244–3253. doi:10.1016/j.jas.2011.06.034

Hay, R.L., 1976. Geology of the Olduvai Gorge: A Study of Sedimentation in a Semiarid Basin. University of California Press.

Hay, R.L., 1973. Lithofacies and environments of Bed I, Olduvai Gorge, Tanzania. Quat. Res. 3, 541 – 560. doi:http://dx.doi.org/10.1016/0033-5894(73)90030-6

Hay, R.L., 1971. Geologic background of Beds I and II, in: Olduvai Gorge. Cambridge University Press, London, pp. 9–18.

Hay, R.L., 1970. Silicate reactions in three lithofacies of a semi-arid basin, Olduvai Gorge, Tanzania. Mineral. Soc. Am. Spec. Pap. 3, 237–255.

Hay, R.L., 1963. Stratigraphy of Beds I through IV, Olduvai Gorge, Tanganyika. Science 139, 829–833. doi:10.1126/science.139.3557.829

Hay, R.L., Kyser, T.K., 2001. Chemical sedimentology and paleoenvironmental history of Lake Olduvai, a Pliocene lake in northern Tanzania. Geol. Soc. Am. Bull. 113, 1505–1521.

Hecky, R.E., Kilham, P., 1973. Diatoms in alkaline, saline lakes: ecology and geochemical implications. Limnol Ocean. 18, 53–71.

Hemp, A. 2002. Ecology of the Pteridophytes on the Southern Slopes of Mt. Kilimanjaro–I. Altitudinal Distribution.Plant Ecology 159 (2), 211–39.

Henry, A.G., Piperno, D.R., 2008. Using plant microfossils from dental calculus to recover human diet: a case study from Tell al-Raqā'i, Syria. J. Archaeol. Sci. 35, 1943–1950. doi:10.1016/j.jas.2007.12.005
Henry, A.G., Ungar, P.S., Passey, B.H., Sponheimer, M., Rossouw, L., Bamford, M., Sandberg, P., de Ruiter, D.J., Berger, L., 2012. The diet of Australopithecus sediba. Nature. doi:10.1038/nature11185
Herlocker, D.J., Dirschl, H., 1972. Vegetation of the Ngorongoro Conservation Area, Tanzania, Canadian Wildlife Service Report Series. Environment Canada Wildlife Service, Ottawa (Canada).
Hodson, M.J., 2005. Phylogenetic Variation in the Silicon Composition of Plants. Ann. Bot. 96, 1027–1046. doi:10.1093/aob/mci255
Holdo, R.M., Holt, R.D., Fryxell, J.M., 2009. Grazers, browsers, and fire influence the extent and spatial pattern of tree cover in the Serengeti. Ecol. Appl. 19, 95–109. doi:10.1890/07-1954.1
Horrocks, M., Nunn, P.D., 2007. Evidence for introduced taro (Colocasia esculenta) and lesser yam (Dioscorea esculenta) in Lapita-era (c. 3050–2500cal.yrBP) deposits from Bourewa, southwest Viti Levu Island, Fiji. J. Archaeol. Sci. 34, 739–748. doi:10.1016/j.jas.2006.07.011
Husson, F., Julie, J., Sebastien, L., Jeremy, M., 2016. Multivariate Exploratory Data Analysis and Data Mining with R. R package version 1.25.
ICSN, 2011. ICSN 2011, The International Code for Starch Nomenclature [WWW Document]. URL http://fossilfarm.org/ICSN/Code.html (accessed 8.25.14).
Iriarte, J., Paz, E.A., 2009. Phytolith analysis of selected native plants and modern soils from southeastern Uruguay and its implications for paleoenvironmental and archeological reconstruction. Quat. Int. 193, 99–123. doi:10.1016/j.quaint.2007.10.008
Isaacs, G.L., 1965. The stratigraphy of the Peninj Group and the provenance of the Natron Australopithecine mandible. Quaternaria 101–130.
Isaacs, G.L., Curtis, G.H., 1974. Age of early Acheulian industries from the Peninj Group, Tanzania. Nature 249, 624–627. doi:10.1038/249624a0
Jaeger, J.J., 1976. Les rongeurs (mammalia, Rodentia) du Pleistocene inferieur d'Olduvai Bed I (Tanzanie), 1ere partie : Les Murides, in: Savage, R.J.G., Coryndon, S.C. (Eds.), Fossil Vertebrates of Africa. Academic Press, London, pp. 57–120.
Jones, R.L., 1964. Note on occurrence of opal phytoliths in some Cenozoic sedimentary rocks. J. Paleontol. 38, 773–775.
Kamau, P.W., 2012. Systematic revision of Pteris L. in tropical Africa and ecology of ferns and lycophytes in lowland tropical rainforests. Universität Koblenz-Landau.
Kappelman, J., 1984. Plio-Pleistocene environments of Bed I and Lower Bed II, Olduvai Gorge, Tanzania. Palaeogeogr. Palaeoclimatol. Palaeoecol. 48, 171–196. doi:10.1016/0031-0182(84)90043-9
Kealhofer, L., Torrence, R., Fullagar, R., 1999. Integrating phytoliths within use-wear/residue studies of stone tools. J. Archaeol. Sci. 26, 527–546.
Kononenko, N., Torrence, R., White, P., 2015. Unexpected uses for obsidian: experimental replication and use-wear/residue analyses of chopping tools. J. Archaeol. Sci. 54, 254–269. doi:10.1016/j.jas.2014.11.010
Kovarovic, K., Slepkov, R., McNulty, K.P., 2013. Ecological continuity between Lower and Upper Bed II, Olduvai Gorge, Tanzania. J. Hum. Evol. 64, 538–555. doi:10.1016/j.jhevol.2013.02.010
Kuhn, M., Johnson, K., 2013. Applied Predictive Modeling. Springer New York, New York, NY.
Leakey, L.S., 1961. New finds at Olduvai Gorge. Nature 189, 649–650.
Leakey, L.S.B., 1959. A new fossil skull from Olduvai. Nature 184, 491–493.
Leakey, L.S., Leakey, M.D., 1964. Recent Discoveries of Fossil Hominids in Tanganyika : At Olduvai and Near Lake Natron. Nature 202, 5–7. doi:10.1038/202005a0

Leakey, L.S., Tobias, P.V., Napier, J.R., 1964. A New Species of Genus Homo from Olduvai Gorge. Nature 202, 7–9.
Leakey, M.D., 1971. Olduvai Gorge Volume 3. Excavations in Beds I and II, 1960-1963. Cambridge University Press, Cambridge.
Leakey, M.D., Hay, R.L., 1982. Fossil footprints of Laetoli. Sci. Am. 246, 50–57.
Lellinger, D.B., 1968. A note to Aspidotis. Am. Fern J. 58, 140–141.
Lemorini, C., Plummer, T.W., Braun, D.R., Crittenden, A.N., Ditchfield, P.W., Bishop, L.C., Hertel, F., Oliver, J.S., Marlowe, F.W., Schoeninger, M.J., Potts, R., 2014. Old stones' song: Use-wear experiments and analysis of the Oldowan quartz and quartzite assemblage from Kanjera South (Kenya). J. Hum. Evol. 72, 10–25. doi:10.1016/j.jhevol.2014.03.002
Liu, L., Ma, S., Cui, J., 2014. Identification of starch granules using a two-step identification method. J. Archaeol. Sci. 52, 421–427. doi:10.1016/j.jas.2014.09.008
Liutkus, C.M., Ashley, G.M., 2003. Facies model of a semiarid freshwater wetland, Olduvai Gorge, Tanzania. J. Sediment. Res. 73, 691–705.
Lombard, M., 2004. Distribution Patterns of Organic Residues on Middle Stone Age Points from Sibudu Cave, Kwazulu-Natal, South Africa. South Afr. Archaeol. Bull. 59, 37. doi:10.2307/3889241
Loth, P.E., Prins, H.H.T., 1986. Spatial Patterns Of The Landscape And Vegetation Of Lake Manyara. ITC J. 115–130.
Loy, T.H., 1994. Methods in the Analysis of Starch Residues on Prehistoric Stone Tools, in: Hather, J.G. (Ed.), Tropical Archaeobotany: Applications and New Developments. Routledge, pp. 86–113.
Lucarini, G., Radini, A., Barton, H., Barker, G., 2016. The exploitation of wild plants in Neolithic North Africa. Use-wear and residue analysis on non-knapped stone tools from the Haua Fteah cave, Cyrenaica, Libya. Quat. Int. doi:10.1016/j.quaint.2015.11.109
Lytle, D.E., Wahl, E.R., 2005. Palaeoenvironmental reconstructions using the modern analogue technique: the effects of sample size and decision rules. The Holocene 15, 554–566.
Mabulla, A., 1996. Middle and latter stone age an lithic technology in the Eyasi Basin, Tanzania. University of Florida.
Madella, M., Alexandre, A., Ball, T., 2005. International Code for Phytolith Nomenclature 1.0. Ann. Bot. 96, 253–260. doi:10.1093/aob/mci172
Madella, M., Lancelotti, C., 2012. Taphonomy and phytoliths: A user manual. Quat. Int. 275, 76–83. doi:10.1016/j.quaint.2011.09.008
Magill, C.R., Ashley, G.M., Domínguez-Rodrigo, M., Freeman, K.H., 2016. Dietary options and behavior suggested by plant biomarker evidence in an early human habitat. Proc. Natl. Acad. Sci. 113, 2874–2879. doi:10.1073/pnas.1507055113
Magill, C.R., Ashley, G.M., Freeman, K.H., 2013a. Water, plants, and early human habitats in eastern Africa. Proc. Natl. Acad. Sci. 110, 1175–1180. doi:10.1073/pnas.1209405109
Magill, C.R., Ashley, G.M., Freeman, K.H., 2013b. Ecosystem variability and early human habitats in eastern Africa. Proc. Natl. Acad. Sci. 110, 1167–1174. doi:10.1073/pnas.1206276110
Maley, J., 1996. The African rain forest–main characteristics of changes in vegetation and climate from the Upper Cretaceous to the Quaternary. Proc. R. Soc. Edinb. Sect. B Biol. Sci. 104, 31–73.
Manega, P.C., 1993. Geochronology, geochemistry and isotope study of the Plio-Pleistocene hominid sites and the Ngorongoro Volcanic Highlands in northern Tanzania. University of Colorado.
Marlowe, F.W., Berbesque, J.C., 2009. Tubers as fallback foods and their impact on Hadza hunter-gatherers. Am. J. Phys. Anthropol. 140, 751–758. doi:10.1002/ajpa.21040
Martínez, A.M., Kak, A.C., 2001. Pca versus lda. Pattern Anal. Mach. Intell. IEEE Trans. On 23, 228–233.

Maslin, M.A., Brierley, C.M., Milner, A.M., Shultz, S., Trauth, M.H., Wilson, K.E., 2014. East African climate pulses and early human evolution. Quat. Sci. Rev. 101, 1–17. doi:10.1016/j.quascirev.2014.06.012

Maslin, M.A., Christensen, B., 2007. Tectonics, orbital forcing, global climate change, and human evolution in Africa: introduction to the African paleoclimate special volume. J. Hum. Evol. 53, 443–464. doi:10.1016/j.jhevol.2007.06.005

Mathew, T., 1989. MANOVA in the Multivariate Components of Variance Model. J. Multivar. Anal. 29, 30–38.

Matthews, W., 2010. Geoarchaeology and taphonomy of plant remains and microarchaeological residues in early urban environments in the Ancient Near East. Quat. Int. 214, 98–113. doi:10.1016/j.quaint.2009.10.019

Mazumdar, J., 2011. Phytoliths of pteridophytes. South Afr. J. Bot. 77, 10–19. doi:10.1016/j.sajb.2010.07.020

Mazumdar, J., Mukhopadhyay, R., 2011. Phytoliths in ferns. IV: In some aquatic ferns and Chinese brake fern. Bioresearch Bull. 6, 385–388.

Meehan, T.J., 1994. Sediment analysis of the middle Whitney Member: Climatic implications of the upper Oligocene of Nebraska, in: Dort, W. (Ed.), Symposium Series. University of Nebraska Press, Lincoln, Nebraska, pp. 57–87.

Mercader, J., 2009. Mozambican Grass Seed Consumption During the Middle Stone Age. Science 326, 1680–1683. doi:10.1126/science.1173966

Mercader, J., Astudillo, F., Barkworth, M., Bennett, T., Esselmont, C., Kinyanjui, R., Grossman, D.L., Simpson, S., Walde, D., 2010. Poaceae phytoliths from the Niassa Rift, Mozambique. J. Archaeol. Sci. 37, 1953–1967. doi:10.1016/j.jas.2010.03.001

Mercader, J., Bennett, T., Esselmont, C., Simpson, S., Walde, D., 2011. Soil Phytoliths from Miombo Woodlands in Mozambique. Quaternary Research 75. 1, 138–50. doi:10.1016/j.yqres.2010.09.008.

Mercader, J., Bennett, T., Esselmont, C., Simpson, S., Walde, D., 2009. Phytoliths in woody plants from the Miombo woodlands of Mozambique. Ann. Bot. 104, 91–113. doi:10.1093/aob/mcp097

Mercader, J., Bennett, T., Raja, M., 2008. Middle Stone Age starch acquisition in the Niassa Rift, Mozambique. Quat. Res. 70, 283–300. doi:10.1016/j.yqres.2008.04.010

Mindzie, C.M., Doutrelepont, Hughes, Vrydaghs, Luc, Swennen, Rony L., Swennen, Rudy J., Beeckman, Hans, de Langhe, Edmond, de Maret, Pierre, 2001. First archaeological evidence of banana cultivation in central Africa during the third millenium before present. Veg. Hist. Archaeobotany 10, 1–6.

Mollel, G.F., Swisher, C.C., 2012. The Ngorongoro Volcanic Highland and its relationships to volcanic deposits at Olduvai Gorge and East African Rift volcanism. J. Hum. Evol. 63, 274–283. doi:10.1016/j.jhevol.2011.09.001

Monahan, C.M., 1996. New zooarchaeological data from Bed II, Olduvai Gorge, Tanzania: implications for hominid behavior in the Early Pleistocene. J. Hum. Evol. 31, 93–128.

Myrbo, A., Morrison, A., McEwan, R., 2011. Tool for Microscopic Identification (TMI) [WWW Document]. URL http://tmi.laccore.umn.edu (accessed 2.23.16).

Neumann, K., Fahmy, A., Lespez, L., Ballouche, A., Huysecom, E., 2009. The Early Holocene palaeoenvironment of Ounjougou (Mali): Phytoliths in a multiproxy context. Palaeogeogr. Palaeoclimatol. Palaeoecol. 276, 87–106. doi:10.1016/j.palaeo.2009.03.001

Nicholson, S.E., Kim, J., 1997. The relationship of the El Nino-Southern oscillation to African rainfall. Int. J. Climatol. 17, 117–135.

Novello, A., 2012. Les phytolithes, marqueurs des environnements mio-pliocènes du Tchad. Reconstitution à partir du signal environnemental des phytolithes dans l'Afrique subsaharienne actuelle (Thèse Paléoécologie). Université de Poitiers.

Novello, A., Barboni, D., Berti-Equille, L., Mazur, J.-C., Poilecot, P., Vignaud, P., 2012. Phytolith signal of aquatic plants and soils in Chad, Central Africa. Rev. Palaeobot. Palynol. 178, 43–58. doi:10.1016/j.revpalbo.2012.03.010

Novello, A., Lebatard, A.-E., Moussa, A., Barboni, D., Sylvestre, F., Bourlès, D.L., Paillès, C., Buchet, G., Decarreau, A., Duringer, P., Ghienne, J.-F., Maley, J., Mazur, J.-C., Roquin, C., Schuster, M., Vignaud, P., 2015. Diatom, phytolith, and pollen records from a 10Be/9Be dated lacustrine succession in the Chad basin: Insight on the Miocene–Pliocene paleoenvironmental changes in Central Africa. Palaeogeogr. Palaeoclimatol. Palaeoecol. 430, 85–103. doi:10.1016/j.palaeo.2015.04.013

Nyenzi, B.S., Kiangi, P.M.R., Rao, N.N.P., 1981. Evaporation values in East Africa. Arch. Meteorol. Geophys. Bioclimatol. Ser. B 29, 37–55.

Oliver, J.S., 1994. Estimates of hominid and carnivore involvement in the {FLK} Zinjanthropus fossil assemblage: some socioecological implications. J. Hum. Evol. 27, 267 – 294. doi:http://dx.doi.org/10.1006/jhev.1994.1046

Ollendorf, A., 1992. Toward a Classification Scheme of Sedge (Cyperaceae) Phytoliths, in: Rapp, J., George, Mulholland, S. (Eds.), Phytolith Systematics, Advances in Archaeological and Museum Science. Springer US, pp. 91–111.

Otsu, N., 1979. Threshold Selection Method from Gray-Level Histograms. IEEE Trans. Syst. Man Cybern. 9, 62–66. doi:10.1109/tsmc.1979.4310076

Pearsall, D.M., Chandler-Ezell, K., Chandler-Ezell, A., 2004a. Maize can still be identified using phytoliths: response to Rovner. J. Archaeol. Sci. 31, 1029–1038. doi:10.1016/j.jas.2003.11.007

Pearsall, D.M., Chandler-Ezell, K., Chandler-Ezell, A., 2003. Identifying maize in neotropical sediments and soilsusing cob phytoliths. J. Archaeol. Sci. 30, 611–627. doi:10.1016/S0305-4403(02)00237-6

Pearsall, D.M., Chandler-Ezell, K., Zeidler, J.A., 2004b. Maize in ancient Ecuador: results of residue analysis of stone tools from the Real Alto site. J. Archaeol. Sci. 31, 423–442. doi:10.1016/j.jas.2003.09.010

Perry, L., 2010. Starch Extraction Protocol [WWW Document]. URL http://fossilfarm.org/Methods/Index.html (accessed 7.15.14).

Perry, L., 2001. Prehispanic subsistence in the Middle Orinoco basin: Starch analyses yield new evidence. Southern Illinois University, Carbondale, Illinois.

Peters, C., Blumenschine, R.J., 1995. Landscape perspectives on possible land use patterns for Early Pleistocene hominids in the Olduvai Basin, Tanzania. J. Hum. Evol. 29, 321–362.

Peters, C.R., 1993. Shell strength and primate seed predation of nontoxic species in eastern and southern Africa. Int. J. Primatol. 14, 315–344.

Pickering, T.R., Domínguez- Rodrigo, M., 2006. The acquisition and use of large mammal carcasses by Oldowan hominins in eastern and southern Africa: a selected review and assessment, in: Schick, K.D., Toth, N.P. (Eds.), The Oldowan: Case Studies into the Earliest Stone Age, Stone Age Institute Publication Series. Stone Age Institute, Gosport, IN, pp. 113–128.

Piperno, D., 1988. Phytoliths: A Comprehensive Guide for Archaeologists and Paleoecologists. Academic Press.

Piperno, D.R., 2009. Identifying crop plants with phytoliths (and starch grains) in Central and South America: A review and an update of the evidence. Quat. Int. 193, 146–159. doi:10.1016/j.quaint.2007.11.011

Piperno, D.R., 2006. Phytoliths. A Comprehensive Guide for Archaeologists and Paleoecologists. AltaMira Press (Rowman & Littlefield), Lanham, New York, Toronto, Oxford.

Plummer, T.W., Bishop, L.C., 1994. Hominid paleoecology at Olduvai Gorge, Tanzania as indicated by antelope remains. J. Hum. Evol. 27, 47 – 75. doi:http://dx.doi.org/10.1006/jhev.1994.1035

Pobiner, B.L., Rogers, M.J., Monahan, C.M., Harris, J.W.K., 2008. New evidence for hominin carcass processing strategies at 1.5Ma, Koobi Fora, Kenya. J. Hum. Evol. 55, 103–130. doi:10.1016/j.jhevol.2008.02.001

Portillo, M., Albert, R.M., 2014. Microfossil evidence for grinding activities. Rev. Arqueol. Ponent 103–112.
Potts, R., 2013. Hominin evolution in settings of strong environmental variability. Quat. Sci. Rev. 73, 1–13. doi:10.1016/j.quascirev.2013.04.003
Potts, R., 1988. Early hominid activities at Olduvai. Aldine de Gruyter, New York.
R Core Team, 2013. R: A language and environment for statistical computing. R Foundation for Statistical Computing, Vienna, Austria.
Reck, H., 1951. A preliminary survey of the tectonics and stratigraphy of Olduvai, in: Olduvai Gorge. Cambridge University Press, New York, p. 163.
Reed, K.E., 1997. Early hominid evolution and ecological change through the African Plio-Pleistocene. J. Hum. Evol. 32, 289–322. doi:10.1006/jhev.1996.0106
Reichert, E.T., 1913. The differentiation and specificity of starches in relation to genera, species, etc.; stereochemistry applied to protoplasmic processes and products, and as a strictly scientific basis for the classification of plants and animals. Carnegie Institution of Washington, Washington D. C.
Rose, L., Marshall, F., 1996. Meat Eating, Hominid Sociality, and Home Bases Revisited. Curr. Anthropol. 37, 307–338.
Rossouw, L., 2009. The application of fossil grass phytolith analysis in the reconstruction of late Ceinozoic environments in the South African interior. University of the Free State, Bloemfontein South Africa.
Roux, J. P. 2011. The Genus Cyrtomium (Pteridophyta: Dryopteridaceae) in Africa and Madagascar. Botanical Journal of the Linnean Society 167 (4), 449–65.
Rovner, I., 2004. On transparent blindfolds. J. Archaeol. Sci. 31, 815–819. doi:10.1016/j.jas.2003.11.008
Runge, F., 1999. The opal phytolith inventory of soils in central Africa —quantities, shapes, classification, and spectra. Rev. Palaeobot. Palynol. 107, 23–53.
Schmitt, C.B., Denich, M., Demissew, S., Friis, I., Boehmer, H.J., 2010. Floristic diversity in fragmented Afromontane rainforests: Altitudinal variation and conservation importance. Appl. Veg. Sci. doi:10.1111/j.1654-109X.2009.01067.x
Shaw, P.J.A., 2003. Multivariate statistics for the environmental sciences. Hodder, Arnold, London.
Shillito, L.-M., 2013. Grains of truth or transparent blindfolds? A review of current debates in archaeological phytolith analysis. Veg. Hist. Archaeobotany 22, 71–82. doi:10.1007/s00334-011-0341-z
Shukla, A.K., Vijayaraghavan, M.R., Chaudhry, B., 1998. Biology Of Pollen. APH Publishing, New Delhi.
Shultz, S., Maslin, M., 2013. Early Human Speciation, Brain Expansion and Dispersal Influenced by African Climate Pulses. PLoS ONE 8, e76750. doi:10.1371/journal.pone.0076750
Sikes, N.E., Ashley, G.M., 2007. Stable isotopes of pedogenic carbonates as indicators of paleoecology in the Plio-Pleistocene (upper Bed I), western margin of the Olduvai Basin, Tanzania. J. Hum. Evol. 53, 574–594. doi:10.1016/j.jhevol.2006.12.008
Stahlschmidt, M.C., Miller, C.E., Ligouis, B., Hambach, U., Goldberg, P., Berna, F., Richter, D., Urban, B., Serangeli, J., Conard, N.J., 2015. On the evidence for human use and control of fire at Schöningen. J. Hum. Evol. doi:10.1016/j.jhevol.2015.04.004
Stanistreet, I.G., 2012. Fine resolution of early hominin time, Beds I and II, Olduvai Gorge, Tanzania. J. Hum. Evol. 63, 300–308. doi:10.1016/j.jhevol.2012.03.001
Stewart, K.M., 2014. Environmental change and hominin exploitation of C4-based resources in wetland/savanna mosaics. J. Hum. Evol. 77, 1–16. doi:10.1016/j.jhevol.2014.10.003
Stromberg, C., 2004. Using phytolith assemblages to reconstruct the origin and spread of grass-dominated habitats in the great plains of North America during the late Eocene to early Miocene. Palaeogeogr. Palaeoclimatol. Palaeoecol. 207, 239–275. doi:10.1016/j.palaeo.2003.09.028

Stromberg, C., 2003. The origin and spread of grass-dominated ecosystems during the Tertiary of North America and how it relates to the evolution of hypsodonty in equids. University of California, Berkeley.
Stromberg, C., 2002. The origin and spread of grass-dominated ecosystems in the late Tertiary of North America: preliminary results concerning the evolution of hypsodonty. Palaeogeogr. Palaeoclimatol. Palaeoecol. 177, 59–75.
Strömberg, C.A.E., 2009. Methodological concerns for analysis of phytolith assemblages: Does count size matter? Quat. Int. 193, 124–140. doi:10.1016/j.quaint.2007.11.008
Strömberg, C.A.E., Werdelin, L., Friis, E.M., Saraç, G., 2007. The spread of grass-dominated habitats in Turkey and surrounding areas during the Cenozoic: Phytolith evidence. Palaeogeogr. Palaeoclimatol. Palaeoecol. 250, 18–49. doi:10.1016/j.palaeo.2007.02.012
Sundue, M., 2009. Silica bodies and their systematic implications in Pteridaceae (Pteridophyta). Bot. J. Linn. Soc. 161, 422–435.
Thomas, D.S.G., Burrough, S.L., 2012. Interpreting geoproxies of late Quaternary climate change in African drylands: Implications for understanding environmental change and early human behaviour. Quat. Int. 253, 5–17. doi:10.1016/j.quaint.2010.11.001
Torrence, R., Wright, R., Conway, R., 2004. Identification of starch granules using image analysis and multivariate techniques. J. Archaeol. Sci. 31, 519–532. doi:10.1016/j.jas.2003.09.014
Trauth, M.H., Maslin, M.A., Deino, A.L., Strecker, M.R., Bergner, A.G.N., Dühnforth, M., 2007. High- and low-latitude forcing of Plio-Pleistocene East African climate and human evolution. J. Hum. Evol. 53, 475–486. doi:10.1016/j.jhevol.2006.12.009
Twiss, P.C., Suess, E., Smith, R.M., 1969. Morphological Classification of Grass Phytoliths. Soil Science Society of America., p. 109.
Tybirk, K., 1993. Pollination, breeding system and seed abortion in some African acacias. Bot. J. Linn. Soc. 112, 107 – 137. doi:http://dx.doi.org/10.1006/bojl.1993.1045
Uribelarrea, D., Domínguez-Rodrigo, M., Pérez-González, A., Vegas Salamanca, J., Baquedano, E., Mabulla, A., Musiba, C., Barboni, D., Cobo-Sánchez, L., 2014. Geo-archaeological and geometrically corrected reconstruction of the 1.84 Ma FLK Zinj paleolandscape at Olduvai Gorge, Tanzania. Quat. Int. 322-323, 7–31. doi:10.1016/j.quaint.2013.12.023
van der Veen, M., 2007. Formation processes of desiccated and carbonized plant remains – the identification of routine practice. J. Archaeol. Sci. 34, 968–990. doi:10.1016/j.jas.2006.09.007
Vergès, J.M., Ollé, A., 2011. Technical microwear and residues in identifying bipolar knapping on an anvil: experimental data. J. Archaeol. Sci. 38, 1016–1025. doi:10.1016/j.jas.2010.11.016
Wadley, L., Sievers, Christine, Bamford, Marion, Godlberg, Paul, Berna, Francesco, Miller, Christopher, 2011. Middle Stone Age Bedding Construction and Settlement Patterns at Sibudu, South Africa. Science 334, 1388–1391. doi:10.1126/science.1213317
Wakjira, F.S., 2006. Biodiversity and ecology of Afromontane rainforests with wild Coffea arabica L. populations in Ethiopia. Cuvillier.
Whistler, R.L., Daniel, J.R., 1984. Molecular structure of starch, in: Whistler, R.L., Bemiller, J.N., PASCHALL, R.L.W.N.B.F. (Eds.), Starch: Chemistry and Technology (Second Edition), Food Science and Technology. Academic Press, San Diego, pp. 153 – 182.
White, F., 1983. The vegetation of Africa: a descriptive memoir to accompany the UNESCO/AETFAT/UNSO vegetation map of Africa.
Williams, Graham, 2011. Data Mining with Rattle and R, Use R! Springer, New York Dordrecht Heidelberg London.
Wilson, J., Hardy, K., Allen, R., Copeland, L., Wrangham, R., Collins, M., 2010. Automated classification of starch granules using supervised pattern recognition of morphological properties. J. Archaeol. Sci. 37, 594–604. doi:10.1016/j.jas.2009.10.024

WoldeGabriel, G., Ambrose, S.H., Barboni, D., Bonnefille, R., Bremond, L., Currie, B., DeGusta, D., Hart, W.K., Murray, A.M., Renne, P.R., Jolly-Saad, M.C., Stewart, K.M., White, T.D., 2009. The Geological, Isotopic, Botanical, Invertebrate, and Lower Vertebrate Surroundings of Ardipithecus ramidus. Science 326, 65–65, 65e1–65e5. doi:10.1126/science.1175817

Wright, P., 2003. Preservation or destruction of plant remains by carbonization? J. Archaeol. Sci. 30, 577–583. doi:10.1016/S0305-4403(02)00203-0

Wynn, J.G., Sponheimer, M., Kimbel, W.H., Alemseged, Z., Reed, K., Bedaso, Z.K., Wilson, J.N., 2013. Diet of Australopithecus afarensis from the Pliocene Hadar Formation, Ethiopia. Proc. Natl. Acad. Sci. 110, 10495–10500. doi:10.1073/pnas.1222559110

Yang, X., Yu, J., Lü, H., Cui, T., Guo, J., Ge, Q., 2009. Starch grain analysis reveals function of grinding stone tools at Shangzhai site, Beijing. Sci. China Ser. Earth Sci. 52, 1164–1171. doi:10.1007/s11430-009-0089-9

Apendices

Appendix 4.2.A. Results of starch granules anticontamination tests.

Test ID	N	Test ID	N
Beaker, 1l 1	0	**Nail polish**	0
Beaker, 1l 2	1	Refrigerator 1	1
Beaker, 25ml 1	0	Refrigerator 2	7
Beaker, 25ml 2	0	Scale 1	0
Laboratory soil 1	0	Scale 2	1
Laboratory soil 2	0	Shaker 1	0
Laboratory soil 3	0	Shaker 2	3
Laboratory soil 4	0	Shaker 3	3
Laboratory soil 5	0	**Slide + coverslip 1**	1
Laboratory soil 6	0	**Slide + coverslip 2**	0
Centrifuge 1-2	6	Sonicator	2
Centrifuge 2-3	1	**SPT**	0
Centrifuge 3-4	4	**SPT**	0
Centrifuge 4-5	2	Tap 1	3
Centrifuge 5-6	0	Tap 2	1
Centrifuge 6-7	8	Tap 3	2
Eppendorf tube 1	0	**Tips 1**	0
Eppendorf tube 2	0	**Tips 2**	0
Falcon tube 1	0	**Tips 3**	0
Falcon tube 2	0	Workbench, center 1	0
Falcon tube 3	0	Workbench, center 2	0
Gloves, PE 1	0	Workbench, center 3	5
Gloves, PE 2	0	Workbench, center 4	2
Gloves, PE 3	0	Workbench, left 1	0
Gloves, vinyl 1	0	Workbench, left 2	3
Gloves, vinyl 2	0	Workbench, left 3	3
Gloves, vinyl 3	0	Workbench, right 1	0
Hood, center 1	0	Workbench, right 2	1
Hood, center 2	0	Workbench, right 3	1
Hood, center 3	0	Workbench, right 4	8
Hood, center 4	1	Protocol control 1	0
Hood, left 1	0	Protocol control 2	0
Hood, left 2	0	Protocol control 3	0
Hood, right 1	3	Protocol control 4	0
Hood, right 2	0	Protocol control 5	0
Hood, right 3	3	Protocol control 6	0
Hood, right 4	1	**Water, ultrapure 1**	0
Microwave	1	**Water, ultrapure 2**	0
pH meter	2	TOTAL	80

Appendix 4.2.B. List of the 123 characters in polarized and in natural light That were used in the starch granules automated classification system.

Nb	Character ID in polarized light	Nb	Character ID in natural light	Definiton	Ref.
1	a1			Coefficient of the degree 10 polynomial fitting the profil	
2	a2			Coefficient of the degree 10 polynomial fitting the profil	
3	a3			Coefficient of the degree 10 polynomial fitting the profil	
4	a4			Coefficient of the degree 10 polynomial fitting the profil	
5	a5			Coefficient of the degree 10 polynomial fitting the profil	
6	a6			Coefficient of the degree 10 polynomial fitting the profil	
7	a7			Coefficient of the degree 10 polynomial fitting the profil	
8	a8			Coefficient of the degree 10 polynomial fitting the profil	
9	a9			Coefficient of the degree 10 polynomial fitting the profil	
10	a10			Coefficient of the degree 10 polynomial fitting the profil	
11	AAC			Area of the central area (= central depression)	
12	Aire	**72**	LN_aire	Area	
13	aire_centrale			Presence/absence of a central area	
14	airesurAAC			Ratio of the total area and the area of the central area	
15	Amplitude_contour	**73**	LN_Amplitude_contour	Amplitude of the shape outline interpreted as a signal	
16	Aplatissement	**74**	LN_Aplatissement	Average of the flattenings (kurtosis) on all lines of the image interpreted as signals (order 4 moment compared to the mean)	1
17	Aplatissement_contour	**75**	LN_Aplatissement_contour	Flattening (kurtosis) of the shape outline interpreted as a signal (order 4 moment compared to the mean)	1
18	Circle_radius			Radius of the total area	1
		76	LN_Compactness	Particle Measurement Factor corresponding to the area divided by the product of Bounding Rect Width and Bounding Rect Height.	1
19	Contrast	**77**	LN_Contrast	Haralick's texture feature	3
20	Correlation	**78**	LN_Correlation	Haralick's texture feature	3
21	CR-CRaire			Difference between the radius of the total area and the radius of the central area	
22	CRaire			Radius of the central area	
23	CRsurCRaire			Ratio of the global radius and the radius of the central area	
24	DHT+bruit_contour	**79**	LN_DHT+bruit_contour	Total harmonic distortion of the outline interpreted as a signal	
25	Dissimilarity	**80**	LN_Dissimilarity	Haralick's texture feature	3
26	Dissymetrie	**81**	LN_Dissymetrie	Average of the computed dissymetry on all lines of the image interpreted as signals (order 3 moment compared to the mean)	1

Appendix 4.2.B. Cont.

27	Dissymetrie_contour	**82**	LN_Dissymetrie_contour	Computed dissymetry of the shape outline interpreted as a signal in natural light (order 3 moment compared to the mean)	1
28	Ecart-type_contour	**83**	LN_Ecart-type_contour	Average of the standard deviations on all lines the shape outline interpreted as signals	1
29	Ecarttype	**84**	LN_Ecarttype	Average of the standard deviations on all lines of the image interpreted as signals	1
		85	LN_Elongation	Particle Measurement Factor corresponding to the max Feret Diameter divided by Equivalent Rect Short Side	
30	Energy	**86**	LN_Energy	Haralick's texture feature	3
31	Entropy	**87**	LN_Entropy	Haralick's texture feature	3
32	entropy	**88**	LN_entropy	Shannon's entropy measurement of the image pixels variations interpreted as a signal	1
33	FourierPower	**89**	LN_FourierPower	Fourier power of the shape outline interpreted as a signal	1
34	Frequence	**90**	LN_Frequence	Main frequency of the image pixels variations interpreted as a signal	1
35	Frequence_contour	**91**	LN_Frequence_contour	Main frequency of the shape outline variations interpreted as a signal	1
36	Fundamentalfrequence_contour	**92**	LN_Fundamentalfrequence_contour	Fundamental frequency of the shape outline variations interpreted as a signal	1
37	GAA			Long length of the fitted ellipse of the central area	
38	Grand_axe	**93**	LN_Grand_axe	Long length of the fitted ellipse	
39	Grand/petit	**94**	LN_grand/petit	Ratio of the lengths of the ellipse	
40	GsurP			Ratio of the lengths of the fitted ellipse of the central area	
41	HarmoSpe	**95**	LN_HarmoSpe	Average of the first specific harmonic of all lines of the image interpreted as signals	1
		96	LN_Heywood	Heywood circularity factor, equivalent to roundness, Perimeter divided by the circumference of a circle with the same area	1
42	Homogeneity	**97**	LN_Homogeneity	Haralick's texture feature	3
43	kurtosis	**98**	LN_kurtosis	Flattenings (kurtosis) on all lines of the image interpreted as signals	1
44	Masse			Relative estimated mass in pg (non calibrated for starch)	2
45	Maxspectrepuiss	**99**	LN_Maxspectrepuiss	Maximum spectrum power of the image pixels variations interpreted as a signal	1
46	Mediane	**100**	LN_Mediane	Average of the values Medians on all lines of the image interpreted as signals	1
47	Mediane_contour	**101**	LN_Mediane_contour	Average of the values Medians on all lines of the shape outline interpreted as signals	1
48	Mode	**102**	LN_Mode	Average of the values modes on all lines of the image interpreted as signals	1
49	Mode_contour	**103**	LN_Mode_contour	Average of the values modes on all lines of the shape outline interpreted as signals	1
50	MoyArith	**104**	LN_MoyArith	Average of the Arithmetic means on all lines of the image interpreted as signals	1

Appendix 4.2.B. Cont.

51	MoyArith_contour	**105**	LN_MoyArith_contour	Average of the Arithmetic means on all lines of the shape outline interpreted as signals	1
52	PAA			Short length of the fitted ellipse of the central area	
53	Peak	**106**	LN_Peak	Haralick's texture feature	3
		107	LN_perimetre	Perimeter of the shape in natural light	1
54	Periode	**108**	LN_Periode	Main Period of the image pixels variations interpreted as a signal	1
55	Petit_axe	**109**	LN_Petit_axe	Short length of the fitted ellipse	1
56	Phase	**110**	LN_Phase	Main Phase of the image pixels variations interpreted as a signal	1
57	Phase_contour	**111**	LN_Phase_contour	Main Phase of the shape outline variations interpreted as a signal	1
58	pics			Number of high values on the long length profile	1
59	Puissance	**112**	LN_Puissance	Main Power of the image pixels variations interpreted as a signal	1
60	roundness			Roundness of the image	1
61	roundness_aire			Roundness of the central area (regularity of the shape compared to a perfect circle)	1
62	SINAD_contour	**113**	LN_SINAD_contour	Measured Signal in Noise and Distortion of the shape outline variations interpreted as a signal	1
63	skewness	**114**	LN_skewness	Skewness indicates the symmetry of the probability density function of the amplitude of the shape outline	1
64	Somme	**115**	LN_Somme	Average of the sums of the values of all lines of the image interpreted as signals	1
65	Somme_contour	**116**	LN_Somme_contour	Average of the sums of the values of all lines of the shape outline interpreted as signals	1
66	taille_contour	**117**	LN_taille_contour	Length of the shape outline	1
67	THD_contour	**118**	LN_THD_contour	Total Harmonic Distortion of the shape outline variations interpreted as a signal	1
		119	LN_Typefactor	Factor relating area to moment of inertia	1
68	ValeurEff	**120**	LN_ValeurEff	Average of the Effective values on all lines of the image interpreted as signals	1
69	Valeurefficace_contour	**121**	LN_Valeurefficace_contour	Effective value of the shape outline interpreted as a signal	1
70	Variance	**122**	LN_Variance	Average of the variances on all lines of the image interpreted as signals	1
71	Variance_contour	**123**	LN_Variance_contour	Average of the variances on all lines of the shape outline interpreted as signals	1

References

1 Barbarin, 2014

2 Beaufort et al., 2014

3 Haralick, 1979

Appendix 4.2.C. Random Forest test values measuring the importance of characters for each species, and mean decrease accuracy and mean decrease gini values for each character. The 24 most important characters as identified by Random Forest test values are marked with *. Characters marked with ** were also plotted in the discriminant analysis scatter plot.

Original names as Barbarin, 2014	English names (figures and text)	Mean Decrease Accuracy	Mean Decrease Gini	Ada_dig	Bra_def	Cad_far	Cap_fas	Cyn_dac	Cyp_rot	Ech_col	Emi_ann	Fai_alb	Fic_sal	Hib_mic	Oly_lat	Pan_sub	Per_sen	Por_ole	Set_pum	Typ_lat	Vig_fru	Vig_vex	Zan_aet
a1		10,85	8,70	0.02	2.49	1.24	1.32	6.15	2.07	2.30	-0.82	0.30	2.61	3.68	4.38	-0.71	3.15	-1.25	-1.26	1.16	-0.44	0.60	0.16
a10		15,24	8,49	0.47	3.09	2.03	0.63	5.76	0.37	3.26	-0.91	5.41	0.63	6.20	-1.05	0.88	6.91	1.65	1.11	0.12	0.91	2.74	-1.44
a2		9,24	7,83	-0.14	2.32	0.68	-0.34	6.72	2.48	0.19	-0.21	4.12	0.06	6.93	1.55	0.49	1.22	-0.89	1.08	-1.34	0.54	-0.60	-0.50
a3		8,31	7,61	-0.81	-0.13	-0.55	1.69	5.33	1.19	0.83	-1.64	2.61	1.40	4.97	0.41	-0.70	2.29	1.44	0.73	0.17	1.97	0.09	-1.20
a4		11,89	7,39	-0.13	0.54	0.68	0.96	5.20	-0.72	1.48	0.80	4.26	0.36	5.38	1.41	1.05	2.57	0.61	0.93	0.41	2.97	1.52	-0.24
a5		12,35	7,34	2.06	1.90	2.67	-0.45	4.44	1.22	3.34	1.59	5.04	1.28	6.09	0.86	1.16	2.48	2.17	0.98	-0.40	2.99	1.48	0.98
a6		10,63	7,38	0.64	1.33	1.44	-1.27	5.48	-0.12	1.03	-0.07	3.81	0.68	6.71	0.61	0.26	3.70	0.53	2.79	-2.12	1.84	0.24	-0.82
a7		14,17	7,58	0.92	1.95	1.01	0.54	6.16	0.01	3.33	-0.24	4.47	-1.50	5.56	-0.60	0.78	3.94	1.65	2.26	-0.49	0.35	1.47	-0.31
a8		14,36	7,78	2.00	1.11	-0.57	-0.92	4.54	-1.96	1.02	0.77	5.14	1.53	6.32	1.48	1.62	4.70	1.87	1.43	0.43	1.96	2.68	-1.47
a9		13,89	8,29	2.56	0.59	1.22	-1.89	5.09	1.20	1.71	2.23	4.44	1.45	7.09	-0.09	1.78	4.42	1.72	1.88	0.20	2.35	1.61	-0.01
AAC		20,85	9,63	2.81	6.09	2.44	3.73	9.73	7.96	8.69	2.51	6.69	2.78	7.91	3.54	5.98	5.27	-0.41	4.73	1.64	3.62	4.27	-0.03
Aire**	Area	17,64	12,58	3.56	5.28	3.18	5.18	8.57	5.03	7.10	4.29	7.75	2.55	9.49	5.35	6.02	7.32	8.36	4.35	2.42	-4.60	6.87	2.77
aire_centrale**	Central area	10,21	2,17	2.00	2.63	1.43	2.47	5.17	4.46	5.46	1.97	1.92	4.04	3.94	-0.92	5.64	0.46	1.67	-0.03	2.85	5.14	4.88	4.16
airesurAAC*	AreaonAAC	32,56	16,64	3.18	13.06	3.27	5.74	12.33	6.63	15.91	2.57	5.57	4.45	12.00	1.61	11.24	7.03	3.14	3.61	5.54	6.62	7.43	3.36
Amplitude_contour		5,08	8,46	1.33	0.70	1.19	-0.91	5.74	1.91	0.47	-0.46	3.12	1.85	7.46	-1.75	0.75	0.32	0.00	1.40	-0.03	1.54	-1.70	0.38
Aplatissement		14,32	9,68	2.55	1.98	0.92	0.60	6.72	2.13	0.61	1.55	6.64	2.60	6.32	5.42	-1.19	0.92	-0.72	0.85	0.49	-2.81	1.18	1.38
Aplatissement_contour		13,32	11,45	4.00	5.62	1.09	3.00	8.69	5.07	3.86	1.41	2.92	0.35	8.02	1.80	6.81	5.89	-0.14	7.35	-1.23	4.59	3.38	4.88
Circle_radius		15,57	12,56	3.52	4.90	4.44	6.71	8.93	4.37	7.30	3.92	5.78	0.77	9.12	6.91	5.75	7.70	7.78	5.62	2.36	1.30	6.49	2.07
Contrast**	Contrast	23,51	13,98	1.31	-0.06	0.14	2.71	13.18	11.65	4.64	-0.44	2.40	4.45	8.87	2.96	0.15	3.15	-1.41	7.50	3.14	8.64	4.14	1.69
Correlation*	Correlation	24,84	15,57	8.80	3.63	0.89	4.72	12.28	6.14	3.18	3.26	5.39	2.44	11.25	8.49	1.18	2.18	7.67	2.15	6.54	1.32	0.74	2.54
CR.CRaire*	CR.Carea	26,35	16,04	2.69	7.50	3.29	7.51	8.88	7.09	10.77	4.27	3.90	2.71	11.37	4.35	7.27	8.77	6.47	2.71	3.75	6.80	7.41	2.66
CRaire		20,66	9,83	4.33	4.93	2.10	3.76	9.61	7.79	7.22	2.35	8.26	2.59	7.65	3.32	4.64	6.82	-1.11	4.49	3.36	4.51	3.95	3.28
CrsurCRaire*	CR.Conarea	31,83	16,12	1.17	14.06	4.50	7.32	12.17	2.06	16.98	3.45	5.97	3.81	12.55	1.97	11.13	8.00	1.35	3.70	6.23	6.72	7.74	2.58
DHT.bruit_contour		15,46	9,51	0.86	3.39	0.06	4.85	6.50	1.44	2.33	1.39	8.60	-0.02	4.86	1.81	-0.48	2.23	1.43	-1.66	0.53	0.49	2.43	0.46
Dissimilarity**	Dissimilarity	22,34	12,74	1.94	1.22	2.22	2.61	10.44	12.07	4.95	0.23	2.66	1.14	9.58	0.00	3.27	4.53	-0.84	4.74	2.50	2.99	5.99	4.71
Dissymetrie**	Dissymetry	23,36	13,08	6.81	6.54	5.55	2.75	8.58	5.16	5.91	-0.42	0.67	0.15	8.97	3.16	0.61	1.99	-0.74	3.61	3.75	2.20	8.41	3.29
Dissymetrie_contour		13,34	11,60	5.99	5.70	3.29	1.61	8.58	3.52	3.05	1.25	3.87	5.09	9.45	3.65	7.28	7.45	-0.43	7.85	0.98	7.08	3.55	3.35
Ecart.type_contour		22,90	12,64	0.23	4.15	-1.44	3.61	5.84	1.96	4.17	3.91	12.24	1.40	6.60	-0.10	-1.57	-2.26	-0.98	0.13	-0.14	1.10	5.66	0.38
Ecarttype**	Ecarttype	22,12	12,73	7.73	4.20	0.64	3.45	8.62	10.21	6.95	2.44	1.19	2.15	9.18	2.67	6.94	6.36	4.13	6.66	5.07	-1.34	4.94	1.25
Energy*	Energy	24,41	15,70	9.01	3.62	1.39	5.20	12.94	4.25	5.02	3.35	5.37	4.68	11.23	9.06	3.20	2.19	7.62	2.77	7.44	0.96	4.08	2.38
entropy		21,88	12,71	4.90	5.69	2.64	2.80	7.73	2.53	5.07	-0.06	6.03	1.12	6.20	3.98	6.83	4.80	2.12	5.22	0.30	3.55	2.32	1.19
Entropy**	Entropy	12,42	10,56	2.67	1.59	1.64	2.41	11.57	12.41	5.19	0.67	0.77	3.52	9.07	1.56	3.25	7.54	-0.38	5.55	1.39	2.01	4.74	1.24
FourierPower		13,93	9,14	4.09	6.36	2.19	1.36	7.72	2.30	4.43	1.83	3.86	1.07	7.21	2.86	5.86	6.19	-0.26	6.21	1.11	5.70	2.99	3.70
Frequence		14,75	9,98	1.12	4.01	2.25	1.57	5.82	2.57	4.00	4.88	6.33	-0.94	6.04	3.84	-2.33	3.59	5.65	5.96	0.86	-3.86	5.54	1.22
Frequence_contour		15,25	8,12	0.11	0.25	0.35	0.33	5.51	1.71	2.23	0.52	6.87	0.73	5.24	1.11	0.03	1.25	1.74	-2.14	1.52	0.06	-2.72	1.22
Fundamentalfrequence_contour		13,21	8,79	0.98	2.67	0.62	-0.36	5.50	-0.26	-1.97	-0.77	7.43	0.59	4.52	-0.05	-0.09	1.52	1.10	0.99	0.37	1.83	3.01	0.43
GAA		22,72	11,60	3.32	4.41	3.66	4.34	9.23	7.49	8.34	1.42	10.09	1.75	7.43	3.86	5.59	2.59	1.05	6.59	2.87	5.05	5.03	3.35
Grand_axe**	Longest_axis	14,62	12,52	2.93	6.26	3.34	5.66	9.31	4.89	8.86	4.59	8.39	2.07	8.91	8.60	5.27	7.85	8.16	5.78	2.56	1.05	7.69	1.28
Grand.petit**	Longest.shortest	18,47	9,35	3.18	4.62	-1.01	2.24	7.34	5.02	3.82	0.84	8.33	0.06	5.54	0.13	1.02	1.17	3.02	2.93	1.94	0.20	2.08	0.53
GsurP		26,03	12,70	1.11	4.65	0.77	4.04	9.48	5.58	12.00	0.68	11.76	4.02	7.93	3.34	8.55	2.75	2.26	2.55	3.81	6.48	5.90	3.33
HarmoSpe**	HarmoSpe	19,92	12,53	8.39	1.64	3.23	4.44	9.70	6.96	7.92	0.48	2.79	2.75	9.29	2.50	7.76	2.55	3.41	3.35	5.98	-0.51	5.27	2.13
Homogeneity**	Homogeneity	21,89	13,43	1.79	2.53	1.13	2.29	9.77	10.66	4.76	-0.54	1.25	1.14	9.68	-0.03	2.58	5.30	-1.70	6.15	2.77	3.18	4.86	4.31
kurtosis		10,89	9,00	2.45	1.64	0.03	-0.82	7.22	2.92	3.71	2.42	6.76	1.92	5.39	-0.16	0.60	1.10	1.32	-0.21	-0.31	2.58	-0.04	0.39
LN_aire**	NL_area	16,94	13,28	2.07	5.09	5.04	6.33	8.90	6.53	8.54	2.91	6.81	1.08	8.51	7.81	5.98	9.43	7.10	6.19	3.90	3.97	7.41	2.73
LN_Amplitude_contour		8,28	8,38	0.01	-0.18	-0.22	-0.44	5.39	1.36	1.79	0.04	-0.06	0.18	5.67	1.47	0.57	1.19	1.12	1.67	1.38	0.92	-0.07	-2.14
LN_Aplatissement*	NL_Flattening	22,99	14,18	6.77	3.67	0.15	4.19	7.86	0.01	1.85	7.45	4.61	4.54	7.19	4.10	-0.20	2.00	5.95	2.29	1.60	6.49	7.76	1.00
LN_Aplatissement_contour*	NL_Flattening_contour	16,63	15,01	2.05	8.80	1.82	4.49	8.99	9.74	6.39	4.53	8.22	6.56	8.06	-0.35	3.99	5.97	0.21	9.15	1.55	8.29	5.38	1.93

Appendix 4.2.C. Cont.

LN_Compactness		15,80	9,74	2.80	1.45	-0.87	0.30	5.32	8.45	0.91	2.26	3.38	3.20	6.32	-2.14	0.43	1.63	5.29	2.14	2.25	2.23	0.61	-1.67
LN_Contrast*	NL_Contrast	31,65	17,07	4.02	7.28	3.39	3.69	9.47	-0.78	4.11	9.10	4.95	6.71	9.27	6.11	-0.74	-0.53	10.97	4.80	5.60	12.17	4.99	2.29
LN_Correlation*	NL_Correlation	39,52	24,33	13.68	14.29	8.17	6.64	16.49	12.57	11.07	5.40	5.11	8.49	14.98	7.75	8.40	11.39	8.16	4.16	12.76	2.05	12.01	8.78
LN_DHT.bruit_contour		13,42	9,07	0.95	-0.08	-2.61	7.37	6.02	1.90	0.77	-1.21	3.19	0.44	3.46	-0.46	1.34	3.44	0.04	-0.63	1.02	1.68	3.10	2.24
LN_Dissimilarity		20,87	11,34	3.98	4.95	3.43	4.96	8.88	0.13	2.75	3.38	3.05	4.05	7.54	4.37	0.71	6.49	4.94	3.94	2.27	3.88	-0.77	2.24
LN_Dissymetrie*	NL_Dissymetry	27,76	15,57	5.15	6.54	4.65	6.89	9.11	4.55	9.37	2.87	4.53	2.82	9.96	2.00	1.93	4.03	8.77	4.25	2.50	-0.97	9.94	3.53
LN_Dissymetrie_contour*	NL_Dissymetry_contour	17,39	15,23	5.05	9.23	4.57	3.94	10.07	10.42	6.29	5.16	8.97	6.70	8.67	3.20	5.92	6.86	2.42	9.48	1.92	8.40	7.51	2.21
LN_Ecart.type_contour		21,59	11,92	5.71	0.39	0.27	8.51	6.69	4.75	4.14	0.24	4.38	1.13	7.67	4.17	1.67	5.14	0.40	0.65	1.07	-0.56	1.19	0.99
LN_Ecarttype*	NL_Ecarttype	26,56	16,45	5.95	10.88	2.58	7.19	10.53	9.02	10.81	2.14	4.45	6.17	10.73	0.75	3.19	5.85	1.35	1.38	4.44	3.86	6.11	2.19
LN_Elongation		19,54	10,67	3.23	5.61	1.42	3.68	7.41	7.09	5.28	0.83	7.81	1.89	5.49	-0.55	2.58	2.48	4.75	4.00	3.22	5.73	0.78	2.49
LN_Energy		19,42	10,07	1.90	7.24	1.76	1.70	5.05	4.06	1.75	2.12	3.35	1.17	8.91	2.64	-1.71	0.18	5.75	4.27	-0.38	5.16	-0.44	0.05
LN_Entropy**	NL_Entropy	24,03	12,73	8.81	2.59	2.26	7.49	8.85	4.94	2.30	0.95	2.67	3.12	6.63	3.30	1.36	8.42	3.08	0.81	4.10	-1.35	5.64	3.86
LN_entropy		14,37	12,70	5.28	8.28	1.06	4.62	9.26	7.96	7.14	-0.61	9.20	8.03	9.87	6.35	4.67	8.58	4.79	6.84	1.05	6.32	6.58	1.68
LN_FourierPower**	NL_FourierPower	16,12	12,91	5.63	9.35	1.97	3.18	9.35	9.14	6.83	3.67	9.18	6.92	6.97	4.78	5.23	7.91	2.07	9.29	3.20	7.04	5.54	1.01
LN_Frequence		17,91	11,65	0.01	8.11	3.25	5.62	7.96	4.21	2.40	2.13	0.83	4.01	7.52	2.63	3.71	6.65	3.12	4.43	2.59	4.37	4.99	2.08
LN_Frequence_contour		17,38	8,92	-0.03	1.32	0.09	4.60	7.11	6.97	1.48	0.48	6.11	3.43	4.89	-1.20	0.56	0.52	5.95	1.70	0.95	1.09	-0.99	1.31
LN_Fundamentalfrequence_contour		11,99	8,66	1.22	4.07	0.29	3.02	6.89	2.41	1.03	-0.23	3.22	0.20	5.46	3.67	-1.67	2.57	1.34	1.28	-0.19	2.83	-0.14	-0.09
LN_Grand_axe*	NL_Longest_axis	18,57	16,70	2.45	7.65	6.45	8.43	11.40	10.02	13.01	5.54	9.23	4.31	11.21	8.80	8.05	10.39	9.46	6.23	5.58	8.75	9.77	3.33
LN_grand.petit*	NL_Longest.shortest	26,30	18,59	5.65	9.07	2.74	1.69	13.04	16.55	5.61	7.82	9.16	10.57	10.75	-1.37	9.29	2.15	6.59	4.51	1.03	10.51	6.69	2.46
LN_HarmoSpe*	NL_HarmoSpe	31,13	17,37	5.01	-0.02	1.37	2.84	11.14	8.43	8.66	3.08	1.57	3.32	9.39	3.20	1.69	4.18	10.51	2.12	2.75	0.90	12.18	3.08
LN_Heywood*	NL_Heywood	26,45	19,66	5.69	9.31	1.60	2.29	12.68	16.84	6.01	5.99	10.03	8.09	8.35	0.33	8.98	2.82	7.74	4.64	2.33	10.63	7.29	3.03
LN_Homogeneity*	NL_Homogeneity	27,69	14,17	2.55	11.27	4.27	0.71	7.56	0.93	3.63	7.21	5.80	3.81	7.18	5.38	0.10	1.94	6.07	4.95	3.63	7.23	-3.98	2.56
LN_kurtosis		11,77	8,92	0.40	3.12	2.26	3.20	4.60	1.49	3.59	0.91	2.02	-0.65	6.51	0.43	3.77	2.85	-0.10	-0.33	-1.02	1.51	0.64	1.36
LN_Maxspectrepuiss		13,43	10,97	4.80	8.41	0.09	5.01	7.37	6.95	5.52	1.79	8.09	5.46	6.77	4.48	3.84	7.52	2.69	8.13	2.52	5.25	4.55	1.71
LN_Mediane**	NL_Median	23,14	13,68	3.60	8.43	0.17	8.95	9.53	7.68	6.21	1.97	2.30	1.54	7.44	-0.19	-0.45	5.68	5.12	2.29	4.59	3.64	4.18	4.91
LN_Mediane_contour		12,63	8,38	2.92	0.92	0.07	3.23	7.24	0.95	-0.56	-0.30	4.89	-0.11	5.78	2.41	0.44	3.54	3.93	3.92	2.71	1.49	-0.94	2.82
LN_Mode*	NL_Mode	25,37	14,43	2.79	5.61	-0.72	2.96	9.43	2.62	6.96	-0.11	6.08	2.57	6.12	4.05	3.78	4.78	11.71	4.84	2.60	0.36	2.45	1.79
LN_Mode_contour		14,13	10,15	4.60	5.37	-0.70	5.19	7.26	2.90	4.90	0.29	6.97	6.58	7.88	4.11	2.04	4.98	2.54	6.96	-0.36	2.21	2.00	-0.52
LN_MoyArith**	LN_ArithMean	21,41	12,96	4.46	7.15	-0.26	7.69	9.65	6.22	5.14	2.21	0.77	4.92	8.01	1.12	1.05	4.41	5.57	1.53	6.27	3.45	0.46	4.12
LN_MoyArith_contour		13,88	10,67	5.35	7.85	0.66	4.66	9.08	6.58	5.45	3.50	7.15	7.78	7.91	4.58	3.32	7.56	2.05	8.12	0.35	5.77	5.45	2.53
LN_Peak		17,93	9,73	-0.99	4.53	-1.22	2.15	6.25	7.72	0.89	-0.83	2.56	-0.04	4.93	-0.99	2.17	3.51	2.43	3.34	1.91	3.98	0.05	2.72
LN_Periode		17,29	10,52	1.10	0.37	2.49	4.78	8.54	4.08	4.88	-0.03	7.90	2.34	6.42	3.77	-0.89	2.94	5.21	3.24	-0.11	1.76	0.64	1.87
LN_Petit_axe**	NL_Shortest_axis	23,87	13,45	2.01	4.07	4.11	5.69	8.76	6.83	7.18	3.25	2.86	0.38	7.47	5.86	3.65	9.15	9.70	4.73	4.00	2.65	4.16	0.33
LN_Phase		6,25	8,41	1.27	2.28	0.15	0.33	4.16	-1.37	1.29	1.06	2.60	1.33	4.71	-2.41	0.45	-0.78	2.40	-1.78	1.22	-0.49	1.28	-1.38
LN_Phase_contour		10,85	9,02	1.88	5.13	1.21	3.58	5.41	5.08	3.65	0.38	6.70	4.81	5.59	2.83	1.24	4.60	2.31	4.83	0.21	2.68	2.21	2.08
LN_Puissance		11,33	9,08	3.94	4.13	1.23	4.84	5.58	4.21	3.00	-1.06	5.95	4.00	5.63	3.60	-0.27	4.35	2.04	4.46	1.38	4.84	0.25	0.58
LN_SINAD_contour		12,86	8,92	2.15	1.88	0.40	7.78	8.44	3.69	1.62	0.34	4.39	-1.91	4.80	0.53	0.37	2.96	1.63	-1.15	0.83	1.32	2.16	2.00
LN_skewness		19,45	11,34	3.92	2.37	0.54	8.40	7.52	4.49	3.03	3.12	4.91	2.47	6.91	2.39	1.47	3.22	0.14	-0.38	-0.90	1.20	2.66	2.24
LN_Somme*	NL_Sum	32,07	18,53	1.43	11.07	0.76	7.64	11.07	14.62	4.56	0.14	2.64	0.90	10.17	0.00	4.20	2.57	8.61	3.54	5.01	1.36	7.47	1.20
LN_Somme_contour		15,18	12,41	4.81	9.49	1.83	4.25	9.00	7.76	7.46	2.94	7.47	5.58	6.99	4.49	3.69	6.40	0.41	9.60	-0.52	6.75	3.41	1.51
LN_taille_contour*	NL_size_contour	16,70	14,11	2.25	4.63	4.75	7.05	9.73	7.02	9.58	3.78	8.74	1.22	8.95	6.97	5.65	9.03	8.09	6.45	5.74	3.81	9.40	2.90
LN_THD_contour		18,12	8,84	0.03	3.27	1.36	3.17	6.28	7.32	1.64	0.07	6.06	-0.40	4.95	-3.68	-0.21	0.13	6.37	1.04	0.11	-0.57	-3.03	0.20
LN_Typefactor		22,54	12,06	5.72	8.45	-1.39	1.09	8.75	8.78	4.16	4.16	5.40	3.36	6.18	-1.38	7.14	2.32	3.71	7.17	2.63	3.79	3.98	0.35
LN_ValeurEff**	NL_ValueEff	22,30	13,62	4.95	8.58	-0.56	9.06	10.74	7.69	7.17	1.52	2.21	5.14	9.25	0.97	3.72	3.75	5.62	1.69	5.22	4.48	3.99	4.65
LN_Valeurefficace_contour*	NL_Valueeffective_contour	16,75	15,53	6.78	8.48	3.83	5.77	10.00	10.27	6.20	2.13	10.32	9.05	10.16	8.86	6.56	10.23	7.07	9.59	2.12	8.58	8.96	2.00
LN_Variance*	NL_Variance	28,86	16,87	6.43	11.39	0.91	10.45	12.06	9.97	14.30	2.88	2.36	7.84	13.04	2.13	3.53	7.50	0.05	0.03	5.64	3.50	5.76	1.21
LN_Variance_contour		12,22	8,78	2.20	0.42	1.09	3.14	5.81	2.30	2.11	1.03	3.05	0.02	5.36	1.48	3.39	1.65	1.51	0.18	1.32	0.34	0.47	3.49
LN.perimetre**	NL_perimeter	16,30	13,51	1.39	4.78	3.78	7.46	10.49	7.41	10.03	3.91	7.68	3.89	8.25	7.81	5.23	9.64	8.48	6.02	4.24	4.39	8.34	1.11
Masse**	Weight	18,96	13,48	4.76	6.51	2.09	4.35	9.36	5.97	8.11	1.63	7.31	2.08	8.81	5.60	7.34	6.39	8.31	5.79	0.87	-3.00	4.93	1.79
Maxspectrepuiss		14,21	9,38	4.60	6.31	2.69	0.89	7.67	1.18	3.84	-1.12	2.55	1.50	5.95	1.65	5.15	4.77	0.48	5.37	1.92	5.30	2.36	2.09
Mediane		25,07	12,46	4.10	3.50	1.73	3.03	9.42	9.51	6.36	1.43	4.76	3.41	8.53	0.55	6.03	5.56	4.32	4.63	2.23	-0.24	2.59	2.31
Mediane_contour		9,27	8,03	1.67	1.71	0.12	2.59	5.69	-0.56	0.94	0.87	6.12	1.27	3.50	1.19	-0.25	1.66	-0.61	1.59	-0.88	1.37	-0.21	-0.52
Mode**	Mode	21,95	13,82	5.23	5.68	2.60	4.50	9.44	6.97	8.19	3.17	3.65	2.76	8.79	3.26	6.90	4.41	10.05	5.48	3.44	-3.96	7.92	3.51

Appendix 4.2.C. Cont.

Mode_contour		16,94	9,58	2.87	5.48	1.21	0.75	7.72	2.52	2.25	-0.23	6.22	0.06	5.65	1.43	8.31	3.93	1.83	5.06	0.52	4.30	-0.61	0.59
MoyArith* **	ArithMean	23,73	12,81	5.20	4.39	1.46	3.21	9.36	9.72	5.39	0.69	3.80	1.96	9.28	-0.43	5.93	5.45	6.42	4.79	4.12	-0.47	4.93	3.22
MoyArith_contour		14,60	9,60	4.25	5.12	2.61	1.59	7.61	3.18	4.04	-2.12	3.46	0.68	7.68	2.24	6.16	4.88	0.91	5.77	1.40	5.45	0.22	1.69
PAA		20,27	9,80	5.71	4.51	2.96	4.09	10.71	7.58	8.58	4.34	6.33	2.74	7.98	3.33	9.70	3.45	1.05	2.77	2.70	6.14	3.98	3.91
Peak*	Peak	28,17	18,18	7.75	1.77	2.53	1.12	13.07	10.56	5.94	-1.00	2.78	3.64	11.43	4.20	-0.09	0.29	-0.21	7.82	11.08	12.49	5.39	2.91
Periode		17,49	9,95	3.61	-0.45	-0.12	0.30	6.66	3.96	1.18	0.48	8.89	1.26	6.17	4.42	1.30	1.95	4.76	3.11	1.39	0.11	-3.49	0.90
Petit_axe **	Shortest_axis	19,03	13,35	1.06	6.38	2.56	4.22	7.77	4.91	7.71	4.85	4.52	1.25	8.76	4.68	4.59	7.10	9.20	3.41	3.62	-1.59	5.86	1.52
Phase		7,94	8,91	0.76	1.30	-0.47	0.17	7.39	1.66	0.60	0.12	2.75	0.16	7.35	-0.04	-1.46	-0.13	0.92	-0.28	1.05	1.67	1.21	-1.15
Phase_contour		16,00	9,84	3.50	5.29	0.29	0.38	7.82	0.59	3.99	-1.55	4.35	-2.26	7.21	1.54	3.99	2.98	1.77	6.09	-0.75	6.60	2.87	1.66
pics **	Pics	11,56	3,59	0.50	0.97	1.08	2.42	4.26	1.85	3.14	-0.05	1.83	1.12	2.47	1.00	1.29	0.90	5.19	-0.05	1.77	-1.24	-0.47	1.08
Puissance		18,14	9,59	3.20	5.25	1.36	1.37	7.19	1.99	3.39	-0.96	4.80	-0.34	6.93	0.14	5.22	4.07	-0.28	4.64	2.89	6.68	-1.67	0.05
roundness		13,21	10,69	3.85	7.40	2.72	1.92	7.21	4.08	5.34	0.46	3.47	1.66	6.31	2.13	5.80	3.25	0.83	7.68	0.31	6.74	1.94	4.21
roundness_aire **	Roundness_area	24,81	13,13	1.12	5.17	2.68	2.48	8.20	8.21	8.03	3.60	13.16	1.97	7.27	1.37	7.43	3.41	1.13	5.53	3.30	5.17	3.43	4.08
SINAD_contour		15,88	9,65	-0.18	3.91	0.94	5.76	6.11	-0.99	2.20	-0.08	8.40	0.94	5.78	1.48	1.45	1.71	-1.15	-0.64	-0.62	1.15	2.10	0.52
skewness **	Skewness	22,51	12,71	1.72	2.50	0.71	3.29	8.38	2.50	4.89	4.21	13.28	1.58	6.04	1.06	0.93	-0.88	1.73	0.92	2.23	2.34	4.44	0.20
Somme		16,06	10,15	1.51	4.61	2.81	3.83	7.32	2.51	1.34	0.81	0.27	1.88	7.60	2.02	1.72	0.84	5.95	1.57	-1.03	0.04	-2.73	0.53
Somme_contour		12,06	10,19	3.50	5.21	0.99	1.16	7.60	2.17	3.24	2.77	1.66	0.92	7.05	2.60	5.23	6.52	1.40	6.39	1.29	5.30	1.94	2.09
taille_contour		14,80	11,47	1.77	5.46	2.89	5.08	8.16	4.92	7.40	3.40	7.29	1.48	9.63	5.87	6.12	7.60	7.82	4.01	2.56	-1.95	5.15	1.88
THD_contour		14,84	8,16	0.14	0.40	-1.63	0.93	5.51	2.86	1.59	-0.70	6.47	-1.38	5.34	1.20	1.54	1.39	1.21	0.83	3.10	-1.17	-0.93	0.19
ValeurEff **	ValueEff	23,95	13,39	5.46	4.77	0.67	3.21	8.78	10.42	7.06	1.18	3.45	1.21	9.16	-0.17	8.27	4.09	5.40	6.18	2.85	-0.84	6.18	1.31
Valeurefficace_contour		12,49	11,87	4.70	5.78	3.77	1.51	7.51	5.20	5.53	1.35	6.51	3.27	8.49	5.33	7.15	7.40	5.02	6.83	2.38	5.53	4.52	3.73
Variance **	Variance	24,93	13,01	7.95	4.31	4.14	4.32	9.49	11.05	6.47	2.21	2.08	0.90	7.85	2.65	7.92	6.43	4.02	6.63	4.77	0.99	5.83	3.51
Variance_contour		11,75	9,03	1.64	1.54	-1.21	-2.40	5.76	1.39	3.14	3.16	7.05	2.71	4.60	-1.52	0.61	-0.33	-1.68	-1.27	0.64	1.99	0.17	-0.82

Appendix 5.A. Detailed phytolith counts, diatoms, and measured tree cover in modern soil samples

	SAMPLE	O34	O35	O36	E54	E55	E56	E57	E58	E59A	E59B	H61	H62	H64	H66	H68	M69	M70	M71	M72	M73	M74	M75
	Tree cover (%)	8	28	39	6	51	78	43	48		49	46	46		7	15	53	64	68	30	79	24	
CODES	ATTRIBUTION																						
Ac1		6	26	5	5	1	9	20	11	7	33	25	7	4	20	9	31	25	6	10	23	35	8
Ac2		2	21	8	1	12	18	0	4	2	36	3	0	0	3	0	8	0	0	12	2	2	7
Ac3		3	0	0	10	0	1	4	3		3	3	4	2	0	0	0	7	2	1	3	9	8
Blo1		0	0	0	0	0	0	1	0		0	0	0	0	2	0	0	0	0	2	12	10	0
Blo2	Grass/Sedge	1	0	0	0	1	0	2	13		0	9	0	0	2	0	0	0	21	1	14	18	0
Blo4	FI	3	256	32	27	35	2	12	9	2	16	12	13	7	0	178	12	2	63	8	6	2	18
Blo5	FI	17	41	25	19	62	131	16	73		7	27	10	31	15	44	16	3	9	2	7	35	0
Blo6	FI	18	55	1	0	54	71	49	2		26	26	36	41	7	21	25	46	18	0	5	0	17
Blo7	FI	2	76	0	5	18	0	49	9		26	23	25	6	34	29	4	17	48	7	14	11	69
Blo8	FI	0	24	0	3	0	0	13	13		2	15	21	22	0	0	0	6	0	0	0	3	2
Blo10		0	0	0	0	0	0	6	4		0	2	0	1	0	12	4	0	1	0	0	0	0
Blo11	Grass/Sedge	7	0	2	0	0	2	14	5	5	0	6	0	0	0	0	4	0	2	2	2	0	6
Blo14	FI	0	0	0	4	13	9	0	0	29	6	6	0	2	0	3	0	2	0	2	0	18	0
Blo17		7	30	2	1	2	4	30	19		9	21	7	5	1	3	2	9	27	5	0	7	9
Com1	FI	0	0	0	0	0	0	0	0		1	0	0	0	0	0	5	0	0	1	0	10	5
Com2	FI	0	0	0	0	0	0	0	0		0	0	0	0	0	0	0	0	0	1	0	0	0
El1	FI	1	0	3	0	21	0	7	12	3	2	0	0	0	0	0	0	0	0	0	0	0	3
El3	FI	8	6	18	2	13	46	21	7		24	15	28	43	9	9	46	46	60	13	26	0	24
El4	Sedge	0	0	3	0	0	0	2	0	2	0	4	0	0	0	0	0	0	0	12	0	2	0
El5	Grass/Sedge	8	9	6	2	1	13	15	77		2	47	3	9	1	15	6	11	9	12	2	11	2
El7	Grass/Sedge	6	1	3	5	0	9	34	59	4	2	37	33	7	1	0	4	2	82	10	25	16	0
El9		1	15	33	4	11	52	23	183	1	58	28	21	27	22	1	22	49	120	23	21	33	12
El10	FI	0	0	0	0	0	10	0	0	10	0	0	0	0	0	3	0	0	2	0	0	0	1
El11		0	8	0	0	2	0	13	25		0	15	0	0	0	0	0	6	0	2	11	0	0
El12		0	18	0	1	0	25	3	12	1	9	0	0	0	0	2	1	0	0	39	30	0	2
El13	Grass	0	1	5	0	1	1	2	4		1	9	0	13	0	0	0	0	12	2	1	0	0
El14										9													
El15	FI	0	0	0	0	0	2	0	0		8	0	0	6	0	2	0	0	22	0	27	12	0
Epi2	Ferns	3	1	2	1	7	0	10	3		0	5	8	42	1	0	0	0	16	0	7	44	0
Glo2	Palms	0	0	0	43	34	219	56	12	4	2	87	23	2	0	1	14	11	93	1	13	113	1
Glo4	Palms	0	0	0	8	26	113	16	6		0	37	9	0	0	0	2	3	41	0	4	28	0
Glo6		0	0	0	0	0	0	2	8		3	0	0	1	0	0	0	2	11	0	0	3	0
Glo9		0	0	0	1	1	16	13	9		2	4	0	0	0	0	0	1	2	0	4	0	0
Glo10	FI	4	0	3	5	10	20	33	19	39	4	26	6	14	7	2	0	0	47	3	40	60	8
Glo11	FI	4	0	0	2	2	5	12	42	5	8	14	5	0	0	0	0	8	0	0	2	9	1

Appendix 5.A. Cont.

	SAMPLE	O34	O35	O36	E54	E55	E56	E57	E58	E59A	E59B	H61	H62	H64	H66	H68	M69	M70	M71	M72	M73	M74	M75
Glo13	FI	22	102	156	60	41	100	36	101	15	105	129	117	98	78	43	27	118	177	23	106	116	120
GSSC1	Grass	7	0	12	3	1	22	6	0		0	2	1	0	0	0	11	0	0	5	1	5	0
GSSC2	Grass	25	13	8	68	3	1	31	7		3	19	6	7	0	7	19	13	3	5	10	0	14
GSSC3	Grass	3	19	29	47	72	35	9	53		11	26	10	18	23	21	32	10	12	0	19	24	21
GSSC4	Grass	0	0	4	0	1	0	3	5	0	2	4	4	0	0	1	0	2	27	2	1	0	0
GSSC5	Grass	4	3	0	3	0	0	2	0	1	25	0	2	0	0	0	0	0	0	2	0	0	
GSSC6	Grass	1	0	2	15	0	0	2	0	1	0	5	0	0	0	0	11	0	1	3	0	1	0
GSSC7	Grass	20	38	8	6	17	19	13	18	0	30	16	31	7	39	22	19	21	10	13	8	9	5
GSSC8	Grass	3	0	0	3	2	0	8	1	2		2	0	7	0	0	0	0	2	0	0	1	
GSSC9	Grass	2	0	0	0	0	0	0	0		0	0	0	0	0	4	0	0	0	0	1	0	0
GSSC10	Grass	0	0	0	0	0	0	0	0		0	0	0	0	0	0	0	0	0	0	9	0	0
GSSC11	Grass	11	8	46	9	12	17	20	25	3	22	16	23	15	2	19	46	23	41	24	46	41	16
GSSC12	Grass	24	20	14	1	5	8	11	9	10	19	16	15	42	22	18	16	19	26	33	23	20	12
GSSC14	Grass	31	33	29	11	7	19	21	12	5	13	34	28	24	21	46	13	37	41	42	13	20	15
GSSC15	Grass	11	0	2	2	4	2	3	1		4	5	1	4	1	4	1	6	4	23	1	2	5
GSSC16	Grass	0	8	1	0	0	2	3	16		2	1	2	17	3	10	2	2	3	11	2	9	6
GSSC17	Grass	1	0	0	1	2	0	2	7		1	0	0	2	0	0	0	0	0	0	0	0	0
GSSC18	Grass	0	0	0	0	0	0	2	1		0	6	2	1	0	1	1	1	6	3	0	1	1
GSSC20	Grass	0	0	0	0	1	0	0	0		0	0	0	2	2	4	1	2	0	0	1	1	0
GSSC22	Grass	64	50	19	17	52	47	45	20	6	34	23	33	20	64	43	18	15	24	21	61	35	63
GSSC23	Grass	18	5	19	5	18	5	8	10	4	12	12	16	12	12	8	8	18	8	3	9	12	15
GSSC24	Grass	6	0	0	0	3	3	3	0		0	2	4	0	1	0	3	12	7	9	12	0	4
Mes	FI	6	28	19	7	3	13	26	48	2	12	49	3	5	21	22	4	61	124	1	153	32	24
Pla1		0	0	0	0	0	0	1	14		0	0	0	0	0	0	0	1	1	0	0	10	0
Pla2	FI	7	2	14	2	2	1	15	15	7	19	22	13	7	5	0	0	0	12	4	2	7	1
Pla5	Sedge									7													
Pla6		2	0	0	0	0	0	0	0		4	2	26	0	0	0	9	0	8	0	0	31	0
Pla7		3	11	35	3	3	6	15	28	25	23	15	7	13	3	0	14	15	15	15	8	19	14
Pla8	Grass/Sedge	0	0	0	0	0	0	0	0		0	2	0	0	0	0	0	0	6	0	0	0	0
Sto		0	0	0	0	1	0	0	0		0	0	0	0	0	0	1	0	0	0	0	0	0
Und1		0	26	5	2	35	1	8	0	4	8	0	30	60	4	1	1	29	9	66	20	198	3
Und3		0	0	0	0	0	2	0	0	1	0	0	19	0	0	0	1	4	11	6	2	35	0
Und4		20	175	2	5	5	139	43	38	69	63	25	5	7	27	0	16	158	223	27	82	76	23
Diatoms		53	104	77	37	26	39	23	397	77	2	61	22	20	7	16	26	20	522	136	15	132	13
	Σ phytoliths	392	1128	575	418	617	1219	813	1071	285	702	939	657	652	452	607	480	822	1515	512	890	1195	565

Appendix 5.B. Datase used in PCA's showed in **Figures 5.1.6**, **5.1.7** and **7.1.3**.

ID	Environment	Country (or site)	Globular _echinate	Globular _granulate	Globular _smooth	Bilobate	Cross	Saddle	Trapeziform	Rondel	Polylobate	Bulliform	D/P	Iph	Ic
LM12	GW	Kenya	0.0	12.8	7.5	39.1	6.8	5.3	1.5	21.8	1.5	3.8	0.2	10.3	32.7
UM12	GW	Kenya	0.4	2.6	0.8	36.1	2.6	4.1	6.0	39.8	3.0	4.5	0.0	9.6	53.3
UM31	GW	Kenya	0.4	1.6	4.4	27.8	3.2	13.3	8.1	24.6	15.3	1.2	0.0	30.0	52.0
B12	W	Kenya	0.0	0.3	3.8	14.1	2.7	3.4	4.5	59.8	1.0	10.3	0.0	16.9	76.3
B23	W	Kenya	0.0	0.4	1.1	10.0	3.2	1.8	2.1	63.6	0.0	17.9	0.0	11.9	81.4
H12	GW	Kenya	0.0	0.8	2.0	9.4	2.0	1.6	4.9	60.4	9.4	9.4	0.0	12.5	85.1
H31	GW	Kenya	0.0	1.9	0.8	9.2	0.0	3.4	2.3	67.0	10.3	5.0	0.0	27.3	86.3
ES12	W	Kenya	0.0	0.0	0.4	4.7	0.0	0.0	0.4	86.3	7.8	0.4	0.0	0.0	95.3
ES23	W	Kenya	0.4	1.4	12.3	13.4	1.4	2.2	2.5	50.4	14.1	1.8	0.0	12.8	79.7
RGW2	GW	Tanzania	0.0	7.8	22.4	30.2	0.9	2.6	0.0	15.5	2.6	18.1	0.2	7.7	35.0
LAS21	G	Kenya	0.0	0.0	6.2	4.9	3.7	2.9	0.0	65.8	16.0	0.4	0.0	25.0	87.7
LAS32	G	Kenya	0.0	0.0	1.5	14.2	0.4	4.5	1.5	56.3	20.1	1.5	0.0	23.5	80.4
UAS11	G	Kenya	0.0	0.4	7.6	3.3	0.0	0.0	0.7	73.9	13.4	0.7	0.0	0.0	96.4
UAS33	G	Kenya	0.0	0.9	0.0	7.0	1.8	1.8	0.0	72.7	15.0	0.9	0.0	16.7	89.2
RGW4	G	Tanzania	0.0	2.7	6.1	54.4	3.0	9.9	0.0	20.9	0.0	3.0	0.0	14.7	23.7
RGW7A	G	Tanzania	0.0	2.0	9.3	24.0	3.7	6.1	0.0	43.1	5.3	6.5	0.0	18.1	58.9
RGW9	G	Tanzania	0.0	2.0	1.6	55.0	0.0	15.5	0.0	7.6	0.0	18.3	0.0	22.0	9.7
RGW17	G	Tanzania	0.0	1.3	0.0	24.7	3.9	3.5	0.0	55.4	0.0	11.3	0.0	10.8	63.4
RGW19	G	Tanzania	0.0	0.3	1.7	36.2	0.0	10.1	0.0	34.5	0.0	17.1	0.0	21.8	42.7
RGW20	G	Tanzania	0.0	0.3	1.1	17.8	0.0	11.2	0.0	60.2	0.0	9.5	0.0	38.6	67.5
RGW23	W	Tanzania	0.0	14.1	4.9	30.1	2.9	7.3	0.0	26.2	0.0	14.6	0.2	18.1	39.4
RGW24	WG	Tanzania	0.0	1.2	1.2	33.3	4.5	14.0	0.0	35.4	0.0	10.3	0.0	27.0	40.6
RGW27	G	Tanzania	0.0	1.1	2.7	30.6	3.2	4.3	0.0	42.5	6.5	9.1	0.0	11.3	56.2
ALEXDIMONI	GW	D.R.Congo	9.1	84.1	0.0	5.5	0.0	1.3	0.0	0.0	0.0	0.0	13.8	18.9	0.0
CAM1	S	Cameroon	73.3	16.6	2.4	2.7	0.0	0.0	0.0	1.0	0.0	4.1	24.2	0.0	27.3
CAM2	W	Cameroon	27.4	57.7	2.9	3.9	0.0	0.7	0.0	1.0	0.0	6.5	15.4	14.3	17.6
CAM3	W	Cameroon	13.1	76.5	0.8	2.8	1.2	0.0	0.0	0.4	0.0	5.2	20.5	0.0	9.1
CAM4	W	Cameroon	0.7	79.6	2.6	5.9	0.0	0.4	0.0	0.0	0.0	10.8	12.7	5.9	0.0
CAM5	W	Cameroon	0.4	83.5	2.5	7.2	0.0	0.4	0.0	0.0	0.4	5.7	10.6	4.8	4.5
CAM6	W	Cameroon	11.2	78.0	2.4	5.6	0.0	0.4	0.0	0.4	0.8	1.2	12.4	6.7	16.7
CAM7	W	Cameroon	3.4	74.4	0.7	13.5	0.0	0.0	0.0	1.3	0.0	6.7	5.3	0.0	9.1
CAM8	W	Cameroon	19.6	65.7	1.6	7.3	2.0	0.8	0.0	0.0	0.4	2.4	8.0	8.0	3.8
CAM9	W	Cameroon	3.1	75.8	1.7	12.8	0.0	0.0	0.0	1.4	0.0	5.2	5.6	0.0	9.8

Appendix 5.B. Cont.

ID	Environment	Country (or site)	Globular _echinate	Globular _granulate	Globular _smooth	Bilobate	Cross	Saddle	Trapeziform	Rondel	Polylobate	Bulliform	D/P	Iph	Ic
CAM10	W	Cameroon	1.0	68.4	2.0	6.6	0.0	0.0	0.0	0.3	0.0	21.7	10.0	0.0	4.8
CAM11	W	Cameroon	23.2	59.6	2.1	8.2	1.1	1.1	0.0	0.7	0.0	3.9	7.5	10.3	6.5
CAM12	W	Cameroon	3.1	72.6	0.9	16.2	0.0	0.0	0.0	1.2	0.3	5.6	4.3	0.0	8.8
CAM13	W	Cameroon	0.0	80.7	0.4	7.4	0.0	0.0	0.0	1.1	0.0	10.4	9.4	0.0	13.0
CAM14	W	Cameroon	2.9	77.7	0.0	13.7	0.0	0.0	0.0	0.0	0.0	5.8	5.9	0.0	0.0
CAM15	W	Cameroon	5.6	67.4	0.7	20.1	0.0	0.0	0.0	0.0	0.0	6.3	3.6	0.0	0.0
CAM16	W	Cameroon	1.1	69.1	1.1	22.9	0.0	0.0	0.0	0.4	0.0	5.5	3.0	0.0	1.6
CAM17	W	Cameroon	0.0	64.4	0.3	28.5	0.0	0.0	0.0	0.3	0.7	5.8	2.2	0.0	3.4
CAM18	W	Cameroon	2.1	54.5	0.7	36.4	0.0	0.0	0.0	0.3	0.7	5.2	1.5	0.0	2.8
CAM19	F	Cameroon	0.6	33.5	0.9	53.5	3.6	0.0	0.0	0.6	0.3	6.9	0.6	0.0	1.6
CAM20	F	Cameroon	0.6	27.9	0.3	51.5	1.7	0.0	0.0	0.6	3.3	14.2	0.5	0.0	6.8
CAM21	F	Cameroon	3.7	44.2	0.6	42.3	3.4	0.0	0.0	0.0	3.1	2.8	1.0	0.0	6.3
CAM22	WG	Cameroon	1.2	55.4	3.0	28.4	2.4	0.6	0.0	0.6	2.4	6.0	1.6	1.9	8.7
CAM23	WG	Cameroon	0.7	53.0	0.7	38.1	0.4	0.0	0.0	0.4	1.5	5.2	1.3	0.0	4.6
CAM24	WG	Cameroon	1.8	49.3	0.0	42.1	1.4	0.0	0.0	0.0	1.4	4.0	1.1	0.0	3.2
CAM25	WG	Cameroon	1.9	50.5	1.4	36.4	1.1	0.0	0.0	0.0	1.6	7.1	1.3	0.0	4.2
CAM26	WG	Cameroon	1.3	47.3	1.9	28.3	0.3	0.0	0.0	0.0	3.5	17.4	1.5	0.0	11.0
S155	W	Senegal	23.8	61.3	3.4	4.3	0.4	2.6	0.0	0.0	0.0	4.3	11.8	35.3	0.0
83151	W	Senegal	22.0	64.2	7.7	3.3	0.8	0.0	0.0	0.0	0.0	2.0	21.2	0.0	0.0
MAS1	G	Tanzania	0.0	30.2	27.3	14.5	0.6	0.0	0.0	0.0	0.0	27.3	2.0	0.0	0.0
MAS3	WG	Tanzania	0.0	34.7	26.1	17.0	0.0	1.1	0.0	0.0	0.0	21.0	1.9	6.3	0.0
MAS7	WG	Tanzania	2.6	31.1	24.8	20.5	1.0	2.6	0.0	0.3	0.0	16.9	1.4	11.0	1.4
MAS8	WG	Tanzania	0.4	25.6	22.7	20.6	0.0	1.7	1.3	1.3	0.0	26.5	1.1	7.5	10.2
MAS9	WG	Tanzania	1.0	39.2	24.7	14.9	1.0	1.5	1.5	1.5	0.0	14.4	2.0	8.8	15.0
MAS14	W	Tanzania	0.4	15.6	33.6	23.6	6.0	2.4	0.0	0.8	0.0	17.6	0.5	7.5	2.4
S7	WG	Senegal	0.7	7.5	10.3	45.2	0.0	2.1	0.0	0.0	0.0	34.2	0.2	4.3	0.0
S5	WG	Senegal	0.0	13.2	2.8	35.4	0.0	9.0	0.0	0.0	0.0	39.6	0.3	20.3	0.0
834	WG	Senegal	4.5	16.6	1.5	38.7	6.0	8.0	0.0	0.0	0.0	24.6	0.4	15.2	0.0
8277	WG	Senegal	0.5	5.8	1.5	50.5	7.8	14.1	0.0	0.0	0.0	19.9	0.1	19.5	0.0
8279	WG	Senegal	0.5	0.5	1.6	66.3	7.1	16.3	0.0	0.0	0.0	7.6	0.0	18.2	0.0
8375	WG	Senegal	0.0	5.2	0.5	61.8	10.4	10.4	0.0	0.0	0.0	11.8	0.1	12.6	0.0
8278	WG	Senegal	0.8	7.5	1.9	72.1	4.9	8.3	0.0	0.0	0.0	4.5	0.1	9.7	0.0

Appendix 5.B. Cont.

ID	Environment	Country (or site)	Globular _echinate	Globular _granulate	Globular _smooth	Bilobate	Cross	Saddle	Trapeziform	Rondel	Polylobate	Bulliform	D/P	Iph	Ic
8370	WG	Senegal	0.0	0.5	0.0	83.3	7.9	6.0	0.0	0.0	0.0	2.3	0.0	6.2	0.0
8383	WG	Senegal	0.0	0.5	0.0	80.9	9.5	6.4	0.0	0.0	0.0	2.7	0.0	6.6	0.0
S84	WG	Senegal	0.0	1.5	0.0	72.9	11.8	8.9	0.0	0.0	0.0	4.9	0.0	9.5	0.0
8368	WG	Senegal	0.5	4.9	1.0	74.1	7.3	5.9	0.0	0.0	0.0	6.3	0.1	6.7	0.0
S118	WG	Senegal	0.0	3.9	0.6	71.9	3.9	6.2	0.0	0.0	0.0	13.5	0.0	7.5	0.0
S88	WG	Senegal	0.5	2.3	1.9	71.8	2.3	13.4	0.0	0.0	0.0	7.9	0.0	15.3	0.0
S91	WG	Senegal	8.4	31.0	5.3	36.3	7.1	1.8	0.0	0.0	0.0	10.2	0.9	3.9	0.0
83120	WG	Senegal	0.4	6.1	2.6	76.5	4.3	4.8	0.0	0.0	0.0	5.2	0.1	5.6	0.0
83122	WG	Senegal	0.0	1.7	0.9	76.4	4.7	9.0	0.0	0.0	0.0	7.3	0.0	10.0	0.0
S122	WG	Senegal	0.0	0.0	0.0	68.4	7.4	9.6	0.0	0.0	0.0	14.7	0.0	11.2	0.0
S93	WG	Senegal	2.9	2.9	1.0	75.1	6.3	5.4	0.0	0.0	0.0	6.3	0.1	6.2	0.0
8398	WG	Senegal	0.6	3.5	0.6	80.0	9.4	4.7	0.0	0.0	0.0	1.2	0.0	5.0	0.0
83127	WG	Senegal	1.0	38.8	4.8	35.9	1.9	2.4	0.0	0.0	0.0	15.3	1.0	6.0	0.0
S128	WG	Senegal	0.5	3.7	9.4	61.8	0.0	4.7	0.0	0.0	0.0	19.9	0.1	7.1	0.0
83100	WG	Senegal	0.0	6.3	1.8	76.8	4.9	5.8	0.0	0.0	0.0	4.5	0.1	6.6	0.0
S130	WG	Senegal	0.0	3.3	1.3	60.7	6.7	8.7	0.0	0.0	0.0	19.3	0.0	11.4	0.0
83103	WG	Senegal	0.5	4.5	1.0	73.2	9.6	4.5	0.0	0.0	0.0	6.6	0.1	5.2	0.0
S138	G	Senegal	0.0	7.4	4.0	50.3	2.7	7.4	0.0	0.0	0.0	28.2	0.1	12.2	0.0
S136	G	Senegal	0.0	9.2	1.8	35.8	2.8	11.9	0.0	0.0	0.0	38.5	0.2	23.6	0.0
83116	G	Senegal	0.6	0.6	0.0	90.2	4.9	2.4	0.0	0.0	0.0	1.2	0.0	2.5	0.0
83115	WS	Senegal	0.0	2.8	0.8	86.3	2.4	4.8	0.0	0.0	0.0	2.8	0.0	5.2	0.0
8335	WS	Mauritanie	0.0	3.3	0.8	4.2	4.2	22.5	0.0	0.0	0.0	65.0	0.1	73.0	0.0
RIM11	WS	Mauritanie	0.0	1.1	1.6	24.5	0.0	22.3	0.0	0.0	0.0	50.5	0.0	47.7	0.0
RIM10	WS	Mauritanie	0.0	4.4	1.5	16.1	0.7	11.7	0.0	0.0	0.0	65.7	0.2	41.0	0.0
RIM1	WS	Mauritanie	1.8	10.7	5.4	20.8	0.6	3.0	0.0	0.0	0.0	57.7	0.5	12.2	0.0
S33	WS	Senegal	0.0	5.8	1.9	54.8	2.4	22.1	0.0	0.0	0.0	13.0	0.1	27.9	0.0
S32	WS	Senegal	0.8	0.8	3.4	40.7	4.2	18.6	0.0	0.0	0.0	31.4	0.0	29.3	0.0
8330	WS	Senegal	0.0	3.1	1.3	53.1	3.8	14.4	0.0	0.0	0.0	24.4	0.0	20.2	0.0
S40	WS	Senegal	0.0	7.5	1.5	36.8	2.0	29.9	0.0	0.0	0.0	22.4	0.1	43.5	0.0
S29	WS	Senegal	0.0	5.7	1.9	49.0	1.9	24.8	0.0	0.0	0.0	16.6	0.1	32.8	0.0
8246	WS	Senegal	0.0	2.4	0.5	56.1	3.3	17.9	0.0	0.0	0.0	19.8	0.0	23.2	0.0
8247	WS	Senegal	1.2	4.8	1.2	59.2	2.8	12.4	0.0	0.0	0.0	18.4	0.1	16.7	0.0
S27	WS	Senegal	0.0	0.5	0.0	56.2	4.9	28.6	0.0	0.0	0.0	9.7	0.0	31.9	0.0
S44	WS	Senegal	0.0	1.7	1.1	51.9	5.5	16.6	0.0	0.0	0.0	23.2	0.0	22.4	0.0

Appendix 5.B. Cont.

ID	Environment	Country (or site)	Globular _echinate	Globular _granulate	Globular _smooth	Bilobate	Cross	Saddle	Trapeziform	Rondel	Polylobate	Bulliform	D/P	Iph	Ic
S24	WS	Senegal	0.0	0.6	0.6	72.1	0.6	19.0	0.0	0.0	0.0	7.3	0.0	20.7	0.0
8346	WS	Senegal	0.4	2.5	0.8	52.1	9.2	27.9	0.0	0.0	0.0	7.1	0.0	31.3	0.0
8320	WS	Senegal	0.0	3.8	0.9	44.8	6.6	36.3	0.0	0.0	0.0	7.5	0.0	41.4	0.0
8315	WS	Senegal	1.3	5.3	2.6	36.8	10.5	14.5	0.0	0.0	0.0	28.9	0.1	23.4	0.0
S54	WS	Mauritanie	0.0	1.3	1.9	60.0	1.9	15.0	0.0	0.0	0.0	20.0	0.0	19.5	0.0
8348	WS	Mauritanie	0.5	1.9	0.5	39.6	6.8	22.7	0.0	0.0	0.0	28.0	0.0	32.9	0.0
S12	WS	Mauritanie	2.0	10.7	8.1	48.3	1.3	12.8	0.0	0.0	0.0	16.8	0.2	20.4	0.0
S58	WS	Mauritanie	0.0	2.1	1.6	50.5	4.2	31.6	0.0	0.0	0.0	10.0	0.0	36.6	0.0
838	WS	Senegal	3.9	6.4	1.7	40.8	4.3	22.7	0.0	0.0	0.0	20.2	0.2	33.5	0.0
8362	WS	Senegal	1.3	1.3	1.9	36.3	11.5	30.6	0.0	0.0	0.0	17.2	0.0	39.0	0.0
8365	WS	Senegal	0.0	2.3	0.5	65.0	6.5	22.9	0.0	0.0	0.0	2.8	0.0	24.3	0.0
RIM3	WS	Mauritanie	2.3	4.6	5.7	20.7	0.0	6.9	0.0	0.0	0.0	59.8	0.3	25.0	0.0
RIM8	WS	Mauritanie	9.3	6.7	2.7	17.3	0.0	6.7	0.0	0.0	0.0	57.3	0.7	27.8	0.0
MAU07	WS	Mauritanie	1.6	7.1	8.7	29.1	0.8	8.7	0.0	0.0	0.0	44.1	0.2	22.4	0.0
MAU06	WS	Mauritanie	0.0	3.1	3.8	46.6	0.0	4.6	0.0	0.0	0.0	42.0	0.1	9.0	0.0
MAU05	WS	Mauritanie	1.2	1.2	2.4	31.7	3.7	6.1	0.0	0.0	0.0	53.7	0.1	14.7	0.0
MAU04	WS	Mauritanie	2.2	2.9	3.6	35.8	1.5	15.3	0.0	0.0	0.0	38.7	0.1	29.2	0.0
RIM2	WS	Mauritanie	3.5	5.8	7.0	9.3	0.0	2.3	0.0	0.0	0.0	72.1	0.8	20.0	0.0
RBOI06	S	Tanzania	0.0	15.3	3.3	10.2	0.0	23.3	0.0	17.7	0.0	30.2	0.3	69.4	34.5
RBOI12	WG	Tanzania	0.6	19.0	0.6	16.7	0.6	18.4	0.0	16.1	0.0	28.2	0.4	51.6	31.1
RBOI14	G	Tanzania	0.0	6.3	1.8	12.5	0.0	14.4	0.0	45.8	0.0	19.2	0.1	53.4	62.9
RBOI15	G	Tanzania	0.0	3.4	6.0	16.7	0.9	9.8	0.0	45.3	0.0	17.9	0.0	35.9	62.4
RBOI17	G	Tanzania	0.0	2.3	1.1	19.2	2.3	15.3	0.0	44.8	0.0	14.9	0.0	41.7	54.9
RBOI10	WG	Tanzania	0.0	1.8	0.9	15.5	0.0	26.8	0.0	24.1	0.0	30.9	0.0	63.4	36.3
RB942	S	Ethiopia	0.0	18.4	0.0	13.8	0.5	10.7	0.0	11.2	0.0	45.4	0.5	42.9	31.0
MA94103	G	Ethiopia	2.3	11.2	0.0	13.5	4.8	17.8	4.6	26.1	0.2	19.7	0.2	49.4	46.1
MA94106	WG	Ethiopia	1.0	20.7	0.0	25.0	8.4	7.4	9.2	8.8	0.8	18.6	0.4	18.1	31.6
MA94101	RW	Ethiopia	0.0	46.5	0.2	13.8	3.1	9.7	6.6	8.3	0.4	11.3	1.1	36.5	36.6
C1	D	Chad	7.5	0.9	3.1	28.6	5.7	14.5	0.4	12.3	0.0	26.9	0.1	29.7	20.7
C2	D	Chad	5.3	4.5	2.9	13.8	3.7	20.8	0.0	8.5	0.0	40.3	0.2	54.4	18.2
A1	S	Chad	22.5	0.0	5.8	21.7	3.5	8.8	2.1	6.3	0.0	29.2	0.5	25.8	19.7
A2	S	Chad	23.7	0.0	5.1	18.2	7.6	5.5	1.3	10.6	0.0	28.0	0.5	17.6	27.5
A3	S	Chad	0.0	0.0	0.0	22.0	6.0	6.7	0.0	4.7	0.0	60.7	0.0	19.2	11.9

Appendix 5.B. Cont.

ID	Environment	Country (or site)	Globular _echinate	Globular _granulate	Globular _smooth	Bilobate	Cross	Saddle	Trapeziform	Rondel	Polylobate	Bulliform	D/P	Iph	Ic
A4	S	Chad	0.0	0.0	1.3	1.3	0.0	2.6	0.0	1.3	0.0	93.4	0.0	66.7	25.0
B	G	Chad	6.9	0.0	1.7	22.2	7.8	5.2	0.0	12.5	0.0	43.6	0.1	14.7	26.2
O34	G	Tanzania	0.0	11.5	0.0	25.0	0.4	31.4	4.2	24.9	0.0	2.7	0.1	55.6	2.9
O35	RW	Tanzania	0.0	34.2	0.0	17.4	2.7	18.5	2.7	24.5	0.0	0.0	0.5	47.8	1.5
O36	RW	Tanzania	0.0	45.0	0.0	12.6	0.3	10.7	13.0	17.8	0.0	0.6	0.8	45.5	0.0
E54	W	Tanzania	16.5	21.7	0.3	4.2	0.3	7.1	2.9	46.9	0.0	0.0	0.6	62.9	3.0
E55	W	Tanzania	19.4	17.2	0.3	5.0	0.6	22.7	3.9	30.5	0.3	0.0	0.6	81.9	1.5
E56	W	Tanzania	51.0	19.2	2.5	4.3	0.3	8.0	2.6	11.8	0.0	0.3	2.6	63.4	0.0
E57	W	Tanzania	19.5	21.9	4.1	9.2	1.4	14.3	5.4	20.0	0.5	3.8	0.8	58.9	5.0
E58	S	Tanzania	4.7	42.0	4.4	5.4	6.0	7.8	6.5	21.8	0.3	1.3	1.0	44.8	0.5
E59A	S	Tanzania	4.0	59.0	0.0	15.0	0.0	10.0	3.0	4.0	0.0	5.0	2.0	40.0	12.3
E59B	GW	Tanzania	0.7	38.8	1.7	11.8	1.0	15.3	7.3	23.5	0.0	0.0	0.7	55.1	13.3
H61	W	Tanzania	25.3	34.5	0.8	11.1	0.2	7.2	3.3	15.1	1.2	1.2	1.6	38.7	1.0
H62	RW	Tanzania	9.6	38.3	0.0	13.2	0.6	14.7	6.9	16.2	0.6	0.0	0.9	51.6	1.0
H64	G	Tanzania	0.7	38.4	0.3	23.6	6.5	11.0	5.1	13.4	1.0	0.0	0.6	27.1	4.4
H66	W	Tanzania	0.0	31.1	0.0	15.8	1.1	27.8	0.7	22.7	0.7	0.0	0.5	62.3	1.0
H68	W	Tanzania	0.4	17.8	0.0	26.3	4.0	20.2	7.5	21.8	2.0	0.0	0.2	40.0	1.7
M69	GW	Tanzania	6.5	11.0	0.0	12.1	0.8	10.6	18.8	37.6	0.8	1.6	0.2	45.2	0.5
M70	GW	Tanzania	4.5	40.5	1.0	19.6	0.6	10.6	7.4	14.8	1.0	0.0	0.8	34.4	1.0
M71	S	Tanzania	23.1	38.6	2.2	12.1	0.5	5.5	7.1	9.5	1.0	0.3	1.7	30.3	0.9
M72	S	Tanzania	0.5	11.9	0.0	44.7	5.0	11.0	11.0	13.7	1.4	0.9	0.1	18.0	0.9
M73	W	Tanzania	4.5	39.5	1.1	9.6	0.5	18.7	12.3	13.1	0.3	0.5	0.8	64.8	0.4
M74	GW	Tanzania	27.7	36.3	0.6	8.1	1.8	9.2	8.1	7.9	0.4	0.0	1.8	48.5	1.0
M75	W	Tanzania	0.3	41.8	0.0	10.2	1.9	25.3	5.2	13.0	0.3	1.9	0.8	67.5	0.0
DB14-29	Zinj	Zinj	7.7	53.8	0.0	0.0	0.0	0.0	32.3	6.2	0.0	0.0	1.6	0.0	0.0
DB14-27	Zinj	Zinj	68.4	8.6	0.0	1.1	0.0	3.0	14.3	2.3	2.3	0.0	3.4	0.0	0.0
DB12-79	Zinj	Zinj	10.6	67.1	5.9	0.0	0.0	0.0	9.4	5.9	0.0	1.2	5.1	0.0	0.0
DB12-69	Zinj	Zinj	10.8	66.2	0.0	0.0	0.0	0.0	20.0	3.1	0.0	0.0	3.3	0.0	0.0
DB12-68	Zinj	Zinj	0.8	84.6	0.0	0.0	0.0	0.0	12.3	1.5	0.0	0.8	6.2	0.0	0.0
DB12-67	Zinj	Zinj	0.9	77.6	1.9	3.7	0.0	0.0	15.0	0.0	0.9	0.0	4.0	0.0	0.0
DB12-124	Zinj	Zinj	19.8	30.2	0.0	2.1	0.0	1.0	35.4	11.5	0.0	0.0	1.0	0.0	0.0
DB12-144	Zinj	Zinj	31.9	15.4	7.7	0.0	0.0	1.1	34.1	9.9	0.0	0.0	1.0	0.0	0.0
DB12-159	Zinj	Zinj	2.0	59.5	0.0	0.0	0.0	0.0	28.4	9.5	0.7	0.0	1.6	0.0	0.0
DB12-160	Zinj	Zinj	7.4	44.4	0.0	3.7	0.0	7.4	18.5	18.5	0.0	0.0	1.1	0.0	0.0
DB12-116	Zinj	Zinj	13.3	33.3	20.0	3.3	0.0	0.0	3.3	10.0	0.0	16.7	2.8	0.0	0.0

Appendix 5.B. Cont.

ID	Environment	Country (or site)	Globular _echinate	Globular _granulate	Globular _smooth	Bilobate	Cross	Saddle	Trapeziform	Rondel	Polylobate	Bulliform	D/P	Iph	Ic
DB12-161	Zinj	Zinj	27.1	11.8	4.7	0.0	0.0	1.2	15.3	37.6	0.0	2.4	0.7	0.0	0.0
DB14-11	Zinj	Zinj	20.7	49.7	0.0	0.0	0.0	0.7	12.4	10.3	2.1	4.1	2.8	0.0	0.0
DB14-09	Zinj	Zinj	0.0	97.4	0.0	0.0	0.0	0.0	0.0	0.0	0.0	2.6	50.0	0.0	0.0
DB12-112	Zinj	Zinj	5.3	82.5	10.5	0.0	0.0	0.0	0.0	1.8	0.0	0.0	50.0	0.0	0.0
DB14-47	Zinj	Zinj	9.8	76.1	0.0	1.1	0.0	0.0	13.0	0.0	0.0	0.0	6.1	0.0	0.0
DB14-40	Zinj	Zinj	18.1	43.8	0.0	0.0	0.0	2.5	27.5	8.1	0.0	0.0	1.6	0.0	0.0
DB14-48	Zinj	Zinj	0.7	86.1	0.0	0.7	0.0	0.0	8.8	2.9	0.7	0.0	6.6	0.0	0.0
DB12-135	Zinj	Zinj	0.0	28.1	0.0	14.6	0.0	0.0	12.5	37.5	0.0	7.3	0.4	0.0	0.0
DB14-46	Zinj	Zinj	2.9	84.0	0.0	2.3	0.0	1.7	8.0	1.1	0.0	0.0	6.6	0.0	0.0
DB12-85	Zinj	Zinj	19.5	7.8	42.9	0.0	0.0	1.3	23.4	5.2	0.0	0.0	0.9	0.0	0.0
DB12-130	Zinj	Zinj	0.0	47.8	0.0	0.0	0.0	2.2	41.3	8.7	0.0	0.0	0.9	0.0	0.0
DB12-10	Zinj	Zinj	0.0	100.0	0.0	0.0	0.0	0.0	0.0	0.0	0.0	0.0	50.0	0.0	0.0
DB14-32	Zinj	Zinj	5.9	86.6	0.0	0.8	0.0	0.0	5.0	1.7	0.0	0.0	12.2	0.0	0.0
M14-1	Zinj	Zinj	15.4	63.4	0.0	0.0	0.0	0.0	12.2	4.9	0.8	3.3	4.4	0.0	0.0
M14-2	Zinj	Zinj	41.9	44.4	0.0	1.3	0.0	1.9	6.9	1.3	0.0	2.5	7.7	0.0	0.0

Appendix 6. Comparison of accuracy rates of identification (in percent) obtained using different datasets of granules and/or characters. Rates of correct allocation are summaries from Random Forest test confusion matrices with granules grouped by species, families, and histological origin (plant parts).

	Accuracy rates in %				
Species	**Selected granules all characters**	**All granules all characters**	**Selected granules selected characters**	**All granules selected characters**	**Blind test Success/Total**
Ada_dig	**53**	48	**53**	39	5/10
Bra_def	71	**73**	70	72	8/13
Cad_far	23	**30**	17	26	1/9
Cap_fas	50	**51**	47	46	0/9
Cyn_dac	**63**	43	59	41	5/11
Cyp_rot	**75**	64	74	61	**1/16**
Ech_col	**76**	62	70	55	2/8
Emi_ann	**33**	27	19	24	1/11
Fai_alb	**64**	59	47	47	11/17
Fic_sal	**47**	41	36	32	0/3
Hib_mic	**56**	32	50	30	4/9
Oly_lat	42	**68**	43	60	0/11
Pan_sub	**63**	59	61	54	2/8
Per_sen	**61**	61	53	45	0/2
Por_ole	**71**	59	70	65	1/3
Set_pum	**38**	36	18	25	0/10
Typ_lat	31	40	38	**44**	0/10
Vig_fru	**53**	49	**50**	50	7/20*
Vig_vex	63	**66**	60	65	7/20*
Zan_aet	25	39	32	**42**	0/9
Mean species	**52.9±16.4**	**50.3±13.7**	**48.3±17.6**	**46.1±14.2**	**Total 48/189**
Family					
CAPPARACEAE	**31**	30	28	28	
FABACEAE	**79**	78	77	78	
MALVACEAE	**53**	40	51	34	
POACEAE	83	**83**	79	80	
Mean family	**61.5±24**	**57.9±26.6**	**58.7±24.2**	**55±27**	
Plant part					
Mesocarp	**66.7**	64.4	61.8	58.8	
Seed	68.9	**69.4**	71	69.1	
USO	80.3	77.7	75	75.4	
Mean plant part	**72±7.3**	**70.5±6.7**	**69.3±6.8**	**67.8±8.4**	
Total Mean	**56.3±17.6**	**53.7±16.3**	**52.9±18.7**	**51.9±17.2**	

* *Vigna vexillata* and *Vigna frutescens* were considered as one single taxon on blind test

Appendix 7.A. Detailed phytolith counts in "Zinj complex" sites samples.

	SAMPLE	DB14 -29	DB14 -27	DB12 -79	DB12 -69	DB12 -68	DB12 -67	DB12 -124	DB12 -144	DB12 -121	DB12 -159	DB12 -160	DB12 -116	DB12 -161	DB14 -11	DB14 -09	DB12 -112	DB14 -47	DB14 -40	DB14 -48	DB12 -135	DB14 -46	DB12 -85	DB12 -130	DB12 -10	DB14 -32	MDR14 -1	MDR14 -2
CODES	**ATTRIBUTION**																											
Ac1		5	1		2	1	5	2	3					10	5	3				1	6					3		
Ac3															3							3						
Blo2	Grass/Sedge	0	3	56	0	0	12	0	0	0	3	8	16	23	10	0	6	13	1	4	9	2	19	6	0	0	7	10
Blo4	Fl	56	5	48	60	0	63	22	28	0	12	54	42	86	48	13	83	35	64	12	0	12	66	45	0	0	48	9
Blo5	Fl		6										47		10	28		26	15	32	3	53		32		45	27	32
Blo8	Fl				13			15	49			43	6	5			41				9			49				
Blo9	Grass		1			9	4				2			2	2								1					
Blo11	Grass/Sedge			1		1							5	2	6	2					7						4	4
Blo13	Fern	0	3	0	17	7	0	0	30	0	2	0	2	8	0	0	0	0	0	0	20	0	4	4	0	0	0	20
Blo14	Fl			16				11	11			17	23	4			7						9	11				
Blo17				1				4	13			16	39	10	19		3	12		6	22		36	26		1	5	19
Com1	Fl																	1										
El1	Fl	0	0	8	19	1	17	0	0	0	16	0	0	28	0	0	0	0	0	0	3	8	0	0	23	0	25	22
El2	Grass/Sedge														2							1					8	
El3	Fl		5					3			7	9	10					21		9		6	6	13	13			
El5	Grass/Sedge	0	16	0	0	0	0	8	0	0	2	9	0	17	1	0	0	0	16	0	0	0	0	4	105	0	0	0
El6			4	3									1							43								
El8	Sedge																						17					
El9		12	12			3	16	8	10		3	5			14	7	8	19		11	4	5	11		21		2	3
El10	Fl	4					8	14							3		17			43		3		28		16		16
El12		36				54		10	3		13	43						3								13	1	
El15	Fl											3	4								18		3			3		
Epi1	Fl					1									2			3	2									1
Glo1	Palms		110	8	7			15	21			2	3	21	5		3	9	14				11			1	4	23
Glo2	Palms	5	72	1		1	1	4	8		3		1	2	25				15	1		5	4			6	15	44
Glo6				5			2																					
Glo9									7				6	4			6						33					
Glo10	Fl	14	11	39	20	25	22	17	14		9	12	10	10	36	2	5	29	13	25	27	29	6	22	13	23	30	30
Glo13	Fl	21	12	18	23	85	61	12			79				36	73	42	41	57	93		118			83	80	48	41
GSSC2	Grass	1	6					2													5	2	2	1			1	
GSSC3	Grass	3		3	2	1		9	9			5	3	7						3	12		2	3		2		1
GSSC4	Grass			2		1					14			25	15		1		13	1	19						5	1
GSSC11	Grass	21	38	8	13	16	16	34	31	0	42	5	1	13	18	0	0	12	44	12	12	14	18	19	0	6	15	11
GSSC12	Grass		1				4														3							
GSSC14	Grass		2					2				1	1					1		1	11	4				1		2
GSSC18	Grass		6				1				1				3					1							1	
GSSC23	Grass		8					1	1			2		1	1				4			3	1	1				3
GSSC24	Grass	0	0	6	9	0	0	0	25	0	0	0	1	0	4	0	0	0	0	0	25	0	0	0	0	0	1	0
Mes	Fl	0	0	38	29	13	25	0	0	0	21	0	9	0	32	0	37	39	0	36	0	3	0	0	0	21	6	7
Pap				1									2	2							7		2					
Pla3	Fl			2	16			18			12	9		28	1				13		8			4		18		
Pla4		2																										
Pla5	Sedge			9	13		2		7		4		16					8			23		19	1				
Pla6		13		12	7	17	20	21			2	6	26		6		28	7		13	47	14	8	19		8	5	
Pla9	Fl	12			21									4														
Sto																		1										
Und1		28	0	14	36	3	0	39	10	0	0	38	42	0	0	0	24	36	0	0	0	14	31	14	0	32	18	4
Und2		50	0	27	1	0	0	0	28	0	0	24	0	0	0	0	0	0	42	0	13	0	0	0	0	22	10	0
Und3			1			27	1	1																				
Und4		11	0	0	0	7	23	29	14	0	95	0	8	0	0	27	0	0	0	2	0	9	2	0	0	0	12	0
	Σ phytoliths	294	323	326	308	273	303	301	322	0	342	311	324	312	307	155	311	316	313	349	313	308	311	302	258	301	298	303

Appendix 7.B. Detailed phytolith counts in BK site samples.

	SAMPLE	DB11 -19	DB11 -20	DB11 -21	DB11 -1	DB11 -2	DB11 -3	DB11 -4	DB11 -5	DB11 -6	DB11 -7	DB11 -8	DB11 -9	DB11 -10	DB11 -13	DB11 -14	DB11 -15	DB11 -16	DB11 -17	DB11 -18	DB12 -71	DB12 -72	DB12 -73	DB12 -18	DB12 -19
CODES	**ATTRIBUTION**																								
Ac1	ND															1	2	3							
Ac3	ND																		2						
Blo2	Grass/Sedge	0	0	0	8	0	0	0	0	0	0	0	0	0	0	0	0	9	0	0	0	0	0	2	0
Blo4	FI	0	15	24	38	9	0	0	39	0	0	0	0	9	7	5	5	54	14	36	0	9	82	7	3
Blo5	FI			58	15	108						48		79		10		73	69	9	8	4	37	19	16
Blo6	FI															31									
Blo9	Grass	0	0	0	0	0	0	0	0	0	0	0	0	0	0	0	3	0	0	0	0	0	0	13	23
Blo11	Grass/Sedge											4		2			1		1					2	
Blo13	Fern			4												26		21	47				3	5	
Blo17	ND		4	14	16	13			6			24		22	20	26	2	28	24	14		12	21	12	46
Com1	FI																								
El1	FI	0	0	0	4	16	0	0	0	0	0	0	0	2	0	11	0	3	0	20	0	0	37	94	30
El3	FI																								5
El5	Grass/Sedge	0	0	0	10	0	0	0	0	0	0	0	0	0	0	0	0	4	0	0	0	0	0	0	0
El6						4										7									
El8	Sedge																								
El9			1		8	8										12		3		7		4	8	13	4
El10	FI	0	0	0	0	4	0	0	0	0	0	0	0	0	0	0	0	0	0	14	0	0	25	0	12
El11			11											38											11
El12														3					27						
El15	FI																							2	
Epi1	FI																							16	
Glo1	Palms																								
Glo2	Palms		11	2		9								1		8	13						2		
Glo3	Palms			2														3							
Glo6						10						8				25	3	8					1		
Glo9																					3		4		3
Glo12	FI		36	3	21	14			20			28		4	11	27	24	20	36	13	8	32	6	26	24
Glo13	FI	0	16	40	36	37	0	0	26	0	0	49	0	14	12	34	28	22	6	14	17	4	8	0	52
GSSC2	Grass																	1							
GSSC3	Grass											1													
GSSC4	Grass		3		7	7			9			3		9	1			6	19		1			1	6
GSSC11	Grass				6	8			14			2		4			13	17	12	3			2	1	
GSSC12	Grass																								
GSSC14	Grass															3		1							
GSSC16	Grass					1																			
GSSC18	Grass																	1							
GSSC21	Grass								4										1						1
GSSC23	Grass				1	2																			
GSSC24	Grass	0	0	0	0	0	0	0	0	0	0	0	0	0	0	0	0	0	0	0	0	0	0	0	0
Mes	FI	0	0	0	0	0	0	0	0	0	0	30	0	9	14	0	24	16	28	0	0	23	0	98	32
Pap																									
Pla1																	1								
Pla2	FI																								
Pla3	FI				26										13	2			17	51	14	23			14
Pla5	Sedge		1															1							
Pla6		0	34	0	0	0	0	0	0	0	0	18	0	16	0	0	6	0	9	0	0	27	0	27	23
Pla7																				4					
Sto																									
Und1		0	0	0	0	0	0	0	0	0	0	3	0	0	1	1	0	0	0	0	0	0	0	0	0
Und2						4																			
Und4		0	0	0	19	0	0	0	60	0	0	0	0	45	0	0	0	26	0	0	0	0	0	0	3
Diatoms																				18	1			1	5
	Σ phytoliths	0	132	147	215	254	0	0	178	0	0	218	0	257	79	229	125	320	312	185	51	138	236	338	308

Appendix 8.A. Detailed phytolith counts in experimental stone tool and experimental soil samples. Letters A-O: soil samples, numbers 2-29: experimental stone tools. Attr.: attribution, Bull.: Bulliform, El.:Elongate, Blo.: Blocky, Pla.: Platelet, Glo.: Globular and Ac.: Acicular.

Phyto ID/ Sample	Group	Attr.	A	B	C	D	E	F	G	H	I	J	K
GSSC Rondel	GSSC	Grass	43	47	38	35	42	53	54	45	41	38	45
GSSC Trapeziform	GSSC	Grass	4	4	3	3	3	4	0	4	3	5	7
GSSC Bilobate	GSSC	Grass	3	5	16	1	3	1	1	0	5	7	2
GSSC Polylobate	GSSC	Grass	19	23	12	30	16	23	30	24	16	16	19
GSSC Saddle	GSSC	Grass	8	3	1	12	4	4	9	5	19	12	10
Bulliform fan shaped	Bull.	Grass	4	0	3	5	0	1	0	3	3	1	1
GSSC Other	GSSC	Grass	0	0	3	1	4	1	3	5	0	9	6
Elongate cylindric	El.	Others	8	18	5	5	12	11	7	15	11	9	4
Elongate tabular	El.	Others	7	11	8	4	7	3	4	1	5	9	9
Elongate granulate	El.	Others	4	14	23	8	27	16	19	9	19	12	19
Elongate echinate	El.	Grass	18	8	5	11	9	9	9	9	5	5	9
Blocky polyhedral rugose	Blo.	Dicot	28	22	20	23	23	18	16	20	22	18	17
Blocky polyhedral psilate	Blo.	Wood	5	9	9	8	14	11	5	8	9	4	1
Blocky irregular rugose	Blo.	Dicot	9	5	11	4	5	3	0	3	9	12	12
Blocky irregular psilate	Blo.	Others	0	1	1	7	5	5	4	1	8	3	21
Puzzle	Pla.	Dicot	8	12	11	14	12	11	9	8	5	14	6
Platelet rugose	Pla.	Dicot	11	16	16	4	8	11	4	22	3	14	10
Platele psilate	Pla.	Dicot	5	3	8	8	3	3	4	3	5	11	1
Globular rugose	Glo.	Wood	4	1	4	4	1	3	0	7	7	7	0
Globular echinate	Glo.	Palm	16	22	7	23	16	19	26	20	18	19	12
Acicular body	Ac.	Others	3	0	3	3	1	1	1	0	3	0	3
Σ phytoliths			207	224	207	213	215	211	205	212	216	225	214
Phyto ID/ Sample	**Group**	**Attr.**	**L**	**M**	**N**	**O**	**2**	**3**	**4**	**5**	**6**	**7**	**8**
GSSC Rondel	GSSC	Grass	42	28	39	33	39	42	28	42	38	49	46
GSSC Trapeziform	GSSC	Grass	6	6	3	8	5	5	4	9	4	3	9
GSSC Bilobate	GSSC	Grass	4	2	8	3	4	5	3	4	3	3	3
GSSC Polylobate	GSSC	Grass	4	27	17	26	19	19	27	23	19	16	8
GSSC Saddle	GSSC	Grass	5	11	0	0	4	3	0	3	11	5	5
Bulliform fan shaped	Bull.	Grass	1	3	9	1	5	0	3	4	3	7	1
GSSC Other	GSSC	Grass	3	4	1	6	0	0	4	4	5	5	0
Elongate cylindric	El.	Others	5	3	7	3	4	11	11	4	4	8	5
Elongate tabular	El.	Others	12	13	3	14	11	4	9	4	9	11	12
Elongate granulate	El.	Others	18	8	25	22	9	24	9	14	16	22	18
Elongate echinate	El.	Grass	11	9	4	3	11	7	9	4	4	8	11
Blocky polyhedral rugose	Blo.	Dicot	27	21	31	19	24	22	16	30	23	22	22
Blocky polyhedral psilate	Blo.	Wood	8	8	1	14	9	4	30	9	3	3	8
Blocky irregular rugose	Blo.	Dicot	6	14	11	21	4	18	24	18	7	16	3
Blocky irregular psilate	Blo.	Others	4	9	6	3	18	4	5	4	18	8	8
Puzzle	Pla.	Dicot	5	12	11	6	14	7	19	8	5	8	5
Platelet rugose	Pla.	Dicot	19	23	12	7	3	12	11	11	9	4	16
Platele psilate	Pla.	Dicot	3	7	2	3	11	8	3	1	4	7	4
Globular rugose	Glo.	Wood	5	3	8	11	1	4	1	1	4	4	5
Globular echinate	Glo.	Palm	15	9	6	19	9	7	5	7	15	1	22
Acicular body	Ac.	Others	0	1	2	3	11	7	0	0	5	3	0
Σ phytoliths			203	221	206	225	215	213	221	204	209	213	211

Appendix 8.A. Cont.

Phyto ID/ Sample	Group	Attr.	9	10	11	12	13	14	15	16	17	18	19
GSSC Rondel	GSSC	Grass	34	34	32	27	49	42	36	39	41	20	65
GSSC Trapeziform	GSSC	Grass	0	3	5	3	3	4	3	8	4	3	4
GSSC Bilobate	GSSC	Grass	3	5	14	3	3	5	8	3	4	3	1
GSSC Polylobate	GSSC	Grass	19	22	22	19	18	23	18	20	7	38	23
GSSC Saddle	GSSC	Grass	1	12	0	12	11	14	8	3	12	3	23
Bulliform fan shaped	Bull.	Grass	0	1	0	4	4	0	0	4	4	0	0
GSSC Other	GSSC	Grass	0	3	1	5	7	0	5	7	1	4	5
Elongate cylindric	El.	Others	14	5	8	5	4	12	9	12	8	3	5
Elongate tabular	El.	Others	12	11	12	8	8	11	9	9	3	8	8
Elongate granulate	El.	Others	15	12	22	22	12	16	16	19	20	8	24
Elongate echinate	El.	Grass	0	3	9	8	4	3	9	3	14	8	9
Blocky polyhedral rugose	Blo.	Dicot	11	22	22	16	26	28	16	26	27	23	54
Blocky polyhedral psilate	Blo.	Wood	19	9	8	9	18	3	9	4	12	8	27
Blocky irregular rugose	Blo.	Dicot	3	8	8	15	4	3	8	11	8	16	5
Blocky irregular psilate	Blo.	Others	28	12	5	3	9	5	4	7	5	7	11
Puzzle	Pla.	Dicot	1	16	19	5	5	16	14	9	7	12	16
Platelet rugose	Pla.	Dicot	11	5	0	16	9	4	5	12	14	18	5
Platele psilate	Pla.	Dicot	22	12	0	9	4	11	8	5	7	11	3
Globular rugose	Glo.	Wood	3	3	7	9	3	3	5	1	0	4	3
Globular echinate	Glo.	Palm	11	11	8	5	5	19	19	14	15	11	22
Acicular body	Ac.	Others	0	3	0	0	3	0	1	0	1	0	3
Σ phytoliths			207	212	202	203	209	222	210	216	214	208	316

Phyto ID/ Sample	Group	Attr.	20	21	22	23	24	25	26	27	28	29
GSSC Rondel	GSSC	Grass	28	28	45	42	39	23	24	39	28	26
GSSC Trapeziform	GSSC	Grass	1	0	0	1	4	0	4	11	9	8
GSSC Bilobate	GSSC	Grass	1	4	11	1	3	5	5	4	9	3
GSSC Polylobate	GSSC	Grass	19	32	16	15	30	58	31	22	18	24
GSSC Saddle	GSSC	Grass	8	3	5	11	3	0	8	3	0	8
Bulliform fan shaped	Bull.	Grass	0	0	8	5	4	1	3	3	3	0
GSSC Other	GSSC	Grass	9	5	3	0	0	4	3	3	5	3
Elongate cylindric	El.	Others	16	3	5	5	8	18	9	3	3	8
Elongate tabular	El.	Others	5	5	11	22	11	9	12	4	11	4
Elongate granulate	El.	Others	11	18	19	8	12	11	18	5	23	14
Elongate echinate	El.	Grass	1	4	8	22	16	3	4	1	9	9
Blocky polyhedral rugose	Blo.	Dicot	36	30	24	26	30	23	20	19	22	24
Blocky polyhedral psilate	Blo.	Wood	12	12	14	11	16	7	9	31	12	7
Blocky irregular rugose	Blo.	Dicot	5	15	11	14	23	3	19	4	15	15
Blocky irregular psilate	Blo.	Others	11	4	8	27	11	12	7	22	8	4
Puzzle	Pla.	Dicot	5	16	16	15	5	8	12	3	4	11
Platelet rugose	Pla.	Dicot	11	15	3	5	5	11	9	11	9	8
Platele psilate	Pla.	Dicot	4	9	5	0	11	5	4	5	3	18
Globular rugose	Glo.	Wood	9	1	5	1	4	1	3	3	4	1
Globular echinate	Glo.	Palm	7	8	15	7	5	5	5	16	4	8
Acicular body	Ac.	Others	3	0	0	0	0	0	1	4	5	4
Σ phytoliths			202	212	232	238	240	207	210	216	204	207

Appendix 8.B. Detailed phytolith counts in FLK West stone tool and paleosol samples.

	SAMPLE		15	17	24	28	29	33	41	42	45	47	54	56	62	68	77	82	87	90	99	100	174	178	184	185	186	188	189	190	191	197	198	201	203	208
CODES	**Taxonomical attribution**	**Dicot plant part signal (if distinctive)**																																		
Ac1					4		7		4										9		3	2		1	3	2	6	2								
Blo1				7			26																											1		
Blo11	Poaceae/Cyperaceae		1																1				1				1							2	
Blo12	Poaceae/Cyperaceae																																			
Blo14	Dicotyledons														32	5	29		11			16	32				16								
Blo2	Poaceae/Cyperaceae																		2																
Blo3	Dicotyledons	Leaves			24	20			4		3	28	79			32	9	12	11	20				6		10	49	23			26			30	7	10
Blo6	Dicotyledons		50	27	0	19	3	27	63	33	101	79	69	75	68	37	21	20	50	39	0	72	16	57	37	49	9	16	56	55	0			44	45	85
Blo8	Dicotyledons	Wood	9	2	48	6	7	7	7	89	54	34	8	59	15	97	21	3	11	20	11	2	116	7	41	50	56	23	38	13	14	0	0	9	20	69
Blo9	Poaceae																1			10			1	1			13	7								
Com1	Commelinaceae														2																					
El1	Dicotyledons		0	0	0	0	33	30	10	0	13	2	0	0	13	0	38	0	0	3	11	0	1	0	10	0	0	0	0	0	25	0	0	6	7	0
El12				11								14														1		7								13
El15	Dicotyledons	Leaves		8	16			22			10		12		1				13	9	8			4	14	6			2	3			3	1	
El2	Poaceae/Cyperaceae										8												1	2				15		3					
El3	Dicotyledons		14	27		31									33								2				16		25		19				
El5	Poaceae/Cyperaceae		8				17												1							3									
El6			0	41	29	0	0	0	0	0	0	0	10	0	0	0	8	11	14	28	0	0	0	2	1	0	8	0	0	6	0	0	0	0	0	18
El7	Poaceae/Cyperaceae						8	3														3														
El8	Cyperaceae																							1												
El9				37	24			31	11	43					16	25	36	6	3	7				3	6	17	6			24	29				21	9
Epi1	Dicotyledons	Leaves																2				18														
Glo1	Arecaceae	Leaves/Fruit		1	10				1		1				4			1	2	8	2				4	3	1								5
Glo10	Dicotyledons	Wood/Bark		3					13									1				5												10		
Glo11	Dicotyledons	Wood/Bark		2									7					1	3									1								
Glo2	Arecaceae	Leaves/Fruit		3	3	2			9	7	1	1			2		2	2	16	14		10		6	9	4	1				2			7	12
Glo3	Arecaceae	Leaves/Fruit	1	5	2				16	4						2	2		6	10		1			1	1	1	5					1		3
Glo4	Arecaceae	Leaves/Fruit		3					6							3			4									1			2					4
Glo5	Dicotyledons								7																											
Glo6										1																2			8					7	
Glo8	Dicotyledons																							24										3		
Glo9																						5					1								
GSSC11	Poaceae								2				3					1	3				15					1								
GSSC12	Poaceae																																			
GSSC14	Poaceae												1									1												1	1	
GSSC18	Poaceae																																			
GSSC2	Poaceae				3				3				6							2		7					12	3					5		
GSSC21	Poaceae															2						3													
GSSC23	Poaceae																				2														
GSSC24	Poaceae																					1														
GSSC3	Poaceae																																		1	
Mes	Dicotyledons	Leaves			33		29			2	6	1	13	27	18		14		19	3	23	19	2	6	23					11	11			24	27	
Pap						11			3				1						1	2		1	1					7	4					1		
Pla2	Dicotyledons		21	7		21									2				17	9		15			35		14			13				14	7
Pla3	Dicotyledons	Leaves	19	4				30	10	26	18	36	19	82			26		10	17	25	20		42	17		32		48	24	27			32	23	
Pla4					13		5		21		5	1					2					2				2										4
Pla5	Cyperaceae																			1																
Pla6						7			8													1								1						
Sto																																				
Und1			0	0	0	0	0	0	0	0	0	0	0	0	2	0	0	0	0	2	0	0	0	0	0	0	0	1	0	0	0	0	0	0	21	0
Und2																					48								28	33						
Und4			98	39	41	51	111	63	9	0	7	18	9	0	40	0	8	80	29	39	84	28	25	79	0	72	7	78	0	80	31			30	16	0
		Σ phytoliths	221	227	250	168	246	213	207	205	227	214	237	243	248	203	217	140	236	243	217	232	213	241	201	222	232	207	207	251	203			190	230	239

Appendix 8.B. Cont.

	SAMPLE		218	219	225	226	227	228	231	237	S1	S2	S3	S4	S5	S6	S7	S8
CODES	**Taxonomical attribution**	**Dicot plant part signal (if distinctive)**																
Ac1			7				20							2				1
Blo1														3				
Blo11	Poaceae/Cyperaceae		1		3					8						2	2	
Blo12	Poaceae/Cyperaceae				4													
Blo14	Dicotyledons				30		13			27								
Blo2	Poaceae/Cyperaceae				3													
Blo3	Dicotyledons	Leaves	11			13	11											1
Blo6	Dicotyledons		14	18	0	43	86		32	32						11	6	9
Blo8	Dicotyledons	Wood	3	92	9	12	3	0	41	61	0	6	0	2	3	0	0	0
Blo9	Poaceae											1						
Com1	Commelinaceae				5							2		4		3	2	1
El1	Dicotyledons		0	0	0	0	8	0	18	0	1	1	0	3	0	0	4	2
El12					4				1									
El15	Dicotyledons	Leaves		8			28		1							2		
El2	Poaceae/Cyperaceae						14		3	3			17	21	4			
El3	Dicotyledons				9													
El5	Poaceae/Cyperaceae		3															
El6			6	0	0	6	0	0	32	2	1	3	12	36	18	14	12	0
El7	Poaceae/Cyperaceae										4	0	0	1	0	3	2	34
El8	Cyperaceae										58	67	26	13	47	29	57	39
El9				7	12	37	12											
Epi1	Dicotyledons	Leaves					4				30	45	85	48	67	52	51	66
Glo1	Arecaceae	Leaves/Fruit			1				3	2	15	22	23	3	7	13	21	14
Glo10	Dicotyledons	Wood/Bark			4		10			1				3	5	3		
Glo11	Dicotyledons	Wood/Bark			1											1	6	7
Glo2	Arecaceae	Leaves/Fruit		1	3					4	12		28	6	23	51	22	
Glo3	Arecaceae	Leaves/Fruit			4						18		17	16	27	6		6
Glo4	Arecaceae	Leaves/Fruit									8							
Glo5	Dicotyledons																	
Glo6	Dicotyledons								7	1				2	2			
Glo8	Dicotyledons																	
Glo9	ND														2			
GSSC11	Poaceae													1	2			2
GSSC12	Poaceae											7				9		5
GSSC14	Poaceae				1							4		4	6	3		10
GSSC18	Poaceae										1			14				
GSSC2	Poaceae				4						13	6	9				4	
GSSC21	Poaceae																	
GSSC23	Poaceae			1							28	28	18	7			3	3
GSSC24	Poaceae															8		
GSSC3	Poaceae				11													
Mes	Dicotyledons	Leaves	13		14	5	8		7	15								
Pap			1				4					7	5	6				
Pla2	Dicotyledons		21															7
Pla3	Dicotyledons	Leaves	1	36	4	42	18		41	35								
Pla4										15								
Pla5	Cyperaceae																	
Pla6																		
Sto					4													
Und1			0	0	0	0	0	0	0	0	0	0	0	0	0	0	0	0
Und2																		
Und4			74	54	100	64	0		19	0	13	6		13			6	4
		Σ phytoliths	155	217	230	222	239		205	206	202	205	240	208	213	210	198	211